



Compilation of SHRIMP U–Pb geochronological data, Yilgarn Craton, Western Australia, 2001–2002

*Geoscience Australia
Record 2003/15*

J.M. Dunphy¹, I.R. Fletcher¹, K.F. Cassidy² and D.C. Champion²

¹ Centre of Excellence for Mass Spectrometry, School of Applied Physics, Curtin University of Technology, GPO Box U1987, Perth WA 6845

² Geoscience Australia, GPO Box 378, Canberra ACT 2601

Geoscience Australia

Chief Executive Officer: Neil Williams

Department of Industry, Tourism and Resources

Minister for Industry, Tourism and Resources: The Hon. Ian Macfarlane, MP

Parliamentary Secretary: The Hon. Warren Entsch, MP

© Commonwealth of Australia 2003

This work is copyright. Apart from any fair dealings for the purposes of study, research, criticism or review, as permitted under the Copyright Act, no part may be reproduced by any process without written permission. Inquiries should be directed to the Communications Unit, Geoscience Australia, GPO Box 378, Canberra ACT 2601.

ISSN: 1039 0073

ISBN: 0 642 46773 0

Bibliographic reference: Dunphy, J.M., Fletcher, I.R., Cassidy, K.F. and Champion, D.C., 2003. Compilation of SHRIMP U–Pb geochronological data, Yilgarn Craton, Western Australia, 2001–2002. Geoscience Australia, Record 2003/15, 139p.

Geoscience Australia has tried to make the information in this product as accurate as possible. However, it does not guarantee that the information is totally accurate or complete. **THEREFORE, YOU SHOULD NOT RELY SOLELY ON THIS INFORMATION WHEN MAKING A COMMERCIAL DECISION.**

Contents

List of Figures	ii
List of Tables	v
Introduction	1
Analytical Procedures	3
Data compilation for the QGNG standard	6
Intercomparison of the TEMORA 1, CZ3 and QGNG standards	9
2001967014: biotite granitic gneiss, Corriding Rock	16
2001967017A: Bali Monzogranite	21
2001967019A: banded biotite granitic gneiss, Quairnie Rock	25
2001967027: quartz-feldspar porphyry dyke, Tower Hill mine	29
2001967028: quartz-feldspar porphyry dyke, Safari prospect	33
2001967039: Meredith monzogranite	36
200196 7040: volcanogenic meta-sandstone, Alabama prospect	40
2001967041A: banded biotite granitic gneiss, Twin Hills	45
2001967043: Galah Monzogranite	49
2001967045: biotite monzogranite dyke, Balarky Rocks	54
2001967048: Republic amphibole porphyry, Wiluna	58
2001967052C: Fifima sandstone	61
2001967053A: biotite migmatite, Mt Dennis	66
2001967053B: biotite monzogranite, Mt Dennis	70
2001967056: deformed pebble meta-conglomerate, Hurleys Reward	74
2001969001: Juglah Monzogranite	79
2001969013A: biotite granodiorite enclave, Ivor Rocks	83
2001969013B: K-feldspar porphyritic monzogranite, Ivor Rocks	88
2001969019A: biotite granodiorite, Ironstone Point	92
2001969019A: biotite granodiorite, Ironstone Point	95
2001969033A: Burtville granodiorite	100
2001969035: Menangina monzogranite	104
2001969039: Donkey Rocks monzogranite	108
2001969043A: foliated biotite monzogranite, Blueys Well	113
2001969044: Mars Bore monzogranite	117
2001969053A: granodiorite leucosome, Turkey Well	121
2001969053C: banded biotite granitic gneiss, Turkey Well	125
2001969111B: gneissic biotite trondhjemite, Wingora Soak	129
2001969122: Mt Joanna granodiorite	134
Acknowledgements	138
References	139

List of Figures

Figure 1.	Approximate locations of samples presented in this Record.	2
Figure 2.	Probability plot of $^{207}\text{Pb}/^{206}\text{Pb}$ ages for QGNG from session Z3963i, prior to low-side $^{207}\text{Pb}/^{206}\text{Pb}$ culling (step 5).	7
Figure 3.	Data for QGNG, in sequence from Table 3.	8
Figure 4.	Histogram of MSWD values for QGNG $^{207}\text{Pb}/^{206}\text{Pb}$ data from the different analytical sessions.	8
Figure 5.	Probability plot of $^{207}\text{Pb}/^{206}\text{Pb}$ ages for QGNG from session Z3673i, omitting points 11-1 and 15-1.	10
Figure 6.	Probability plot of $^{206}\text{Pb}/^{238}\text{U}$ ages for QGNG from session Z3673i, omitting points 11-1 and 15-1.	11
Figure 7.	Probability plot of $^{206}\text{Pb}/^{238}\text{U}$ ages for TEMORA 1 from session 3673i.	11
Figure 8.	Probability plot of $^{206}\text{Pb}/^{238}\text{U}$ ages for CZ3 from session 3673i.	12
Figure 9.	Correlation between apparent $^{206}\text{Pb}/^{238}\text{U}$ age defects and Hf content of the three samples (calibrated against QGNG).	12
Figure 10.	Representative SEM images for sample 2001967014: biotite granitic gneiss, Corriding Rock.	17
Figure 11.	Concordia plot for zircon data from 2001967014: biotite granitic gneiss, Corriding Rock.	18
Figure 12.	Enlargement of main group of zircon analyses for sample 2001967014: biotite granitic gneiss, Corriding Rock.	19
Figure 13.	Probability plot for data from high-U zircons in 2001967014: biotite granitic gneiss, Corriding Rock.	19
Figure 14.	Representative SEM images for sample 2001967017A: Bali Monzogranite.	22
Figure 15.	Concordia plot for zircons from sample 2001967017A: Bali Monzogranite.	24
Figure 16.	Concordia plot for the main data cluster for sample 2001967017A: Bali Monzogranite.	24
Figure 17.	Representative SEM images for sample 2001967019A: banded biotite granitic gneiss, Quairnie Rock.	26
Figure 18.	Concordia plot for zircon data from sample 2001967019A: banded biotite granitic gneiss, Quairnie Rock.	28
Figure 19.	Enlargement of main data cluster from sample 2001967019A: banded biotite granitic gneiss, Quairnie Rock.	28
Figure 20.	Representative SEM images for sample 2001967027: quartz-feldspar porphyry dyke, Tower Hill mine.	30
Figure 21.	Concordia plot for zircon data from sample 2001967027: quartz-feldspar porphyry dyke, Tower Hill mine showing the strong zero-age Pb-loss trend.	32
Figure 22.	Enlargement of the main group of zircon data from sample 2001967027: quartz-feldspar porphyry dyke, Tower Hill mine.	32
Figure 23.	Representative SEM images for sample 2001967028: quartz-feldspar porphyry dyke, Safari prospect.	34
Figure 24.	Concordia plot of zircon data from sample 2001967028: quartz-feldspar porphyry dyke, Safari prospect.	35
Figure 25.	Representative SEM images for sample 2001967039: Meredith monzogranite.	37
Figure 26.	Concordia plot for zircons from sample 2001967039: Meredith monzogranite.	39
Figure 27.	Enlargement of the main data group from sample 2001967039: Meredith monzogranite.	39
Figure 28.	Representative SEM images for sample 2001967040: volcanogenic meta-sandstone, Alabama prospect.	41
Figure 29.	Concordia plot for zircons from sample 2001967040: volcanogenic meta-sandstone, Alabama prospect.	42
Figure 30.	Cumulative probability plot for concordant data for zircons from sample 2001967040: volcanogenic meta-sandstone, Alabama prospect.	43
Figure 31.	Representative SEM images for sample 2001967041A: banded biotite granitic gneiss, Twin Hills.	46
Figure 32.	Concordia plot for zircons from sample 2001967041A: banded biotite granitic gneiss, Twin Hills.	48

Figure 33. Concordia plot for the main group of data from sample 2001967041A: banded biotite granitic gneiss, Twin Hills.	48
Figure 34. Representative SEM images for sample 2001967043: Galah Monzogranite.	50
Figure 35. Concordia plot for zircons from sample 2001967043: Galah Monzogranite.	51
Figure 36. Cumulative probability plot for the main data cluster for sample 2001967043: Galah Monzogranite.	52
Figure 37. Enlargement of main data cluster for sample 2001967043: Galah Monzogranite.	52
Figure 38. Representative SEM images for sample 2001967045: biotite monzogranite dyke, Balarky Rocks.	55
Figure 39. Concordia plot for zircons from sample 2001967045: biotite monzogranite dyke, Balarky Rocks.	57
Figure 40. Concordia plot for the main data group from sample 2001967045: biotite monzogranite dyke, Balarky Rocks.	57
Figure 41. Representative SEM images for sample 2001967048: Republic amphibole porphyry, Wiluna.	59
Figure 42. Concordia plot for zircons from sample 2001967048: Republic amphibole porphyry, Wiluna.	60
Figure 43. Representative SEM images for sample 2001967052C: Fifima sandstone.	62
Figure 44. Concordia plot for zircons from sample 2001967052C: Fifima sandstone.	63
Figure 45. Cumulative probability plot of concordant $^{207}\text{Pb}/^{206}\text{Pb}$ data for zircons from sample 2001967052C: Fifima sandstone.	64
Figure 46. Representative SEM images for sample 2001967053A: biotite migmatite, Mt Dennis.	67
Figure 47. Concordia plot for zircons from sample 2001967053A: biotite migmatite, Mt Dennis.	69
Figure 48. Concordia plot of the main data cluster for sample 2001967053A: biotite migmatite, Mt Dennis.	69
Figure 49. Representative SEM images for sample 2001967053B: biotite monzogranite, Mt Dennis.	71
Figure 50. Concordia plot of all data for zircons from sample 2001967053B: biotite monzogranite, Mt Dennis.	73
Figure 51. Cumulative probability plot for concordant data for zircons from sample 2001967053B: biotite monzogranite, Mt Dennis.	73
Figure 52. Representative SEM images for sample 2001967056: deformed pebble meta-conglomerate, Hurleys Reward.	75
Figure 53. Concordia plot for zircons from sample 2001967056: deformed pebble meta-conglomerate, Hurleys Reward.	76
Figure 54. Cumulative probability plot of concordant $^{207}\text{Pb}/^{206}\text{Pb}$ data for zircon from sample 2001967056: deformed pebble meta-conglomerate, Hurleys Reward.	77
Figure 55. Representative SEM images for sample 2001969001: Juglah Monzogranite.	80
Figure 56. Concordia plot for zircons from sample 2001969001: Juglah Monzogranite.	81
Figure 57. Representative SEM images for sample 2001969013A: biotite granodiorite enclave, Ivor Rocks.	84
Figure 58. Concordia plot for zircons from sample 2001969013A: biotite granodiorite enclave, Ivor Rocks.	85
Figure 59. Cumulative probability plot of $^{207}\text{Pb}/^{206}\text{Pb}$ data from concordant data for sample 2001969013A: biotite granodiorite enclave, Ivor Rocks.	86
Figure 60. Representative SEM images for sample 2001969013B: K-feldspar porphyritic monzogranite, Ivor Rocks.	89
Figure 61. Concordia plot for zircons from sample 2001969013B: K-feldspar porphyritic monzogranite, Ivor Rocks.	91
Figure 62. Cumulative probability plot of concordant data for sample 2001969013B: K-feldspar porphyritic monzogranite, Ivor Rocks.	91
Figure 63. Concordia plot for supplementary analyses of zircon from sample 2001969019A: biotite granodiorite, Ironstone Point.	93
Figure 64. Concordia plot for all zircon data from sample 2001969019A: biotite granodiorite, Ironstone Point.	94
Figure 65. SHRIMP Pb/Pb data for rutile standard WH-1.	97

Figure 66. Concordia plot of rutile data from sample 2001969019A: biotite granodiorite, Ironstone Point.	98
Figure 67. SHRIMP Pb/Pb data for rutile from sample 2001969019A: biotite granodiorite, Ironstone Point.	98
Figure 68. Representative SEM images for sample 2001969033A: Burtville granodiorite.	101
Figure 69. Concordia plot for zircons from sample 2001969033A: Burtville granodiorite.	103
Figure 70. Concordia plot for the main data group for sample 2001969033A: Burtville granodiorite.	103
Figure 71. Representative SEM images for sample 2001969035: Menangina monzogranite.	105
Figure 72. Concordia plot for zircon data from sample 2001969035: Menangina monzogranite.	106
Figure 73. Representative SEM images for sample 2001969039: Donkey Rocks monzogranite.	109
Figure 74. Probability plot for data from sample 2001969039: Donkey Rocks monzogranite.	110
Figure 75. Concordia plot for zircons from 2001969039: Donkey Rocks monzogranite.	111
Figure 76. Representative SEM images for sample 2001969043A: foliated biotite monzogranite, Blueys Well.	114
Figure 77. Concordia plot for zircons from sample 2001969043A: foliated biotite monzogranite, Blueys Well.	115
Figure 78. Representative SEM images for sample 2001969044: Mars Bore monzogranite.	118
Figure 79. Concordia plot for zircons from sample 2001969044: Mars Bore monzogranite.	119
Figure 80. Representative SEM images for sample 2001969053A: granodiorite leucosome, Turkey Well.	122
Figure 81. Concordia plot for zircons from sample 2001969053A: granodiorite leucosome, Turkey Well.	123
Figure 82. Representative SEM images for sample 2001969053C: banded biotite granitic gneiss, Turkey Well.	126
Figure 83. Concordia plot for zircons from sample 2001969053C: banded biotite granitic gneiss, Turkey Well.	127
Figure 84. Representative SEM images for sample 2001969111B: gneissic biotite trondhjemite, Wingora Soak.	130
Figure 85. Concordia plot for zircons from sample 2001969111B: gneissic biotite trondhjemite, Wingora Soak.	132
Figure 86. Concordia plot for the main data group from sample 2001969111B: gneissic biotite trondhjemite, Wingora Soak.	132
Figure 87. Representative SEM images for sample 2001969122: Mt Joanna granodiorite.	135
Figure 88. Concordia plot for zircons from sample 2001969122: Mt Joanna granodiorite.	137
Figure 89. Concordant data from sample 2001969122: Mt Joanna granodiorite.	137

List of Tables

Table 1.	Run table for SHRIMP zircon analyses.	4
Table 2.	Run table for SHRIMP rutile analyses.	4
Table 3:	Data for QGNG, for 12 analytical sessions.	7
Table 4.	Summary of SHRIMP $^{206}\text{Pb}/^{238}\text{U}$ age data for standards on mount Z3673.	10
Table 5.	SHRIMP analytical results for standard QGNG on mount Z3673.	13
Table 6.	SHRIMP analytical results for standard TEMORA 1 on mount Z3673.	14
Table 7.	SHRIMP analytical results for standard CZ3 on mount Z3673.	15
Table 8.	SHRIMP analytical results for zircon from sample 2001967014: biotite granitic gneiss, Corriding Rock.	20
Table 9.	SHRIMP analytical results for zircon from sample 2001967017A: Bali Monzogranite.	23
Table 10.	SHRIMP analytical results for zircon from sample 2001967019A: banded biotite granitic gneiss, Quairnie Rock.	27
Table 11.	SHRIMP analytical results for zircon from sample 2001967027: quartz-feldspar porphyry dyke, Tower Hill mine.	31
Table 12.	SHRIMP analytical results for zircon from sample 2001967028: quartz-feldspar porphyry dyke, Safari prospect.	35
Table 13.	SHRIMP analytical results for zircon from sample 2001967039: Meredith monzogranite.	38
Table 14	SHRIMP analytical results for zircon from sample 2001967040: volcanogenic meta-sandstone, Alabama prospect.	44
Table 15.	SHRIMP analytical results for zircon from sample 2001967041A: banded biotite granitic gneiss, Twin Hills.	47
Table 16.	SHRIMP analytical results for zircon from sample 2001967043: Galah Monzogranite.	53
Table 17.	SHRIMP analytical results for zircon from sample 2001967045: biotite monzogranite dyke, Balarky Rocks.	56
Table 18.	SHRIMP analytical results for zircon from sample 2001967048: Republic amphibole porphyry, Wiluna.	60
Table 19.	SHRIMP analytical results for zircon from sample 2001967052C: Fifima sandstone.	65
Table 20.	SHRIMP analytical results for zircon from sample 2001967053A: biotite migmatite, Mt Dennis.	68
Table 21.	SHRIMP analytical results for zircon from sample 2001967053B: biotite monzogranite, Mt Dennis.	72
Table 22.	SHRIMP analytical results for zircon from sample 2001967056: deformed pebble meta-conglomerate, Hurleys Reward.	78
Table 23.	SHRIMP analytical results for zircon from sample 2001969001: Juglah Monzogranite.	82
Table 24.	SHRIMP analytical results for zircon from sample 2001969013A: biotite granodiorite enclave, Ivor Rocks.	87
Table 25.	SHRIMP analytical results for zircon from sample 2001969013B: K-feldspar porphyritic monzogranite, Ivor Rocks.	90
Table 26.	Supplementary SHRIMP analytical results for zircon from sample 200196 9019A: biotite granodiorite, Ironstone Point.	93
Table 27.	SHRIMP analytical results for rutile WH-1 standard.	96
Table 28.	SHRIMP analytical results for rutile from sample 2001969019A: biotite granodiorite, Ironstone Point.	96
Table 29.	SHRIMP analytical results for zircon from sample 2001969033A: Burtville granodiorite.	102
Table 30.	SHRIMP analytical results for zircon from sample 2001969035: Menangina monzogranite.	107
Table 31.	SHRIMP analytical results for zircon from sample 2001969039: Donkey Rocks monzogranite.	112
Table 32.	SHRIMP analytical results for zircon from sample 200196 9043A: foliated biotite monzogranite, Blueys Well.	116
Table 33.	SHRIMP analytical results for zircon from sample 2001969044: Mars Bore monzogranite.	120

Table 34.	SHRIMP analytical results for zircon from sample 2001969053A: granodiorite leucosome, Turkey Well.	124
Table 35.	SHRIMP analytical results for zircon from sample 2001969053C: banded biotite granitic gneiss, Turkey Well.	128
Table 36.	SHRIMP analytical results for zircon from sample 2001969111B: gneissic biotite trondhjemite, Wingora Soak.	133
Table 37.	SHRIMP analytical results for zircon from sample 2001969122: Mt Joanna granodiorite.	136

Introduction

This Record contains zircon U–Pb geochronological data obtained between September 2001 and June 2002 on rocks from the Yilgarn Craton, Western Australia. In addition, data are presented for rutile from sample 2001969019A. Zircon from this sample was analysed in the first year of the project (Fletcher et al., 2001). Additional zircon data for this sample are also reported here. Approximate positions of sampling localities are shown in Figure 1.

The data were collected as part of the Norseman-Wiluna Synthesis project, a National Geoscience Accord project that operates in collaboration with the Geological Survey of Western Australia. The results are helping to meet the objective of providing an improved geological and metallogenic framework for the Norseman-Wiluna region of the eastern Yilgarn Craton, and help provide geochronological constraints on geodynamic and tectonic models for the region. The data were acquired through a collaborative research agreement between Curtin University of Technology, Bentley, Western Australia and Geoscience Australia.

This Record describes the analysed samples and data obtained from them, and provides a brief discussion of their geochronological interpretation. The broader geological implications of the data will be published elsewhere. The complete data files, including data for QGNG standards and data for intercomparisons between QGNG and the TEMORA 1 and CZ3 standards (L.P. Black et al., in prep.), are stored in the Geoscience Australia database, OZCHRON.

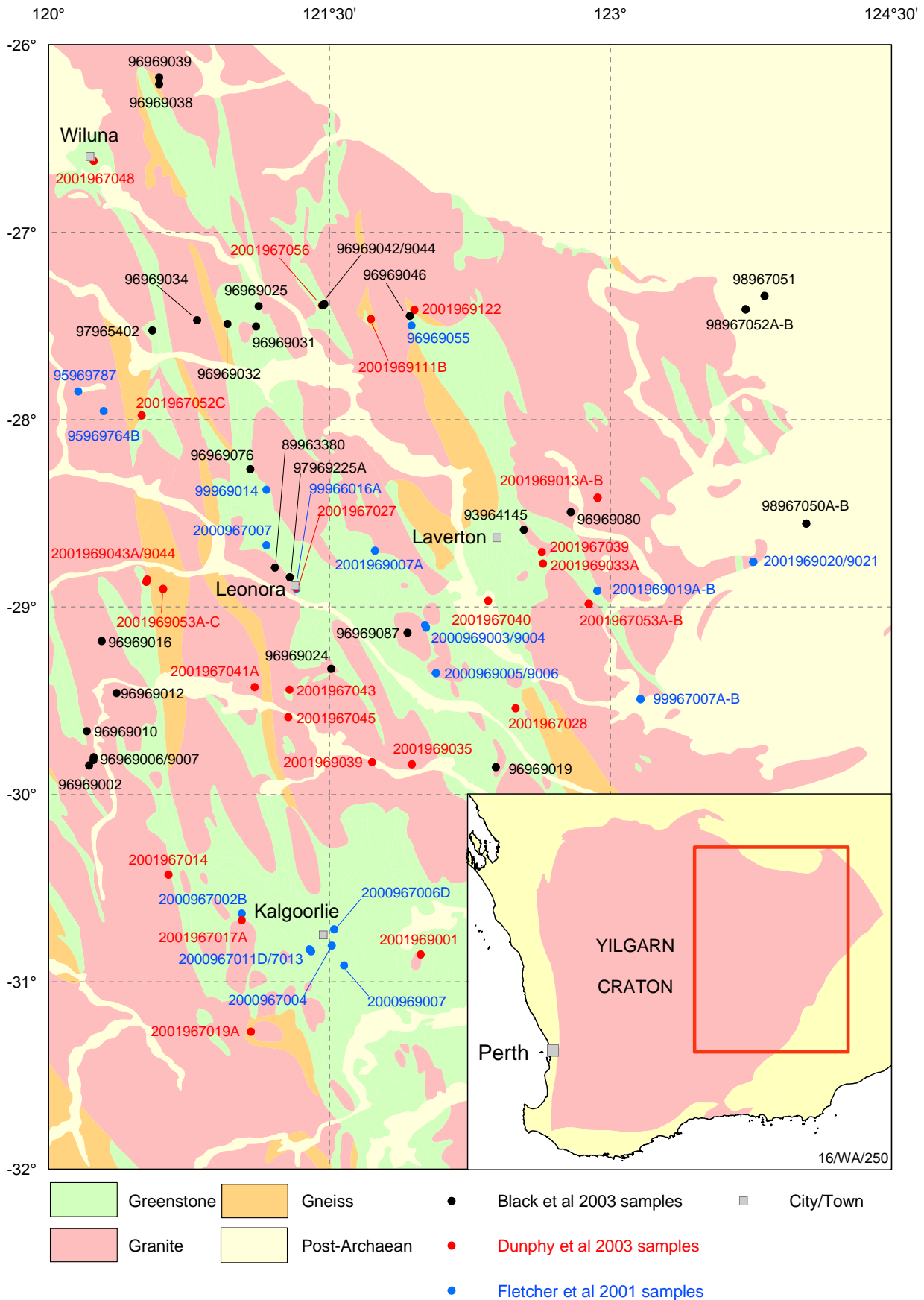


Figure 1. Approximate locations of samples presented in this Record (Dunphy et al. 2003 samples), as well as locations of samples from Fletcher et al. (2001) and Black et al. (2003). The geology, towns and coastline are derived from Geoscience Australia's national geoscience dataset.

Analytical Procedures

Sample processing

Sampling involved the splitting of boulders to access fresh rock, although blasting of solid outcrop was required for some samples. Other samples were obtained from drillcore in collaboration with company geologists. The locations of field samples (± 50 m) were determined using a hand-held GPS; drillcore collar locations were obtained from company data. Sample locations in this Record are referred to the Geocentric Datum of Australia 1994 (GDA94) through Map Grid Australia (MGA) coordinates, Zone 51.

At the field site, the rock was broken into fist-size fragments, having regard to cleanliness at all times, to avoid contamination of the sample. Typically, the sample weighed between 10 kg and 20 kg, sometimes more if a low zircon yield was suspected, but less if only drillcore was available. In the mineral separation lab at Geoscience Australia each rock was cleaned and broken down to 2–5 cm pieces using a pre-cleaned hydraulic splitter. The pieces were ultrasonically washed in water, dried under heat lamps and crushed using a jaw crusher or Rocklabs Boyd crusher. A rotary disc mill or a Rocklabs Continuous Ring Mill was used for milling.

For most samples, for which the main geochronological question is their magmatic age, zircon selection was biased towards the least magnetic, clearest grains, without discrimination between grain morphologies. The initial mineral-density separation was undertaken using a Wilfley table, reducing the sample to about 5% of its original weight. The highly magnetic grains were then removed using a hand magnet. A second density separation stage, using Tetrabromoethane (2.96 g/ml), was followed by magnetic separation using a Frantz isodynamic separator. The non-magnetic fraction then went to a third density separation in Methylene Iodide (3.3 g/ml) and additional Frantz separation. Approximately 100–150 zircon grains per sample were selected for mounting by handpicking under a binocular microscope. For the metasedimentary samples, where zircon provenance is the main factor, zircons were hand-picked without discrimination from the heavy mineral concentrate.

The zircon grains were encapsulated in epoxy, together with similar quantities of one of the in-house Geoscience Australia multi-grain standards, QGNG (Daly et al., 1998), and a small quantity of the Perth standard CZ3 (Pidgeon et al., 1994). The mounts were polished to expose grains in section, and all grains were photographed in transmitted and reflected light, and imaged by cathodoluminescence (CL) on a Hitachi S2250 NSEM located in the Electron Microscopy Unit at the Australian National University. After analysis, backscattered electron (BSE) and additional CL images of typical grains of each sample were obtained at the Centre for Microscopy and Microanalysis (CMM) at The University of Western Australia for inclusion in this report.

Rutile grains were hand-picked from the heavy mineral fraction of sample 2001969019A, together with the zircon recovered for this sample, and mounted with the zircon in mount Z3734. The reference standard for rutile analyses was a small split of the Windmill Hill rutile (2625 Ma, Clark et al., 2000; referred to as WH-1) in a separate mount (UWA mount 96-58).

All SHRIMP mounts were ultrasonically cleaned in petroleum spirit and a 10% Extran solution, triple rinsed in quartz-distilled water, and dried overnight at 30°C in an oven prior to gold-coating with high-purity gold at the CMM.

Data acquisition for zircon

SHRIMP analyses were undertaken on the SHRIMP II located at Curtin University of Technology, Perth, Western Australia, using procedures from Compston et al. (1984) and Smith et al. (1998). In general, attempts were made to analyse examples of all identified grain types. A raster (surface-

cleaning) time of 3 minutes was used, and data were acquired over 7 scans through the mass sequence, which is listed in Table 1. The primary O₂⁻ beam was typically ~3 nA, but up to ~5 nA, and produced an approximately 20–30 µm elliptical spot. The mass resolution at 1% peak height was 4,500–5,000 with secondary ion sensitivity on CZ3 > 15 cps/ppm Pb/nA. For the few samples of detrital zircons extracted from sedimentary or volcano-sedimentary rock, data acquisition was reduced to five scans of the mass spectrum.

Most analytical sessions involved analyses of two samples on one mount over a continuous 48-hour period, with re-tuning of the instrument after 24 hours. One session analysing three magmatic samples and another session on detrital zircons lasted 3-days. Another session was shortened to ~30 hours, the remaining time being used to analyse possible cores in grains on other mounts.

Table 1. Run table for SHRIMP zircon analyses.

Nominal Mass	Species	Count time (s)
196	ZrO ₂	2
204	Pb	10
204.045	background	10
206	Pb	10
207	Pb	40
208	Pb	10
238	U	5
248	ThO	5
254	UO	2

Data acquisition for rutile

Data for rutile were also obtained using the Perth SHRIMP, following the procedures outlined by Clark et al. (2000). The data acquisition sequence is shown in Table 2. The three U species were recorded to provide options for data reduction. Thorium abundances were too small to measure.

Table 2. Run table for SHRIMP rutile analyses.

Nominal Mass	Species	Count time (s)
208Ti	Ti ₃ O ₄	2
204	Pb	10
204.1	background	10
206	Pb	10
207	Pb	40
208Pb	Pb	10
238	U	5
254	UO	2
270	UO ₂	2

Data reduction for zircon

QGNG was used for calibration of U/Pb, and CZ3 for U content (550 ppm U; Nelson, 1997). The reference $^{206}\text{Pb}/^{238}\text{U}$ age for QGNG, determined by replicate analyses using thermal ionisation mass spectrometry (TIMS), is 1843.1 Ma (L.P. Black, pers. comm., 2001).

Data reduction was undertaken using SQUID 1.02c (Ludwig, 2001). For most analytical sessions, the slope of the $\ln[\text{Pb}/\text{U}]:\ln[\text{UO}/\text{U}]$ calibration line was sufficiently well defined and different from the nominal value (2.0) to justify using a value determined from the data.

Corrections for common Pb were based on measured ^{204}Pb and the isotopic composition of Broken Hill galena. Data are only used for age determinations if the common-Pb component is sufficiently small such that corrections for its effect on radiogenic $^{207}\text{Pb}/^{206}\text{Pb}$ data are so minor that the dates are insensitive to the choice of common Pb composition used in making the corrections (over a wide range of Proterozoic–Archaean common-Pb compositions). Analyses requiring larger corrections commonly give discordant data and are presumed to have experienced some open-system disturbance. The origin and age (and hence composition) of their common Pb components are unknown, but largely irrelevant, since these data are not used for age determinations.

Data reduction for rutile

Rutile data were processed using the software package Krill (Kinny, 1997). Pb/U calibration was based on a $\text{Pb}^+/\text{UO}^+:\text{UO}_2^+/\text{UO}^+$ correlation. Uranium abundances were estimated from $\text{UO}^+/\text{Ti}_3\text{O}_4^+$, using an average value of 164 ppm (Clark et al., 2000) for WH-1. Given the variability of WH-1, the resulting abundances are probably accurate to only $\pm\sim 50\%$.

Data presentation

All data from individual analyses are tabulated, and shown in concordia plots, at $\pm 1\text{s}$ precision. All tabulated data are common-Pb corrected. Abbreviations used in table headings are

4f206: the proportion of total ^{206}Pb calculated to be common Pb,

conc.: concordance, defined as $100 \cdot t[^{206}\text{Pb}/^{238}\text{U}]/t[^{207}\text{Pb}/^{206}\text{Pb}]$.

Weighted mean $^{207}\text{Pb}/^{206}\text{Pb}$ ages determined from grouped data are given in the text with 95% confidence limits. The final ages are rounded off to integers and the corresponding uncertainties are rounded up to cover the range that is required by additional decimal places (e.g., 2660.2 ± 5.2 rounds to 2660 ± 6 Ma).

Data compilation for the QGNG standard

Introduction

Zircon grains from the QGNG standard were used for Pb/U calibration and as a monitor of $^{207}\text{Pb}/^{206}\text{Pb}$ reproducibility and accuracy. As in the previous period of this work (Fletcher et al., 2001), these analyses were interspersed with sample analyses (typically after every second unknown), and were collected under the same standardised conditions. Data for one session involving detrital zircons, for which only five scans of the mass spectrum were recorded, are not included in this summary. Data from a short (< 1 day) session following session Z3963j, which included data from two mounts, have also been omitted from this summary. However, the data in both these cases are compatible with those reported here. A total of 383 QGNG analyses from 12 analytical sessions are reported.

Data processing

The full datasets (i.e. both $^{206}\text{Pb}/^{238}\text{U}$ and $^{207}\text{Pb}/^{206}\text{Pb}$) have been assessed in a standardised way, as described in Fletcher et al. (2001), as rigorously as possible. The standard procedure is:

1. SQUID data reduction and preliminary Pb/U calibration;
2. deletion of outliers in $^{206}\text{Pb}/^{238}\text{U}$ (essentially as identified by SQUID), and final Pb/U calibration;
3. deletion of 'abnormal' $^{207}\text{Pb}/^{206}\text{Pb}$ data (>5% discordance; >1000 ppm U; low-precision, possibly due to primary beam instability);
4. deletion of any $>3\sigma$ $^{207}\text{Pb}/^{206}\text{Pb}$ outliers;
5. progressive deletion of $^{207}\text{Pb}/^{206}\text{Pb}$ data from the low side, until MSWD is the smallest possible value >1.0 . (Note that in 3 sessions MSWD <1.0 without culling.)

In three sessions (Z3812i, Z3922i, Z3963i) the $^{207}\text{Pb}/^{206}\text{Pb}$ data distribution is too broad to permit low-side culling to force MSWD close to 1.0 (step 5) without excluding an unreasonable portion of the data. These data sets have the appearance of single populations when shown on a probability plot (Fig. 2), but they are more dispersed than anticipated from the precision of individual analyses. For session Z3963i (Fig. 2), ~60% culling would be required to force MSWD down to 1.0. For these three cases, data culling was stopped at MSWD ≥ 1.3 . All QGNG data sets are discussed in later chapters, with their corresponding sample data.

Data compilation

The weighted mean $^{207}\text{Pb}/^{206}\text{Pb}$ dates for each session are compiled in Table 3 and shown in Fig. 3. Both the grand mean (1850.0 ± 0.8 Ma) and between-session reproducibility (MSWD = 1.07) are similar to values for the first year of the program (1848.9 ± 0.8 Ma; MSWD = 0.8; Fletcher et al., 2001). The compiled MSWD values for $^{207}\text{Pb}/^{206}\text{Pb}$ data from the different analytical sessions (Fig. 4) show a distribution consistent with the form of the MSWD function (Wendt and Carl, 1991), but displaced to higher values, indicating that the applied culling procedure does not lead to excessively restricted distributions amongst the data retained.

As in the first year of the project (Fletcher et al., 2001), we conclude that there are no significant between-session variations in $^{207}\text{Pb}/^{206}\text{Pb}$ data for QGNG, and therefore that there are no significant between-session variations in the sample data recorded in the following chapters, and no re-normalisation has been applied to these data. However, comments in Fletcher et al. (2001) regarding absolute uncertainties in ages also apply to these sample data.

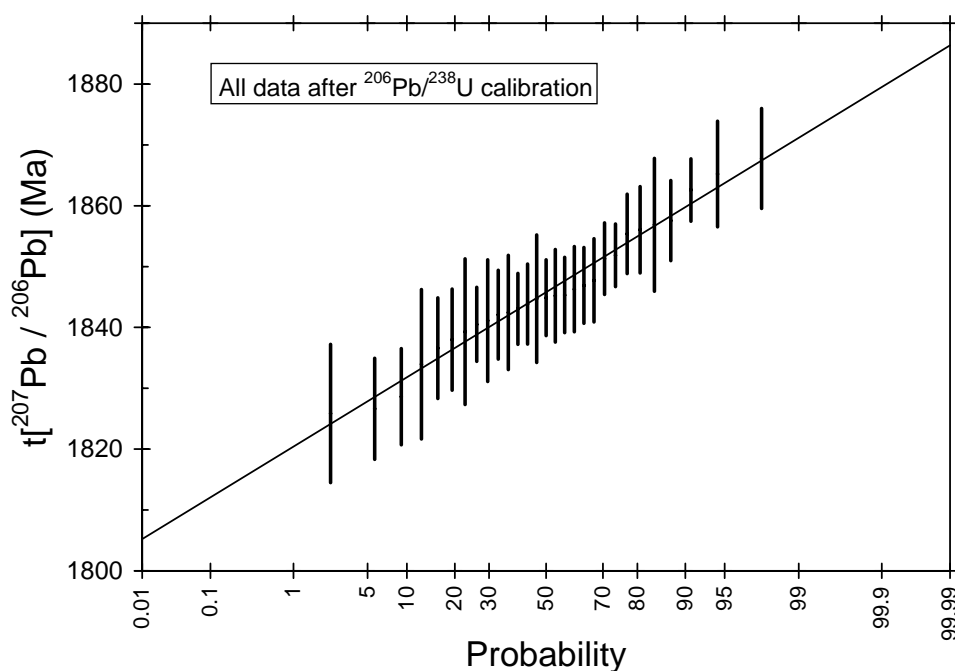


Figure 2. Probability plot of $^{207}\text{Pb}/^{206}\text{Pb}$ ages for QGNG from session Z3963i, after SQUID $^{206}\text{Pb}/^{238}\text{U}$ calibration but prior to low-side $^{207}\text{Pb}/^{206}\text{Pb}$ culling (step 5). Point precisions shown as 1s.

Table 3. Data for QGNG, for 12 analytical sessions.

Session	Date	t[207/206]	\pm 95%	MSWD	n-used	n-total
Z3739i	16/11/01	1850.8	2.6	1.03	33	34
Z3805i* ¹	10/11/01	1850.5	2.7	0.98	28	31
Z3805j	02/12/01	1849.2	2.8	1.15	32	36
Z3812i* ²	17/12/01	1852.3	3.7	1.30	20	25
Z3877i	26/02/02	1851.4	2.1	1.04	30	41
Z3878i	15/03/02	1849.9	2.5	1.07	28	38
Z3878j* ¹	22/03/02	1847.5	2.7	0.89	33	37
Z3881i	26/04/02	1847.9	2.4	1.11	35	36
Z3881j	03/05/02	1850.3	2.4	1.00	29	33
Z3922i* ²	13/05/02	1851.7	3.7	1.40	21	22
Z3963i* ²	27/05/02	1849.2	3.3	1.30	25	31
Z3963j* ^{1,3}	07/06/02	1849.8	4.3	0.76	18	19

t[207/206] is the weighted mean $^{207}\text{Pb}/^{206}\text{Pb}$ age, in Ma.

n-used is the number of analyses in the data subset averaged to give t[207/206].

n-total is the number of analyses recorded for the session.

*¹ MSWD < 1.0 before any low-side $^{207}\text{Pb}/^{206}\text{Pb}$ culling.

*² abnormally broad $^{207}\text{Pb}/^{206}\text{Pb}$ distributions; culling stopped at MSWD \geq 1.3.

*³ one-day session.

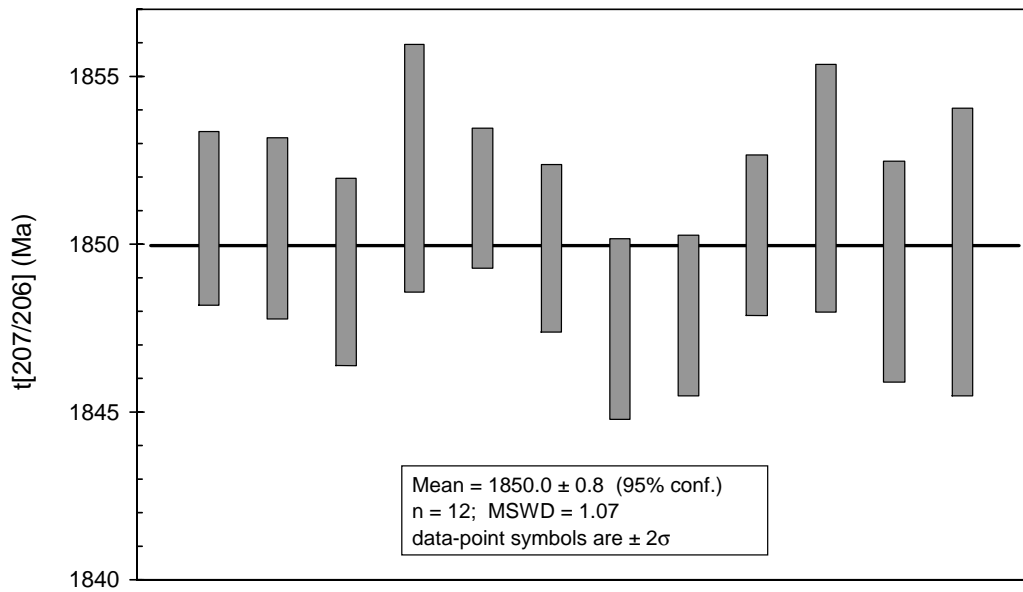


Figure 3. Data for QGNG, in sequence from Table 3. The TIMS reference age is 1851.8 \pm 0.6 Ma (2 σ ; L.P. Black, pers. comm., 2001).

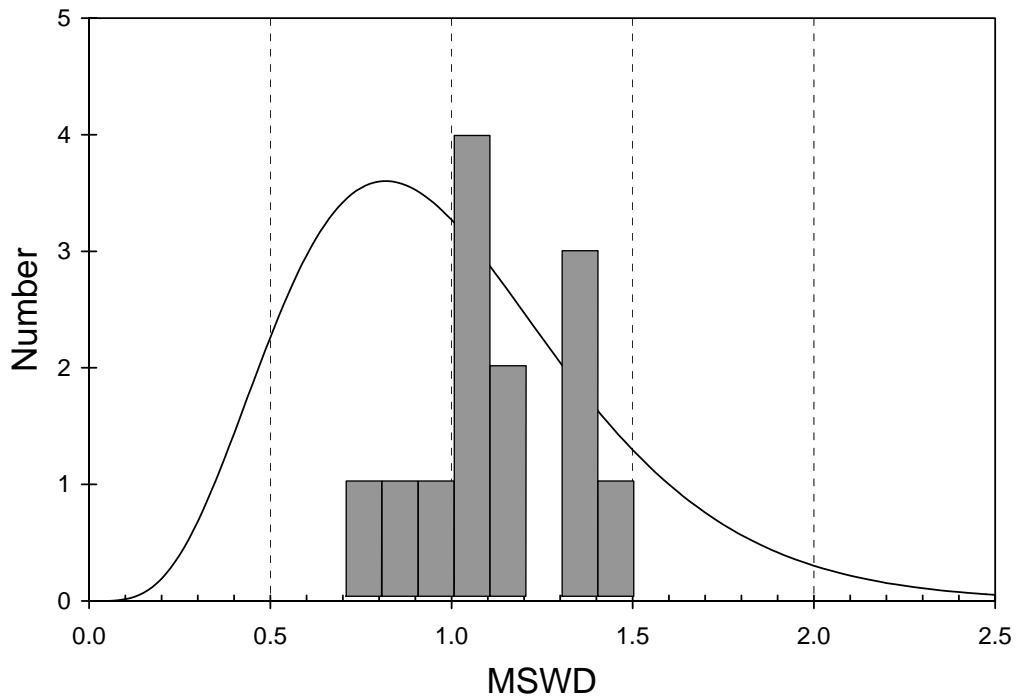


Figure 4. Histogram of MSWD values for QGNG $^{207}\text{Pb}/^{206}\text{Pb}$ data from the different analytical sessions. The curve represents the distribution function of the MSWD for the appropriate degrees of freedom for this sample population (Wendt and Carl, 1991).

Intercomparison of the TEMORA 1, CZ3 and QGNG standards

Introduction

During the first year of this project (Fletcher et al., 2001), one analytical session was dedicated to analyses of standards, to complement work being carried out on potential new standards at Geoscience Australia in Canberra, and to improve the database for Perth/Canberra interlaboratory comparisons. The materials analysed were: TEMORA 1, a new standard under consideration in Canberra (L.P. Black, pers. comm., 2001); CZ3, the current Perth standard (Nelson, 1997); and QGNG, the Geoscience Australia standard used throughout this project (L.P. Black, pers. comm., 2001).

Data acquisition

A large quantity of the TEMORA 1 and QGNG multi-grain samples, and multiple fragments of CZ3 were placed on a single mount (Z3673). Data were collected over a 2-day analytical session, using a continuous 3-sample rotation as for other analyses in this project. Since the prime interest in this comparison is the $^{206}\text{Pb}/^{238}\text{U}$ characteristics of the samples, rather than $^{207}\text{Pb}/^{206}\text{Pb}$, five data scans were recorded for each analysis instead of the usual seven. This is normal practice for Palaeozoic samples, and for detrital zircon samples, maximising the number of analyses without significantly degrading $^{206}\text{Pb}/^{238}\text{U}$ data, but at some cost to the precision of $^{207}\text{Pb}/^{206}\text{Pb}$ data.

Data processing

Data were processed the same way throughout this report, using QGNG as the $^{206}\text{Pb}/^{238}\text{U}$ reference and CZ3 as the U abundance reference. The QGNG data were duplicated in the data file to be processed as samples, to allow direct comparison of the three sample datasets after processing. The 1σ reproducibility of $^{206}\text{Pb}/^{238}\text{U}$ is similar for the three samples, so the output data distributions would be little changed if a different sample was used as the initial $^{206}\text{Pb}/^{238}\text{U}$ reference (but see comments below on CZ3).

For QGNG, the data were corrected for common Pb on the basis of measured ^{204}Pb and Broken Hill galena isotopic composition, as done for other data sets in this Record. The common Pb correction for Temora 1 and CZ3 for $^{206}\text{Pb}/^{238}\text{U}$ was based on measured $^{207}\text{Pb}/^{206}\text{Pb}$ and a Stacey and Kramers (1975) model Pb composition at the apparent age of the samples, as is common procedure for Palaeozoic samples. For all three samples, the average measured $^{204}\text{Pb}^+$ was indistinguishable from zero (95% confidence limits), so none of the data are significantly affected by choices of common Pb compositions, or of correction procedure.

One QGNG analysis (15-1) is a $>3\sigma$ (low) outlier in $^{207}\text{Pb}/^{206}\text{Pb}$ and another analysis (11-1) of relatively poor precision was $>2\sigma$ low. These two analyses are also the lowest in $^{206}\text{Pb}/^{238}\text{U}$; they have both been omitted from detailed data considerations. The remaining 45 analyses comprise a single population in $^{207}\text{Pb}/^{206}\text{Pb}$ (Fig. 5) with weighted mean age of 1851.1 ± 4.2 Ma (MSWD = 1.4).

Results

The main characteristics of the data are summarised in Table 4 and all data are listed in Tables 5–7. Probability plots of $^{207}\text{Pb}/^{206}\text{Pb}$ (Fig. 5) and $^{206}\text{Pb}/^{238}\text{U}$ (Figs. 6–8) show all three to conform to the linear trends expected of data from homogeneous samples. However, MSWD for CZ3 is sufficiently large (1.4) to suggest that this sample is less uniform than the others (ignoring the two deleted analyses for QGNG). Omitting one 3σ outlier (analysis 9-1) from CZ3 would reduce MSWD to 1.3 and change the weighted mean $^{206}\text{Pb}/^{238}\text{U}$ age from 567.4 ± 3.2 Ma to 568.0 ± 2.6 Ma.

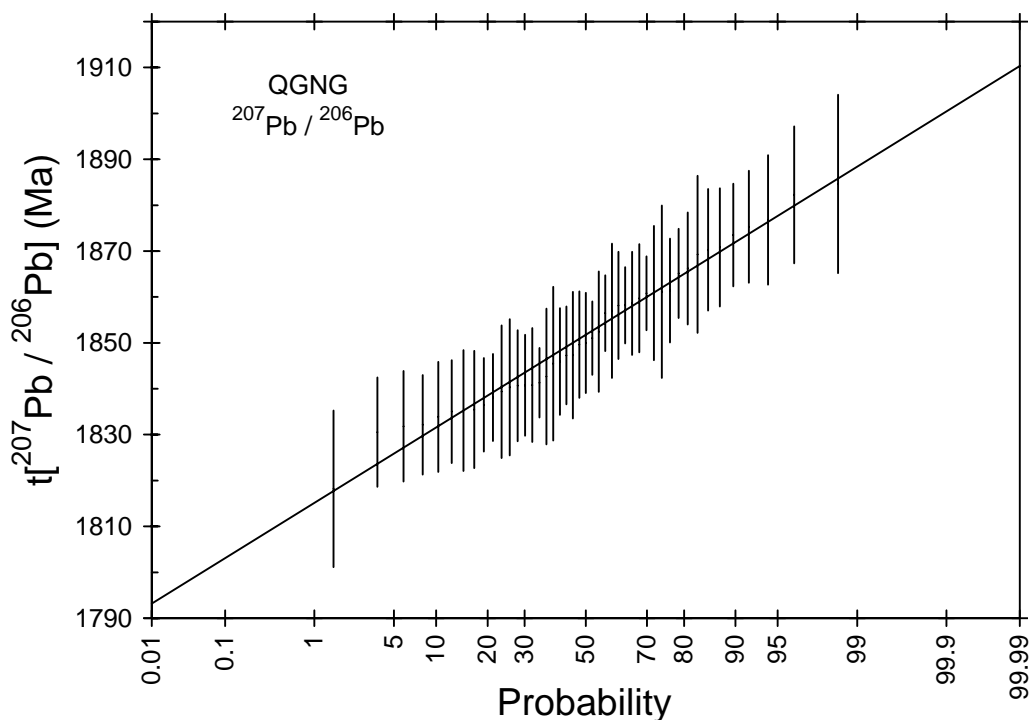


Figure 5. Probability plot of $^{207}\text{Pb}/^{206}\text{Pb}$ ages for QGNG from session Z3673i, omitting points 11-1 and 15-1. Point precisions shown as 1s.

Table 4. Summary of SHRIMP $^{206}\text{Pb}/^{238}\text{U}$ age data (ages in Ma) for standards on mount Z3673.

Sample	n	Ref. age	Meas. age	\pm	MSWD	% error	% \pm
QGNG	45	1843.1	--	9.1	--	--	0.43
Tem1	47	416.8	416.5	2.2	1.09	-0.04	0.53
CZ3	47	564.0	567.4	3.2	1.40	+0.63	0.57

All uncertainties are 95% confidence limits.

n is the number of analyses used.

% error is the percent difference between the measured age and reference age.

% \pm is the percent 95% confidence limits for the measured age.

CZ3 is inconsistent with the other two samples, in that its SHRIMP-measured age does not match the reference age (Table 4) when one of the other two is used for calibration. There appears to be three possible reasons for this:

1. The Pb^+/U^+ data vary with position on the mount surface. This is considered unlikely, particularly since the analysed fragments of each sample were more widely distributed across the mount than the distance between the sample clusters.
2. The reference age for CZ3 is wrong. While this is possible, and there are less reference TIMS data for CZ3 than the other samples, there are no other published data to support such a conclusion.
3. There is a trace element (matrix) effect causing a Pb^+/U^+ data perturbation. There is a variation of ~ 1 wt.% in the HfO_2 contents of these samples (Figure 9), and it is well known that variations of this size in other elements (notably U) can cause significant variations in secondary ion ratios (Williams, 1998).

There are insufficient grounds to choose between these possibilities at this stage.

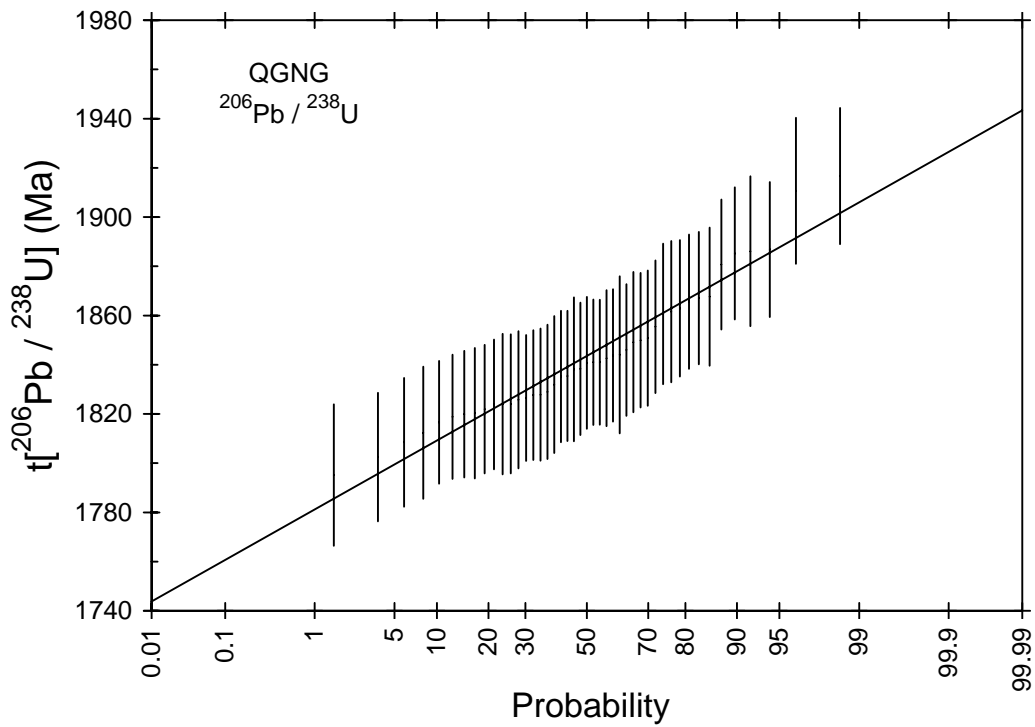


Figure 6. Probability plot of $^{206}\text{Pb}/^{238}\text{U}$ ages for QGNG from session Z3673i, omitting points 11-1 and 15-1. Point precisions shown as 1σ .

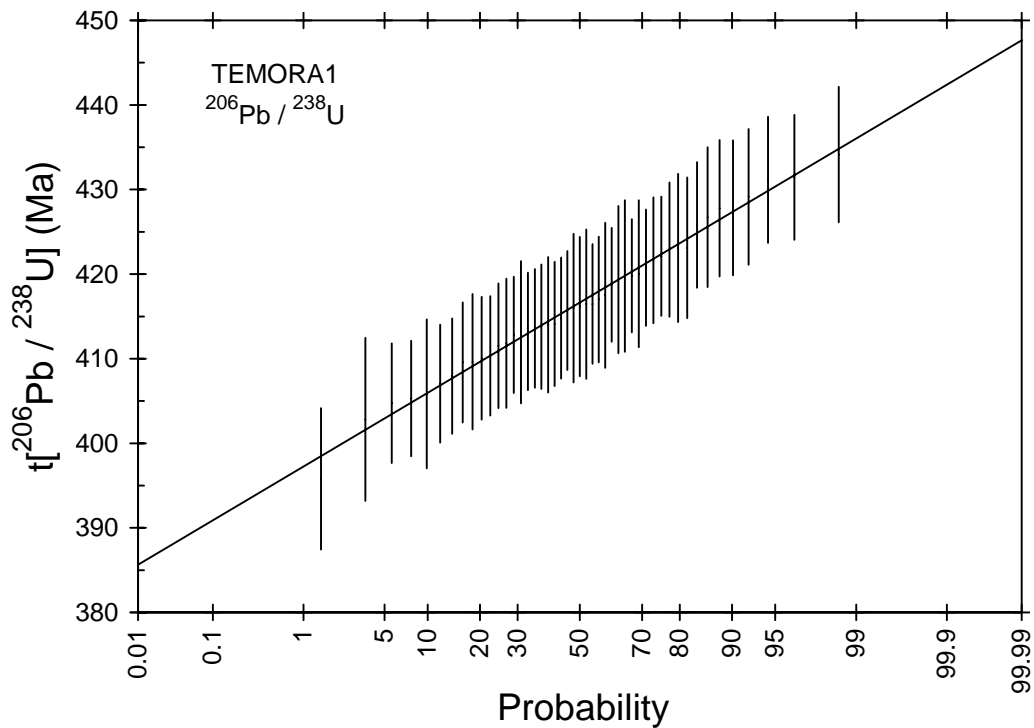


Figure 7. Probability plot of $^{206}\text{Pb}/^{238}\text{U}$ ages for TEMORA 1 from session 3673i. Point precisions shown as 1σ .

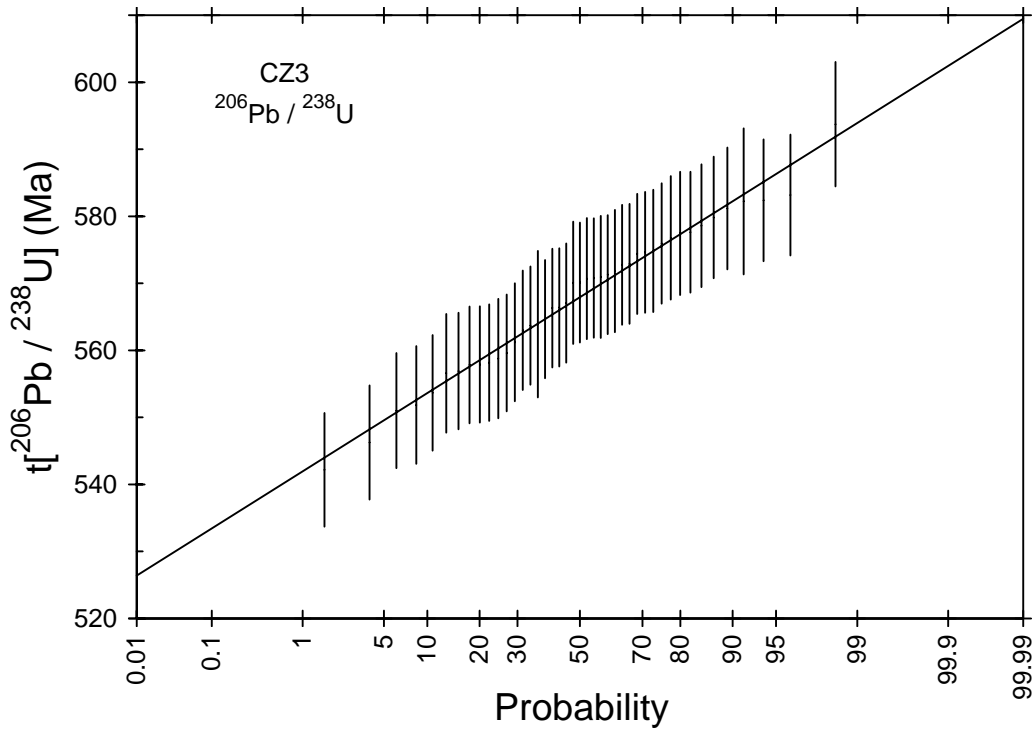


Figure 8. Probability plot of $^{206}\text{Pb}/^{238}\text{U}$ ages for CZ3 from session 3673i. Point precisions shown as 1σ .

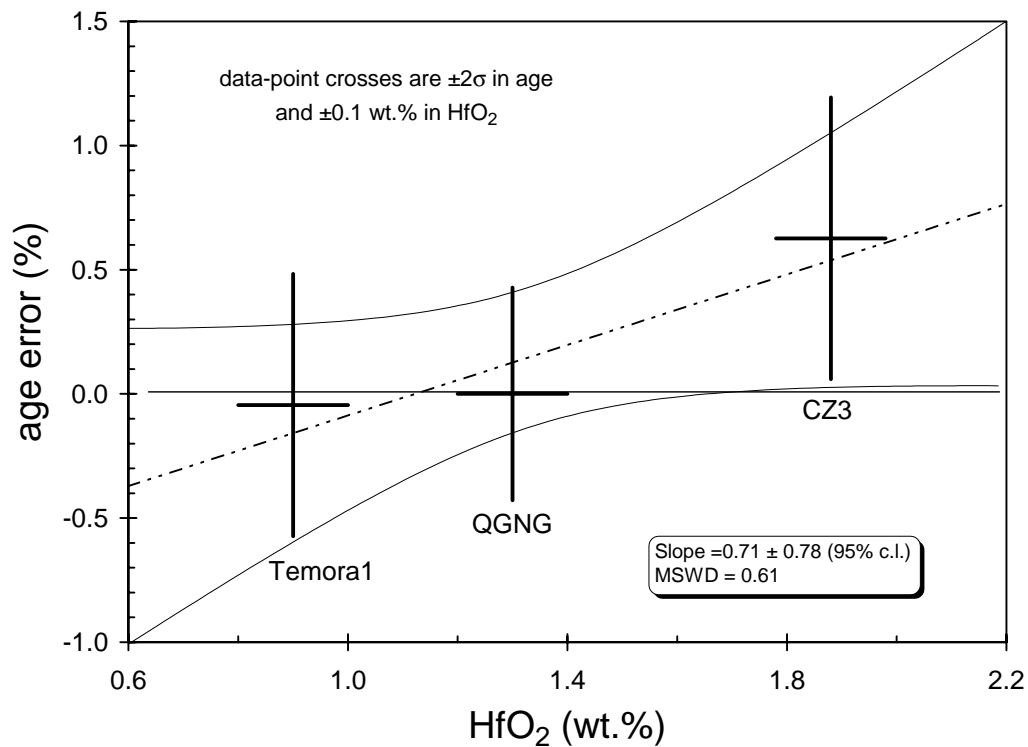


Figure 9. Correlation between apparent $^{206}\text{Pb}/^{238}\text{U}$ age defects and Hf content of the three samples (calibrated against QGNG), illustrating a possible trace-element cause for the apparent age offset in CZ3. HfO_2 data provided by L.P. Black (pers. comm., 2002).

Table 5. SHRIMP analytical results for standard QGNG on mount Z3673.

grain-spot	U (ppm)	Th (ppm)	4f206 (%)	$^{207}\text{Pb}/^{206}\text{Pb}$		$^{206}\text{Pb}/^{238}\text{U}$		$^{207}\text{Pb}/^{235}\text{U}$		$^{208}\text{Pb}/^{232}\text{Th}$	conc. (%)	$^{207}\text{Pb}/^{206}\text{Pb}$		$^{206}\text{Pb}/^{238}\text{U}$	
					\pm		\pm		\pm			Age (Ma)	\pm	Age (Ma)	\pm
Q.1-1	226	183	0.133	0.1138	0.0009	0.3305	0.0055	5.185	0.096	0.0963	99	1861	15	1841	27
Q.2-1	241	241	0.062	0.1137	0.0007	0.3335	0.0056	5.230	0.094	0.0953	100	1860	12	1855	27
Q.3-1	243	263	0.292	0.1122	0.0007	0.3226	0.0054	4.990	0.089	0.0929	98	1835	11	1802	26
Q.4-1	434	210	0.329	0.1135	0.0005	0.3260	0.0052	5.102	0.085	0.0930	98	1856	8	1819	25
Q.5-1	221	219	0.144	0.1138	0.0007	0.3311	0.0055	5.197	0.093	0.0948	99	1861	11	1844	27
Q.6-1	180	184	0.127	0.1122	0.0008	0.3281	0.0056	5.075	0.095	0.0971	100	1835	13	1829	27
Q.7-1	270	164	0.296	0.1144	0.0008	0.3294	0.0055	5.197	0.094	0.0949	98	1871	13	1835	26
Q.8-1	454	408	0.329	0.1136	0.0005	0.3262	0.0053	5.110	0.086	0.0934	98	1858	8	1820	26
Q.9-1	271	242	0.305	0.1129	0.0007	0.3238	0.0054	5.043	0.089	0.0938	98	1847	11	1808	26
Q.10-1	159	87	0.148	0.1129	0.0009	0.3274	0.0057	5.098	0.097	0.0917	99	1847	14	1826	28
Q.12-1	178	190	0.251	0.1144	0.0008	0.3309	0.0057	5.219	0.098	0.0945	99	1870	13	1843	28
Q.13-1	238	261	0.021	0.1119	0.0007	0.3293	0.0055	5.082	0.091	0.0945	100	1831	12	1835	27
Q.14-1	270	239	0.507	0.1147	0.0008	0.3266	0.0054	5.166	0.092	0.0950	97	1875	12	1822	26
Q.16-1	381	277	0.155	0.1124	0.0006	0.3276	0.0053	5.075	0.086	0.0937	99	1838	9	1827	26
Q.17-1	258	209	-0.101	0.1125	0.0007	0.3326	0.0057	5.160	0.093	0.0960	101	1841	11	1851	27
Q.18-1	235	255	0.191	0.1136	0.0007	0.3300	0.0055	5.170	0.093	0.0961	99	1858	12	1838	27
Q.19-1	122	66	0.518	0.1143	0.0011	0.3211	0.0059	5.062	0.104	0.0962	96	1869	17	1795	29
Q.20-1	147	103	-0.416	0.1127	0.0009	0.3399	0.0063	5.279	0.107	0.0969	102	1843	15	1886	30
Q.21-1	182	194	-0.034	0.1133	0.0008	0.3361	0.0058	5.248	0.098	0.0955	101	1852	13	1868	28
Q.22-1	131	81	0.111	0.1128	0.0010	0.3300	0.0060	5.133	0.105	0.0939	100	1845	17	1838	29
Q.23-1	248	243	0.120	0.1125	0.0008	0.3278	0.0055	5.086	0.092	0.0947	99	1841	12	1828	27
Q.24-1	160	154	-0.145	0.1125	0.0009	0.3346	0.0059	5.190	0.101	0.0965	101	1840	15	1861	29
Q.25-1	165	142	-0.053	0.1124	0.0009	0.3322	0.0059	5.151	0.100	0.0955	101	1839	14	1849	28
Q.26-1	197	174	-0.207	0.1122	0.0008	0.3351	0.0057	5.184	0.096	0.0951	101	1835	13	1863	28
Q.27-1	140	77	0.128	0.1138	0.0012	0.3270	0.0059	5.132	0.107	0.0949	98	1861	19	1824	29
Q.28-1	470	288	0.201	0.1138	0.0005	0.3305	0.0053	5.186	0.086	0.0947	99	1861	8	1841	25
Q.29-1	226	216	0.485	0.1141	0.0008	0.3246	0.0055	5.109	0.093	0.0930	97	1866	12	1812	27
Q.30-1	276	295	-0.178	0.1125	0.0008	0.3359	0.0056	5.213	0.094	0.0966	101	1841	12	1867	27
Q.31-1	286	262	0.021	0.1120	0.0007	0.3278	0.0054	5.062	0.089	0.0954	100	1832	11	1828	26
Q.32-1	153	137	0.535	0.1152	0.0010	0.3271	0.0058	5.193	0.102	0.0957	97	1882	15	1824	28
Q.33-1	150	114	-0.466	0.1135	0.0009	0.3450	0.0062	5.401	0.106	0.0987	103	1857	15	1911	30
Q.34-1	250	262	-0.027	0.1121	0.0007	0.3316	0.0055	5.125	0.092	0.0957	101	1873	12	1846	27
Q.35-1	265	274	0.429	0.1146	0.0007	0.3263	0.0054	5.155	0.092	0.0955	97	1834	11	1820	26
Q.36-1	596	392	0.229	0.1126	0.0005	0.3255	0.0051	5.052	0.082	0.0947	99	1841	8	1817	25
Q.37-1	178	130	0.062	0.1111	0.0010	0.3287	0.0057	5.037	0.100	0.0914	101	1818	17	1832	28
Q.38-1	325	252	-0.377	0.1123	0.0006	0.3397	0.0056	5.258	0.091	0.0959	103	1836	10	1885	27
Q.38-2	509	456	0.124	0.1132	0.0005	0.3305	0.0052	5.158	0.085	0.0947	99	1851	8	1841	25
Q.39-1	252	245	-0.259	0.1137	0.0007	0.3400	0.0057	5.328	0.095	0.0976	102	1859	11	1887	27
Q.39-2	281	279	0.213	0.1131	0.0007	0.3270	0.0054	5.099	0.091	0.0943	99	1850	12	1824	26
Q.40-1	158	134	0.130	0.1148	0.0009	0.3348	0.0059	5.299	0.103	0.0952	99	1877	14	1862	29
Q.41-1	227	230	-0.150	0.1120	0.0007	0.3324	0.0056	5.132	0.094	0.0952	101	1832	12	1850	27
Q.42-1	266	277	-0.583	0.1131	0.0007	0.3462	0.0058	5.400	0.096	0.0992	104	1850	11	1917	28
Q.42-2	240	254	-0.187	0.1129	0.0007	0.3356	0.0056	5.223	0.094	0.0963	101	1846	12	1866	27
Q.43-1	83	47	0.118	0.1153	0.0012	0.3312	0.0066	5.265	0.119	0.0983	98	1885	19	1844	32
Q.44-1	327	327	-0.099	0.1141	0.0006	0.3388	0.0055	5.328	0.091	0.0975	101	1865	10	1881	26
Young outliers															
Q.11-1	123	64	0.471	0.1098	0.0013	0.3151	0.0057	4.771	0.104	0.0879	98	1796	22	1766	28
Q.15-1	223	233	0.101	0.1094	0.0007	0.3173	0.0053	4.786	0.086	0.0904	99	1789	12	1777	26

Data are at 1σ precision. All Pb data are common-Pb corrected (see text for details).

Analysis date: 11/06/01; session Z3673i.

Table 6. SHRIMP analytical results for standard TEMORA 1 on mount Z3673.

grain-spot	U (ppm)	Th (ppm)	4f206 (%)	$^{207}\text{Pb}/^{206}\text{Pb}$		$^{206}\text{Pb}/^{238}\text{U}$		$^{207}\text{Pb}/^{235}\text{U}$		$^{208}\text{Pb}/^{232}\text{Th}$		$^{207}\text{Pb}/^{206}\text{Pb}$ Age (Ma)	
					\pm		\pm		\pm		\pm		\pm
TEM.1-1	99	31	-0.124	0.0583	0.0016	0.0670	0.0013	0.538	0.018	0.0220	416	8	
TEM.2-1	182	106	-0.007	0.0560	0.0012	0.0664	0.0012	0.513	0.014	0.0207	414	7	
TEM.3-1	238	129	-0.066	0.0536	0.0024	0.0661	0.0011	0.488	0.023	0.0205	413	7	
TEM.4-1	259	69	0.434	0.0543	0.0020	0.0648	0.0011	0.485	0.020	0.0182	405	7	
TEM.5-1	65	25	0.224	0.0381	0.0070	0.0632	0.0016	0.332	0.062	0.0115	403	10	
TEM.6-1	295	175	0.156	0.0564	0.0010	0.0654	0.0011	0.509	0.012	0.0208	408	7	
TEM.7-1	88	30	-0.244	0.0443	0.0026	0.0653	0.0014	0.399	0.025	0.0154	413	8	
TEM.8-1	192	78	0.070	0.0578	0.0012	0.0665	0.0012	0.530	0.015	0.0215	414	7	
TEM.9-1	173	93	0.007	0.0520	0.0028	0.0657	0.0012	0.471	0.027	0.0198	412	7	
TEM.10-1	181	116	-0.035	0.0504	0.0025	0.0653	0.0012	0.454	0.024	0.0189	410	7	
TEM.11-1	241	56	0.198	0.0549	0.0012	0.0667	0.0012	0.505	0.014	0.0193	416	7	
TEM.12-1	228	130	0.369	0.0546	0.0017	0.0652	0.0011	0.491	0.018	0.0197	407	7	
TEM.13-1	228	104	0.101	0.0564	0.0011	0.0693	0.0012	0.539	0.014	0.0204	431	7	
TEM.14-1	212	106	0.153	0.0572	0.0015	0.0658	0.0012	0.519	0.016	0.0211	410	7	
TEM.15-1	219	121	0.152	0.0554	0.0012	0.0665	0.0012	0.508	0.014	0.0211	415	7	
TEM.16-1	295	158	0.164	0.0557	0.0013	0.0662	0.0011	0.508	0.014	0.0203	413	7	
TEM.17-1	216	58	0.268	0.0578	0.0012	0.0685	0.0012	0.545	0.015	0.0220	426	7	
TEM.18-1	436	107	0.027	0.0559	0.0009	0.0672	0.0011	0.518	0.012	0.0205	419	7	
TEM.19-1	106	29	0.108	0.0537	0.0024	0.0677	0.0014	0.501	0.025	0.0203	423	8	
TEM.20-1	474	278	-0.045	0.0553	0.0008	0.0673	0.0011	0.513	0.011	0.0205	420	7	
TEM.21-1	113	50	-0.138	0.0630	0.0015	0.0663	0.0013	0.576	0.018	0.0230	410	8	
TEM.22-1	127	66	-0.017	0.0601	0.0015	0.0688	0.0014	0.570	0.018	0.0226	427	8	
TEM.23-1	91	30	-0.096	0.0582	0.0020	0.0681	0.0014	0.546	0.022	0.0239	423	9	
TEM.24-1	197	74	0.085	0.0530	0.0018	0.0676	0.0013	0.494	0.020	0.0200	423	8	
TEM.25-1	197	114	0.189	0.0609	0.0024	0.0673	0.0012	0.565	0.025	0.0223	417	7	
TEM.26-1	94	26	0.255	0.0515	0.0037	0.0666	0.0014	0.473	0.036	0.0160	418	9	
TEM.27-1	218	49	0.310	0.0592	0.0012	0.0652	0.0012	0.532	0.014	0.0214	405	7	
TEM.28-1	84	41	0.159	0.0645	0.0055	0.0674	0.0015	0.600	0.053	0.0259	416	9	
TEM.29-1	266	98	0.172	0.0510	0.0021	0.0659	0.0011	0.464	0.021	0.0185	414	7	
TEM.30-1	207	115	-0.104	0.0494	0.0023	0.0671	0.0012	0.457	0.022	0.0204	422	7	
TEM.31-1	139	39	-0.045	0.0527	0.0016	0.0686	0.0013	0.499	0.018	0.0198	429	8	
TEM.32-1	248	129	-0.188	0.0518	0.0016	0.0689	0.0012	0.492	0.017	0.0209	431	7	
TEM.33-1	100	52	0.095	0.0474	0.0033	0.0644	0.0014	0.421	0.031	0.0182	406	9	
TEM.33-2	83	28	-0.119	0.0517	0.0025	0.0670	0.0015	0.477	0.025	0.0212	420	9	
TEM.34-1	383	154	-0.008	0.0545	0.0013	0.0674	0.0011	0.506	0.015	0.0207	421	7	
TEM.35-1	156	93	-0.134	0.0532	0.0022	0.0695	0.0013	0.510	0.023	0.0209	434	8	
TEM.36-1	150	62	0.187	0.0583	0.0014	0.0662	0.0012	0.532	0.016	0.0211	412	8	
TEM.37-1	317	187	-0.101	0.0544	0.0009	0.0676	0.0011	0.507	0.012	0.0202	422	7	
TEM.38-1	69	23	0.232	0.0468	0.0024	0.0627	0.0013	0.404	0.023	0.0169	396	8	
TEM.39-1	82	27	-0.167	0.0654	0.0056	0.0676	0.0015	0.610	0.054	0.0265	416	9	
TEM.40-1	92	48	0.290	0.0500	0.0031	0.0668	0.0014	0.461	0.031	0.0184	419	9	
TEM.40-2	94	49	-0.122	0.0511	0.0021	0.0670	0.0014	0.472	0.022	0.0201	420	9	
TEM.41-1	250	150	0.136	0.0481	0.0031	0.0652	0.0012	0.433	0.029	0.0178	410	7	
TEM.42-1	124	63	-0.016	0.0522	0.0018	0.0661	0.0013	0.475	0.019	0.0190	414	8	
TEM.43-1	283	153	-0.224	0.0499	0.0018	0.0662	0.0011	0.455	0.018	0.0196	416	7	
TEM.44-1	134	74	0.105	0.0562	0.0014	0.0687	0.0013	0.532	0.017	0.0220	428	8	
TEM.45-1	117	64	-0.095	0.0574	0.0020	0.0688	0.0013	0.544	0.022	0.0225	428	8	

Data are at 1 σ precision. All Pb data are common-Pb corrected (see text for details).

Analysis date: 11/06/01; session Z3673i.

Table 7. SHRIMP analytical results for standard CZ3 on mount Z3673.

grain-spot	U (ppm)	Th (ppm)	4f206 (%)	^{207}Pb		^{206}Pb		^{207}Pb		^{208}Pb		$^{207}\text{Pb}/^{206}\text{Pb}$	
				^{206}Pb	\pm	^{238}U	\pm	^{235}U	\pm	^{232}Th	Age (Ma)	\pm	
CZ3.1-1	537	28	-0.024	0.0589	0.0007	0.0899	0.0015	0.731	0.014	0.0287	555	9	
CZ3.2-1	556	29	0.012	0.0595	0.0006	0.0920	0.0015	0.754	0.014	0.0309	567	9	
CZ3.3-1	548	29	0.107	0.0603	0.0007	0.0930	0.0015	0.773	0.015	0.0317	573	9	
CZ3.4-1	556	29	0.105	0.0602	0.0006	0.0933	0.0015	0.774	0.015	0.0291	574	9	
CZ3.5-1	556	30	-0.117	0.0581	0.0006	0.0925	0.0015	0.741	0.015	0.0283	571	9	
CZ3.6-1	531	28	-0.077	0.0581	0.0007	0.0901	0.0015	0.722	0.015	0.0269	557	9	
CZ3.7-1	543	28	-0.098	0.0575	0.0006	0.0913	0.0018	0.724	0.016	0.0247	564	11	
CZ3.8-1	569	30	0.077	0.0592	0.0008	0.0894	0.0015	0.730	0.016	0.0273	552	9	
CZ3.9-1	559	29	0.035	0.0587	0.0006	0.0878	0.0014	0.710	0.014	0.0285	542	8	
CZ3.10-1	558	29	0.059	0.0602	0.0006	0.0906	0.0014	0.753	0.014	0.0317	558	9	
CZ3.11-1	572	30	-0.077	0.0589	0.0006	0.0926	0.0015	0.753	0.014	0.0287	571	9	
CZ3.12-1	522	26	-0.259	0.0556	0.0008	0.0929	0.0015	0.711	0.015	0.0218	575	9	
CZ3.13-1	550	29	0.186	0.0614	0.0008	0.0915	0.0015	0.775	0.016	0.0321	563	9	
CZ3.13-1	553	29	0.074	0.0593	0.0008	0.0907	0.0014	0.741	0.015	0.0286	560	9	
CZ3.15-1	540	28	-0.335	0.0569	0.0006	0.0936	0.0015	0.734	0.014	0.0302	579	9	
CZ3.16-1	569	30	0.104	0.0590	0.0007	0.0885	0.0014	0.720	0.015	0.0257	546	9	
CZ3.17-1	534	28	-0.065	0.0573	0.0009	0.0916	0.0015	0.724	0.017	0.0220	566	9	
CZ3.18-1	560	30	0.091	0.0596	0.0006	0.0898	0.0014	0.738	0.014	0.0292	554	9	
CZ3.19-1	541	28	0.019	0.0587	0.0008	0.0892	0.0014	0.722	0.015	0.0291	551	9	
CZ3.20-1	572	30	0.034	0.0589	0.0008	0.0904	0.0014	0.735	0.015	0.0297	558	9	
CZ3.21-1	539	28	0.049	0.0591	0.0007	0.0937	0.0015	0.763	0.015	0.0277	578	9	
CZ3.22-1	529	28	0.043	0.0602	0.0006	0.0946	0.0018	0.785	0.017	0.0295	582	11	
CZ3.23-1	551	29	-0.088	0.0577	0.0007	0.0912	0.0015	0.726	0.015	0.0262	564	9	
CZ3.24-1	564	30	0.044	0.0593	0.0011	0.0928	0.0015	0.758	0.019	0.0290	572	9	
CZ3.25-1	571	30	0.001	0.0590	0.0006	0.0918	0.0015	0.747	0.014	0.0276	566	9	
CZ3.26-1	528	27	-0.028	0.0603	0.0013	0.0921	0.0015	0.766	0.020	0.0356	567	9	
CZ3.27-1	540	28	0.190	0.0593	0.0007	0.0903	0.0014	0.738	0.014	0.0258	557	9	
CZ3.28-1	557	29	0.196	0.0602	0.0011	0.0911	0.0015	0.756	0.019	0.0268	561	9	
CZ3.29-1	550	29	-0.089	0.0588	0.0006	0.0934	0.0015	0.757	0.014	0.0300	576	9	
CZ3.29-2	552	29	-0.076	0.0581	0.0006	0.0925	0.0015	0.741	0.015	0.0275	571	9	
CZ3.29-3	562	30	-0.130	0.0570	0.0009	0.0943	0.0015	0.741	0.016	0.0209	582	9	
CZ3.29-4	548	28	-0.167	0.0590	0.0009	0.0941	0.0015	0.766	0.017	0.0339	580	9	
CZ3.30-1	541	29	0.194	0.0612	0.0010	0.0927	0.0015	0.782	0.018	0.0315	570	9	
CZ3.31-1	533	28	-0.117	0.0578	0.0010	0.0931	0.0015	0.742	0.018	0.0273	575	9	
CZ3.31-2	558	30	-0.184	0.0582	0.0011	0.0935	0.0015	0.750	0.018	0.0302	577	9	
CZ3.32-1	555	29	0.057	0.0598	0.0006	0.0927	0.0015	0.764	0.015	0.0310	571	9	
CZ3.32-2	556	29	0.080	0.0590	0.0008	0.0906	0.0015	0.737	0.015	0.0258	559	9	
CZ3.33-1	544	29	-0.004	0.0598	0.0009	0.0925	0.0015	0.763	0.016	0.0315	570	9	
CZ3.33-2	550	29	0.089	0.0595	0.0006	0.0905	0.0014	0.742	0.014	0.0291	558	9	
CZ3.33-3	555	29	0.077	0.0592	0.0007	0.0943	0.0015	0.770	0.016	0.0283	581	9	
CZ3.34-1	543	29	-0.063	0.0582	0.0007	0.0915	0.0015	0.734	0.015	0.0276	565	9	
CZ3.24-2	540	28	0.105	0.0583	0.0009	0.0928	0.0015	0.746	0.017	0.0261	573	9	
CZ3.17-2	566	30	-0.034	0.0591	0.0006	0.0932	0.0015	0.760	0.015	0.0292	574	9	
CZ3.17-3	558	29	-0.027	0.0575	0.0007	0.0935	0.0015	0.741	0.015	0.0231	577	9	
CZ3.35-1	547	28	-0.276	0.0575	0.0006	0.0962	0.0015	0.763	0.015	0.0315	594	9	
CZ3.35-3	536	28	0.067	0.0591	0.0007	0.0929	0.0015	0.757	0.015	0.0263	573	9	
CZ3.35-3	545	29	-0.232	0.0568	0.0008	0.0944	0.0015	0.740	0.016	0.0246	583	9	

Data are at 1σ precision. All Pb data are common-Pb corrected (see text for details).

Analysis date: 11/06/01; session Z3673i.

2001967014: biotite granitic gneiss, Corriding Rock

1:250,000 sheet: Kalgoorlie (SH5109)

1:100,000 sheet: Davyhurst (3037)

MGA: 273443 mE 6631389 mN

Location: The sample was taken from the north-east side of a large outcrop located about 100 m north of Corriding Rock and approximately 500 m north of Emu Rock Dam.

Description: The sample is from a grey, banded, seriate to variably K-feldspar porphyritic, medium-grained biotite quartzofeldspathic gneiss. The gneiss is cut by several generations of variably deformed pegmatite and biotite granite dykes. The banded gneiss displays a strong sub-vertical, SSE-striking gneissosity. It contains common biotite-rich schlieren and thin (<50 cm), strongly-deformed, biotite-rich disrupted dykes and xenoliths.

The sample is characterised by a granular to granoblastic texture. Principal minerals are quartz (35–40%), K-feldspar (30–35%), plagioclase (25–30%) and biotite (5–6%), with K-feldspar > plagioclase. K-feldspar is subhedral to anhedral, with larger grains commonly poikilitic, and displays well-developed tartan twinning, and common minor perthite. Plagioclase forms subhedral grains which are very weakly zoned. Twinning is common and minor myrmekite is present. Plagioclase is characterised by very minor to locally moderate replacement by white mica and rare epidote/clinozoisite and carbonate. Quartz is anhedral, moderately to locally strongly undulose, with common minor to moderate sub-grain development. Biotite forms anhedral to ragged, light yellow to medium-dark red-brown flakes that are locally partly replaced by chlorite, rutile and minor epidote/clinozoisite and/or white mica. Accessory phases include zircon, apatite, anhedral opaque minerals, and interstitial white mica.

Mount, pop: Z3805D

Description of zircons

Zircon from this sample generally occurs as euhedral elongate (aspect ratios of 2:1 to 3:1) grains with well-defined crystal faces, but some equant grains and fragments are also present. The grains range from about 80 μm to 200 μm in length. They are predominantly colourless to pale grey-brown and slightly turbid, but some grains are clear or dark grey-brown. Small rounded and/or rod-like inclusions are present in many grains. Continuous core to rim euhedral concentric zoning is common in many grains in CL (Fig. 10), but areas of disrupted zoning and dark patches are present, indicative of recrystallisation and metamictisation. Grains with distinct cores and rim overgrowths are present, but rare.

Concurrent standard data

After omitting two outliers identified by SQUID, the apparent calibration slope for QGNG is 2.26 ($n = 34$). The concurrent sample data also suggest a slope >2, and a value of 2.2 was used for the calibration exponent. This gives a Pb/U calibration with 1σ scatter of 1.08% and MSWD = 4.5. Omitting the two Pb/U calibration outliers and one 3σ (low) outlier, and culling one other low point, leaves 32 points with a weighted mean $^{207}\text{Pb}/^{206}\text{Pb}$ age of 1849.2 ± 2.8 Ma (MSWD = 1.15).

Element abundance calibration was based on CZ3 ($n = 2$).

Sample data

A total of 36 analyses were recorded from 35 grains (Table 8; Fig. 11). Two analyses (13-1, 18-2) are >5% discordant and are not used for age interpretation. The concordant data fall into two distinct groups on the basis of U content, those >500 ppm U and those <250 ppm. All 16 low-U data fall in a single cluster (Fig. 12) yielding a weighted mean $^{207}\text{Pb}/^{206}\text{Pb}$ age of 2686.8 ± 4.4 Ma

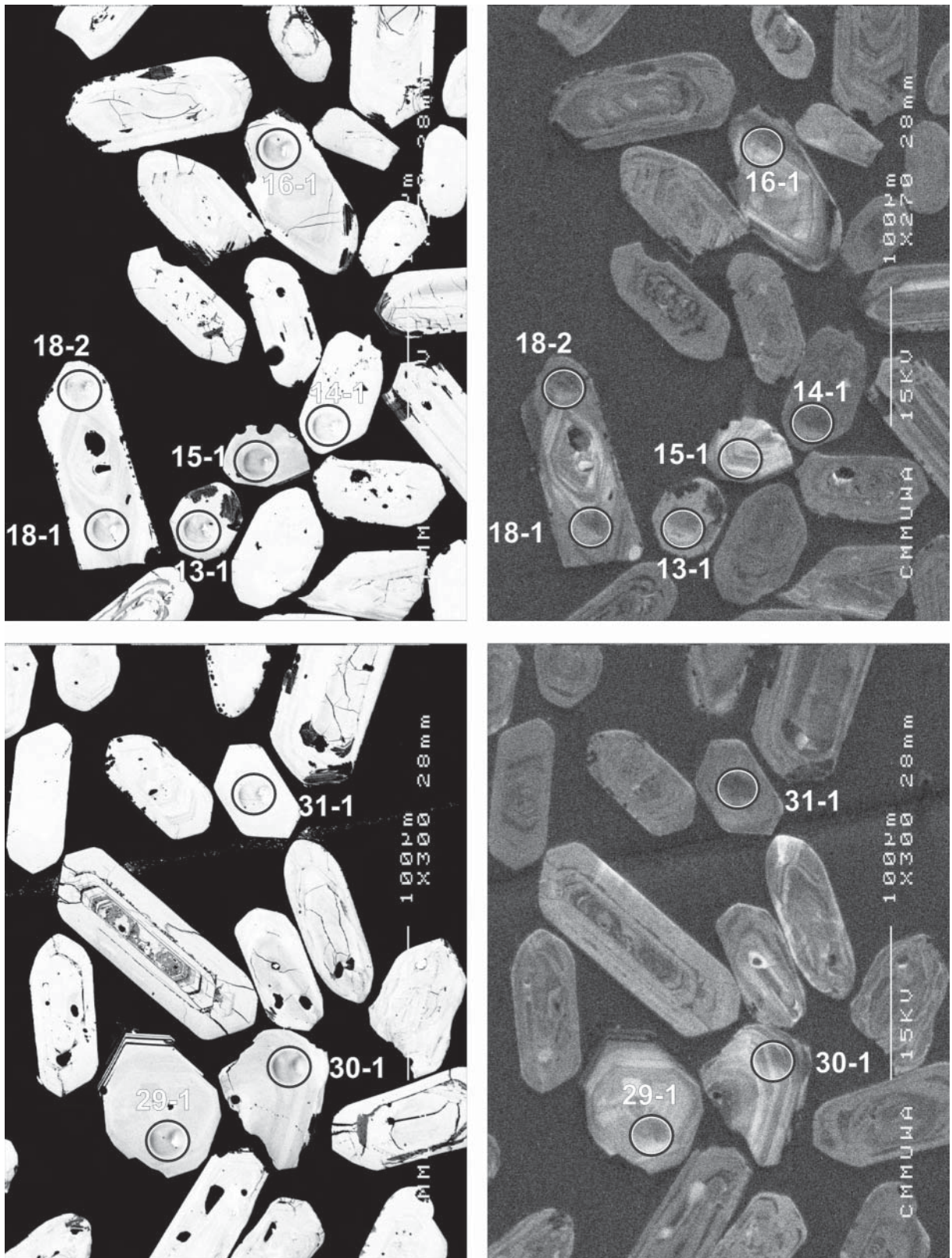


Figure 10. Representative SEM images (BSE on left, CL on right) for sample 2001967014: biotite granitic gneiss, Corriding Rock. SHRIMP analysis spots are labelled. Remnant pits from the ion microprobe analyses are faintly visible in some grains. Scale bar is 100 μ m.

(MSWD = 1.4). Omitting two 2σ outliers (2-1, 36-1) would leave a slightly over-restricted group (MSWD = 0.79) with an age of 2686.4 ± 3.7 Ma.

The high-U data scatter and include both older and younger dates, probably reflecting zircon inheritance and early Pb-loss, respectively (Fig. 11). Within these data there is a possible subgroup of eight analyses (Fig. 13) that gives a poorly constrained age of 2701.4 ± 4.3 Ma (MSWD = 3.8).

Geochronological interpretation

The 2687 ± 5 Ma date from the low-U group most likely represents the age of the granitic protolith of the gneiss, which contains inherited high-U grains. The low-U zircons could be either grains that crystallised from the granite or inherited grains with reset U-Pb. Alternatively, the high-U grains might date the crystallisation of the granite (~ 2700 Ma), in which case 2687 Ma is the probable time of formation of the gneiss, but this can only be true if the granite also included older high-U inherited grains (e.g., 7-1, 17-1, 23-1).

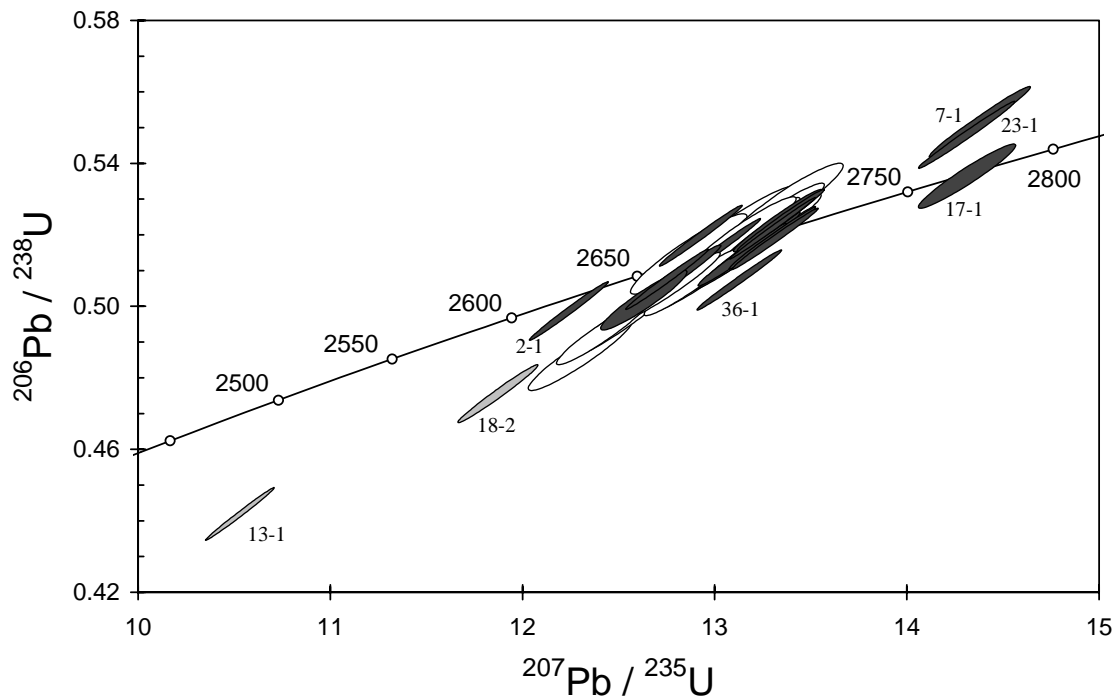


Figure 11. Concordia plot for zircon data from 2001967014: biotite granitic gneiss, Corriding Rock. White filled symbols are from low-U analyses and are used to define an age in the sample; high-U analyses are dark grey; discordant analyses are light grey.

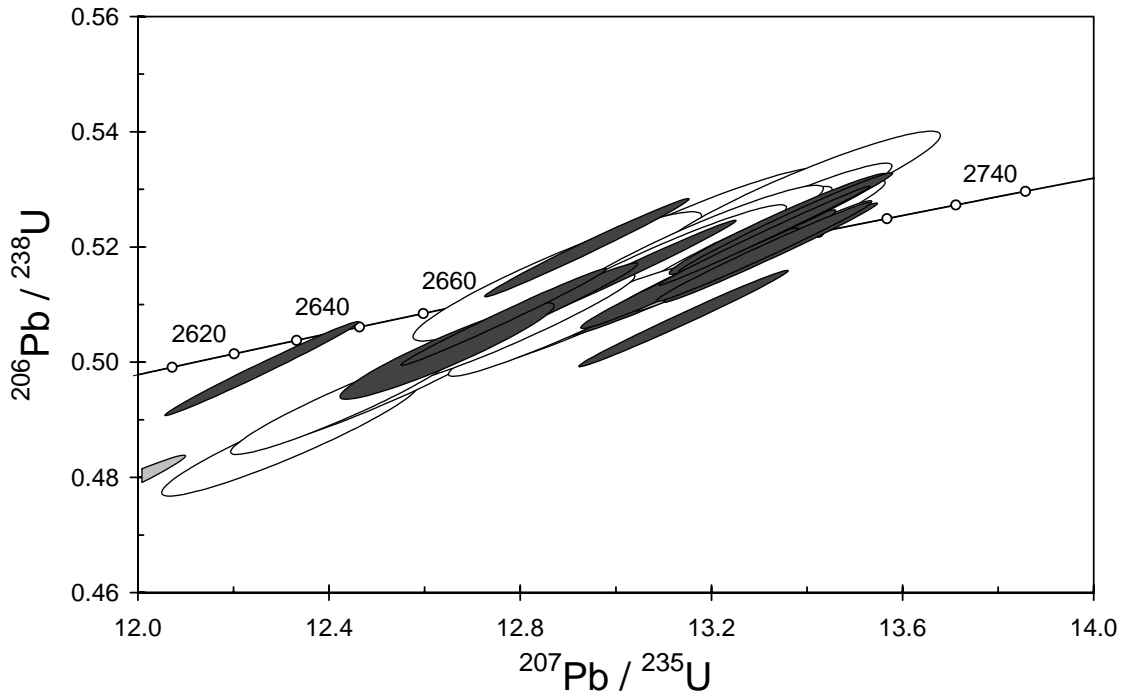


Figure 12. Enlargement of main group of zircon analyses for sample 2001967014: biotite granitic gneiss, Corriding Rock. Symbol shading as in Figure 11.

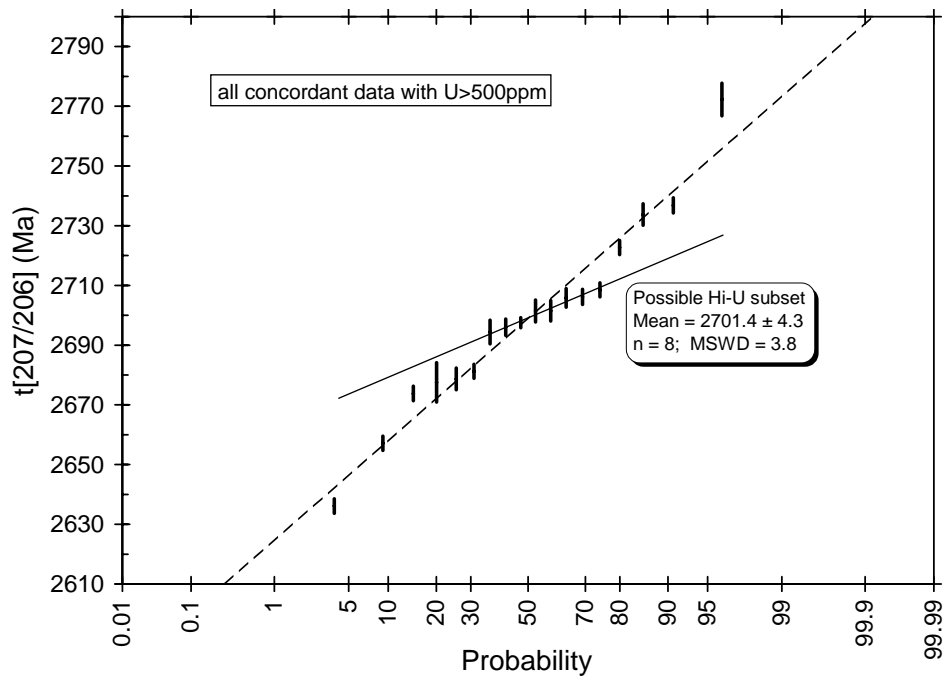


Figure 13. Probability plot for data from high-U zircons in 2001967014: biotite granitic gneiss, Corriding Rock.

Table 8. SHRIMP analytical results for zircon from sample 2001967014: biotite granitic gneiss, Corriding Rock.

grain-spot	U (ppm)	Th (ppm)	4f206 (%)	$^{207}\text{Pb}/^{206}\text{Pb}$		$^{206}\text{Pb}/^{238}\text{U}$		$^{207}\text{Pb}/^{235}\text{U}$		$^{208}\text{Pb}/^{232}\text{Th}$	conc. (%)	$^{207}\text{Pb}/^{206}\text{Pb}$	
					\pm		\pm		\pm			Age (Ma)	\pm
Low-U group													
3-1	88	60	0.111	0.1833	0.0009	0.508	0.007	12.83	0.18	0.139	99	2683	8
15-1	92	63	0.119	0.1823	0.0010	0.520	0.009	13.08	0.23	0.140	101	2673	9
16-1	116	73	0.017	0.1831	0.0008	0.495	0.007	12.50	0.17	0.134	97	2682	7
18-1	185	207	0.016	0.1834	0.0006	0.506	0.006	12.79	0.16	0.138	98	2684	5
19-1	80	60	0.094	0.1836	0.0009	0.486	0.007	12.31	0.18	0.130	95	2686	8
20-1	111	87	0.007	0.1835	0.0007	0.517	0.007	13.08	0.18	0.143	100	2685	7
21-1	140	97	-0.036	0.1849	0.0006	0.522	0.007	13.30	0.17	0.145	100	2697	6
24-1	209	148	0.593	0.1829	0.0007	0.493	0.006	12.42	0.16	0.153	96	2680	7
26-1	183	136	-0.013	0.1846	0.0007	0.507	0.006	12.90	0.17	0.141	98	2694	6
29-1	78	89	0.090	0.1833	0.0010	0.529	0.007	13.38	0.20	0.142	102	2683	9
30-1	96	83	-0.039	0.1837	0.0008	0.520	0.007	13.17	0.18	0.142	100	2686	7
33-1	113	76	-0.091	0.1833	0.0008	0.521	0.007	13.16	0.18	0.143	101	2683	7
34-1	99	70	0.019	0.1840	0.0008	0.524	0.007	13.30	0.18	0.148	101	2689	7
35-1	71	52	0.129	0.1843	0.0010	0.508	0.007	12.92	0.19	0.138	98	2692	9
Low-U 2 σ age out liers													
2-1	60	46	0.166	0.1814	0.0010	0.515	0.007	12.87	0.20	0.140	100	2665	9
36-1	137	121	0.032	0.1852	0.0006	0.514	0.006	13.12	0.17	0.140	99	2700	6
Possible high-U subgroup													
1-1	543	274	0.551	0.1854	0.0004	0.517	0.006	13.21	0.16	0.163	99	2701	4
4-1	1342	701	0.282	0.1848	0.0003	0.524	0.006	13.35	0.15	0.144	101	2696	3
8-1	721	198	0.196	0.1859	0.0003	0.518	0.006	13.28	0.16	0.149	100	2706	3
10-1	1299	317	0.288	0.1854	0.0004	0.515	0.006	13.15	0.15	0.142	99	2702	3
12-1	886	95	0.144	0.1846	0.0004	0.524	0.006	13.34	0.15	0.161	101	2694	4
14-1	1697	382	0.004	0.1849	0.0002	0.522	0.006	13.31	0.15	0.140	100	2698	2
25-1	849	70	0.023	0.1862	0.0003	0.519	0.006	13.32	0.15	0.140	99	2709	2
31-1	825	182	0.120	0.1859	0.0003	0.519	0.006	13.31	0.15	0.135	100	2706	3
Other high-U													
5-1	868	289	0.610	0.1827	0.0007	0.502	0.006	12.64	0.15	0.163	98	2678	7
6-1	1783	991	0.018	0.1782	0.0003	0.499	0.005	12.25	0.14	0.133	99	2636	2
7-1	1596	172	0.252	0.1890	0.0004	0.552	0.007	14.38	0.17	0.283	104	2734	4
9-1	2229	202	0.425	0.1805	0.0003	0.520	0.006	12.94	0.14	0.161	102	2657	2
11-1	1331	309	0.453	0.1823	0.0003	0.508	0.006	12.76	0.14	0.142	99	2674	2
17-1	1370	757	0.010	0.1935	0.0006	0.537	0.006	14.32	0.17	0.141	100	2772	5
23-1	1129	774	0.016	0.1894	0.0003	0.548	0.006	14.32	0.16	0.130	103	2737	3
27-1	862	638	0.022	0.1831	0.0003	0.515	0.006	13.01	0.16	0.129	100	2681	2
28-1	1183	85	0.106	0.1878	0.0003	0.507	0.006	13.14	0.15	0.180	97	2723	2
32-1	561	352	0.013	0.1828	0.0004	0.508	0.006	12.82	0.15	0.143	99	2679	4
>5% discordant													
13-1	1730	362	0.229	0.1732	0.0002	0.442	0.005	10.54	0.12	0.117	91	2588	2
18-2	549	398	0.019	0.1813	0.0004	0.475	0.005	11.88	0.14	0.132	94	2665	3

Data are at 1 σ precision. All Pb data are common-Pb corrected (based on ^{204}Pb and Broken Hill Pb composition). Analysis date: 2/12/01; session Z3805j.

2001967017A: Bali Monzogranite

1:250,000 sheet: Kalgoorlie (SH5109)

1:100,000 sheet: Kalgoorlie (3136)

MGA: 311413mE 6605289mN

Location: The sample was collected from a large flat outcrop located about 200 m east of a track and about 400 m southeast of Camel Dam.

Description: This strongly deformed, grey, K-feldspar-megacrystic, medium-grained biotite monzogranite is intruded, in 'net-vein' style, by several generations of pink, fine-grained biotite monzogranite dykes and aplites, and minor pegmatites and late quartz veins. It also contains minor biotite-rich clots and patches. The foliation is sub-vertical and strikes ESE.

The sample has a recrystallised granoblastic texture. Principal minerals are quartz (35–40%), plagioclase (30–35%), K-feldspar (20–25%) and biotite (5–7%), with plagioclase > K-feldspar. Plagioclase occurs as subhedral to anhedral grains. Zoning is common, with mainly complex oscillatory zoning in cores, but the rims are largely unzoned rims. Myrmekite is common. Plagioclase is locally partly replaced by minor white mica and traces of epidote/clinozoisite. K-feldspar is generally anhedral, with some poikilitic grains to >1 cm (containing sub- to euhedral plagioclase and/or quartz inclusions), and with common tarten twinning, minor simple twinning, and common perthite, particularly in the poikilitic grains. Quartz is anhedral of variable grain size, from <<1 mm to 1 cm, and displays common weakly to moderately undulose extinction and minor weak sub-grain development. Biotite occurs as aligned, pale yellow to dark red-brown elongate flakes that are locally altered to chlorite and rutile and/or white mica. Accessory phases include apatite, zircon and opaque minerals. Secondary minerals include very minor to trace amounts of white mica, chlorite, rutile and epidote/clinozoisite.

Mount, pop: Z3877C

Description of zircons

The zircon in this sample consists of stubby to elongate subhedral grains with slight to moderate rounding of crystal faces, and grains which are more equant and rounded. Both types vary in size, with the subhedral grains ranging from about 50 μm to 280 μm in length (aspect ratios from 2:1 to 4:1), and the equant rounded grains from approximately 65 μm to 150 μm in diameter. The zircon varies from colourless to pale yellow-brown. Most grains contain cracks and small inclusions. Continuous euhedral concentric zoning is visible in many grains in CL, and some also contain sector zoning or distinct cores (Fig. 14). Other grains are more homogeneous in CL, or contain irregular patches and zones, indicative of recrystallisation.

Concurrent standard data

This three-day session was interrupted mid-way by several arc 'drop-outs' and related instabilities. There is a calibration change across this period but it is considered too minor to justify splitting the data into two blocks. The observed calibration slope is 2.16, with the corresponding sample data suggesting values >2.3. A value of 2.2 was used for data reduction. Using all data (including several of poor precision, which have little bearing on the result), the Pb/U calibration has a 1σ scatter of 1.16% (MSWD = 7.82; $n = 41$). The $^{207}\text{Pb}/^{206}\text{Pb}$ data display a small amount of excess scatter that is difficult to characterise. Omitting two 3σ outliers and three points with internal precision >15 Ma gives a weighted mean $^{207}\text{Pb}/^{206}\text{Pb}$ age of 1849.9 ± 2.4 Ma, with MSWD = 1.4 ($n = 36$). Further omitting three $\geq 2\sigma$ outliers (two low, one high) gives 1850.0 ± 2.0 Ma (MSWD = 1.10), while the preferred "standard" low-side culling procedure gives 1851.4 ± 2.1 Ma (MSWD = 1.04; $n = 30$).

Element abundance calibration was based on CZ3 ($n = 3$).

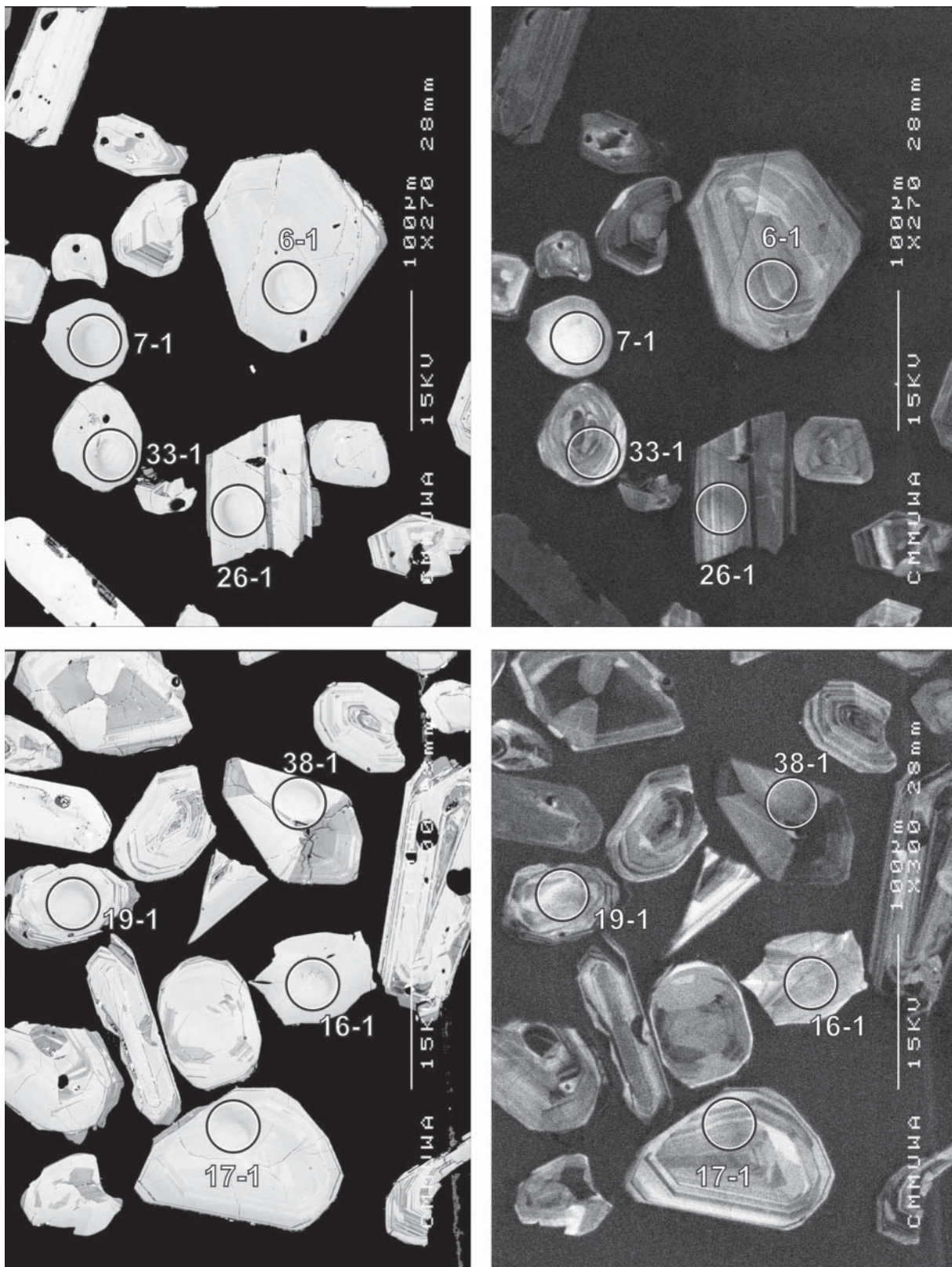


Figure 14. Representative SEM images (BSE on left, CL on right) for sample 2001967017A: Bali Monzogranite. SHRIMP analysis spots are labelled. Remnant pits from the ion microprobe analyses are faintly visible in some grains. Scale bar is 100 μ m.

Sample data

Thirty nine analyses were obtained from separate grains (Table 9). The data show a distinct zero-age discordance trend (Fig. 15), nine of the points being >5% discordant. The discordant data, and one extremely low-U analysis (6-1) are not considered for age interpretation. Of the remainder, one (8-1) is anomalously young and two (20-1, 26-1) are $\sim 3\sigma$ young outliers. The remaining 27 analyses form a single population (Fig. 16) with a weighted mean $^{207}\text{Pb}/^{206}\text{Pb}$ age of 2666.8 ± 2.2 Ma (MSWD = 0.78).

Geochronological interpretation

The age of 2667 ± 3 Ma is taken to be the crystallization age of the granite.

Table 9. SHRIMP analytical results for zircon from sample 2001967017A: Bali Monzogranite.

grain-spot	U (ppm)	Th (ppm)	4f206 (%)	^{207}Pb		^{206}Pb		^{207}Pb		^{208}Pb	conc. (%)	$^{207}\text{Pb}/^{206}\text{Pb}$	
				^{206}Pb	\pm	^{238}U	\pm	^{235}U	\pm			^{232}Th	Age (Ma)
Main group													
1-1	90	36	0.051	0.1813	0.0007	0.507	0.007	12.66	0.17	0.143	99	2665	6
3-1	183	115	0.192	0.1819	0.0006	0.493	0.006	12.37	0.16	0.144	97	2670	5
5-1	150	82	0.078	0.1807	0.0005	0.502	0.006	12.49	0.16	0.140	99	2659	5
7-1	80	37	-0.012	0.1820	0.0007	0.506	0.007	12.69	0.18	0.139	99	2671	6
9-1	84	46	0.072	0.1819	0.0008	0.481	0.006	12.07	0.17	0.112	95	2670	7
10-1	107	46	0.032	0.1803	0.0007	0.504	0.007	12.53	0.17	0.138	99	2656	6
11-1	67	44	0.055	0.1827	0.0008	0.505	0.007	12.71	0.18	0.140	98	2678	7
12-1	81	12	0.096	0.1820	0.0008	0.504	0.007	12.65	0.18	0.136	99	2671	7
13-1	169	26	0.004	0.1820	0.0005	0.519	0.007	13.02	0.18	0.144	101	2671	4
14-1	78	44	-0.007	0.1813	0.0007	0.512	0.007	12.79	0.18	0.144	100	2664	6
15-1	59	29	0.036	0.1819	0.0009	0.502	0.007	12.59	0.19	0.141	98	2670	8
16-1	86	45	0.004	0.1814	0.0007	0.498	0.007	12.46	0.17	0.139	98	2666	6
17-1	81	51	-0.009	0.1826	0.0006	0.509	0.007	12.83	0.18	0.142	99	2677	6
18-1	79	46	0.011	0.1810	0.0007	0.510	0.007	12.74	0.18	0.141	100	2662	6
19-1	83	33	-0.008	0.1809	0.0006	0.501	0.007	12.48	0.17	0.142	98	2661	6
21-1	59	30	0.110	0.1815	0.0009	0.511	0.007	12.79	0.19	0.140	100	2667	8
22-1	84	40	0.263	0.1822	0.0009	0.529	0.015	13.29	0.39	0.107	102	2673	8
23-1	148	86	0.131	0.1811	0.0006	0.513	0.007	12.80	0.17	0.142	100	2663	6
24-1	92	37	0.250	0.1818	0.0008	0.496	0.007	12.43	0.17	0.142	97	2670	8
28-1	147	105	0.010	0.1817	0.0005	0.515	0.006	12.89	0.17	0.142	100	2668	5
30-1	111	44	0.055	0.1819	0.0006	0.507	0.007	12.72	0.17	0.141	99	2670	6
32-1	119	48	0.044	0.1805	0.0006	0.495	0.006	12.31	0.16	0.145	97	2658	5
34-1	145	74	0.392	0.1815	0.0008	0.484	0.006	12.11	0.16	0.119	95	2667	7
35-1	244	153	0.085	0.1816	0.0004	0.509	0.006	12.74	0.16	0.142	99	2668	4
37-1	211	108	0.002	0.1814	0.0004	0.511	0.006	12.79	0.16	0.135	100	2666	4
38-1	206	105	0.186	0.1815	0.0005	0.505	0.006	12.64	0.16	0.135	99	2667	5
Young outliers													
8-1	51	35	-0.170	0.1277	0.0010	0.378	0.006	6.66	0.11	0.109	100	2067	14
20-1	120	55	0.086	0.1784	0.0009	0.497	0.006	12.22	0.17	0.138	99	2638	9
26-1	71	44	0.108	0.1786	0.0008	0.523	0.007	12.89	0.19	0.141	103	2640	8
Discordant or low U													
2-1	108	88	0.562	0.1805	0.0011	0.435	0.006	10.83	0.16	0.123	88	2657	10
4-1	150	93	1.358	0.1821	0.0018	0.424	0.005	10.65	0.17	0.150	85	2672	16
6-1	8	3	0.330	0.1813	0.0029	0.483	0.012	12.06	0.35	0.145	95	2664	27
25-1	119	64	0.546	0.1822	0.0010	0.443	0.006	11.12	0.16	0.153	88	2673	9
27-1	139	54	1.305	0.1828	0.0017	0.483	0.006	12.16	0.19	0.183	94	2678	15
29-1	61	68	0.203	0.1826	0.0010	0.462	0.006	11.64	0.17	0.069	91	2677	9
31-1	111	30	0.575	0.1799	0.0010	0.458	0.006	11.36	0.16	0.142	92	2652	9
33-1	105	46	0.378	0.1842	0.0009	0.457	0.006	11.61	0.16	0.143	90	2691	8
36-1	111	65	1.127	0.1814	0.0017	0.364	0.005	9.10	0.15	0.130	75	2666	16
39-1	247	78	2.336	0.1823	0.0028	0.349	0.004	8.77	0.17	0.188	72	2674	26

Data are at 1σ precision. All Pb data are common-Pb corrected (based on ^{204}Pb and Broken Hill Pb composition). Analysis date: 26/02/02; session Z3877i.

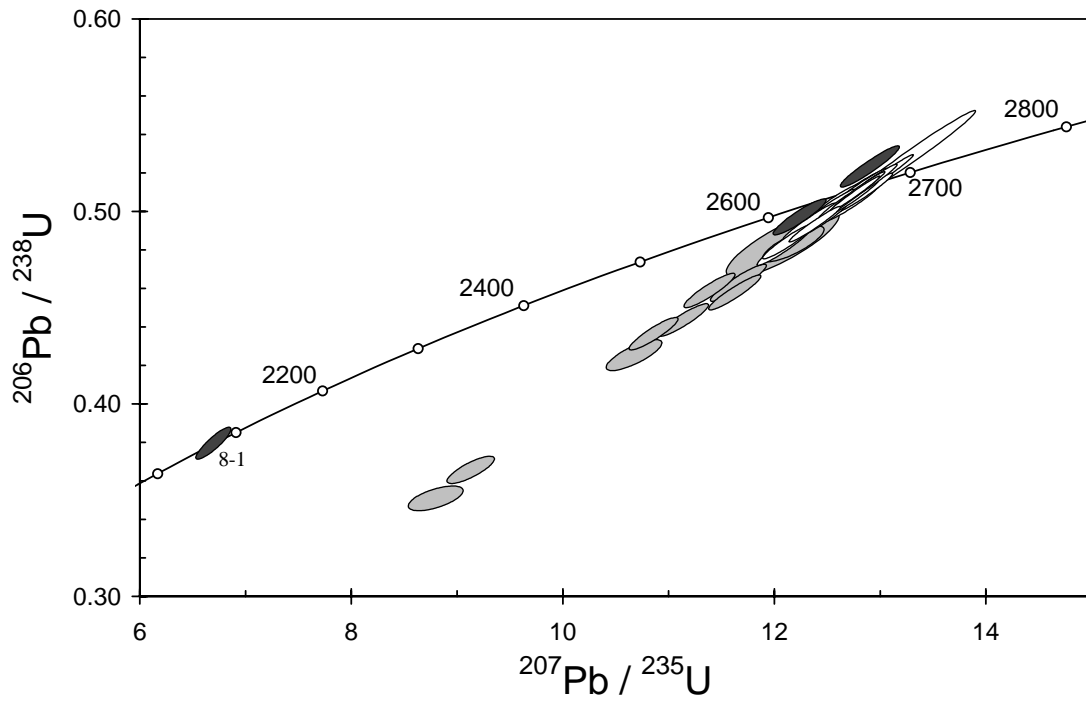


Figure 15. Concordia plot for zircons from sample 2001967017A: Bali Monzogranite. White filled symbols are used to define the age of the sample; discordant analyses are light grey; young outliers are dark grey.

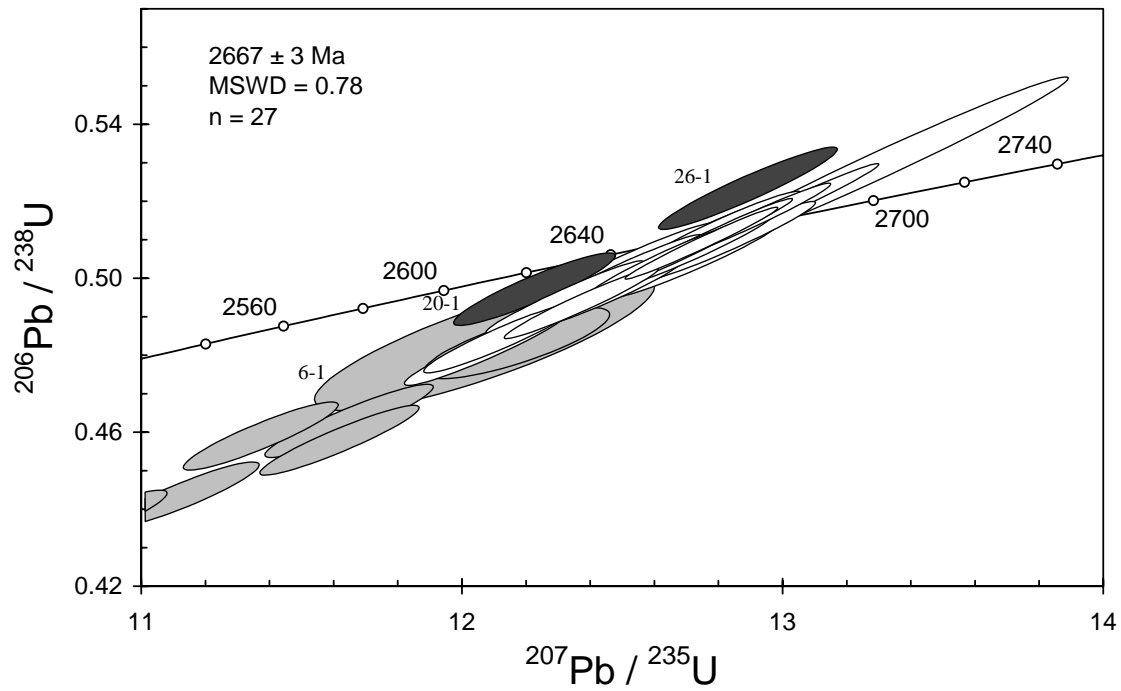


Figure 16. Concordia plot for the main data cluster for sample 2001967017A: Bali Monzogranite. Shading as in Figure 15.

2001967019A: banded biotite granitic gneiss, Quairnie Rock

1:250,000 sheet: Boorabbin (SH5113)

1:100,000 sheet: Yilmia (3135)

MGA: 317248mE 6539438mN

Location: The sample was taken from the western side of a large, low whaleback that forms part of Quairnie Rock, about 11 km south of the abandoned Nepean Ni mine.

Description: This light grey, fine- to medium-grained, seriate, biotite-poor (<5%), biotite monzogranite is interlayered with grey, fine- to medium-grained, equigranular to seriate, biotite-rich (8-10%), biotite monzogranite. The bands of biotite-poor and biotite-rich monzogranite form a complex, banded biotite quartzofeldspathic gneiss. The biotite-rich bands may constitute highly-deformed, disrupted dykes or enclaves, and are generally sub-parallel and typically parallel to a moderately NE-dipping, SSE-striking foliation that developed after generation of the gneiss. Both phases are cut by several generations of thin, syn- and post-kinematic felsic granite and pegmatite veins, minor late quartz veins, and rare late monzogranite dykes. The sample has a granoblastic texture. Principal minerals are quartz (30–35%), plagioclase (30–35%), K-feldspar (30–35%) and biotite (5–7%). Plagioclase occurs as subhedral grains with no visible zoning, variably developed and locally bent twinning, and rare minor myrmekite. The plagioclase is commonly partly altered to white mica, carbonate and/or epidote/clinozoisite, and contains traces of hematite. K-feldspar is generally anhedral, commonly with tarten twinning and minor perthite. Quartz is anhedral, and mostly has weakly to moderately developed undulose extinction. Biotite occurs as aligned, pale yellow to dark-brown flakes that are locally partly altered to chlorite and rutile and/or white mica. Accessory phases include zircon, opaque minerals and apatite. Secondary minerals are minor white mica, chlorite, rutile, and trace epidote/clinozoisite and hematite.

Mount, pop: Z3805C

Description of zircons

The zircon crystals and fragments range from ~70 µm to >250 µm in length and up to 180 µm in width. Most grains are subhedral and elongate with aspect ratios to 4:1, but some stubby, equant grains and anhedral fragments are also present. Slight rounding of crystal faces is common. About 25% of the grains are colourless and relatively clear in transmitted light, and are either homogeneous and bright in CL or finely zoned (Fig. 17). The remainder are pale yellow-brown or darker and turbid in transmitted light. Many have disrupted zoning patterns in CL or are completely metamict and/or recrystallised. Fractures are pervasive in these grains. Cores are visible in some grains.

Concurrent standard data

After omitting two outliers identified by SQUID, the apparent calibration slope for QGNG is 2.26 ($n = 34$). The concurrent sample data also suggest a slope >2, and a value of 2.2 was used for the calibration exponent. This gives a Pb/U calibration with 1σ scatter of 1.08% and $MSWD = 4.5$. For $^{207}\text{Pb}/^{206}\text{Pb}$, omitting the two Pb/U calibration outliers and one 3σ (low) outlier, and culling one other low point, leaves 32 points with a weighted mean $^{207}\text{Pb}/^{206}\text{Pb}$ age of 1849.2 ± 2.8 Ma ($MSWD = 1.15$).

Element abundance calibration was based on CZ3 ($n = 2$).

Sample data

Thirty five analyses were recorded from 33 grains (Table 10, Fig. 18). Two analyses (18-1, 33-1) are >5% discordant and not considered reliable for geochronology. Three others (1-1, 2-1, 3-1) have $U > 1000$ ppm, well above values that generally lead to metamictisation and Pb-loss in Archaean grains. These also are not used for age interpretation, although two of them (2-1, 3-1)

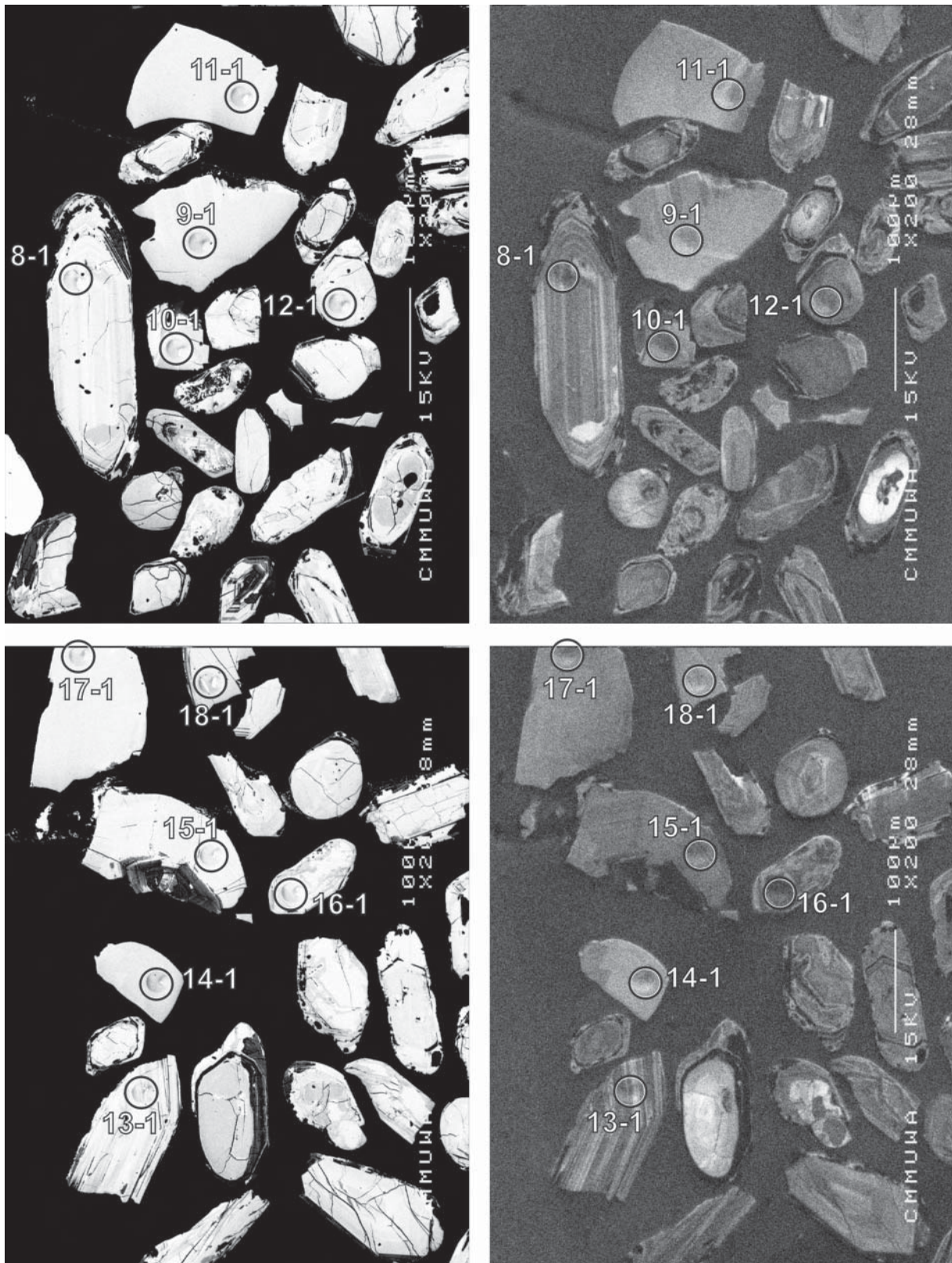


Figure 17. Representative SEM images (BSE on left, CL on right) for sample 2001967019A: banded biotite granitic gneiss, Quairnie Rock. SHRIMP analysis spots are labelled. Remnant pits from the ion microprobe analyses are faintly visible in some grains. Scale bar is 100 µm.

are consistent with the main group of data. Several of these analyses (1-1, 33-1), as well as one concordant analysis (24-1) with a moderate U content, are clearly older than the main data group, suggesting that these grains are xenocrysts (Fig. 18). The remaining data fall in a single cluster (Fig. 19) that has a weighted mean $^{207}\text{Pb}/^{206}\text{Pb}$ age of 2673.7 ± 2.7 Ma, with some excess scatter (MSWD = 1.5). Omitting two analyses (4-1, 9-1) that are low-age outliers at $\sim 3\sigma$ leaves 27 with an age of 2674.7 ± 2.1 Ma (MSWD = 0.95).

Geochronological interpretation

The 2675 ± 3 Ma date is probably the age of the monzogranite that now constitutes the gneiss, although it is also possible that this is the age of the gneiss-forming event, with the lower U (typically magmatic) grains being recrystallised from high-U precursors.

Table 10. SHRIMP analytical results for zircon from sample 2001967019A: banded biotite granitic gneiss, Quairnie Rock.

grain-spot	U (ppm)	Th (ppm)	4f206 (%)	^{207}Pb		^{206}Pb		^{207}Pb		^{208}Pb	conc. (%)	$^{207}\text{Pb}/^{206}\text{Pb}$	
				^{206}Pb	\pm	^{238}U	\pm	^{235}U	\pm			^{232}Th	Age (Ma)
Main group													
5-1	128	74	0.063	0.1837	0.0007	0.504	0.006	12.77	0.17	0.139	98	2687	6
6-1	150	51	0.053	0.1823	0.0006	0.519	0.006	13.04	0.17	0.143	101	2674	6
8-1	230	211	0.393	0.1825	0.0008	0.492	0.006	12.38	0.16	0.138	96	2676	8
10-1	249	147	0.022	0.1822	0.0005	0.504	0.006	12.65	0.15	0.139	98	2673	5
11-1	127	67	0.040	0.1817	0.0009	0.514	0.007	12.87	0.18	0.143	100	2668	8
12-1	198	86	-0.043	0.1833	0.0006	0.499	0.006	12.61	0.16	0.138	97	2683	6
13-1	187	117	0.083	0.1818	0.0006	0.502	0.006	12.58	0.16	0.138	98	2669	6
14-1	89	35	0.010	0.1818	0.0008	0.515	0.007	12.90	0.19	0.142	100	2669	8
15-1	219	100	0.068	0.1814	0.0006	0.515	0.006	12.89	0.16	0.141	101	2666	5
16-1	740	80	0.015	0.1824	0.0003	0.504	0.006	12.69	0.15	0.139	98	2675	3
17-1	176	90	0.009	0.1814	0.0006	0.496	0.007	12.41	0.18	0.136	97	2666	6
18-2	186	66	0.008	0.1825	0.0006	0.514	0.006	12.92	0.16	0.143	100	2675	5
19-1	194	69	0.079	0.1815	0.0006	0.505	0.006	12.64	0.16	0.139	99	2667	5
20-1	80	48	0.000	0.1824	0.0009	0.515	0.007	12.96	0.19	0.142	100	2674	8
21-1	162	99	-0.038	0.1833	0.0006	0.504	0.007	12.72	0.17	0.140	98	2683	6
21-2	191	118	-0.042	0.1827	0.0006	0.513	0.008	12.92	0.20	0.141	100	2678	5
22-1	134	53	0.329	0.1836	0.0008	0.492	0.006	12.46	0.17	0.144	96	2685	7
23-1	130	1	0.000	0.1829	0.0007	0.518	0.007	13.05	0.17	0.152	100	2679	6
25-1	128	51	-0.014	0.1820	0.0007	0.515	0.008	12.93	0.20	0.145	100	2671	6
26-1	173	88	0.021	0.1817	0.0006	0.512	0.006	12.81	0.16	0.140	100	2668	5
27-1	93	54	0.054	0.1823	0.0008	0.522	0.007	13.11	0.18	0.144	101	2674	7
28-1	258	74	0.098	0.1827	0.0005	0.509	0.006	12.83	0.16	0.142	99	2677	5
29-1	76	38	0.031	0.1826	0.0010	0.520	0.007	13.10	0.20	0.142	101	2676	9
30-1	103	44	0.032	0.1830	0.0008	0.509	0.007	12.84	0.18	0.139	99	2680	7
31-1	128	58	-0.025	0.1829	0.0007	0.517	0.007	13.04	0.17	0.141	100	2679	6
32-1	169	84	0.023	0.1826	0.0006	0.508	0.006	12.79	0.16	0.143	99	2677	6
34-1	43	20	0.162	0.1814	0.0012	0.505	0.008	12.62	0.23	0.138	99	2665	11
Old outlier													
24-1	114	54	0.132	0.2008	0.0009	0.536	0.007	14.85	0.20	0.151	98	2833	7
Young outliers													
4-1	204	72	0.170	0.1802	0.0007	0.488	0.006	12.11	0.15	0.134	96	2655	6
9-1	121	59	0.047	0.1803	0.0007	0.503	0.007	12.51	0.18	0.139	99	2655	7
Discordant or high-U													
1-1	2175	243	0.003	0.1889	0.0005	0.541	0.007	14.08	0.18	0.151	102	2732	4
2-1	1127	37	0.000	0.1812	0.0003	0.507	0.006	12.66	0.14	0.138	99	2664	3
3-1	1407	81	0.198	0.1824	0.0003	0.499	0.006	12.56	0.14	0.220	98	2675	3
18-1	163	64	0.564	0.1829	0.0010	0.407	0.005	10.26	0.14	0.123	82	2679	9
33-1	66	<1	-0.130	0.2161	0.0012	0.514	0.007	15.32	0.24	---	91	2952	9

Data are at 1σ precision. All Pb data are common-Pb corrected (based on ^{204}Pb and Broken Hill Pb composition). Analysis date: 2/12/01; session Z3805j.

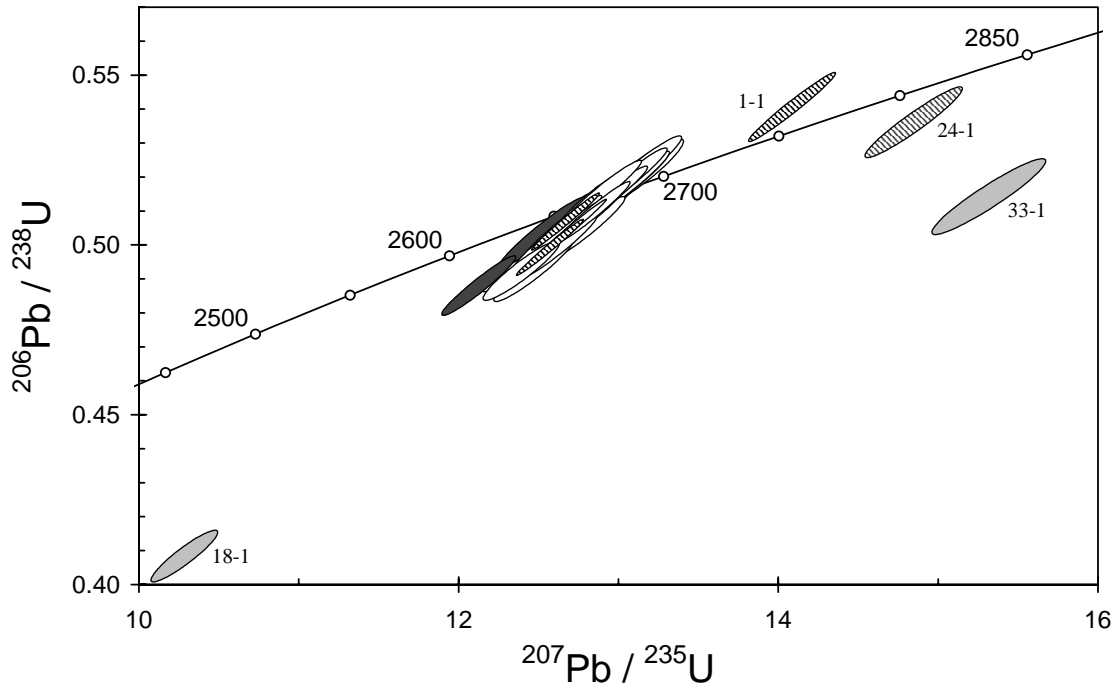


Figure 18. Concordia plot for zircon data from sample 2001967019A: banded biotite granitic gneiss, Quairnie Rock. White filled symbols are used to define the age of the sample; younger outliers are dark grey; inherited grains and/or high-U analyses have diagonal shading; discordant analyses are light grey.

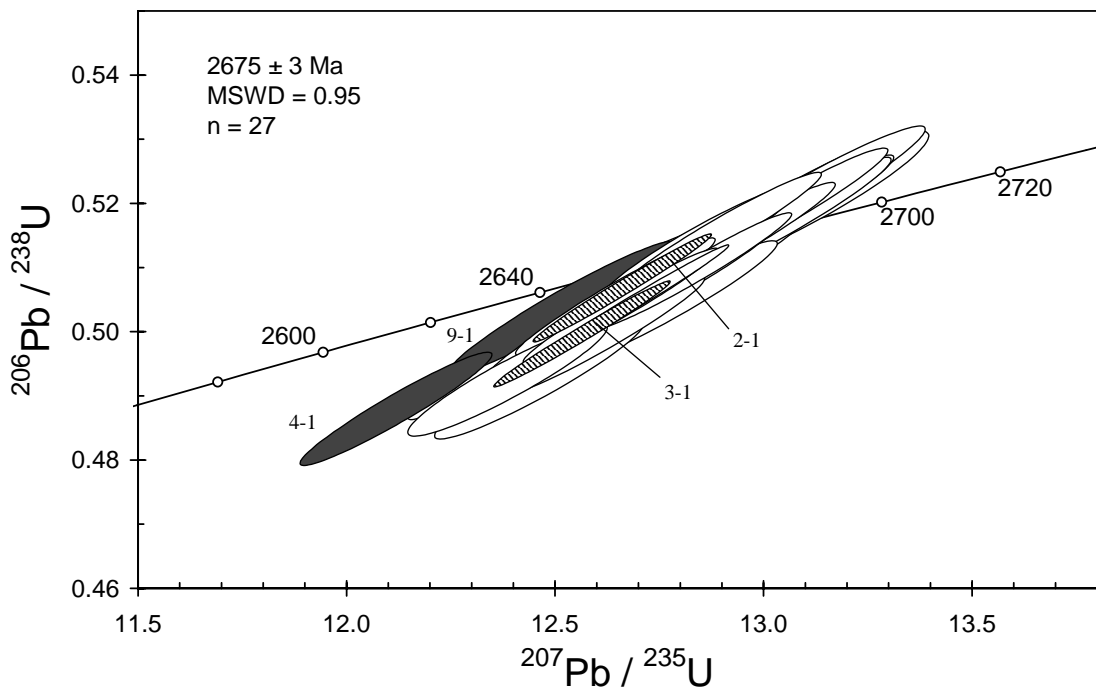


Figure 19. Enlargement of main data cluster from sample 2001967019A: banded biotite granitic gneiss, Quairnie Rock. Shading as in Fig. 18.

2001967027: quartz-feldspar porphyry dyke, Tower Hill mine**1:250,000 sheet:** Leonora (SH5101)**1:100,000 sheet:** Leonora (3140)**MGA:** 336556mE 6802345mN**Location:** The sample was collected along the access ramp in the northeast corner of the Tower Hill open-pit, about 1 km southwest of Leonora.**Description:** It is from a grey-pink, strongly deformed and altered, quartz-feldspar porphyry that intrudes a mafic volcanic sequence. Both units are cut by quartz veins and associated hydrothermal alteration; the selected sample is free from obvious quartz veins.

This rock is characterised by a distinctly recrystallised porphyroclastic texture, largely the product of pervasive hydrothermal alteration and moderate deformation of a quartz-feldspar porphyritic microgranite. Principal minerals are albite (~35–40%), white mica (8–12%), biotite (5–8%), chlorite (3–5%), carbonate (3–5%), monocrystalline quartz (1–2%), tourmaline (1–2%), minor opaque minerals and trace zircon and apatite, in a very-fine grained quartzofeldspathic groundmass (~35–40%). Albite, with minor white mica, carbonate and biotite, forms porphyroclasts of variable size (mainly <2 mm, to 5 mm) that display moderate twinning. The albite porphyroclasts are the product of recrystallisation and hydrothermal alteration of igneous feldspar phenocrysts. Quartz phenocrysts show minor recrystallisation and minor to moderate undulose extinction. White mica is present as clusters of small (<0.1 mm), elongate grains that form seams and lenses, are largely in optical continuity and define the strong foliation. Biotite occurs as light yellow to dark brown, subhedral to ragged and irregular grains (<0.5 mm) and clusters of grains, generally in alignment with the white mica-defined foliation. Retrograde alteration has locally replaced biotite with chlorite and opaque minerals. Carbonate occurs mainly as disseminated, irregular grains (<0.1 mm), and as clusters of irregular grains that may represent the replacement product of igneous Fe-Mg silicates. Tourmaline forms minor, disseminated, large (to 1 mm), blue-green-brown poikiloblastic grains. The fine-grained quartzo-feldspathic mosaic contains minor white mica, carbonate, biotite and opaque minerals, and sometimes displays radiating intergrowths of quartz and feldspar (?albite).

Mount, pop: Z3739B**Description of zircons**

Zircon from this sample is mostly turbid, pale grey to grey-brown, whole crystals, with a small proportion of fragments. The grains are predominantly euhedral to subhedral, with slightly rounded crystal faces. They vary from roughly equant to elongate grains, 50 μm to 200 μm in size (aspect ratios up to 5:1). The grains have well-defined continuous euhedral and concentric zoning (clearly visible in reflected light and CL; Fig. 20), but patches of disrupted zoning in the central regions of some grains are interpreted to result from recrystallisation. Some grains contain distinct cores which have zoning that is structurally truncated by new growth of euhedrally-zoned zircon.

Concurrent standard data

There was a calibration shift after re-tuning half-way through this session, and the data were therefore processed in two blocks. In the first block, the apparent calibration slope for all QGNG ($n = 16$) data is ~2.3. Omitting one outlier identified by SQUID reduces this to 2.2, for a highly linear array with 1σ scatter in Pb/U of 0.5% (MSWD = 1.7). For the second block ($n = 18$) the slope is even higher (2.5) but not as well defined (1σ scatter in Pb/U = 1.05%; MSWD = 3.9). A value of 2.2 was used for the calibration exponent in both cases. The $^{207}\text{Pb}/^{206}\text{Pb}$ data form a single population. Omitting only the one calibration outlier leaves 33 points with a weighted mean $^{207}\text{Pb}/^{206}\text{Pb}$ age of 1850.8 ± 2.6 Ma (MSWD = 1.03).

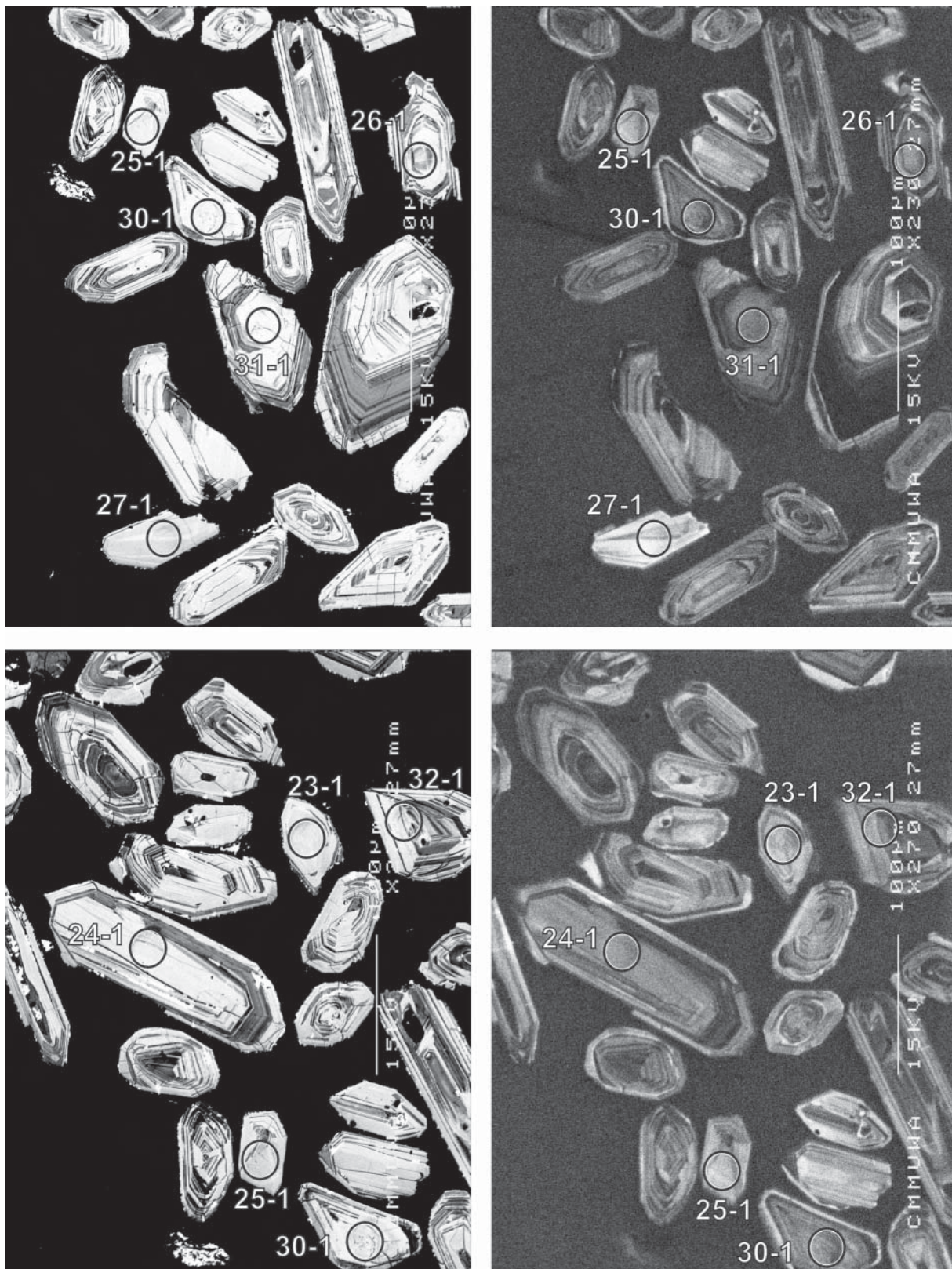


Figure 20. Representative SEM images (BSE on left, CL on right) for sample 2001967027: quartz-feldspar porphyry dyke, Tower Hill mine. SHRIMP analysis spots are labelled. Remnant pits from the ion microprobe analyses are faintly visible in some grains. Scale bar is 100 µm.

Element abundance calibration was based on CZ3 (n = 1 in each block).

Sample data

Thirty four analyses were made on separate grains (Table 11). Many analyses are discordant, with a strong zero-age Pb-loss trend (Fig. 21). There is also evidence for ancient Pb loss in several of the data (9-1, 11-1, 15-1, 30-1) that are close to concordia (Fig. 22); these analyses also have high-U. Amongst the concordant data, there is one distinct old outlier (3-1), possibly from a xenocryst. The remaining 13 concordant points produce a weighted mean $^{207}\text{Pb}/^{206}\text{Pb}$ age of 2670.3 ± 4.6 Ma, with MSWD = 0.88.

Geochronological interpretation

The 2670 ± 5 Ma date is considered to be the crystallization age of the dyke.

Table 11. SHRIMP analytical results for zircon from sample 2001967027: quartz-feldspar porphyry dyke, Tower Hill mine.

grain-spot	U (ppm)	Th (ppm)	4f206 (%)	$^{207}\text{Pb}/^{206}\text{Pb}$	\pm	$^{206}\text{Pb}/^{238}\text{U}$	\pm	$^{207}\text{Pb}/^{235}\text{U}$	\pm	$^{208}\text{Pb}/^{232}\text{Th}$	conc. (%)	Age (Ma)	\pm
Main concordant group													
1-1	82	50	0.315	0.1822	0.0012	0.487	0.004	12.24	0.12	0.087	96	2673	11
2-1	80	52	0.185	0.1812	0.0009	0.513	0.004	12.81	0.11	0.100	100	2664	8
6-1	102	34	0.107	0.1831	0.0011	0.493	0.005	12.44	0.14	0.101	96	2681	10
8-1	115	54	0.281	0.1802	0.0010	0.487	0.004	12.11	0.12	0.066	96	2655	10
10-1	89	32	0.148	0.1816	0.0010	0.484	0.005	12.11	0.14	0.122	95	2667	10
14-1	85	28	0.033	0.1818	0.0010	0.503	0.005	12.61	0.14	0.132	98	2669	9
17-1	116	55	0.609	0.1803	0.0010	0.477	0.006	11.84	0.17	0.091	95	2655	9
19-1	72	17	-0.019	0.1823	0.0009	0.499	0.007	12.54	0.19	0.137	98	2674	8
23-1	92	38	0.100	0.1816	0.0009	0.507	0.007	12.70	0.18	0.134	99	2668	8
25-1	96	46	0.013	0.1820	0.0009	0.486	0.007	12.19	0.18	0.109	96	2671	8
27-1	57	22	0.052	0.1831	0.0013	0.518	0.008	13.08	0.22	0.143	100	2682	12
31-1	183	43	0.167	0.1822	0.0006	0.509	0.006	12.80	0.16	0.133	99	2673	6
33-1	81	24	0.234	0.1831	0.0009	0.503	0.007	12.70	0.19	0.113	98	2681	8
Old outlier													
3-1	103	58	0.217	0.1889	0.0008	0.544	0.004	14.17	0.12	0.144	103	2732	7
Obvious early Pb loss													
9-1	341	156	0.323	0.1747	0.0006	0.458	0.002	11.04	0.07	0.126	93	2603	6
11-1	308	101	0.130	0.1752	0.0006	0.473	0.002	11.42	0.07	0.131	96	2608	6
15-1	419	146	0.145	0.1715	0.0006	0.453	0.005	10.72	0.13	0.121	94	2572	5
30-1	403	190	0.133	0.1618	0.0004	0.438	0.005	9.76	0.11	0.123	95	2475	4
>5% discordant													
4-1	196	67	0.513	0.1834	0.0007	0.425	0.003	10.76	0.07	0.080	85	2684	6
5-1	133	112	1.714	0.1865	0.0016	0.409	0.003	10.53	0.12	0.058	82	2712	14
7-1	166	111	0.536	0.1791	0.0011	0.341	0.003	8.43	0.08	0.054	72	2645	10
12-1	163	137	0.201	0.1822	0.0009	0.439	0.003	11.03	0.10	0.053	88	2673	8
13-1	214	139	2.177	0.1787	0.0018	0.297	0.003	7.32	0.11	0.041	63	2641	17
16-1	175	197	1.729	0.1826	0.0016	0.366	0.005	9.20	0.14	0.041	75	2677	15
18-1	98	127	0.504	0.1820	0.0024	0.395	0.018	9.91	0.46	0.029	80	2671	22
20-1	120	81	0.709	0.1831	0.0012	0.452	0.006	11.41	0.17	0.068	90	2681	11
21-1	161	169	1.076	0.1833	0.0015	0.404	0.005	10.22	0.15	0.051	82	2683	13
22-1	152	128	0.467	0.1808	0.0010	0.396	0.005	9.87	0.13	0.042	81	2660	9
24-1	151	78	0.367	0.1815	0.0008	0.459	0.006	11.50	0.15	0.053	91	2667	8
26-1	188	62	0.053	0.1838	0.0006	0.483	0.006	12.23	0.16	0.096	94	2687	5
28-1	162	218	1.191	0.1903	0.0011	0.422	0.005	11.08	0.15	0.048	83	2745	9
29-1	140	114	0.787	0.1810	0.0010	0.407	0.005	10.15	0.14	0.063	83	2662	9
32-1	216	373	0.732	0.1834	0.0009	0.345	0.004	8.72	0.11	0.013	71	2684	8
34-1	98	43	0.301	0.1815	0.0009	0.468	0.006	11.72	0.17	0.073	93	2666	8

Data are at 1σ precision. All Pb data are common-Pb corrected (based on ^{204}Pb and Broken Hill Pb composition). Analysis date 16/11/01; session Z3739i.

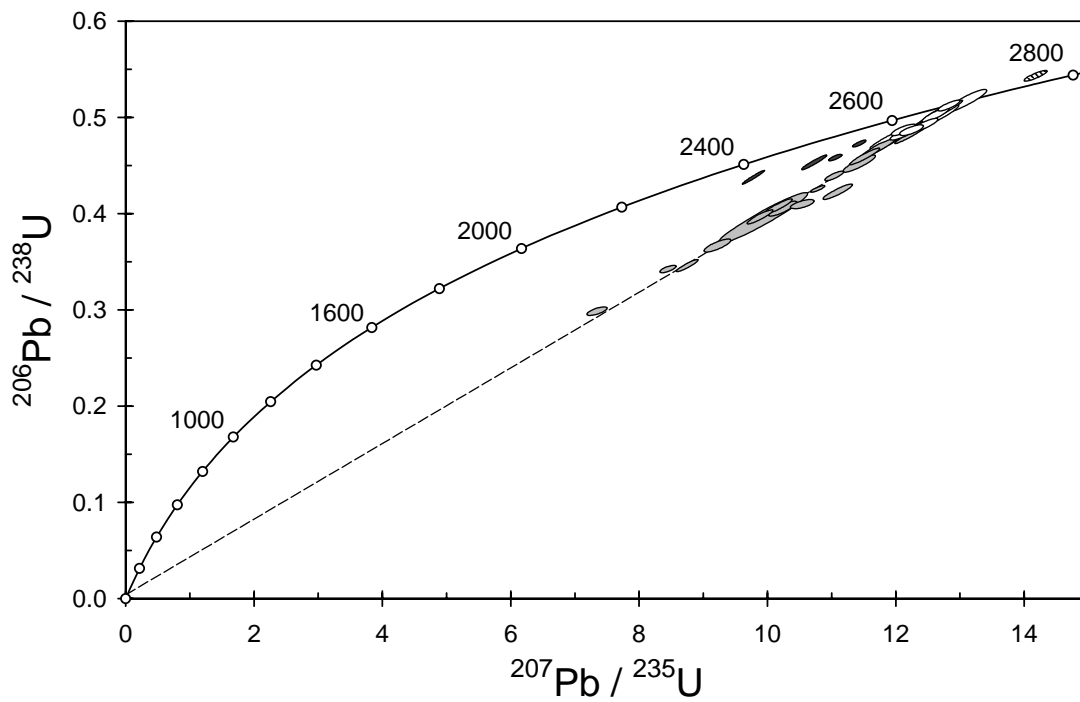


Figure 21. Concordia plot for zircon data from sample 2001967027: quartz-feldspar porphyry dyke, Tower Hill mine, showing the strong zero-age Pb-loss trend.

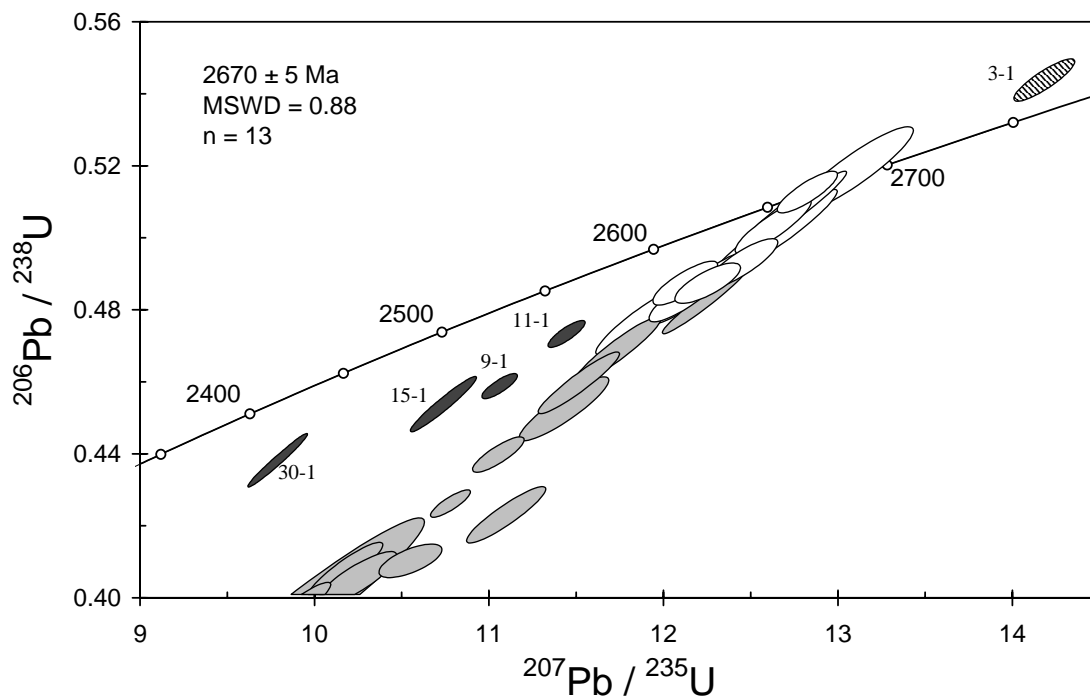


Figure 22. Enlargement of the main group of zircon data from sample 2001967027: quartz-feldspar porphyry dyke, Tower Hill mine. White filled symbols are used to define the age of the sample; older outlier (xenocryst?) has diagonal shading; analyses displaying ancient Pb loss are dark grey; discordant analyses are light grey.

2001967028: quartz-feldspar porphyry dyke, Safari prospect

1:250,000 sheet:	Edjudina (SH5106)
1:100,000 sheet:	Edjudina (3338)
MGA:	450887mE 6732052mN
Location:	This sample was taken from Sons of Gwalia Ltd diamond drillhole MCD031, depth interval 203.75–205.27 m. The collar site is located within the Safari mining locality, about 3 km west of Safari Bore.
Description:	This is a grey, strongly deformed and altered, quartz-feldspar porphyry that intrudes a felsic to intermediate volcanoclastic sequence. Both units are cut by quartz veins and associated hydrothermal alteration. The porphyry contains quartz and feldspar phenocrysts in a moderately altered groundmass of sericite, quartz, albite, carbonate and minor pyrite. The porphyry is strongly foliated and contains minor thin quartz-carbonate veins, which are not present in the collected sample.
Mount, pop:	Z3922B

Description of zircons

Colourless to pale grey-brown, euhedral to subhedral zircon fragments and whole crystals are present. The grains are stubby to elongate, and range in size from about 60 μm to 200 μm , with aspect ratios of 2:1 to 3:1. Inclusions are present in some grains. Continuous oscillatory zoning is visible in some grains in transmitted light, but in CL nearly all grains display zoning, as well as recrystallisation features such as disrupted or irregular zoning (Fig. 23). Cores are locally visible.

Concurrent standard data

During this analytical session, the primary beam progressively became unstable. Following assessment, data were truncated after 30 hours, leaving a relatively short data file. Nevertheless, the remaining QGNG data give an acceptable Pb/U calibration (1σ scatter = 0.96%; $n = 22$; MSWD = 4.6; calibration slope = 2.1). Assessing the $^{207}\text{Pb}/^{206}\text{Pb}$ data is difficult, partly because of the variable data quality and the modest number of points. The standard culling procedure does not work well, removing a rather large proportion of the data. Culling was stopped at MSWD ≥ 1.3 (refer to chapter on “Data compilation for the QGNG standard”), resulting in a weighted mean $^{207}\text{Pb}/^{206}\text{Pb}$ age of 1851.7 ± 3.7 Ma (MSWD = 1.4; $n = 21$).

Element abundance calibration was based on CZ3 ($n = 3$).

Sample data

Individual analyses on 17 grains are presented for this sample (Fig. 24; Table 7). Although the zircon appears to have suffered significant disturbance, its effect on $^{207}\text{Pb}/^{206}\text{Pb}$ dates is difficult to determine. A large proportion of analyses record high common Pb. In order to remove the data most likely to have been disturbed, those with $>2\%$ common ^{206}Pb or >300 ppm U were not considered for chronology, although one of these (12-1) falls in the main group of data. The remaining 11 analyses, which are all concordant (Fig. 24), give a weighted mean $^{207}\text{Pb}/^{206}\text{Pb}$ age of 2673.1 ± 5.1 Ma, with MSWD = 1.5. This level of scatter is similar to that seen in the concurrent standards.

Geochronological interpretation

The 2673 ± 5 Ma date is considered to be the crystallisation age of the intrusion.

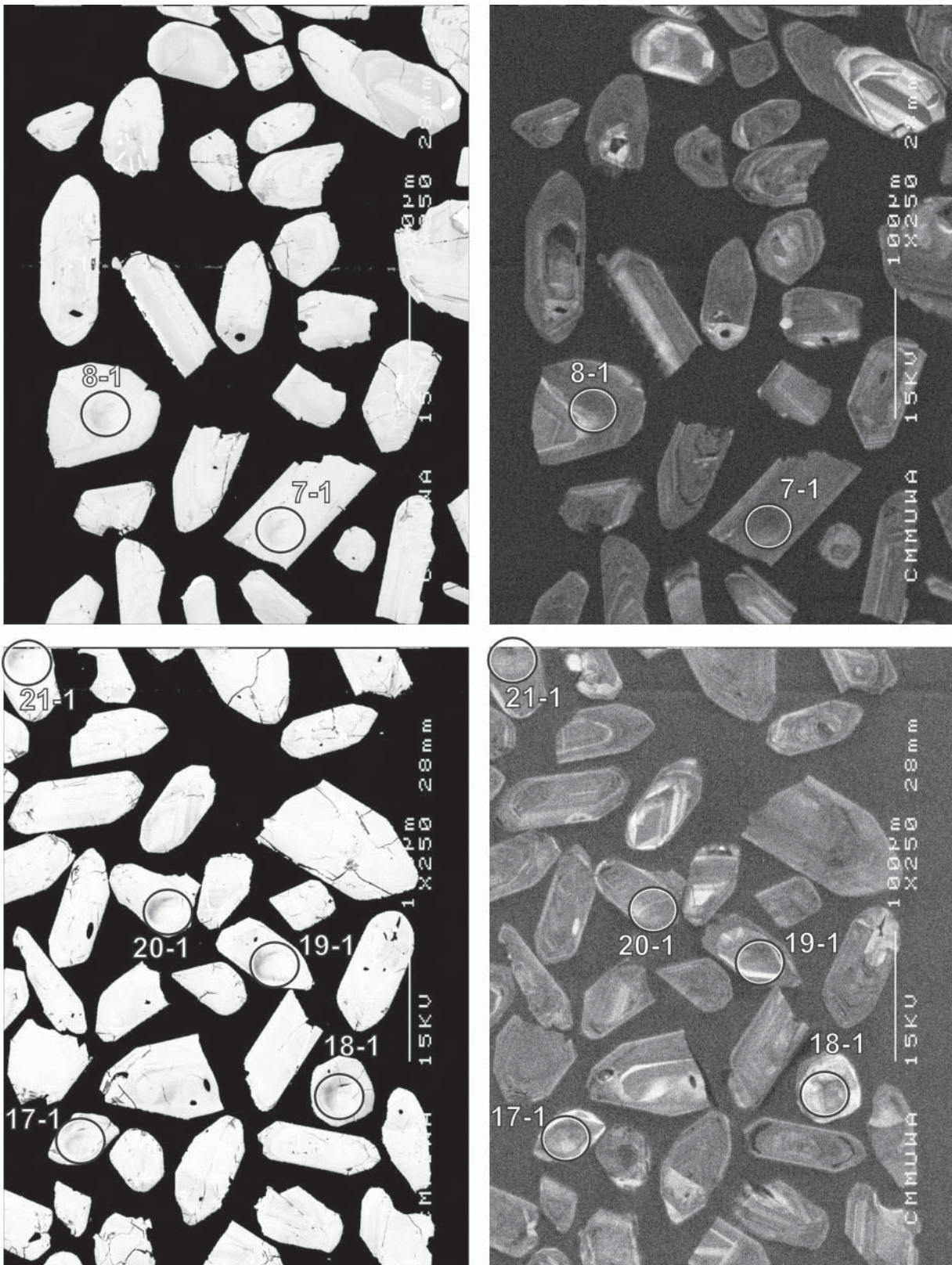


Figure 23. Representative SEM images (BSE on left, CL on right) for sample 2001967028: quartz-feldspar porphyry dyke, Safari prospect. SHRIMP analysis spots are labelled. Remnant pits from the ion microprobe analyses are faintly visible in some grains. Scale bar is 100 μm.

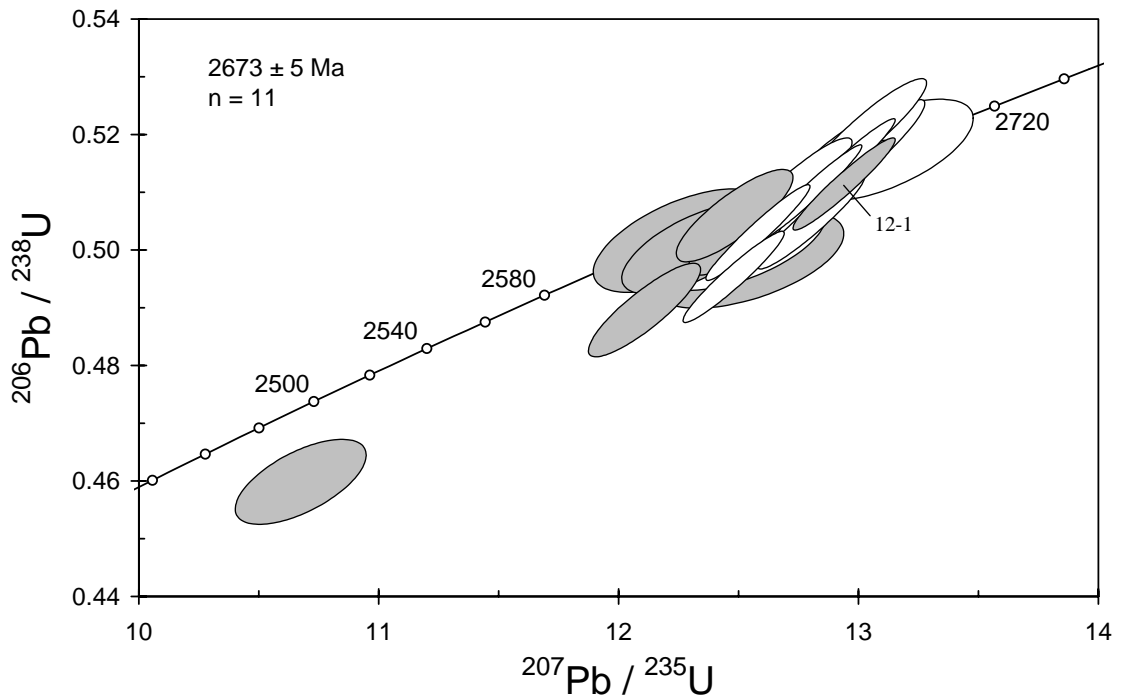


Figure 24. Concordia plot of zircon data from sample 2001967028: quartz-feldspar porphyry dyke, Safari prospect. White filled symbols are used to define the age of the sample; high common Pb and high-U data are light grey. One analysis with very high common Pb (1-1) is not plotted.

Table 12. SHRIMP analytical results for zircon from sample 2001967028: quartz-feldspar porphyry dyke, Safari prospect.

grain-spot	U (ppm)	Th (ppm)	4f206 (%)	$\frac{^{207}\text{Pb}}{^{206}\text{Pb}}$	\pm	$\frac{^{206}\text{Pb}}{^{238}\text{U}}$	\pm	$\frac{^{207}\text{Pb}}{^{235}\text{U}}$	\pm	$\frac{^{208}\text{Pb}}{^{232}\text{Th}}$	conc. (%)	Age (Ma)	\pm
Main group													
2-1	254	62	0.685	0.1808	0.0029	0.501	0.006	12.49	0.24	0.128	98	2660	26
3-1	209	61	0.538	0.1838	0.0007	0.505	0.005	12.79	0.15	0.146	98	2688	6
7-1	225	55	0.044	0.1819	0.0005	0.510	0.006	12.79	0.14	0.139	99	2670	4
8-1	206	49	0.050	0.1822	0.0005	0.514	0.006	12.92	0.14	0.141	100	2673	5
9-1	236	64	0.254	0.1808	0.0009	0.511	0.006	12.73	0.16	0.141	100	2660	8
11-1	247	81	0.279	0.1827	0.0006	0.495	0.005	12.47	0.14	0.140	97	2677	6
15-1	70	31	0.134	0.1827	0.0009	0.516	0.006	13.01	0.17	0.141	100	2677	8
18-1	111	63	0.747	0.1814	0.0009	0.521	0.006	13.03	0.16	0.142	101	2666	8
19-1	166	102	0.547	0.1830	0.0007	0.510	0.006	12.88	0.15	0.143	99	2680	6
20-1	110	32	0.231	0.1838	0.0026	0.517	0.006	13.11	0.24	0.139	100	2687	24
21-1	151	93	0.131	0.1813	0.0006	0.503	0.006	12.57	0.14	0.138	99	2665	5
>2% 4f206 or >300ppm U													
1-1	54	23	37.435	0.1799	0.0403	0.452	0.019	11.22	2.56		90	2652	372
4-1	177	51	2.297	0.1793	0.0011	0.489	0.005	12.10	0.15	0.128	97	2646	11
5-1	497	184	1.058	0.1684	0.0022	0.459	0.005	10.66	0.18	0.122	96	2541	22
6-1	208	73	3.750	0.1824	0.0032	0.498	0.006	12.53	0.26	0.131	97	2675	29
10-1	94	46	3.198	0.1771	0.0028	0.501	0.006	12.25	0.24	0.126	100	2626	26
12-1	342	185	0.132	0.1834	0.0006	0.511	0.005	12.93	0.14	0.141	99	2683	5
13-1	302	108	4.273	0.1789	0.0013	0.506	0.005	12.47	0.16	0.127	100	2642	12
14-1	270	73	2.732	0.1798	0.0011	0.503	0.007	12.47	0.18	0.127	99	2651	10
16-1	460	107	1.423	0.1784	0.0022	0.500	0.005	12.30	0.20	0.137	99	2638	20
17-1	142	87	3.913	0.1805	0.0014	0.504	0.006	12.54	0.17	0.131	99	2657	13

Data are at 1 σ precision. All Pb data are common-Pb corrected (based on ^{204}Pb and Broken Hill Pb composition). Analysis date: 13/05/02; session Z3922i.

2001967039: Meredith monzogranite

- 1:250,000 sheet:** Laverton (SH5102)
1:100,000 sheet: Burtville (3440)
MGA: 464232mE 6824490mN
Location: The sample was taken from bouldery outcrop about 100 m south of a track around 1 km west of Meredith Well.
Description: This is a grey-pink, seriate to sparsely K-feldspar porphyritic, fine-grained biotite monzogranite. Moderate foliation and weak lineation is defined by aligned biotite and elongate quartz grains. The monzogranite contains minor, small, biotite-rich schlieren and seams.
The unit is characterised by granular to granoblastic texture. Principal minerals are quartz (40–45%), K-feldspar (30–35%), plagioclase (20–25%), biotite (4–5%) and muscovite (1–2%), with K-feldspar > plagioclase. K-feldspar is subhedral to locally poikilitic, and displays well-developed tartan twinning, and very minor perthite. Plagioclase occurs as subhedral to anhedral grains, with no visible to very weak normal zoning. Twinning is common and trace quantities of myrmekite have been developed. Much of the plagioclase has been replaced by white mica, epidote/clinozoisite and carbonate, including some large grains of muscovite. Quartz is anhedral, with commonly weakly to moderately undulose extinction, and very minor sub-grain development. Biotite forms aligned, light yellow to medium-dark red-brown ragged flakes that are generally partly to completely replaced by chlorite, epidote/clinozoisite, rutile and/or white mica. Muscovite forms large (?primary) flakes, to >1 mm, localised within biotite grain clusters, and as large (?secondary) grains in altered plagioclase. Accessory phases include zircon, apatite, and opaque minerals. Secondary minerals include minor to locally more abundant chlorite, white mica/muscovite, epidote/clinozoisite, rutile, carbonate, and trace hematite.
Mount, pop: Z3881C

Description of zircons

Zircon predominantly occurs as euhedral to subhedral zircon crystals, with only slight rounding of crystal faces, although some fragments are also present. The grains are generally pale grey and many are stained yellowish-brown. Grains range from small (~45 µm) equant zircon, to stubby crystals (aspect ratios 2:1 to 3:1), to elongate grains up to 200 µm long (aspect ratios to 4:1). Small rod-like and/or equant inclusions are locally present. Most grains have continuous euhedral oscillatory zoning from core to rim, as seen in transmitted light and CL (Fig. 25). Irregular and discordant patches of recrystallised zircon in some grains are only visible in CL. A few grains are homogeneous in CL. Some have distinct cores in which zoning is discordantly truncated by new zircon growth.

Concurrent standard data

The apparent calibration slope for QGNG was 1.93. Neither of the concurrent samples was sufficiently single-aged to provide an alternate estimate, and the default slope of 2.0 was used. Omission of two outliers identified by SQUID produces a 1σ scatter in the Pb/U calibration of 0.88% (MSWD = 5.1; n = 31). The standardised assessment of $^{207}\text{Pb}/^{206}\text{Pb}$ requires the omission of three low- $^{207}\text{Pb}/^{206}\text{Pb}$ analyses and gives a weighted mean age of 1850.3 ± 2.4 (n = 29; MSWD = 1.00). Element abundance calibration was based on CZ3 (n = 4).

Sample data

Thirty one analyses were obtained from separate grains (Table 13). Approximately half of the analysed zircons have obviously disturbed U–Pb systems, either giving discordant data or having

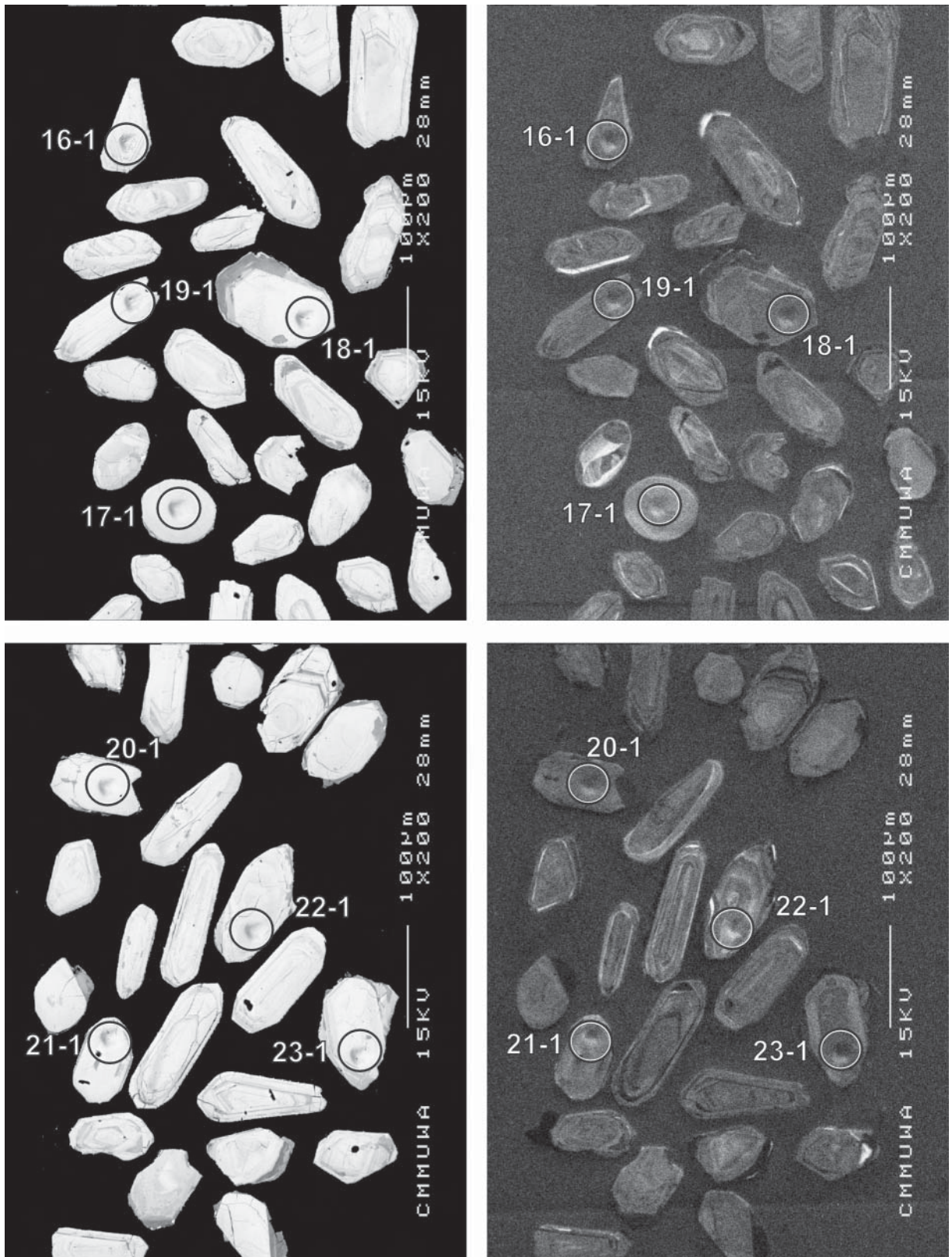


Figure 25. Representative SEM images (BSE on left, CL on right) for sample 2001967039: Meredith monzogranite. SHRIMP analysis spots are labelled. Remnant pits from the ion microprobe analyses are faintly visible in some grains. Scale bar is 100 μm .

high common Pb (Fig. 26). Amongst the concordant data are four analyses (11-1, 15-1, 21-1, 27-1) that clearly represent xenocrystic grains, and there is another 3σ outlier (8-1) at the older edge of the main data group (Fig. 27). The removal of all these data leaves only 10 analyses, which have some excess scatter (MSWD = 1.7) but still define a reasonably precise weighted mean $^{207}\text{Pb}/^{206}\text{Pb}$ age of 2658.4 ± 4.6 Ma.

Geochronological interpretation

The 2658 ± 5 Ma date is taken to be the crystallization age of the monzogranite.

Table 13. SHRIMP analytical results for zircon from sample 2001967039: Meredith monzogranite.

grain-spot	U (ppm)	Th (ppm)	4f206 (%)	$^{207}\text{Pb}/^{206}\text{Pb}$		$^{206}\text{Pb}/^{238}\text{U}$		$^{207}\text{Pb}/^{235}\text{U}$		$^{208}\text{Pb}/^{232}\text{Th}$	conc. (%)	$^{207}\text{Pb}/^{206}\text{Pb}$ Age (Ma)	
					\pm		\pm		\pm				\pm
Main group													
14-1	49	81	0.023	0.1812	0.0011	0.521	0.007	13.03	0.18	0.144	102	2664	10
17-1	134	104	-0.015	0.1824	0.0006	0.503	0.005	12.65	0.14	0.136	98	2675	6
18-1	361	161	-0.004	0.1806	0.0004	0.502	0.005	12.50	0.12	0.138	99	2658	3
20-1	244	304	-0.004	0.1807	0.0005	0.509	0.005	12.68	0.13	0.140	100	2659	4
22-1	189	148	1.040	0.1812	0.0010	0.490	0.005	12.25	0.14	0.140	96	2664	9
23-1	404	132	0.143	0.1808	0.0004	0.498	0.005	12.41	0.12	0.143	98	2660	4
24-1	146	154	0.108	0.1801	0.0007	0.513	0.005	12.75	0.14	0.141	101	2653	6
25-1	479	56	0.049	0.1796	0.0004	0.494	0.005	12.24	0.12	0.128	98	2650	4
26-1	77	47	0.227	0.1802	0.0011	0.522	0.006	12.97	0.17	0.146	102	2655	10
31-1	205	114	0.020	0.1808	0.0005	0.503	0.005	12.55	0.13	0.139	99	2660	5
Old outlier													
8-1	125	90	-0.078	0.1828	0.0007	0.511	0.005	12.87	0.14	0.141	99	2678	6
Inherited grains													
11-1	457	441	0.872	0.1860	0.0005	0.528	0.005	13.54	0.13	0.137	101	2707	4
15-1	279	149	0.009	0.1934	0.0005	0.523	0.005	13.94	0.14	0.144	98	2771	4
21-1	129	64	0.088	0.1926	0.0007	0.520	0.005	13.80	0.15	0.143	98	2764	6
27-1	168	59	0.733	0.1919	0.0008	0.528	0.005	13.96	0.15	0.155	99	2758	7
>5% discordant or 4f206 >2%													
1-1	525	187	1.556	0.1762	0.0030	0.459	0.005	11.15	0.23	0.148	93	2617	29
2-1	85	70	9.151	0.2100	0.0032	0.385	0.005	11.15	0.23	0.116	72	2906	25
3-1	129	142	4.126	0.1771	0.0022	0.388	0.004	9.49	0.16	0.153	81	2626	21
4-1	386	29	3.823	0.1819	0.0043	0.448	0.006	11.24	0.30	0.408	89	2670	39
5-1	308	285	3.752	0.1826	0.0049	0.487	0.005	12.27	0.35	0.164	96	2677	44
6-1	136	95	4.638	0.1781	0.0049	0.452	0.005	11.10	0.33	0.173	91	2635	46
7-1	352	65	0.667	0.1806	0.0013	0.466	0.006	11.60	0.16	0.158	93	2658	12
9-1	70	73	12.576	0.1826	0.0142	0.579	0.014	14.56	1.18	0.223	110	2676	128
10-1	366	166	2.220	0.1803	0.0009	0.440	0.004	10.94	0.12	0.148	89	2656	8
12-1	260	126	3.213	0.1917	0.0016	0.525	0.005	13.87	0.18	0.190	99	2757	14
13-1	139	79	7.591	0.1900	0.0024	0.468	0.006	12.26	0.21	0.165	90	2742	20
16-1	452	196	0.729	0.1767	0.0005	0.446	0.005	10.87	0.12	0.126	91	2622	5
19-1	480	187	0.162	0.1753	0.0004	0.462	0.004	11.18	0.11	0.129	94	2609	4
28-1	134	90	3.310	0.1899	0.0054	0.488	0.006	12.79	0.39	0.172	94	2742	47
29-1	224	63	0.158	0.1835	0.0013	0.483	0.007	12.21	0.19	0.139	94	2685	11
30-1	1030	457	0.633	0.1369	0.0007	0.340	0.004	6.41	0.08	0.098	86	2188	9

Data are at 1σ precision. All Pb data are common-Pb corrected (based on ^{204}Pb and Broken Hill Pb composition). Analysis date: 2/05/02; session Z3881j.

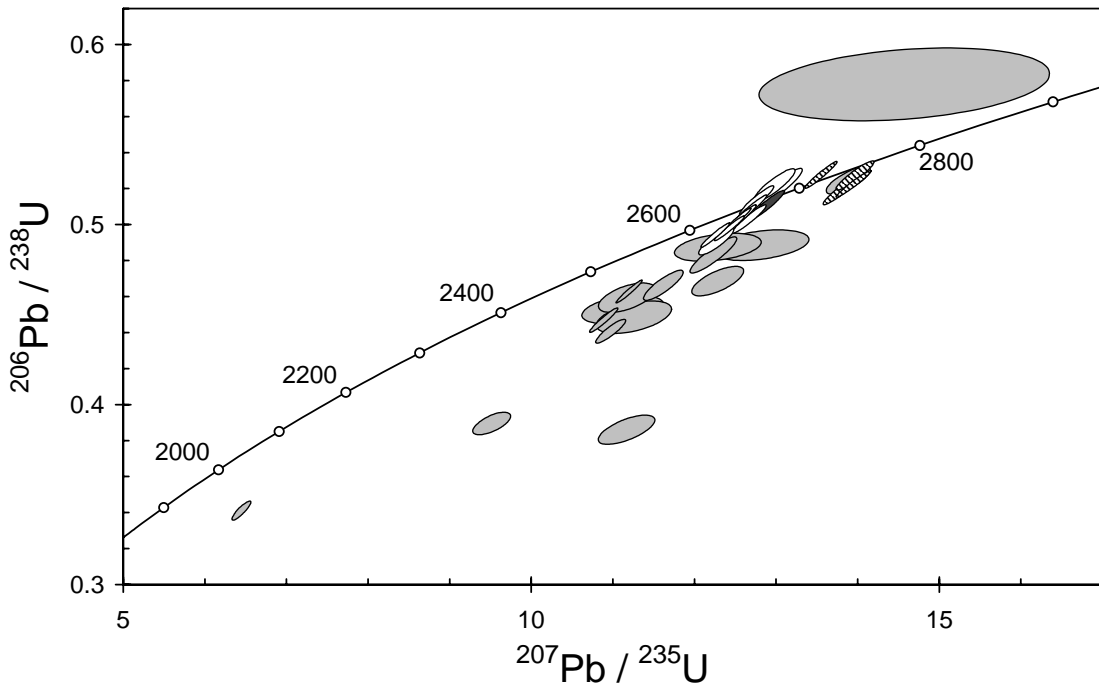


Figure 26. Concordia plot for zircons from sample 2001967039: Meredith monzogranite. White filled symbols are used to define the age of the sample; inherited grains have diagonal shading; older statistical outlier is dark grey; discordant and/or high common Pb analyses are light grey.

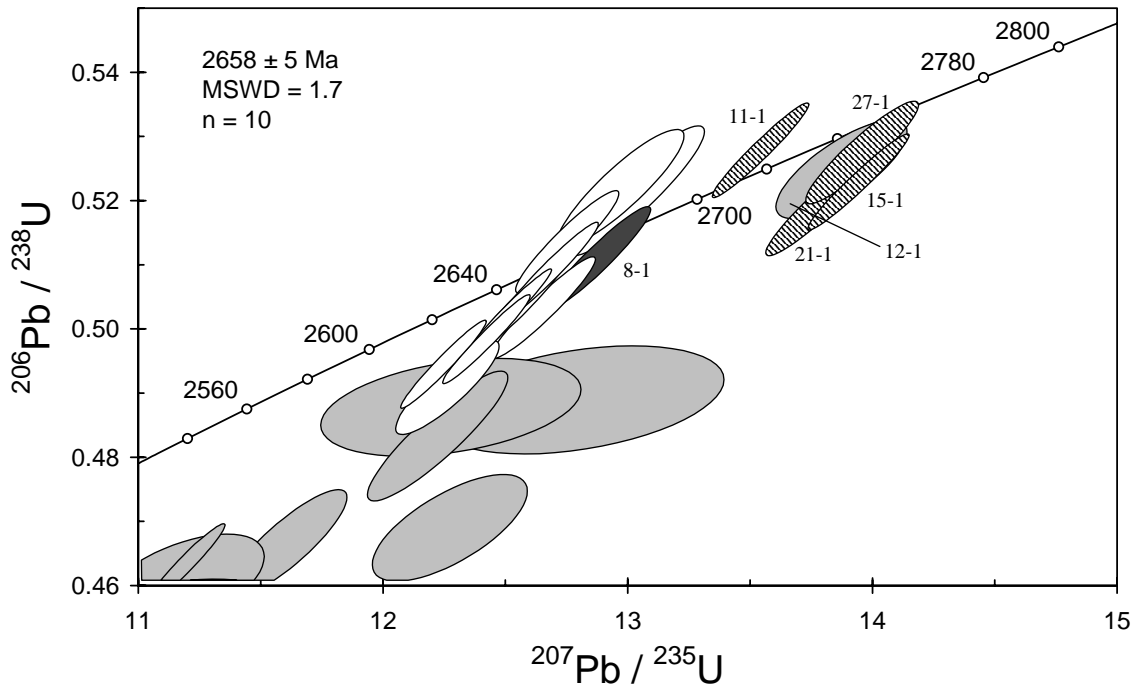


Figure 27. Enlargement of the main data group from sample 2001967039: Meredith monzogranite. Shading as in Figure 26.

200196 7040: volcanogenic meta-sandstone, Alabama prospect

1:250,000 sheet: Laverton (SH5102)

1:100,000 sheet: Laverton (3340)

MGA: 436437mE 6795660mN

Location: The sample was taken from Placer Dome Ltd diamond drillhole ALAD002, depth interval 266.50–268.00 m. The collar site is located in the Alabama prospect, approximately 10 km west-southwest of Brumby Well.

Description: This is from a grey, intensely altered, graded volcanogenic meta-sandstone unit, which is part of a strongly deformed and altered felsic to intermediate volcanoclastic and sedimentary sequence. The medium-grained, graded sandstone contains a variety of altered, sub-mm to 5 mm size angular to sub-rounded, quartz, quartzo-feldspathic, and lithic clasts. The lithic clasts include felsic, intermediate and mafic lithologies.

Principal minerals are micro-crystalline quartz and/or feldspar (45%), discrete poly- and monocrystalline quartz (10%), very-fine grained sericite (~25%), carbonate (8–10%), chlorite (5–8%), opaque minerals (2–3%), leucoxene/rutile (2–3%), and trace zircon. The sample is a strongly recrystallised, and intensely altered, poorly-sorted, clast-rich rock with a very fine-grained quartz-feldspar-rich matrix forming up to 25% of the rock. Recrystallised and altered clasts, generally < 3 mm, form about 75% of the rock and include monocrystalline quartz (~5%), chert (~5%), feldspar (~5%) and a variety of rock fragments. The quartz and chert clasts are generally sub-angular to sub-rounded, whereas recrystallisation and alteration hamper identification of the other clast types. The rock fragments have a variety of assemblages, including quartz-feldspar, quartz-sericite-carbonate, sericite-chlorite-carbonate-leucoxene/rutile and chlorite-rich assemblages, indicating a range of precursor lithologies. Opaque minerals occur as subhedral to anhedral and irregular grains disseminated throughout the matrix and concentrated in sericite-, chlorite- and carbonate-rich rock fragments. Carbonate also forms irregular to anhedral grains disseminated throughout the various rock fragments and matrix. Accessory phases include trace zircon.

Mount, pop: Z3813C

Description of zircons

Zircon from this sample comprises colourless and clear fragments and crystals. They are predominantly subhedral to euhedral, with moderate rounding of crystal faces. The zircon ranges from relatively small (~50 μm), equant or stubby grains, to elongate (aspect ratios of 2:1 to 3:1), grains which are generally larger (to about 170 μm , with one very large grain at 230 μm in length). Some grains contain small rounded and/or acicular inclusions, and some have pervasive fractures. Continuous euhedral concentric zoning is visible in transmitted light in about half the grains, but most display well-defined zoning in CL (Fig. 28). Distinct cores, overgrown by oscillatory-zoned zircon are common. Patchy or irregular zoning throughout some entire grains, and parts of grains, is typical of recrystallisation.

Concurrent standard data

This three-day session, analysing detrital zircon grains, used a shortened runtable (five scans instead of the standard seven). The session was interrupted twice: it was necessary to re-tune the primary ion column after eight analyses, and the duoplasmatron arc “dropped out” about 12 hours later. Both these interruptions caused a distinct shift in Pb/U calibration. The early analyses could not be properly assessed or recombined with later data, and were deleted. The second data block was also too small ($n = 7$ for QGNG) for a robust calibration. However, this calibration shift was smaller than the first. As the second block of data overlaps with others towards the end

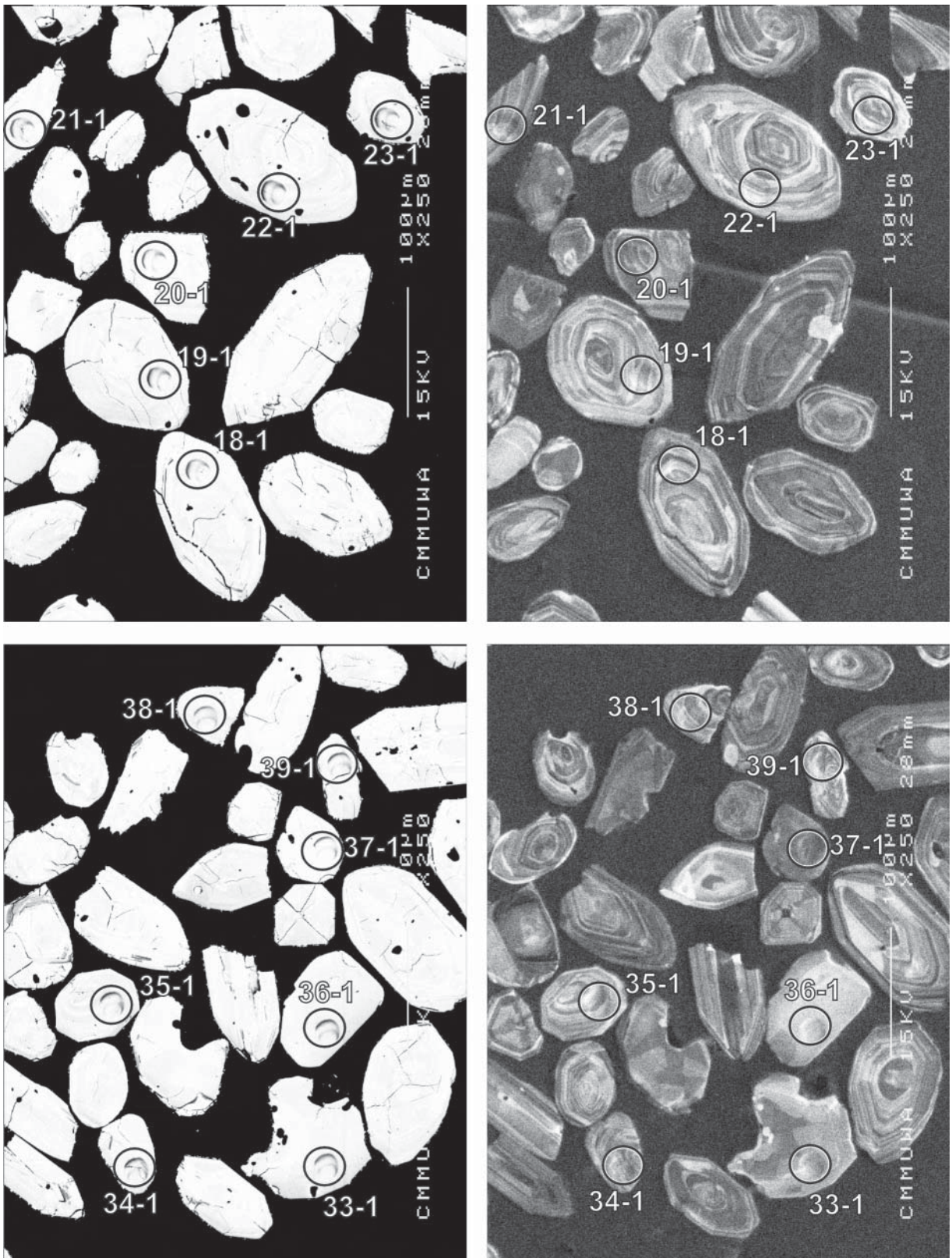


Figure 28. Representative SEM images (BSE on left, CL on right) for sample 2001967040: volcanogenic meta-sandstone, Alabama prospect. SHRIMP analysis spots are labelled. Remnant pits from the ion microprobe analyses are faintly visible in some grains. Scale bar is 100 μ m.

of the session, the data were all retained in a single block for processing. The resulting calibration is less precise than usual, but acceptable. The data produce a 1σ Pb/U scatter of 1.5% with MSWD = 10.4. The observed calibration slope is 1.95, and the default value of 2.0 was used. Omitting one $\sim 3\sigma$ (low) outlier and two other points leaves 41, with a weighted mean $^{207}\text{Pb}/^{206}\text{Pb}$ age of 1851.1 ± 2.5 Ma (MSWD = 1.01).

Element abundance calibration was based on CZ3 (n = 3).

Sample data

The 53 analyses on 52 grains (Table 14) are mostly concordant and apparently group fairly closely on a concordia plot (Fig. 29), but there is considerable real spread and unusual distribution of $^{207}\text{Pb}/^{206}\text{Pb}$ ages (Fig. 30), being weighted towards older values. There are possible source age peaks at ~ 2710 Ma and ~ 2670 Ma, with a minor peak at ~ 2650 Ma. The youngest single date is 2639 ± 5 Ma (1σ) from a grain (4-1) with moderate U content. A weighted mean $^{207}\text{Pb}/^{206}\text{Pb}$ age of 2648 ± 10 Ma (MSWD = 1.20) is obtained from the youngest 7 analyses.

Geochronological interpretation

The preferred interpretation for this sample is that the maximum depositional age for the rock is ~ 2650 Ma, although this peak is not strongly defined, with input from older sources at ~ 2670 Ma and 2710 Ma.

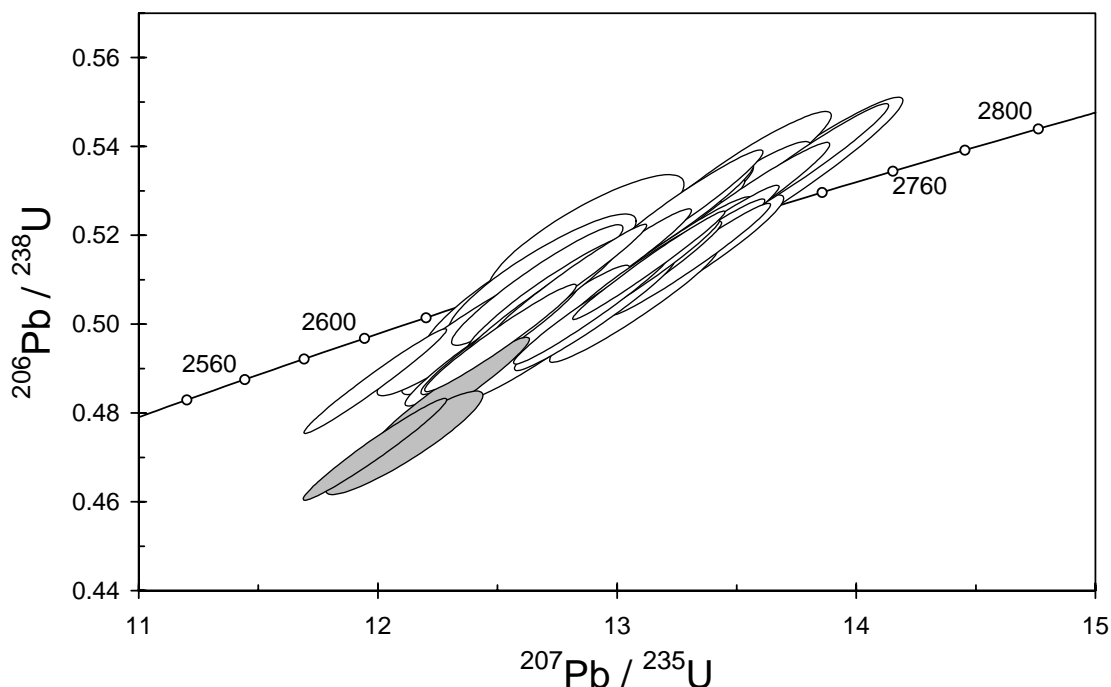


Figure 29. Concordia plot for zircons from sample 2001967040: volcanogenic meta-sandstone, Alabama prospect. White filled symbols are used to define the age of the sample and/or zircon sources; discordant analyses are light grey.

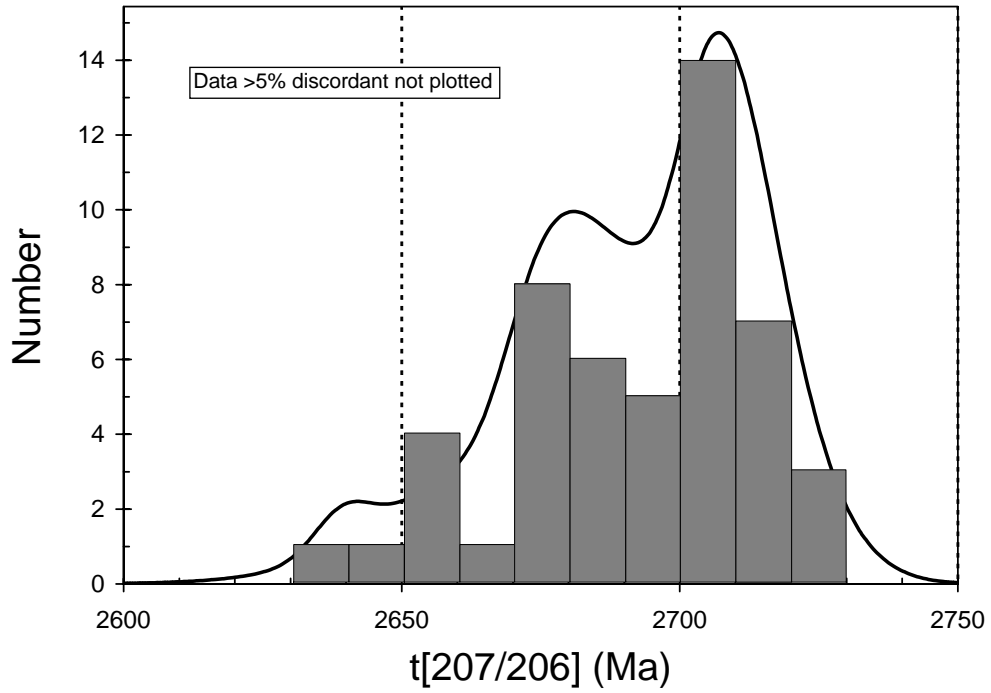


Figure 30. Cumulative probability plot for concordant data for zircons from sample 2001967040: volcanogenic meta-sandstone, Alabama prospect.

Table 14. SHRIMP analytical results for zircon from sample 2001967040: volcanogenic meta-sandstone, Alabama prospect, listed in order of $^{207}\text{Pb}/^{206}\text{Pb}$ age.

grain-spot	U (ppm)	Th (ppm)	4f206 (%)	^{207}Pb		^{206}Pb		^{207}Pb		^{208}Pb	conc. (%)	$^{207}\text{Pb}/^{206}\text{Pb}$	
				^{206}Pb	±	^{238}U	±	^{235}U	±			^{232}Th	Age (Ma)
4-1	246	81	0.057	0.1785	0.0006	0.487	0.008	11.98	0.20	0.132	97	2639	5
38-1	95	39	-0.032	0.1795	0.0020	0.520	0.009	12.86	0.27	0.145	102	2649	19
49-1	50	19	0.103	0.1801	0.0017	0.511	0.009	12.68	0.26	0.138	100	2654	16
32-1	50	23	0.032	0.1803	0.0012	0.497	0.009	12.35	0.24	0.131	98	2655	11
10-1	133	59	-0.034	0.1803	0.0019	0.507	0.010	12.60	0.28	0.136	100	2655	17
7-1	64	24	0.093	0.1806	0.0011	0.508	0.009	12.66	0.24	0.137	100	2658	10
16-1	47	17	0.089	0.1817	0.0013	0.498	0.009	12.47	0.25	0.137	98	2669	12
20-1	192	59	0.025	0.1821	0.0006	0.510	0.008	12.80	0.21	0.139	99	2672	6
48-1	61	20	0.038	0.1822	0.0011	0.507	0.009	12.73	0.24	0.141	99	2673	10
45-1	124	86	0.054	0.1823	0.0008	0.504	0.008	12.67	0.22	0.131	98	2674	7
52-1	24	9	0.000	0.1825	0.0016	0.505	0.011	12.71	0.31	0.141	98	2676	15
15-1	140	78	0.066	0.1827	0.0007	0.496	0.008	12.51	0.21	0.139	97	2678	6
34-1	101	31	0.074	0.1827	0.0009	0.496	0.008	12.50	0.22	0.134	97	2678	8
18-1	98	34	-0.033	0.1827	0.0009	0.494	0.008	12.44	0.22	0.128	96	2678	8
39-1	90	49	-0.001	0.1829	0.0008	0.526	0.009	13.26	0.23	0.145	102	2679	7
35-1	84	31	0.024	0.1833	0.0009	0.523	0.009	13.21	0.24	0.141	101	2683	8
27-1	78	30	-0.018	0.1833	0.0011	0.522	0.009	13.20	0.24	0.149	101	2683	10
41-2	115	49	0.039	0.1834	0.0008	0.513	0.009	12.97	0.22	0.139	99	2684	7
31-1	56	25	0.165	0.1836	0.0012	0.533	0.010	13.50	0.26	0.143	103	2685	11
19-1	71	22	-0.010	0.1836	0.0010	0.504	0.009	12.77	0.24	0.138	98	2686	9
17-1	73	24	0.078	0.1839	0.0011	0.519	0.009	13.17	0.24	0.139	100	2689	9
47-1	60	29	0.008	0.1841	0.0011	0.505	0.009	12.81	0.24	0.137	98	2691	10
50-1	109	38	0.032	0.1843	0.0009	0.500	0.008	12.71	0.22	0.135	97	2692	8
24-1	66	20	-0.039	0.1843	0.0010	0.513	0.009	13.04	0.24	0.139	99	2692	9
42-1	63	22	-0.041	0.1845	0.0011	0.514	0.009	13.07	0.24	0.147	99	2694	9
22-1	64	22	0.048	0.1848	0.0011	0.527	0.009	13.43	0.25	0.141	101	2696	10
13-1	55	41	0.075	0.1855	0.0012	0.506	0.009	12.95	0.25	0.140	98	2703	11
9-1	58	26	0.033	0.1856	0.0012	0.495	0.009	12.67	0.24	0.136	96	2703	10
30-1	279	128	0.004	0.1856	0.0005	0.513	0.008	13.13	0.21	0.140	99	2704	4
43-1	56	29	0.038	0.1856	0.0011	0.514	0.009	13.15	0.25	0.141	99	2704	10
36-1	43	23	0.048	0.1857	0.0014	0.512	0.010	13.12	0.27	0.141	99	2705	13
46-1	189	102	-0.007	0.1858	0.0008	0.511	0.008	13.10	0.22	0.140	98	2705	7
14-1	152	95	-0.014	0.1859	0.0007	0.503	0.008	12.89	0.22	0.140	97	2706	6
40-2	90	31	-0.001	0.1859	0.0009	0.515	0.009	13.21	0.23	0.141	99	2706	8
12-1	52	25	0.028	0.1860	0.0013	0.512	0.009	13.14	0.26	0.139	98	2708	12
23-1	86	48	0.045	0.1861	0.0009	0.504	0.009	12.93	0.23	0.141	97	2708	8
25-1	106	50	-0.011	0.1861	0.0008	0.527	0.009	13.53	0.24	0.141	101	2708	7
51-1	56	30	0.200	0.1861	0.0012	0.511	0.009	13.11	0.25	0.141	98	2708	11
14-2	129	58	-0.019	0.1862	0.0008	0.510	0.008	13.10	0.22	0.139	98	2709	7
21-1	115	42	-0.034	0.1862	0.0008	0.504	0.008	12.95	0.22	0.141	97	2709	7
8-1	115	49	-0.081	0.1863	0.0008	0.536	0.009	13.77	0.24	0.150	102	2710	7
44-1	75	66	0.165	0.1864	0.0010	0.512	0.009	13.16	0.24	0.140	98	2711	9
54-1	111	72	0.145	0.1865	0.0008	0.502	0.008	12.90	0.22	0.140	97	2712	7
3-1	55	22	0.128	0.1865	0.0012	0.533	0.012	13.70	0.33	0.139	101	2712	11
5-1	158	76	0.008	0.1866	0.0007	0.518	0.009	13.34	0.22	0.142	99	2713	6
26-1	63	44	0.088	0.1868	0.0016	0.509	0.010	13.12	0.27	0.139	98	2714	14
37-1	153	74	0.043	0.1869	0.0007	0.515	0.008	13.28	0.22	0.140	99	2715	6
33-1	65	47	-0.034	0.1875	0.0011	0.515	0.009	13.31	0.25	0.143	98	2720	10
6-1	162	65	0.001	0.1876	0.0007	0.514	0.008	13.30	0.22	0.143	98	2721	6
11-1	85	34	-0.052	0.1881	0.0009	0.504	0.009	13.07	0.23	0.144	96	2725	8
>5% discordant													
29-1	236	88	0.040	0.1858	0.0013	0.472	0.008	12.10	0.22	0.128	92	2705	12
28-1	108	41	0.059	0.1843	0.0009	0.484	0.008	12.30	0.21	0.128	94	2692	8
53-1	247	117	0.037	0.1844	0.0007	0.471	0.008	11.98	0.20	0.127	92	2693	6

Data are at 1σ precision. All Pb data are common-Pb corrected (based on ^{204}Pb and Broken Hill Pb composition). Analysis date: 28/01/02; session Z3813i.

2001967041A: banded biotite granitic gneiss, Twin Hills

1:250,000 sheet: Menzies (SH5105)

1:100,000 sheet: Melita (3139)

MGA: 315817mE 6743149mN

Location: This sample comes from a small pavement about 300 m south of a fence-line track, and about 2.5 km northwest of Jasper Well.

Description: The sample is from a grey-white, seriate to sparsely K-feldspar porphyritic, medium-grained biotite quartz-feldspathic gneiss. The granitic gneiss is intruded by sub-parallel dykes (<2 m in width) of foliated, fine- to medium-grained, biotite-poor seriate to quartz-K-feldspar porphyritic biotite monzogranite. Both phases are intruded by cross-cutting dykes (<3 m in width) of weakly-foliated, equigranular to moderately quartz-K-feldspar porphyritic, fine-grained biotite monzogranite. The foliation is not as strongly expressed in the later phases of monzogranite relative to the earlier granitic gneiss phase. Several generations of pegmatite veins cut the various granitic phases.

The sample has a recrystallised granoblastic texture. Principal minerals are quartz (35–40%), plagioclase (35–40%), K-feldspar (15–20%) and biotite (7–9%). Plagioclase occurs as subhedral to anhedral grains with no visible to very faint normal zoning, moderately common twinning, and trace myrmekite development. There is very minor, weakly- and locally-developed alteration to white mica, epidote/clinozoisite and carbonate. K-feldspar is anhedral, and displays common tartan twinning. Quartz is anhedral, commonly with very weak to moderate undulose extinction and minor, very weak sub-grain development. Biotite occurs as aligned, pale yellow to moderate green-brown elongate flakes, and clusters of flakes associated with minor titanite that display very minor and local replacement by chlorite, epidote/clinozoisite and rutile. Accessory phases include subhedral to anhedral titanite (1–2%; some grains may be secondary), apatite, zircon, and opaque minerals, and minor altered allanite (<1%). Secondary minerals include very minor to trace amounts of epidote/clinozoisite, chlorite, white mica, carbonate, rutile and titanite(?).

Mount, pop: 3881D

Description of zircons

Most zircon from this sample are pale grey-brown, euhedral to subhedral crystals with only slightly rounded crystal faces. Slight yellowish staining is present on some grains. The grains are generally stubby to elongate, with aspect ratios from about 2:1 to 4:1 (75 μm to 165 μm long), but some longer grains (up to 190 μm in length, aspect ratio 7:1) and smaller equant grains (from 40 μm) are also present. Small rod-like inclusions are visible in some grains. Continuous euhedral oscillatory zoning and some cores are clearly visible in transmitted light and CL (Fig. 31). Patches of recrystallised zircon occur in some grains.

Concurrent standard data

The apparent calibration slope for QGNG was 1.93. Neither of the concurrent samples was sufficiently single-aged to provide an alternate estimate and the default slope of 2.0 was used. Culling two outliers identified by SQUID, yields a 1σ scatter in the Pb/U calibration of 0.88% (MSWD = 5.1; $n = 31$). Applying the standardised assessment of $^{207}\text{Pb}/^{206}\text{Pb}$ data results in the omission of three low- $^{207}\text{Pb}/^{206}\text{Pb}$ points, and gives a weighted mean age of 1850.3 ± 2.4 ($n = 29$; MSWD = 1.00).

Element abundance calibration was based on CZ3 ($n = 4$).

Sample data

Thirty one analyses were obtained from individual grains (Table 15). Several show a strong zero-age discordance trend (Fig. 32), and there is one obviously inherited grain (1-1), and one anomalously

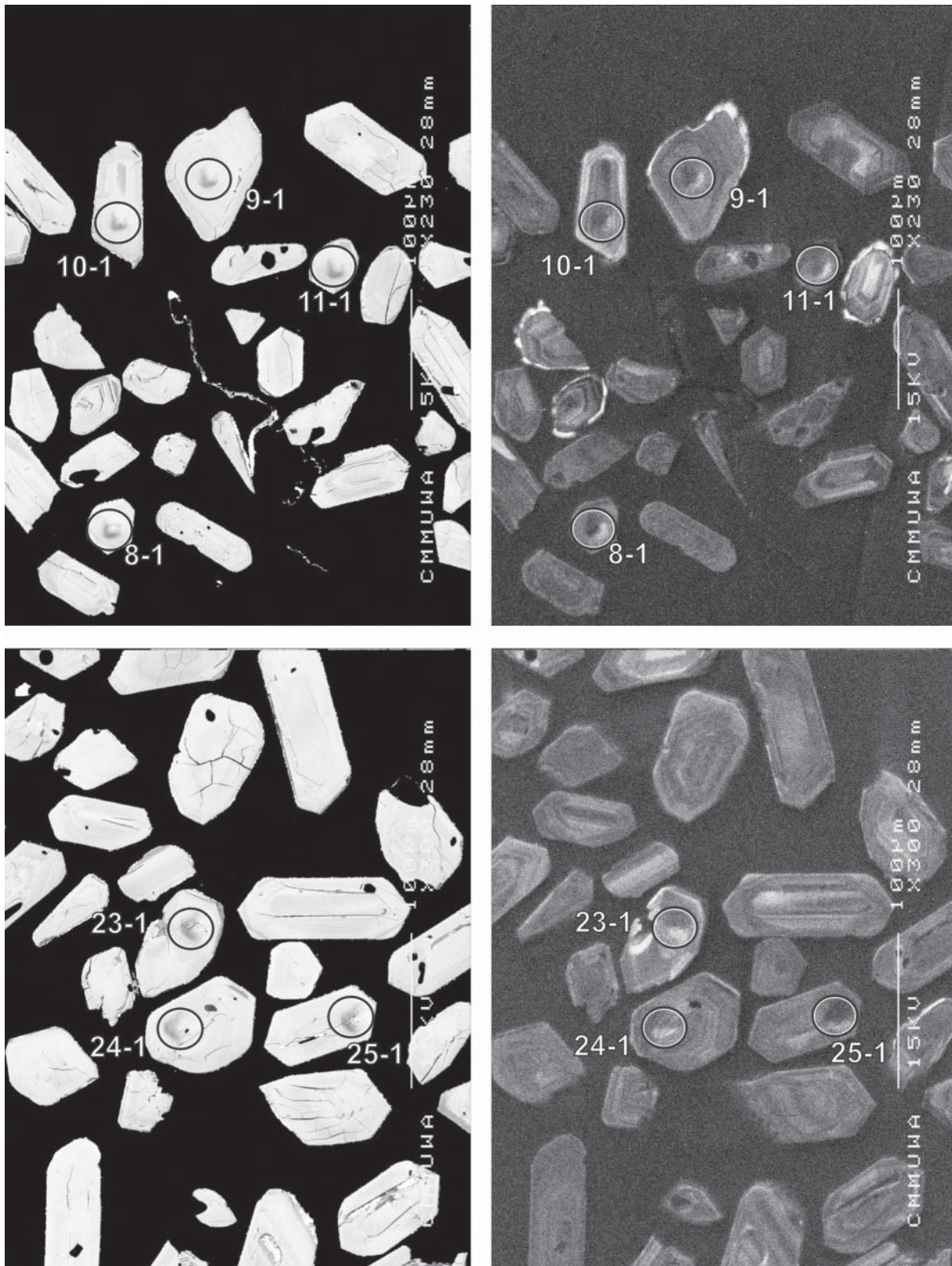


Figure 31. Representative SEM images (BSE on left, CL on right) for sample 2001967041A: banded biotite granitic gneiss, Twin Hills. SHRIMP analysis spots are labelled. Remnant pits from the ion microprobe analyses are faintly visible in some grains. Scale bar is 100 μ m.

young analysis which also has very high-U (13-1). The remaining 23 analyses fall in a single group (Fig.33), but are considerably scattered (MSWD = 3.3). Omitting three analyses (20-1, 22-1, 27-1) that are $>3\sigma$ outliers to the main group leaves 20 analyses with a weighted mean $^{207}\text{Pb}/^{206}\text{Pb}$ age of 2802.8 ± 2.8 (essentially unchanged date, but with MSWD = 1.9).

Geochronological interpretation

The age of 2803 ± 3 Ma is considered most likely to be the age of the granitic protolith of the gneiss.

Table 15. SHRIMP analytical results for zircon from sample 2001967041A: banded biotite granitic gneiss, Twin Hills.

grain-spot	U (ppm)	Th (ppm)	4f206 (%)	$^{207}\text{Pb}/^{206}\text{Pb}$		$^{206}\text{Pb}/^{238}\text{U}$		$^{207}\text{Pb}/^{235}\text{U}$		$^{208}\text{Pb}/^{232}\text{Th}$	conc. (%)	$^{207}\text{Pb}/^{206}\text{Pb}$ Age (Ma)	
					\pm		\pm		\pm				\pm
Main group													
2-1	547	417	0.081	0.1977	0.0003	0.526	0.005	14.34	0.13	0.145	97	2807	3
3-1	219	66	0.058	0.1966	0.0005	0.528	0.006	14.30	0.18	0.143	98	2798	4
5-1	221	96	0.033	0.1985	0.0010	0.531	0.006	14.53	0.19	0.140	97	2814	8
6-1	120	57	0.032	0.1971	0.0007	0.534	0.006	14.52	0.16	0.145	98	2803	6
7-1	492	365	0.013	0.1982	0.0003	0.525	0.005	14.35	0.13	0.143	97	2811	3
9-1	162	62	0.031	0.1961	0.0006	0.536	0.005	14.50	0.15	0.144	99	2794	5
10-1	200	123	0.005	0.1976	0.0005	0.545	0.005	14.85	0.15	0.150	100	2807	4
11-1	125	57	0.006	0.1981	0.0007	0.547	0.006	14.94	0.17	0.151	100	2810	6
12-1	181	78	0.016	0.1960	0.0006	0.545	0.005	14.72	0.15	0.147	100	2793	5
15-1	239	124	0.012	0.1971	0.0005	0.543	0.005	14.75	0.15	0.149	100	2802	4
16-1	403	224	0.159	0.1974	0.0004	0.520	0.005	14.16	0.14	0.145	96	2805	3
18-1	232	134	0.173	0.1971	0.0006	0.529	0.005	14.37	0.15	0.144	98	2803	5
19-1	87	41	-0.077	0.1963	0.0009	0.544	0.006	14.74	0.18	0.150	100	2796	7
21-1	250	117	0.049	0.1964	0.0005	0.545	0.005	14.77	0.15	0.147	100	2797	4
23-1	134	75	0.169	0.1967	0.0007	0.512	0.005	13.89	0.15	0.127	95	2799	6
24-1	208	84	0.127	0.1963	0.0005	0.529	0.005	14.32	0.15	0.132	98	2795	5
25-1	529	267	0.001	0.1966	0.0003	0.531	0.005	14.41	0.14	0.153	98	2799	3
26-1	314	93	0.038	0.1981	0.0013	0.537	0.006	14.68	0.18	0.147	99	2811	10
29-1	113	58	0.008	0.1970	0.0007	0.540	0.006	14.67	0.17	0.149	99	2802	6
30-1	95	45	0.024	0.1981	0.0008	0.536	0.006	14.64	0.17	0.149	98	2810	7
Inherited													
1-1	264	204	0.155	0.2100	0.0008	0.538	0.005	15.58	0.16	0.133	95	2905	6
Young outlier													
13-1	1907	793	0.017	0.1877	0.0009	0.500	0.004	12.94	0.13	0.122	96	2722	8
3σ outliers													
20-1	392	271	0.016	0.1952	0.0006	0.536	0.006	14.43	0.16	0.140	99	2786	5
22-1	597	195	0.030	0.1983	0.0003	0.541	0.005	14.80	0.14	0.154	99	2812	3
27-1	479	263	0.019	0.1959	0.0003	0.536	0.005	14.48	0.14	0.140	99	2793	3
$>5\%$ discordant													
4-1	811	232	0.287	0.1872	0.0023	0.294	0.012	7.60	0.32	0.110	61	2718	20
8-1	1241	280	0.066	0.1870	0.0012	0.463	0.005	11.92	0.14	0.126	90	2716	10
14-1	174	50	0.446	0.1953	0.0008	0.471	0.007	12.67	0.18	0.132	89	2788	6
17-1	256	207	0.257	0.1988	0.0012	0.496	0.005	13.61	0.15	0.126	92	2816	10
28-1	173	98	0.357	0.1949	0.0010	0.340	0.003	9.12	0.10	0.071	68	2784	8
31-1	119	58	0.310	0.1972	0.0009	0.499	0.005	13.58	0.16	0.156	93	2803	7

Data are at 1σ precision. All Pb data are common-Pb corrected (based on ^{204}Pb and Broken Hill Pb composition). Analysis date: 2/05/02; session Z3881j.

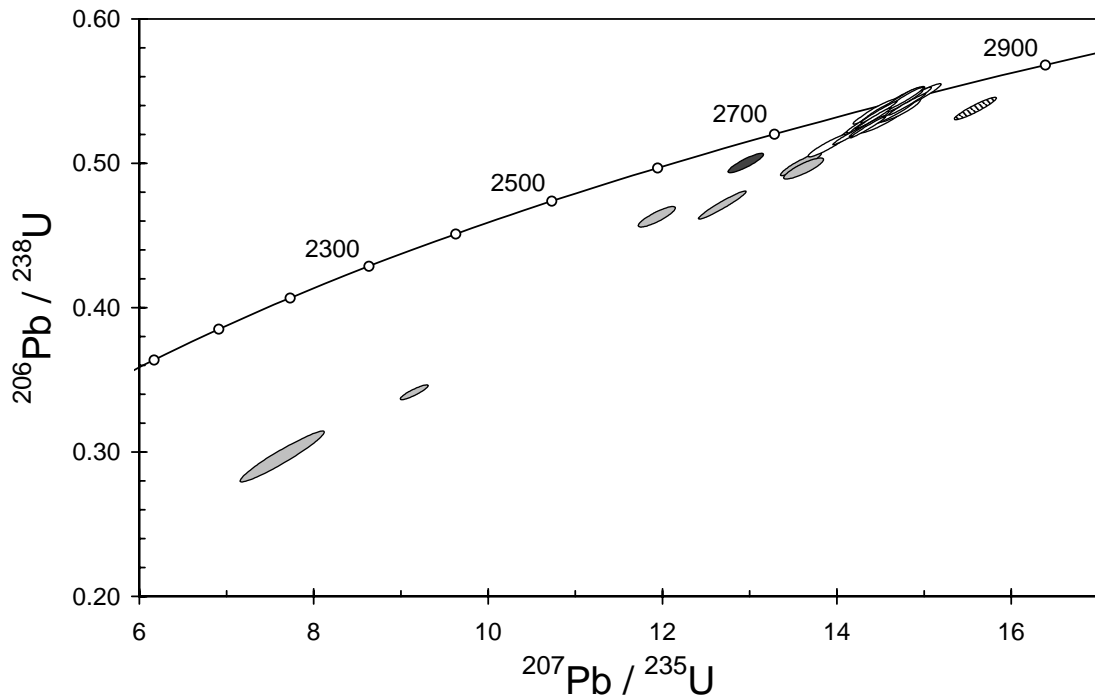


Figure 32. Concordia plot for zircons from sample 2001967041A: banded biotite granitic gneiss, Twin Hills. White filled symbols are used to define the age of the sample; inherited grain has diagonal shading; three younger and one older outliers are dark grey; discordant analyses are light grey.

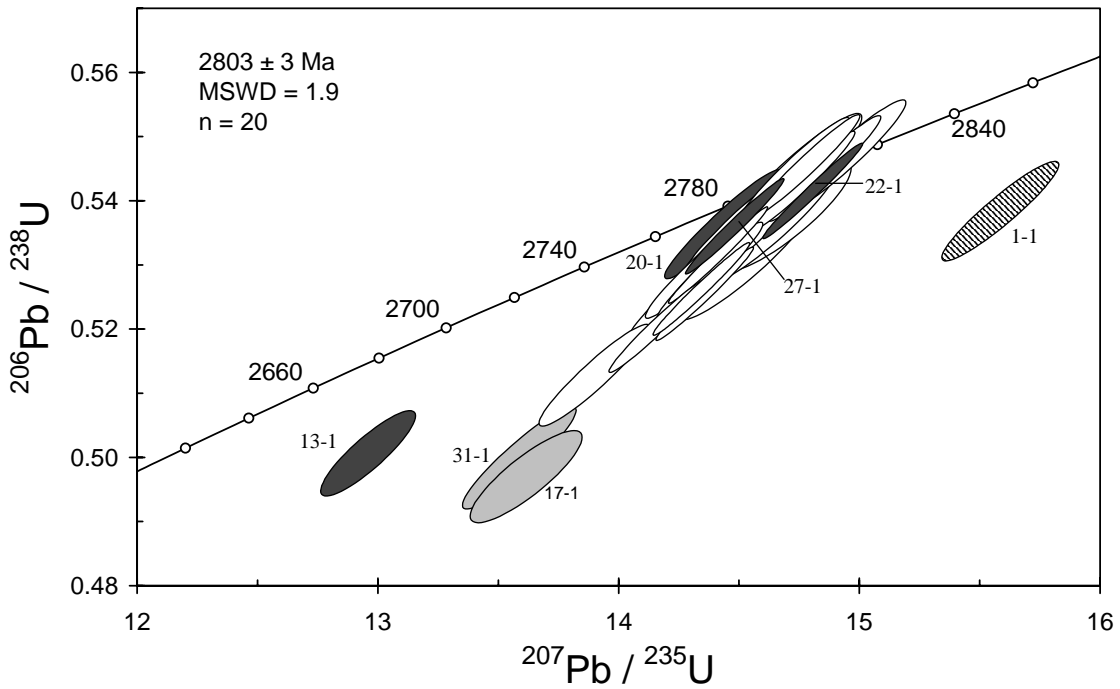


Figure 33. Concordia plot for the main group of data from sample 2001967041A: banded biotite granitic gneiss, Twin Hills. Shading as in Figure 32.

2001967043: Galah Monzogranite

- 1:250,000 sheet:** Menzies (SH5105)
- 1:100,000 sheet:** Melita (3139)
- MGA:** 333794mE 6741934mN
- Location:** The sample was collected from an old blast site near Galah Rockhole about 2 km east of the Menzies - Leonora Road.
- Description:** This is a cream to grey-pink, seriate to weakly K-feldspar porphyritic, medium to coarse-grained biotite monzogranite. It contains minor biotite-rich schlieren, and is cut by minor thin pegmatite veins and joints.
- The unit is characterised by a granular texture. The principal minerals are K-feldspar (30–35%), quartz (30–35%), plagioclase (25–30%), biotite (4–5%) and muscovite (2–3%). K-feldspar is subhedral to anhedral, with common well-developed tartan twinning, and minor perthite, particularly in larger grains. Plagioclase is subhedral to anhedral, and displays locally-developed, faint oscillatory or normal zoning, mostly in grain cores. Twinning is common and some myrmekite is present. Locally, plagioclase is variably replaced by white mica, epidote/clinozoisite and carbonate, including some large grains of muscovite. Quartz is anhedral, with moderately-developed undulose extinction and minor sub-grain development along grain boundaries. Biotite occurs as light yellow to medium-dark red-brown elongate flakes that are generally partly to completely replaced by chlorite, epidote/clinozoisite, rutile, fluorite and/or white mica. Muscovite forms large (?primary) flakes (to >1 mm) localised with biotite grain clusters, and as large (?secondary) grains in altered plagioclase. Accessory phases include zircon, opaque minerals, and rare altered titanite. Secondary minerals include minor chlorite, white mica/muscovite, epidote/clinozoisite, rutile, fluorite, carbonate, and trace hematite.
- Mount, pop:** Z3812B

Description of zircons

The zircon grains are predominantly euhedral to subhedral whole crystals, but some anhedral fragments are also present. The grains vary from equant to elongate (aspect ratio to 4:1) and from 65 μm to >350 μm in size. Some rounding of crystal faces is noted, and fracturing is common. The zircon are pale grey to brown, mostly turbid, but occasionally clear. Continuous core to rim euhedral zoning is common, as is recrystallisation and metamictisation (Fig.34). Some grains contain well-rounded or euhedral cores with clear overgrowths.

Concurrent standard data

The primary beam became increasingly unstable during the last 12 hours of this analytical session, and the last ~8 hours of data were subsequently deleted from files. The retained data for QGNG give a robust Pb/U calibration; after omitting one outlier identified by SQUID, the apparent calibration slope is 2.08 ($n = 24$), with 1σ scatter in Pb/U = 1.04% and MSWD = 5.7. This slope is sufficiently close to the default value (2.0) for it to be used.

Assessment of $^{207}\text{Pb}/^{206}\text{Pb}$ for these data is difficult. Omitting only the single U/Pb calibration outlier results in a typical weighted mean $^{207}\text{Pb}/^{206}\text{Pb}$ age (1850 ± 4 Ma) but with considerable excess scatter (MSWD = 1.7). This might be associated with primary beam instability late in the session — if the data had been truncated ~8 hours earlier, there would be no scatter (MSWD = 1.08, $n = 16$) and the mean age similar (1848.2 ± 3.9 Ma). Alternatively, omitting two 2σ outliers (one high and one low value) and two other points very close to 2σ (also one high and one low) gives 1849.4 ± 3.2 Ma with MSWD = 1.03. The nature of the excess scatter is such that the preferred data assessment protocol (refer to chapter on “Data compilation for the QGNG standard”) does not work well. Applying a low-side culling procedure to force MSWD close to

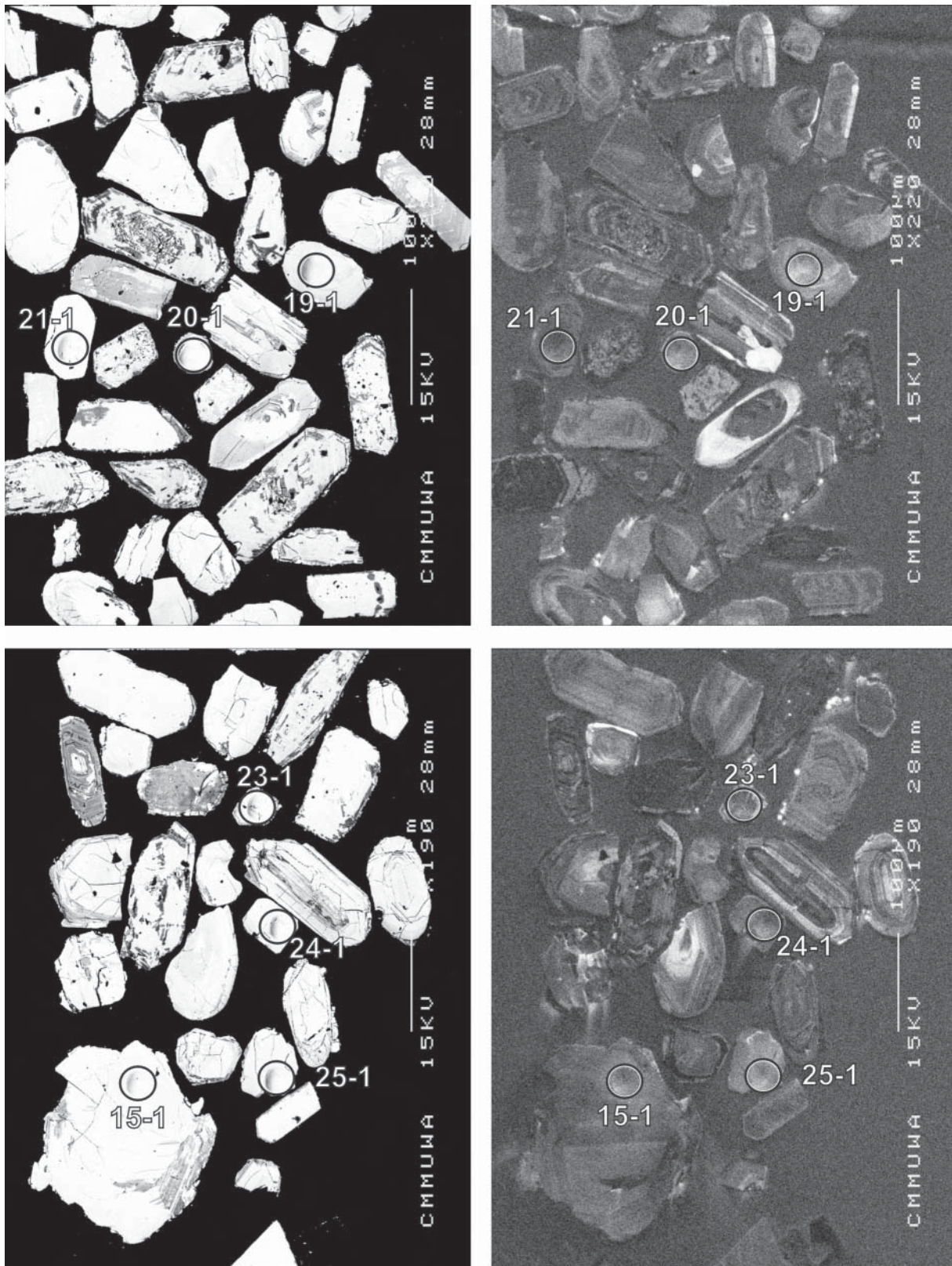


Figure 34. Representative SEM images (BSE on left, CL on right) for sample 2001967043: Galah Monzogranite. SHRIMP analysis spots are labelled. Remnant pits from the ion microprobe analyses are faintly visible in some grains. Scale bar is 100 μ m.

unity results in an abnormally high number of data rejections (>30% of data). For consistency with other data sets, we have applied low-side culling, but stopped at MSWD = 1.3, which retains 20 analyses. The corresponding weighted mean $^{207}\text{Pb}/^{206}\text{Pb}$ age is 1852.3 ± 3.7 Ma.

Element abundance calibration was based on CZ3 (n = 2).

Sample data

Twenty four analyses were taken, each on separate grains (Table 16). Three analyses (1-1, 7-1, 17-1) are strongly discordant and another (20-1) is anomalously young, presumably due to Pb loss (Fig. 35). Two analyses (11-1, 21-1) are clearly old outliers, interpreted to represent inherited grains, and one low-precision analysis (2-1) is also apparently older than the main group. The remaining cluster of data is internally complex, including data from at least two age populations (Fig. 36). A possible older group of five analyses gives a weighted mean $^{207}\text{Pb}/^{206}\text{Pb}$ age of 2689.3 ± 3.5 Ma (MSWD = 0.78), while the youngest six give 2641.6 ± 6.7 Ma, with MSWD = 1.3 (Fig. 37).

Geochronological interpretation

Given that the monzogranite shows no signs of intense metamorphism, and the youngest data subgroup is from zircons with modest U contents (i.e. they do not have the typically low U of metamorphic grains), the age of the youngest subgroup is taken to be the crystallisation age of the rock (2642 ± 8 Ma). There is a significant xenocrystic component at ~ 2690 Ma, although this date could be partially reset from an older value.

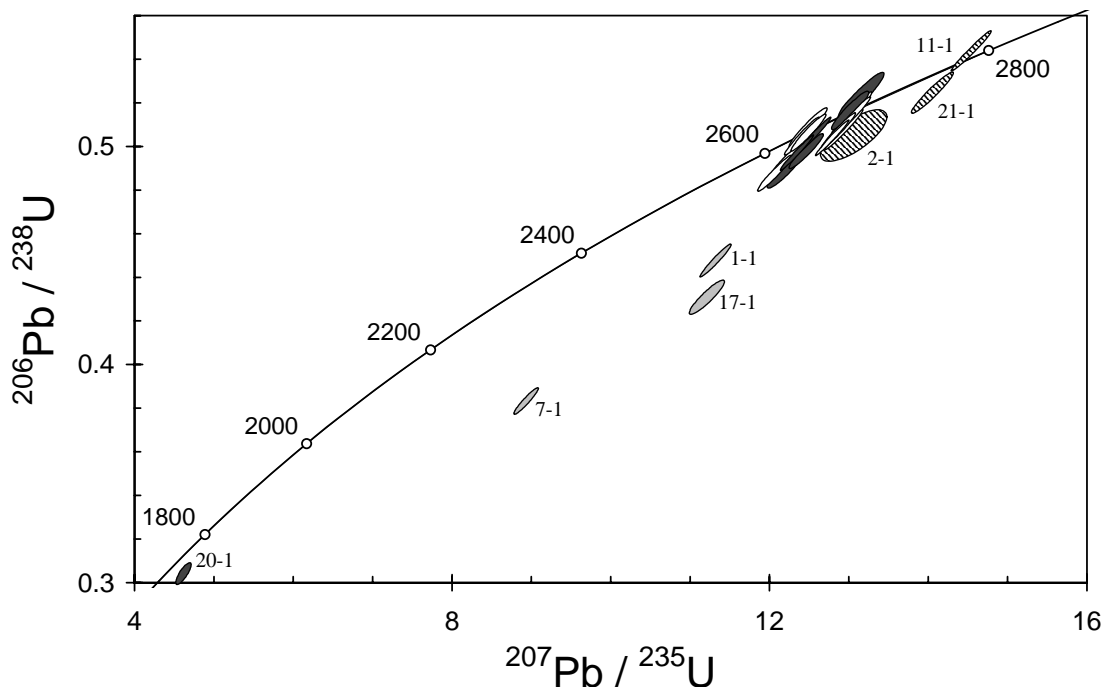


Figure 35. Concordia plot for zircons from sample 2001967043: Galah Monzogranite. White filled symbols are used to define ages for the two groups in the main data cluster; inherited grains have diagonal shading; statistical outliers are dark grey; discordant analyses are light grey.

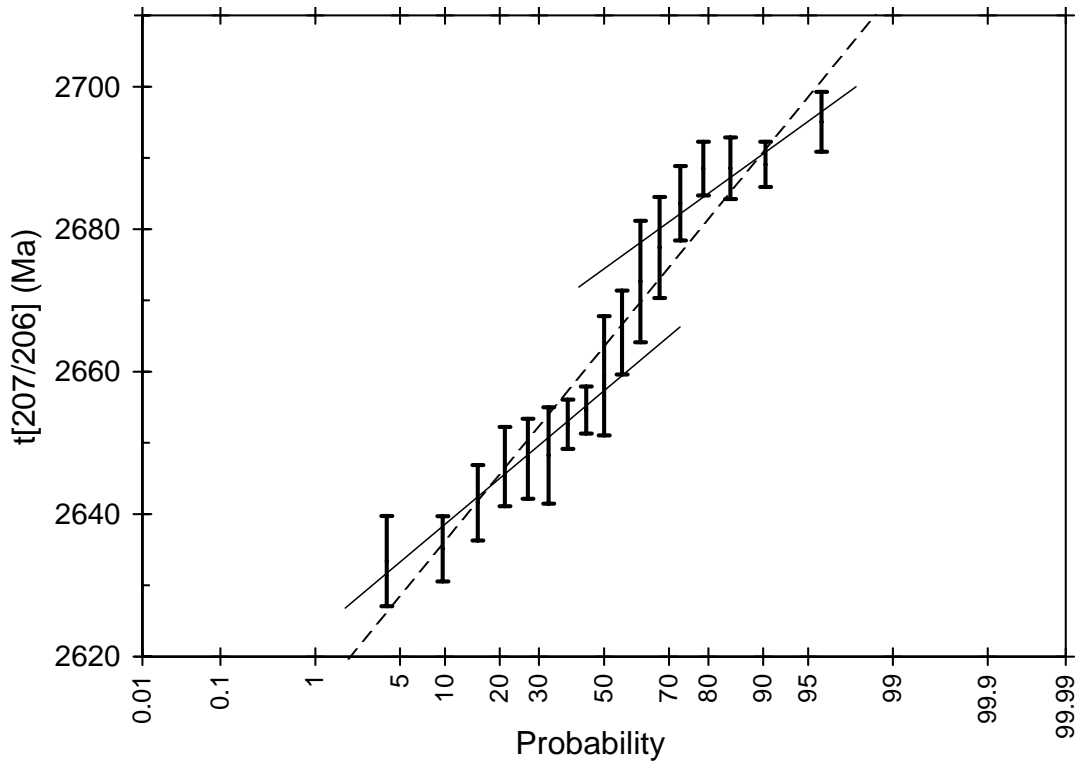


Figure 36. Cumulative probability plot for the main data cluster ($n = 17$) for sample 2001967043: Galah Monzogranite showing (poorly defined) multiple age sub-populations.

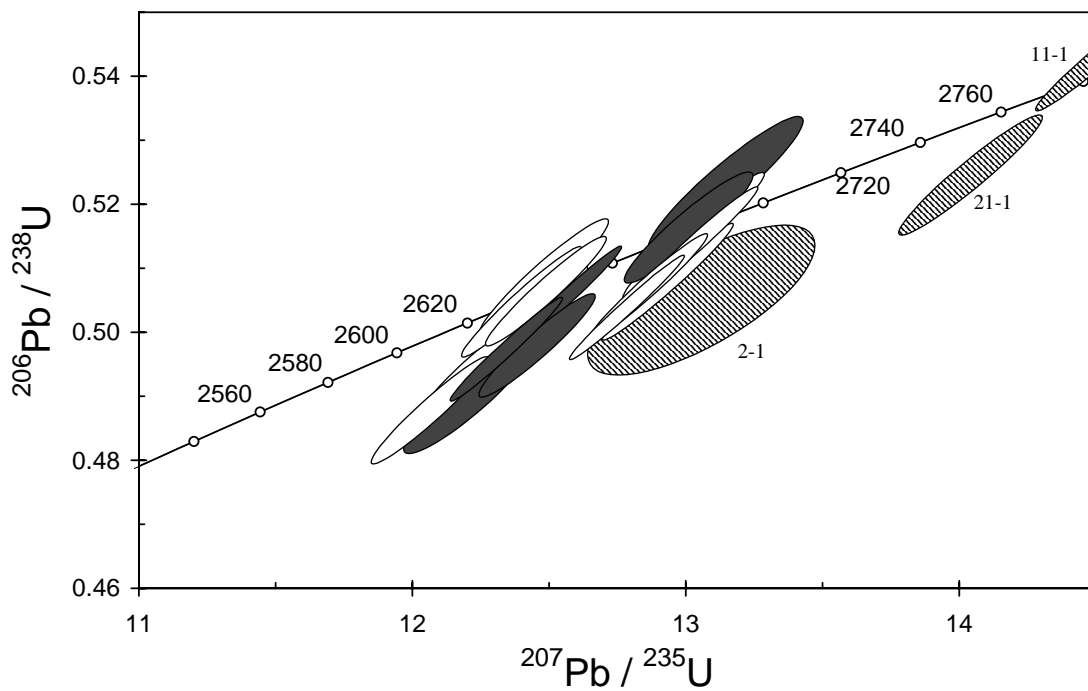


Figure 37. Enlargement of main data cluster for sample 2001967043: Galah Monzogranite. Shading as in Fig. 35.

Table 16. SHRIMP analytical results for zircon from sample 2001967043:Galah Monzogranite.

grain-spot	U (ppm)	Th (ppm)	4f206 (%)	^{207}Pb		^{206}Pb		^{207}Pb		^{208}Pb	conc. (%)	$^{207}\text{Pb}/^{206}\text{Pb}$	
				^{206}Pb	±	^{238}U	±	^{235}U	±			^{232}Th	Age (Ma)
Possibly magmatic grains													
10-1	136	165	0.044	0.1793	0.0006	0.488	0.006	12.05	0.14	0.137	97	2647	6
12-1	208	189	0.020	0.1788	0.0006	0.506	0.006	12.48	0.15	0.139	100	2642	5
14-1	219	200	-0.006	0.1781	0.0005	0.505	0.006	12.39	0.15	0.140	100	2635	5
15-1	130	108	0.046	0.1779	0.0007	0.509	0.006	12.47	0.16	0.139	101	2633	6
18-1	150	174	0.013	0.1794	0.0006	0.501	0.006	12.41	0.15	0.138	99	2648	6
25-1	144	70	0.152	0.1795	0.0007	0.495	0.006	12.24	0.15	0.136	98	2648	7
Inherited													
2-1	84	36	-0.007	0.1875	0.0027	0.505	0.008	13.05	0.28	0.140	97	2720	24
11-1	251	113	-0.012	0.1938	0.0005	0.544	0.006	14.53	0.17	0.149	101	2775	4
21-1	119	40	0.081	0.1941	0.0007	0.525	0.006	14.04	0.18	0.138	98	2778	6
Possibly inherited													
3-1	414	99	0.006	0.1800	0.0004	0.497	0.005	12.34	0.14	0.135	98	2653	3
4-1	382	94	-0.035	0.1839	0.0004	0.514	0.006	13.04	0.15	0.143	99	2689	4
5-1	266	132	-0.002	0.1846	0.0005	0.508	0.006	12.93	0.16	0.139	98	2695	4
6-1	218	128	0.121	0.1834	0.0006	0.515	0.007	13.02	0.17	0.141	100	2684	5
9-1	344	122	0.001	0.1802	0.0004	0.505	0.005	12.55	0.14	0.138	99	2655	3
13-1	57	23	0.102	0.1822	0.0009	0.523	0.007	13.14	0.19	0.139	101	2673	9
16-1	198	59	0.457	0.1807	0.0009	0.489	0.006	12.19	0.15	0.210	96	2659	8
19-1	478	224	0.006	0.1840	0.0004	0.504	0.005	12.78	0.14	0.140	98	2689	3
22-1	342	150	0.153	0.1827	0.0008	0.516	0.006	13.01	0.16	0.145	100	2677	7
23-1	433	238	0.280	0.1814	0.0006	0.498	0.005	12.45	0.14	0.142	98	2665	6
24-1	309	112	-0.016	0.1839	0.0005	0.507	0.006	12.86	0.15	0.140	98	2689	4
>5% discordant or anomalously young													
1-1	413	231	0.078	0.1831	0.0006	0.447	0.005	11.30	0.13	0.124	89	2682	5
7-1	1638	2374	0.255	0.1688	0.0006	0.383	0.004	8.91	0.10	0.095	82	2546	6
17-1	229	122	0.021	0.1885	0.0010	0.431	0.005	11.19	0.15	0.115	85	2729	9
20-1	573	423	0.513	0.1095	0.0008	0.304	0.003	4.58	0.06	0.087	95	1791	14

Data are at 1σ precision. All Pb data are common-Pb corrected (based on ^{204}Pb and Broken Hill Pb composition). No analysis was made on grain 8. Analysis date: 17/12/01; session Z3812i.

2001967045: biotite monzogranite dyke, Balarky Rocks

1:250,000 sheet: Menzies (SH5105)

1:100,000 sheet: Menzies (3138)

MGA: 333452mE 6725745mN

Location: The sample was taken from a large boulder, on the eastern edge of the extensive rocky outcrops at Balarky Rock, about 2 km west-southwest of Balarky Tank.

Description: It is from a grey-pink, equigranular to moderately quartz-feldspar porphyritic, fine-grained biotite monzogranite dyke which intrudes the Balarky monzogranite, a seriate to sparsely K-feldspar porphyritic, medium-grained biotite monzogranite. The dyke contains minor, small (<10 cm), biotite-rich clots and schlieren, K-feldspar, quartz, and plagioclase phenocrysts. It is cut by rare, thin, pegmatite veins.

The sample has a granular texture. Principal minerals are K-feldspar (32–37%), quartz (32–37%), plagioclase (22–27%), and biotite (5–6%). K-feldspar is subhedral to anhedral, and displays common well-developed tartan twinning, rare simple twinning, and minor to locally moderate perthite. Plagioclase occurs as subhedral to anhedral grains, that are unzoned to variably zoned. Patchy normal or oscillatory zoning occurs in grain cores. Minor to moderate twinning is present. Minor to locally moderate myrmekite developed. The plagioclase is locally altered to white mica and epidote/clinozoisite. Quartz is anhedral, with common minor to moderate undulose extinction and minor sub-grain development along grain boundaries. Biotite forms small, light yellow to medium-dark red-brown, ragged flakes that are variably replaced by chlorite, epidote/clinozoisite, rutile, fluorite and/or white mica. Accessory phases include zircon, opaque minerals and trace apatite. Secondary minerals include minor chlorite, white mica, epidote/clinozoisite, rutile, and trace fluorite and hematite.

Mount, pop: Z3812A

Description of zircons

The zircon consists of fragments and crystals ranging from small (~65 μm) and equant, to larger (up to 200 μm) elongated (aspect ratio 3:1) grains. Most grains are subhedral to euhedral and have relatively well-defined crystal faces, although some rounding is present. The grains are colourless to yellow-brown (due to Fe-oxide staining?), and are either clear or turbid. Fractures are common, and the grains contain some rod-like and/or rounded inclusions. Many grains display well-defined zoning in CL (Fig. 38), but some recrystallisation and metamictisation is present. Both euhedral and well-rounded cores with thin rims are visible in transmitted and reflected light, and in CL. In rare cases, up to two stages of overgrowth are visible.

Concurrent standard data

The primary beam became increasingly unstable during the last 12 hours of this analytical session, and the last ~8 hours of data were subsequently deleted from files. The retained data for QGNG give a sound Pb/U calibration; after omitting one outlier identified by SQUID, the apparent calibration slope is 2.08 ($n = 24$), with 1σ scatter in Pb/U = 1.04% and MSWD = 5.7. This slope is sufficiently close to the default value (2.0) for it to be used.

Assessment of $^{207}\text{Pb}/^{206}\text{Pb}$ for these data is difficult. Omitting only the single U/Pb calibration outlier results in a typical weighted mean $^{207}\text{Pb}/^{206}\text{Pb}$ age (1850 ± 4 Ma) but there is considerable excess scatter (MSWD = 1.7). This might be associated with primary beam instability late in the session — if the data had been truncated ~8 hours earlier, there would be no scatter (MSWD = 1.08, $n = 16$) and the mean age similar (1848.2 ± 3.9 Ma). Alternatively, omitting two 2σ outliers (one high and one low value) and two other points very close to 2σ (also one high and one low) gives 1849.4 ± 3.2 Ma with MSWD = 1.03. The nature of the excess scatter is such

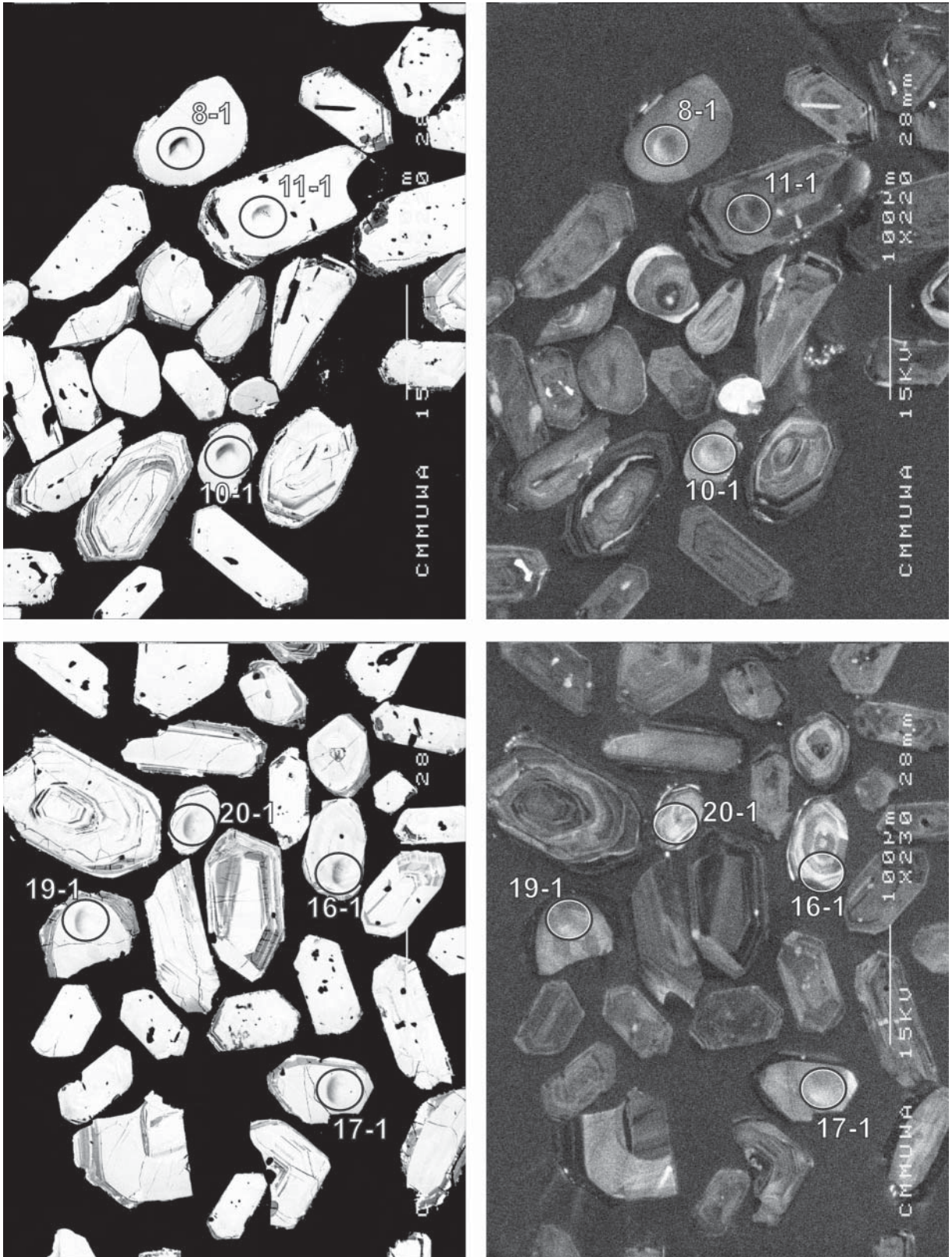


Figure 38. Representative SEM images (BSE on left, CL on right) for sample 2001967045: biotite monzogranite dyke, Balarky Rocks. SHRIMP analysis spots are labelled. Remnant pits from the ion microprobe analyses are faintly visible in some grains. Scale bar is 100 μ m.

that the preferred data assessment protocol (refer to chapter on “Data compilation for the QGNG standard”) does not work well. Applying a low-side culling procedure to force MSWD close to unity results in an abnormally high number of data rejections (>30% of data). For consistency with other data sets, we have applied low-side culling, but stopped at MSWD = 1.3, which retains 20 analyses. The corresponding weighted mean $^{207}\text{Pb}/^{206}\text{Pb}$ age is 1852.3 ± 3.7 Ma.

Element abundance calibration was based on CZ3 (n = 2).

Sample data

Twenty two analyses were obtained from individual grains (Table 17). Several analyses were disregarded, including one discordant analysis (22-1), one with high common Pb (21-1), two with very high U and Th (11-1 and 24-1), and five (3-1, 12-1, 16-1, 20-1, 23-1) that appear to represent inherited grains (Fig. 39). One of the latter appears to be derived from a metamorphosed rock (23-1; very low U and Th). The remaining 13 analyses appear to form a single group (Fig. 40), and give a weighted mean $^{207}\text{Pb}/^{206}\text{Pb}$ age of 2651.3 ± 5.8 Ma, but with some excess scatter (MSWD = 1.9). Omitting one $\sim 2\sigma$ old outlier (13-1) improves this to MSWD = 1.5 and gives an age of 2649.4 ± 5.7 Ma (Fig. 34).

Geochronological interpretation

The crystallisation age of the dyke is interpreted to be 2649 ± 7 Ma.

Table 17. SHRIMP analytical results for zircon from sample 2001967045: biotite monzogranite dyke, Balarky Rocks.

grain-spot	U (ppm)	Th (ppm)	4f206 (%)	$^{207}\text{Pb}/^{206}\text{Pb}$	\pm	$^{206}\text{Pb}/^{238}\text{U}$	\pm	$^{207}\text{Pb}/^{235}\text{U}$	\pm	$^{208}\text{Pb}/^{232}\text{Th}$	conc. (%)	Age (Ma)	\pm
Main group													
6-1	224	285	0.143	0.1795	0.0006	0.505	0.006	12.50	0.15	0.143	100	2648	6
1-1	61	76	0.413	0.1805	0.0011	0.499	0.007	12.43	0.19	0.144	98	2658	10
4-1	141	121	0.169	0.1809	0.0008	0.497	0.006	12.39	0.16	0.147	98	2661	7
8-1	77	128	0.078	0.1798	0.0008	0.486	0.006	12.04	0.16	0.136	96	2651	8
9-1	157	85	0.021	0.1803	0.0005	0.512	0.006	12.74	0.15	0.143	100	2656	5
10-1	60	54	0.048	0.1809	0.0009	0.494	0.006	12.33	0.17	0.137	97	2662	9
14-1	73	52	-0.003	0.1782	0.0009	0.511	0.007	12.56	0.17	0.139	101	2636	9
15-1	125	175	0.204	0.1784	0.0009	0.483	0.006	11.89	0.15	0.129	96	2638	8
17-1	66	85	0.036	0.1789	0.0009	0.506	0.007	12.47	0.18	0.140	100	2643	9
18-1	107	93	0.141	0.1779	0.0009	0.485	0.006	11.90	0.16	0.134	97	2634	8
19-1	119	134	0.021	0.1799	0.0007	0.493	0.006	12.22	0.16	0.137	97	2652	7
25-1	107	156	0.068	0.1788	0.0009	0.500	0.007	12.33	0.19	0.139	99	2642	8
Old outliers													
3-1	118	17	0.762	0.1864	0.0019	0.534	0.007	13.71	0.22	0.396	102	2710	16
12-1	102	38	0.067	0.1889	0.0008	0.527	0.006	13.73	0.18	0.145	100	2733	7
13-1	150	61	0.044	0.1812	0.0006	0.511	0.006	12.76	0.15	0.141	100	2664	5
16-1	85	53	0.329	0.1965	0.0011	0.530	0.007	14.36	0.20	0.149	98	2797	9
20-1	68	48	0.099	0.1923	0.0010	0.516	0.007	13.68	0.19	0.151	97	2762	8
23-1	12	3	0.058	0.1825	0.0025	0.492	0.011	12.39	0.32	0.127	96	2675	23
>5% discordant, high common Pb or high U+Th													
11-1	898	994	0.024	0.1847	0.0003	0.515	0.005	13.12	0.14	0.143	99	2695	2
21-1	117	130	1.840	0.1800	0.0027	0.537	0.006	13.33	0.25	0.207	104	2653	24
22-1	61	17	0.258	0.1800	0.0021	0.403	0.006	10.01	0.20	0.099	82	2653	19
24-1	874	1074	0.043	0.1774	0.0011	0.530	0.006	12.97	0.17	0.151	104	2628	10

Data are at 1σ precision. All Pb data are common-Pb corrected (based on ^{204}Pb and Broken Hill Pb composition). Analysis date: 17/12/01; session Z3812i. Analyses 2-1, 5-1, 7-1 were lost due to technical problems.

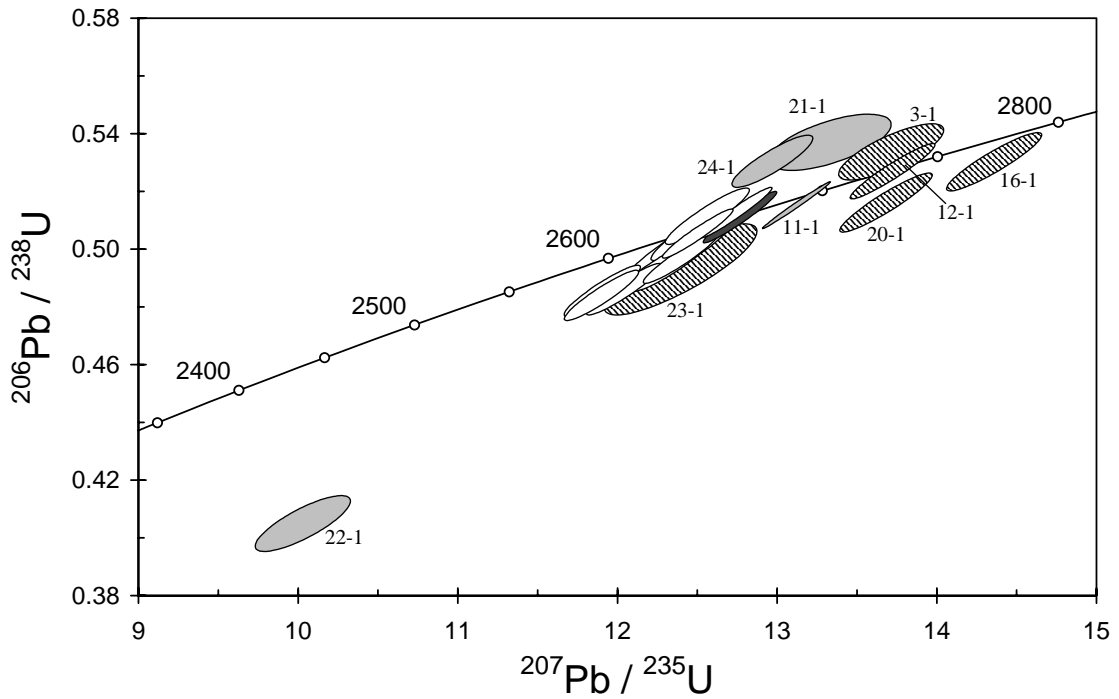


Figure 39. Concordia plot for zircons from sample 2001967045: biotite monzogranite dyke, Balarky Rocks. White filled symbols might define the age of the sample; inherited grains have diagonal shading; older outlier is dark grey; discordant, high common Pb and high U+Th analyses are light grey.

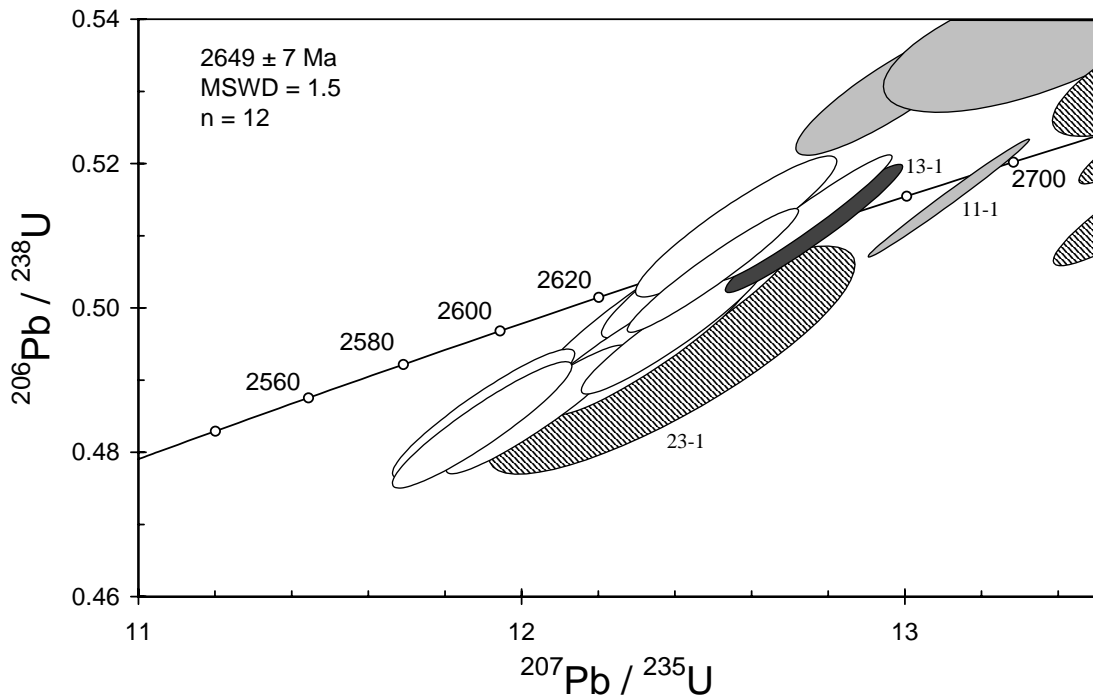


Figure 40. Concordia plot for the main data group from sample 2001967045: biotite monzogranite dyke, Balarky Rocks. Shading as in Figure 39.

2001967048: Republic amphibole porphyry, Wiluna

1:250,000 sheet:	Wiluna (SG5109)
1:100,000 sheet:	Wiluna (2944)
MGA:	225386mE 7052780mN
Location:	The sample comes from Newmont Australia Ltd diamond drillhole WD494, depth interval 1080.10–1085.30 m. The collar site is located above the Golden Age deposit, approximately 5 km southeast of Wiluna.
Description:	This is a small, moderately altered, medium-grained amphibole-feldspar porphyry dyke, locally referred to as the Republic porphyry. The ~20 m thick intrusion is one of several, stratigraphy-parallel dykes localised beneath the Golden Age reef and interpreted to be syn-kinematic. The porphyry contains altered amphibole and feldspar phenocrysts within a moderately altered groundmass of chlorite, sericite, carbonate, quartz and albite.
Mount, pop:	Z3922A

Description of zircons

Zircon from this sample are strikingly uniform in size, morphology and colour. The population consists of predominantly prismatic euhedral crystals with little, if any, rounding of crystal faces. The grains are all colourless to very pale yellow-grey, and are very clear, although small inclusions are locally present. Fractures are absent. Most grains range from about 50 μm to 100 μm in length (aspect ratios of 2:1), but a few larger, more elongate grains are also present (up to 170 μm long, aspect ratios to 4:1). There are no obvious internal features in transmitted or reflected light, but in CL many grains display distinct sector zoning and/or oscillatory zoning (Fig. 41).

Concurrent standard data

During this analytical session, the primary beam progressively became unstable. Following assessment, data were truncated after 30 hours, leaving a relatively short data file. Nevertheless, the remaining QGNG data give an acceptable Pb/U calibration (1σ scatter = 0.96%; $n = 22$; MSWD = 4.6). Assessing the $^{207}\text{Pb}/^{206}\text{Pb}$ data is difficult, partly because of the variable data quality and the modest number of points. The standard culling procedure does not work well, removing a rather large proportion of the data. Culling was stopped at MSWD ≥ 1.3 (refer to chapter on “Data compilation for the QGNG standard”), resulting in a weighted mean $^{207}\text{Pb}/^{206}\text{Pb}$ age of 1851.7 ± 3.7 Ma (MSWD = 1.4; $n = 21$).

Element abundance calibration was based on CZ3 ($n = 3$).

Sample data

Twenty one analyses were obtained from separate grains (Table 18). The data are all concordant and group closely on a concordia plot (Fig. 42), but with some excess scatter in $^{207}\text{Pb}/^{206}\text{Pb}$ (MSWD = 1.5). Omitting one $>2\sigma$ outlier (10-1) gives a weighted mean $^{207}\text{Pb}/^{206}\text{Pb}$ age of 2770.1 ± 2.4 Ma for the remaining 20 analyses, with MSWD = 1.3. This level of scatter is similar to that seen in the concurrent data for QGNG, and might result from some unidentified systematic problem during this session. Additional culling of data is not justified.

Geochronological interpretation

The age of 2770 ± 3 Ma is considered to be the crystallisation age of the lamprophyre.

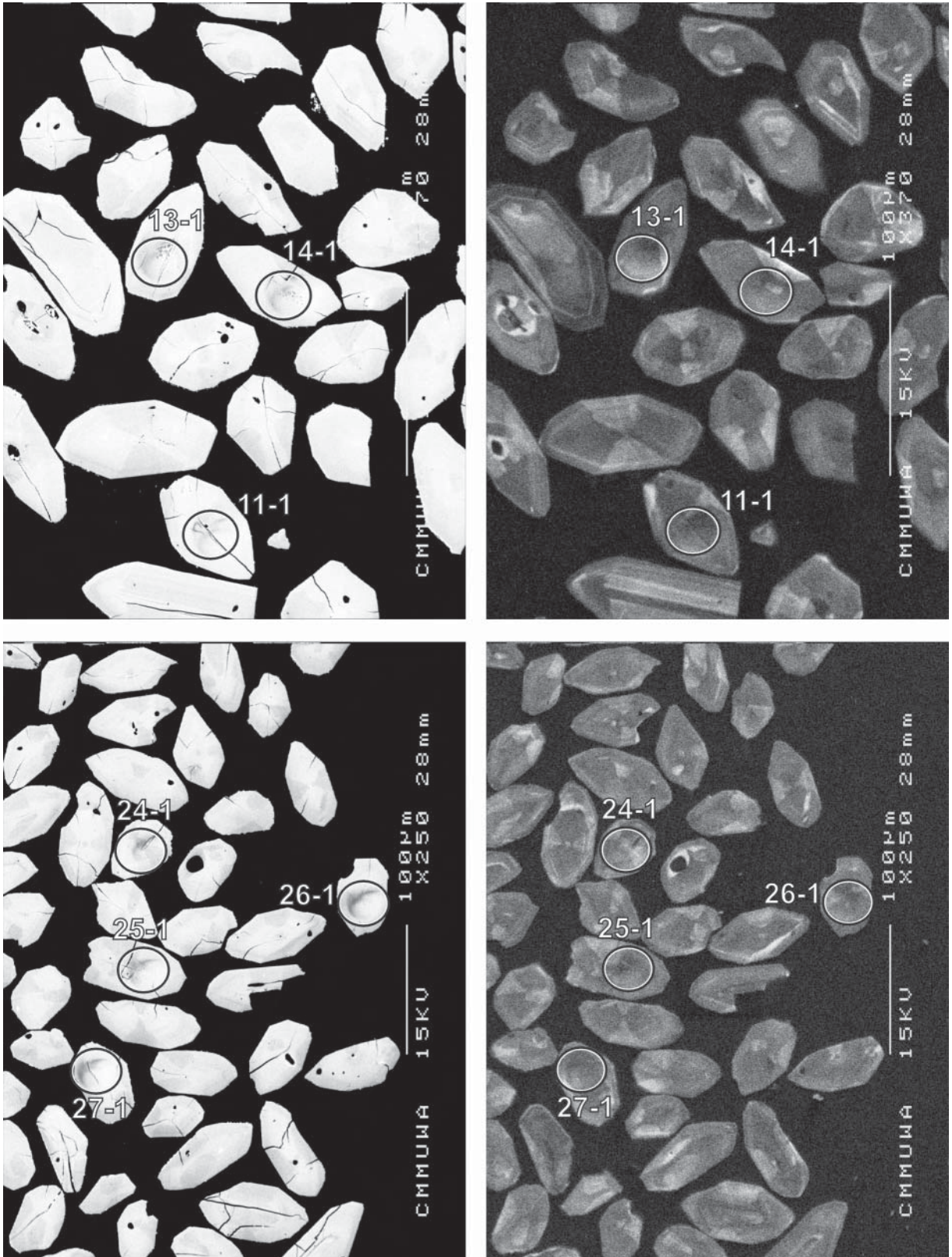


Figure 41. Representative SEM images (BSE on left, CL on right) for sample 2001967048: Republic amphibole porphyry, Wiluna. SHRIMP analysis spots are labelled. Remnant pits from the ion microprobe analyses are faintly visible in some grains. Scale bar is 100 μm .

Table 18. SHRIMP analytical results for zircon from sample 2001967048: Republic amphibole porphyry, Wiluna.

grain-spot	U (ppm)	Th (ppm)	4f206 (%)	$^{207}\text{Pb}/^{206}\text{Pb}$		$^{206}\text{Pb}/^{238}\text{U}$		$^{207}\text{Pb}/^{235}\text{U}$		$^{208}\text{Pb}/^{232}\text{Th}$	conc. (%)	$^{207}\text{Pb}/^{206}\text{Pb}$ Age (Ma)	
					\pm		\pm		\pm				\pm
Main group													
1-1	163	66	0.013	0.1935	0.0005	0.526	0.006	14.02	0.16	0.142	98	2772	5
2-1	170	64	0.016	0.1929	0.0005	0.529	0.006	14.07	0.16	0.146	99	2767	4
3-1	205	78	-0.001	0.1927	0.0005	0.532	0.006	14.14	0.16	0.143	99	2766	4
4-1	179	75	0.007	0.1943	0.0005	0.527	0.006	14.13	0.16	0.145	98	2779	4
5-1	171	63	0.023	0.1926	0.0005	0.537	0.006	14.26	0.16	0.146	100	2765	5
6-1	164	66	-0.003	0.1932	0.0005	0.533	0.006	14.20	0.16	0.143	99	2770	4
7-1	181	68	0.020	0.1925	0.0005	0.532	0.006	14.11	0.16	0.148	99	2764	4
8-1	153	61	0.053	0.1934	0.0006	0.541	0.007	14.42	0.18	0.148	101	2772	5
9-1	208	89	0.010	0.1935	0.0005	0.533	0.006	14.21	0.16	0.147	99	2772	4
11-1	190	67	0.047	0.1934	0.0005	0.539	0.006	14.36	0.16	0.146	100	2771	4
12-1	183	72	0.043	0.1929	0.0005	0.524	0.006	13.94	0.16	0.145	98	2767	5
13-1	145	56	0.011	0.1931	0.0006	0.536	0.006	14.28	0.16	0.144	100	2769	5
14-1	148	63	0.013	0.1944	0.0007	0.529	0.006	14.19	0.17	0.147	98	2780	6
15-1	162	63	-0.012	0.1932	0.0005	0.535	0.006	14.26	0.16	0.147	100	2770	5
16-1	166	54	-0.002	0.1939	0.0005	0.536	0.006	14.33	0.16	0.148	100	2775	4
17-1	186	67	-0.004	0.1937	0.0005	0.538	0.006	14.37	0.16	0.148	100	2774	4
18-1	219	91	0.013	0.1923	0.0004	0.523	0.006	13.87	0.17	0.145	98	2762	4
19-1	145	65	0.022	0.1924	0.0007	0.535	0.009	14.20	0.24	0.148	100	2763	6
20-1	160	65	0.065	0.1935	0.0005	0.527	0.006	14.05	0.16	0.146	98	2772	4
21-1	162	60	0.026	0.1943	0.0007	0.531	0.006	14.21	0.16	0.145	99	2779	6
Young outlier													
10-1	139	53	0.025	0.1918	0.0006	0.540	0.006	14.28	0.16	0.147	101	2758	5

Data are at 1 σ precision. All Pb data are common-Pb corrected (based on ^{204}Pb and Broken Hill Pb composition). Analysis date: 13/05/02; session Z3922j.

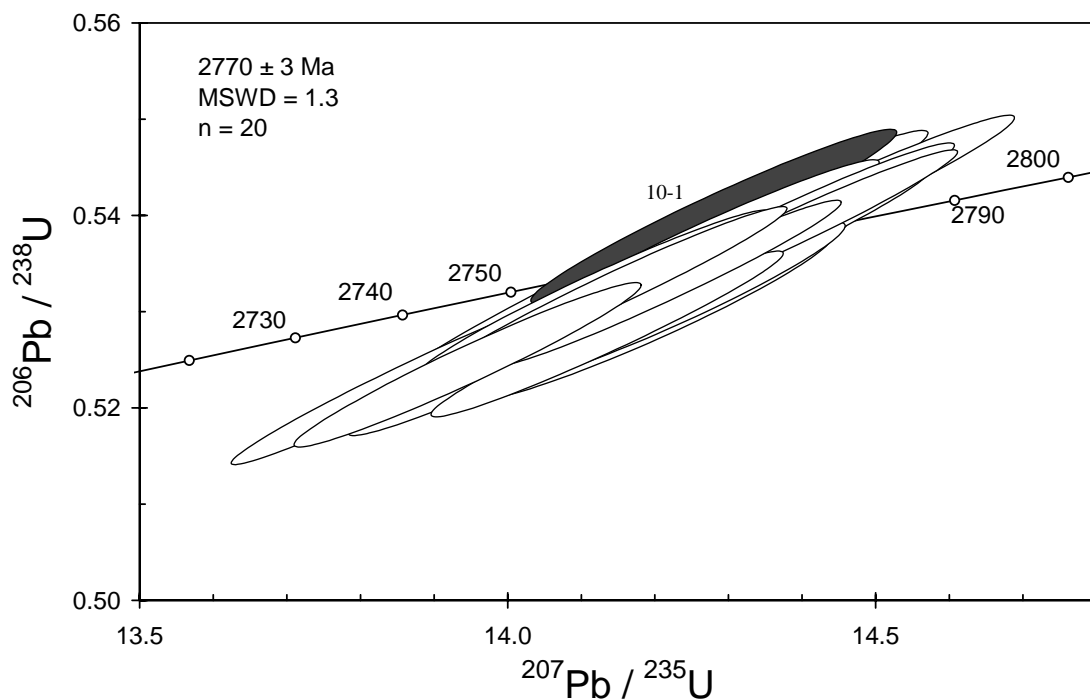


Figure 42. Concordia plot for zircons from sample 2001967048: Republic amphibole porphyry, Wiluna. White filled symbols are used to define the age of the sample; young outlier is dark grey.

2001967052C: Fifima sandstone

1:250,000 sheet: Sir Samuel (SG5113)

1:100,000 sheet: Depot Springs (2942)

MGA: 253813mE 6902721mN

Location: The sample was taken from Barrick Gold of Australia Ltd diamond drillhole GSUG0072, interval 293.00–294.00 m. The collar for the west-directed subhorizontal drillhole is in the Genesis South underground mine, about 2.5 kms northwest of Agnew.

Description: It is an altered, medium-grained meta-sandstone that is locally referred to as the Fifima sandstone. It contains cyclic graded beds of fine- to very coarse-grained sandstone, with pebbly and silty horizons, granitoid and rip-up clasts. The sandstone is characterised by trough cross-bedding, scours with armoured bases and pebble layers, and asymmetric ripple marks. This rock is part of the Scotty Creek conglomerate, a west-facing, cyclic-graded siltstone to conglomerate sequence that dips very steeply to the west and is locally overturned.

Principal minerals are quartz (47–52%), plagioclase (22–27%), biotite (12–17%) and carbonate (8–12%), with minor opaque minerals, white mica, chlorite, leucoxene/rutile and trace zircon and apatite. The sample exhibits a strongly recrystallised, granulated quartz, feldspar and biotite mosaic, with a typical grain size of 0.1 to 0.2 mm through which larger, recrystallised quartz, feldspar, and lithic clasts, up to >1 mm, are disseminated. The quartz and feldspar clasts are broken and variably recrystallised. Lithic clasts include recrystallised granitoid, chert and more mica-rich lithologies (characterised by biotite-rich aggregates). Chert clasts are identified by fine-grained disseminated opaque minerals, and the granitoid clasts by variably recrystallised and altered quartz and feldspar grains in a finer-grained quartz-feldspathic matrix. The rock is strongly foliated, as defined by aligned, elongate clusters of yellow to red-brown biotite flakes and the fine-grained quartzofeldspathic mosaic. Feldspar grains display weak to moderate albite twinning, and are variably altered to white mica and carbonate. Carbonate also occurs as irregular to anhedral grains. Accessory phases include zircon and apatite. Retrograde alteration minerals include minor chlorite and white mica.

Mount, pop: Z3813B

Description of zircons

The zircon ranges in size from approximately 50 μm to over 200 μm in length (aspect ratios from 1:1 to 4:1). The colourless to pale grey-brown crystals and fragments are subhedral to euhedral with slight rounding of crystal faces. Inclusions and fractures are locally present. Systematic euhedral oscillatory zoning is visible in most grains in CL (Fig. 43), although some grains display recrystallisation features. A number of grains are comprised of small cores and overgrowths.

Concurrent standard data

This three-day session, analysing detrital zircon grains, used a shortened runtable (five scans instead of the standard seven). The session was interrupted twice: it was necessary to re-tune the primary ion column after eight analyses, and the duoplasmatron arc “dropped out” about 12 hours later. Both these interruptions caused a distinct shift in Pb/U calibration. The early analyses could not be properly assessed or recombined with later data, and were deleted. The second data block was also too small ($n = 7$ for QGNG) for a robust calibration. However, this calibration shift was smaller than the first, and as the second block of data overlaps with others towards the end of the session, the data were all retained in a single block for processing. The resulting calibration is less precise than usual, but acceptable. The data produce a 1σ Pb/U scatter of 1.5% with MSWD = 10.4. The observed calibration slope is 1.95, and the default value of 2.0 was used. Omitting one $\sim 3\sigma$ (low) outlier and two other points leaves 41 analyses with a weighted

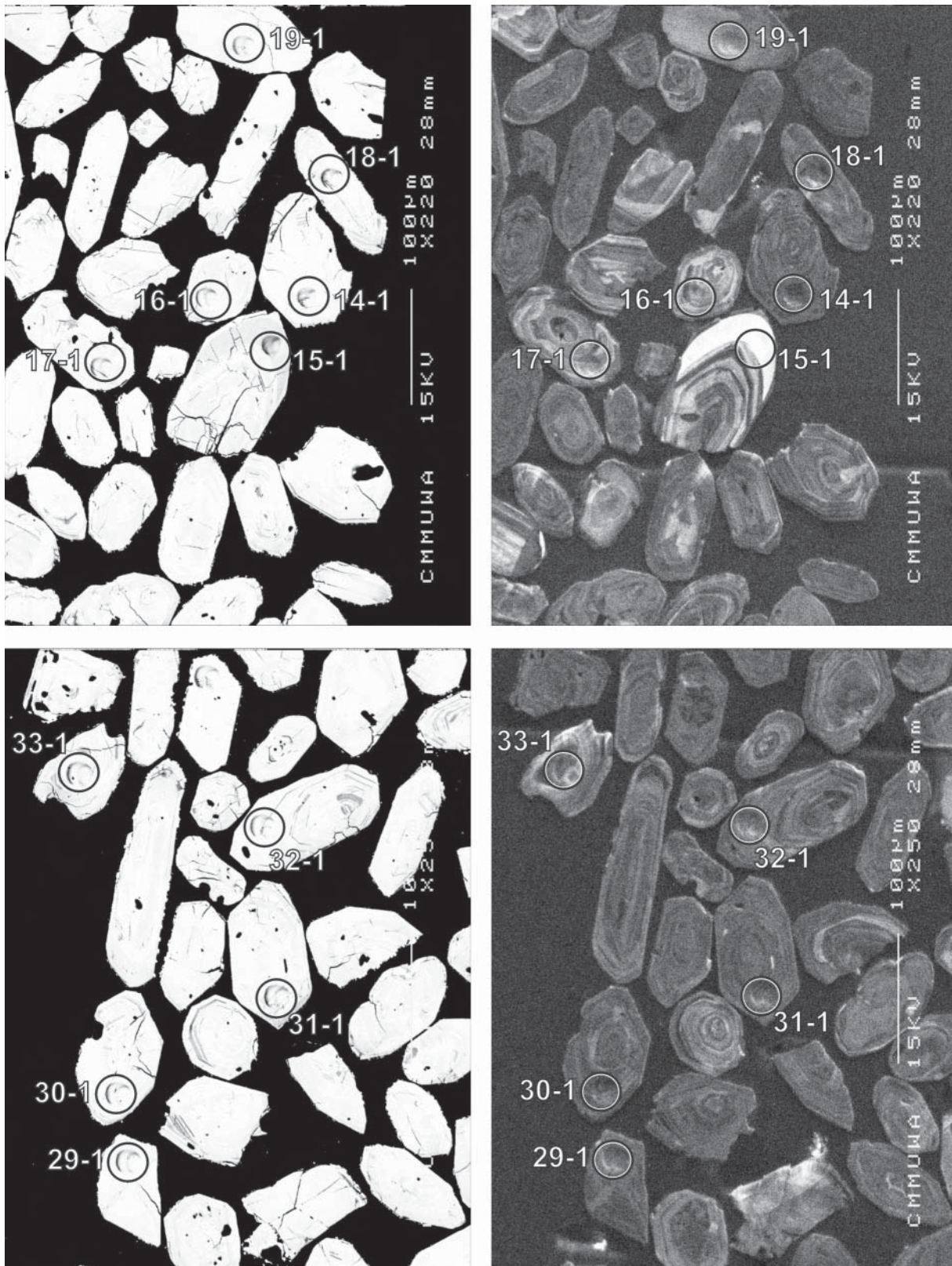


Figure 43. Representative SEM images (BSE on left, CL on right) for sample 2001967052C: Fijima sandstone. SHRIMP analysis spots are labelled. Remnant pits from the ion microprobe analyses are faintly visible in some grains. Scale bar is 100 µm.

mean $^{207}\text{Pb}/^{206}\text{Pb}$ age of 1851.1 ± 2.5 Ma (MSWD = 1.01).

Element abundance calibration was based on CZ3 (n = 3).

Sample data

A modest number of the 53 grains that were analysed show signs of U–Pb disturbance, with ~30% of analyses being >5% discordant (Table 19, Fig.44). Although those grains are not used for age interpretation, they demonstrate a complex pattern including both ancient and recent Pb loss. This is important for the interpretation of the concordant data. There is one distinctly old concordant grain (39-1, ~2816 Ma) and a preponderance of grains at ~2690 Ma (Figs. 44, 45). The age distribution tails to lower values (Fig. 45), ending at 2655 Ma except for analysis 23-1, which has a $^{207}\text{Pb}/^{206}\text{Pb}$ age of 2635 ± 7 Ma (1σ). This analysis also has $4f_{206} > 0.2\%$, higher than almost all other analyses for this sample and a level commonly associated with minor U–Pb disturbance. It also has low $^{208}\text{Pb}/^{232}\text{Th}$. Given these features, and the clearly disturbed character of many other grains in this sample, this analysis is not considered reliable for chronology. The next youngest date is 2655 ± 6 Ma (1σ). A weighted mean $^{207}\text{Pb}/^{206}\text{Pb}$ age of 2662 ± 5 Ma is obtained from the youngest eight analyses, excluding 23-1 (MSWD = 1.05).

Geochronological interpretation

The maximum depositional age for this sample is considered to be 2662 ± 5 Ma, despite indications for a younger age from one lower-quality analysis.

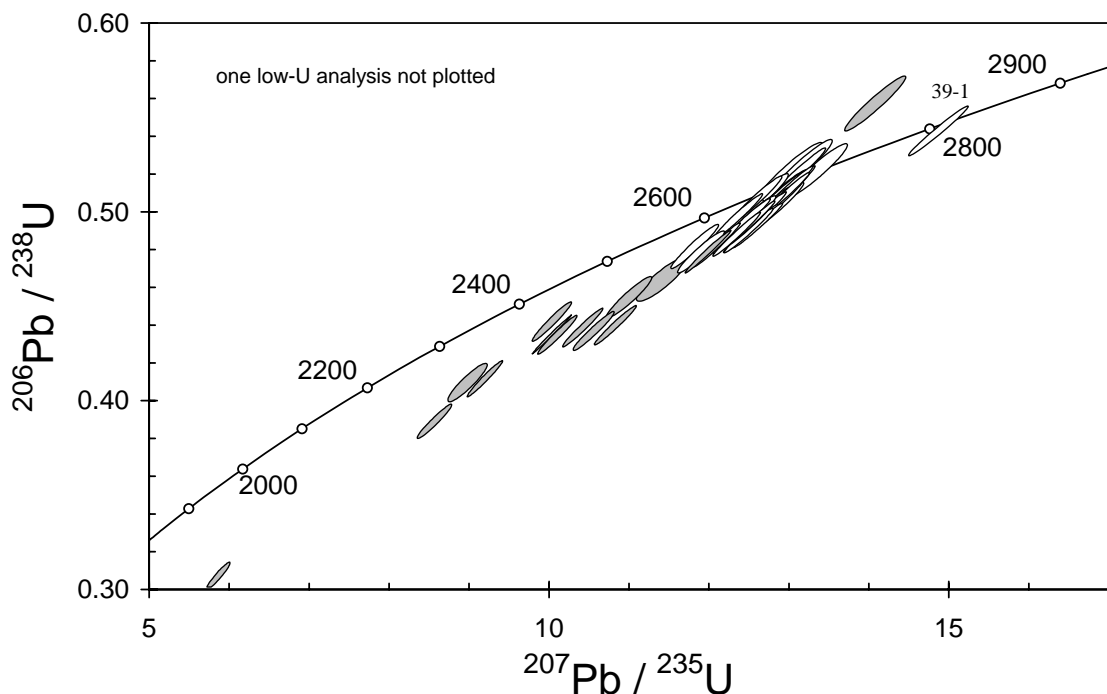


Figure 44. Concordia plot for zircons from sample 2001967052C: Fifima sandstone. White filled symbols are used to define the age of the sample; discordant analyses are light grey. One low-U analysis (15-1) is not plotted.

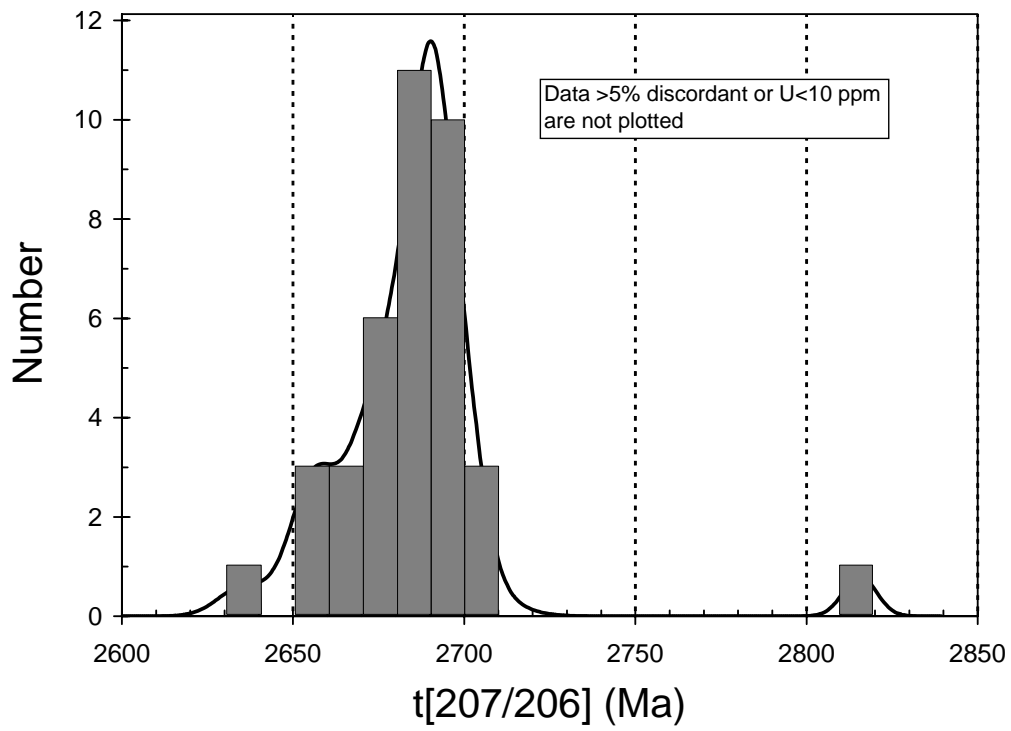


Figure 45. Cumulative probability plot of concordant $^{207}\text{Pb}/^{206}\text{Pb}$ data for zircons from sample 2001967052C: Fifima sandstone. One low-U analysis (15-1) is not plotted.

Table 19. SHRIMP analytical results for zircon from sample 2001967052C: Fifima sandstone, in order of $^{207}\text{Pb}/^{206}\text{Pb}$ age.

grain-spot	U (ppm)	Th (ppm)	4f206 (%)	$^{207}\text{Pb}/^{206}\text{Pb}$		$^{206}\text{Pb}/^{238}\text{U}$		$^{207}\text{Pb}/^{235}\text{U}$		$^{208}\text{Pb}/^{232}\text{Th}$	conc. (%)	$^{207}\text{Pb}/^{206}\text{Pb}$ Age (Ma)	
					±		±		±				±
23-1	209	118	0.277	0.1781	0.0008	0.481	0.008	11.81	0.20	0.123	96	2635	7
7-1	195	268	0.001	0.1802	0.0006	0.497	0.008	12.35	0.20	0.138	98	2655	6
45-1	161	1	0.043	0.1803	0.0007	0.506	0.008	12.58	0.21	0.067	99	2655	7
22-1	414	287	0.056	0.1803	0.0009	0.478	0.008	11.89	0.20	0.129	95	2656	8
46-1	121	21	0.022	0.1809	0.0010	0.507	0.008	12.65	0.22	0.145	99	2661	9
52-1	36	24	0.053	0.1811	0.0013	0.521	0.010	13.01	0.26	0.143	102	2663	12
51-1	107	49	0.068	0.1814	0.0011	0.493	0.008	12.34	0.22	0.132	97	2665	10
12-1	324	225	0.005	0.1819	0.0005	0.482	0.008	12.09	0.20	0.137	95	2670	5
10-1	86	48	0.144	0.1820	0.0010	0.490	0.008	12.30	0.22	0.138	96	2671	9
47-1	53	29	-0.012	0.1823	0.0011	0.524	0.010	13.16	0.25	0.145	101	2674	10
53-1	57	40	0.025	0.1823	0.0017	0.497	0.009	12.49	0.25	0.139	97	2674	16
40-1	258	138	0.163	0.1825	0.0006	0.495	0.008	12.45	0.20	0.138	97	2676	5
43-1	144	124	0.053	0.1827	0.0007	0.521	0.009	13.11	0.22	0.143	101	2678	6
55-1	322	401	-0.006	0.1830	0.0005	0.489	0.008	12.33	0.20	0.136	96	2680	4
48-1	349	226	0.267	0.1830	0.0008	0.496	0.008	12.52	0.20	0.138	97	2680	7
16-1	139	117	0.040	0.1834	0.0007	0.503	0.008	12.72	0.22	0.138	98	2684	6
17-1	119	77	0.042	0.1834	0.0008	0.508	0.008	12.85	0.22	0.140	99	2684	7
20-1	344	194	0.025	0.1835	0.0007	0.508	0.008	12.86	0.21	0.138	99	2685	6
41-1	296	203	0.099	0.1836	0.0005	0.487	0.008	12.34	0.20	0.132	95	2685	5
38-1	175	78	0.037	0.1836	0.0007	0.510	0.008	12.90	0.22	0.141	99	2686	6
50-1	326	153	0.053	0.1840	0.0005	0.494	0.008	12.52	0.20	0.134	96	2689	4
28-1	265	135	0.102	0.1840	0.0006	0.492	0.008	12.48	0.20	0.134	96	2689	5
44-1	294	122	0.119	0.1840	0.0005	0.512	0.008	12.98	0.21	0.150	99	2689	5
32-1	206	156	-0.002	0.1841	0.0006	0.500	0.008	12.69	0.21	0.140	97	2690	5
33-1	210	135	0.071	0.1841	0.0006	0.505	0.008	12.81	0.21	0.128	98	2690	5
5-1	350	244	0.246	0.1842	0.0006	0.498	0.008	12.65	0.20	0.138	97	2691	5
26-1	207	51	-0.004	0.1842	0.0006	0.511	0.008	12.98	0.22	0.140	99	2691	5
27-1	222	90	-0.031	0.1844	0.0006	0.506	0.008	12.86	0.21	0.138	98	2693	5
49-1	178	62	0.099	0.1844	0.0007	0.508	0.008	12.92	0.21	0.145	98	2693	6
30-1	261	144	0.043	0.1846	0.0005	0.508	0.008	12.93	0.21	0.140	98	2694	5
54-1	232	57	-0.005	0.1847	0.0007	0.505	0.008	12.85	0.21	0.141	98	2695	6
13-1	239	182	0.014	0.1849	0.0005	0.490	0.008	12.48	0.20	0.136	95	2697	5
11-1	250	101	0.041	0.1850	0.0006	0.490	0.008	12.49	0.20	0.136	95	2698	5
6-1	237	148	0.021	0.1851	0.0006	0.491	0.008	12.54	0.21	0.136	95	2699	5
25-1	90	110	-0.062	0.1852	0.0009	0.502	0.009	12.83	0.23	0.139	97	2700	8
4-1	244	124	-0.014	0.1856	0.0005	0.492	0.008	12.60	0.20	0.135	95	2704	5
3-1	61	28	0.032	0.1856	0.0011	0.521	0.009	13.34	0.26	0.138	100	2704	10
39-1	213	107	0.000	0.1987	0.0006	0.543	0.009	14.86	0.24	0.150	99	2816	5
>5% discordant or U <10ppm													
8-1	254	112	0.100	0.1785	0.0006	0.439	0.007	10.81	0.18	0.114	89	2639	5
9-1	946	261	0.308	0.1384	0.0007	0.306	0.005	5.84	0.10	0.089	78	2207	9
14-1	419	343	0.210	0.1753	0.0007	0.436	0.007	10.54	0.17	0.120	89	2609	7
15-1	3	1	0.140	0.1961	0.0079	0.535	0.023	14.45	0.86	0.198	99	2794	66
18-1	798	289	0.095	0.1590	0.0011	0.409	0.007	8.96	0.16	0.112	90	2446	12
19-1	133	36	-0.044	0.1832	0.0009	0.557	0.010	14.07	0.25	0.165	106	2682	9
21-1	468	258	0.005	0.1816	0.0004	0.478	0.007	11.98	0.19	0.132	94	2668	4
24-1	259	158	0.110	0.1785	0.0016	0.463	0.007	11.40	0.21	0.099	93	2639	15
29-1	764	416	0.430	0.1598	0.0007	0.388	0.006	8.55	0.14	0.108	86	2453	8
31-1	657	604	0.093	0.1620	0.0005	0.411	0.006	9.17	0.15	0.109	90	2477	6
34-1	1632	483	0.001	0.1673	0.0002	0.434	0.007	10.01	0.16	0.136	92	2531	2
35-1	595	425	0.179	0.1685	0.0006	0.434	0.007	10.08	0.16	0.117	91	2543	6
36-1	780	430	0.029	0.1647	0.0007	0.441	0.007	10.01	0.16	0.120	94	2504	7
37-1	381	245	0.232	0.1724	0.0006	0.438	0.007	10.41	0.17	0.120	91	2581	6
42-1	249	129	0.051	0.1755	0.0010	0.454	0.007	10.99	0.19	0.122	92	2611	10

Data are at 1σ precision. All Pb data are common-Pb corrected (based on ^{204}Pb and Broken Hill Pb composition). Analysis date: 20/01/02; session Z3813i.

2001967053A: biotite migmatite, Mt Dennis

1:250,000 sheet: Laverton (SH5102)

1:100,000 sheet: Burtville (3440)

MGA: 488672mE 6793990mN

Location: The sample was taken from the northern side of a large outcrop about 250 m east of the Coglia - Merolia Road, and about 1 km north of Mt Dennis.

Description: The sample is from a grey, seriate to moderately feldspar-porphyrific, medium-grained biotite quartzofeldspathic migmatite. This is the earliest phase of a granitoid complex that contains more than five generations of biotite granodiorite and monzogranite, several generations of pegmatite veins, and evidence for several deformation events. Successive phases of biotite granodiorite and monzogranite record decreasing intensities of deformation. The last major phase is a seriate to moderately K-feldspar porphyritic fine-grained biotite monzogranite, of which sample 2001967053B is representative.

This rock has a recrystallised granoblastic texture. Principal minerals are quartz (37–42%), plagioclase (37–42%), K-feldspar (10–15%) and biotite (7–9%). Plagioclase occurs as subhedral to anhedral grains with variably developed normal and oscillatory zoning, particularly in grain cores. Twinning is well-developed and locally bent. Trace quantities of myrmekite are present. The plagioclase grains are locally replaced by white mica and epidote/clinozoisite. K-feldspar is anhedral, with common tartan twinning and very minor perthite. Quartz is anhedral with common weak to moderate undulose extinction. Biotite occurs as aligned and elongate, pale yellow to moderate-dark red-brown ragged flakes, and clusters of flakes associated with minor titanite and opaque minerals. The biotite is locally replaced by chlorite, epidote/clinozoisite, white mica, rutile, and titanite. Accessory phases include apatite, anhedral titanite, zircon and opaque minerals. Secondary minerals include rare epidote/clinozoisite, chlorite, white mica, rutile and titanite(?).

Mount, pop: Z3881A

Description of zircons

Zircon occurs as euhedral to subhedral crystals and fragments with slightly rounded crystal faces. The grains vary from roughly equant to elongate, and from 35 μm to 165 μm in length (aspect ratios to 4:1). Most are colourless to pale grey, with a faint reddish-yellow stain. Small sub-rounded and rod-like inclusions are present in a number of grains. Continuous concentric oscillatory zoning is visible in most grains in transmitted and reflected light and in CL (Fig. 46). Recrystallised zones and possible cores are also revealed by CL.

Concurrent standard data

The apparent calibration slope for QGNG was 1.93. Neither of the concurrent samples was sufficiently single-aged to provide an alternate estimate and the default slope of 2.0 was used. The calibration is highly precise with 36 points giving a 1σ scatter in Pb/U of 0.49% (MSWD = 2.15). The standardised assessment of $^{207}\text{Pb}/^{206}\text{Pb}$ data results in a weighted mean age of 1847.9 ± 2.4 (n = 35; MSWD = 1.11).

Element abundance calibration was based on CZ3 (n = 3).

Sample data

About 40% of the 35 analyses (Table 20) are discordant, showing both early and recent Pb loss (Fig. 47). Six of the more concordant analyses are 4–5% discordant, which have also suffered early Pb loss (Fig. 47). The remaining 15 analyses give a weighted mean $^{207}\text{Pb}/^{206}\text{Pb}$ age of 2767 ± 3.3 Ma with significant excess scatter (MSWD = 2.1). Given the evidence in other data for early Pb loss, and the lack of any obvious inheritance in the analysed grains, the younger

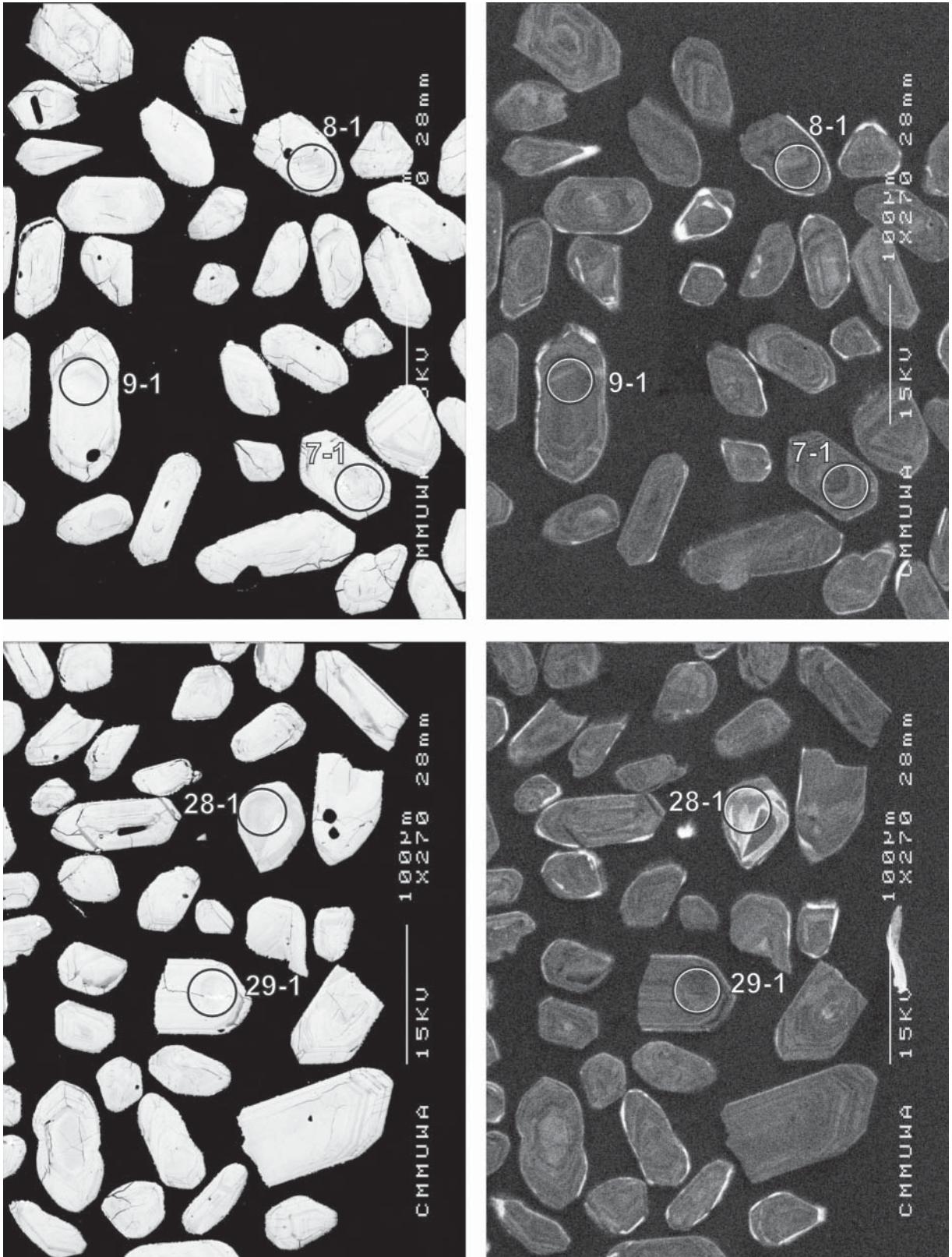


Figure 46. Representative SEM images (BSE on left, CL on right) for sample 2001967053A: biotite migmatite, Mt Dennis. SHRIMP analysis spots are labelled. Remnant pits from the ion microprobe analyses are faintly visible in some grains. Scale bar is 100 μm .

dates in this group are considered the least reliable. Culling from the low-age side leads to an age of 2770.0 ± 3.3 Ma ($n = 10$; MSWD = 1.2; Fig. 48).

Geochronological interpretation

The 2770 ± 4 Ma is considered to be the age of the precursor granite, with ancient Pb loss possibly a result of migmatitisation.

Table 20. SHRIMP analytical results for zircon from sample 2001967053A: biotite migmatite, Mt Dennis.

grain-spot	U (ppm)	Th (ppm)	4f206 (%)	$^{207}\text{Pb}/^{206}\text{Pb}$		$^{206}\text{Pb}/^{238}\text{U}$		$^{207}\text{Pb}/^{235}\text{U}$		$^{208}\text{Pb}/^{232}\text{Th}$	conc. (%)	$^{207}\text{Pb}/^{206}\text{Pb}$ Age (Ma)	
					\pm		\pm		\pm				\pm
Main group													
3-1	182	56	0.143	0.1926	0.0006	0.520	0.003	13.80	0.10	0.145	98	2765	5
4-1	217	130	0.028	0.1928	0.0008	0.514	0.006	13.67	0.16	0.142	97	2766	7
6-1	275	142	0.215	0.1929	0.0005	0.516	0.003	13.73	0.09	0.137	97	2767	4
11-1	528	365	0.296	0.1937	0.0004	0.515	0.003	13.75	0.08	0.137	96	2774	4
14-1	559	568	0.053	0.1930	0.0003	0.512	0.003	13.64	0.08	0.138	96	2768	3
15-1	249	169	0.127	0.1941	0.0006	0.533	0.008	14.27	0.21	0.144	99	2777	5
26-1	271	139	0.071	0.1934	0.0005	0.515	0.003	13.74	0.09	0.140	97	2771	4
28-1	88	47	0.300	0.1926	0.0010	0.504	0.004	13.40	0.14	0.148	95	2765	9
29-1	393	191	0.190	0.1941	0.0004	0.530	0.003	14.20	0.09	0.138	99	2777	4
34-1	412	110	0.052	0.1928	0.0004	0.522	0.004	13.87	0.10	0.141	98	2766	3
Possible young outliers													
2-1	371	292	0.183	0.1922	0.0004	0.509	0.003	13.49	0.08	0.128	96	2761	3
21-1	232	45	0.038	0.1921	0.0005	0.505	0.003	13.36	0.09	0.137	95	2760	4
22-1	335	242	0.067	0.1921	0.0006	0.507	0.003	13.42	0.09	0.140	96	2760	5
24-1	228	153	0.270	0.1918	0.0006	0.519	0.003	13.72	0.10	0.145	98	2757	5
30-1	226	59	0.215	0.1921	0.0006	0.519	0.003	13.74	0.10	0.140	98	2760	5
Near concordant; early Pb loss													
7-1	260	155	0.657	0.1883	0.0006	0.498	0.003	12.92	0.09	0.136	95	2727	5
9-1	315	145	0.153	0.1900	0.0004	0.502	0.003	13.14	0.09	0.137	95	2742	4
12-1	429	321	0.049	0.1840	0.0003	0.491	0.003	12.47	0.08	0.131	96	2689	3
17-1	474	237	0.319	0.1884	0.0005	0.499	0.003	12.97	0.08	0.130	96	2728	4
19-1	497	345	0.698	0.1861	0.0010	0.496	0.003	12.74	0.10	0.130	96	2708	9
33-1	260	139	0.556	0.1895	0.0009	0.499	0.004	13.03	0.11	0.138	95	2737	8
>5% discordant or high common Pb													
1-1	337	157	0.155	0.1862	0.0004	0.480	0.003	12.31	0.08	0.127	93	2709	4
5-1	351	268	0.173	0.1906	0.0004	0.484	0.003	12.73	0.08	0.138	93	2748	4
8-1	600	381	0.504	0.1607	0.0004	0.402	0.002	8.90	0.05	0.107	88	2463	4
10-1	344	109	0.150	0.1852	0.0005	0.486	0.003	12.42	0.08	0.138	94	2700	4
13-1	444	177	0.151	0.1807	0.0004	0.452	0.003	11.26	0.07	0.125	90	2660	4
16-1	1005	892	0.154	0.1755	0.0002	0.457	0.003	11.06	0.06	0.126	93	2611	2
18-1	686	344	1.659	0.1843	0.0006	0.439	0.002	11.17	0.07	0.126	87	2692	5
20-1	292	260	0.435	0.1884	0.0006	0.474	0.003	12.32	0.09	0.130	92	2728	5
23-1	293	193	0.469	0.1892	0.0006	0.477	0.003	12.44	0.08	0.133	92	2735	5
25-1	469	278	0.377	0.1803	0.0005	0.464	0.003	11.53	0.09	0.127	93	2655	5
27-1	458	246	0.383	0.1925	0.0007	0.489	0.003	12.98	0.09	0.141	93	2764	6
31-1	250	169	0.661	0.1895	0.0010	0.487	0.003	12.74	0.11	0.128	93	2738	9
32-1	208	139	0.629	0.1895	0.0008	0.479	0.003	12.51	0.10	0.127	92	2738	7
35-1	241	145	0.460	0.1767	0.0010	0.431	0.003	10.50	0.09	0.119	88	2622	9

Data are at 1σ precision. All Pb data are common-Pb corrected (based on ^{204}Pb and Broken Hill Pb composition). Analysis date: 26/04/02; session Z3881i

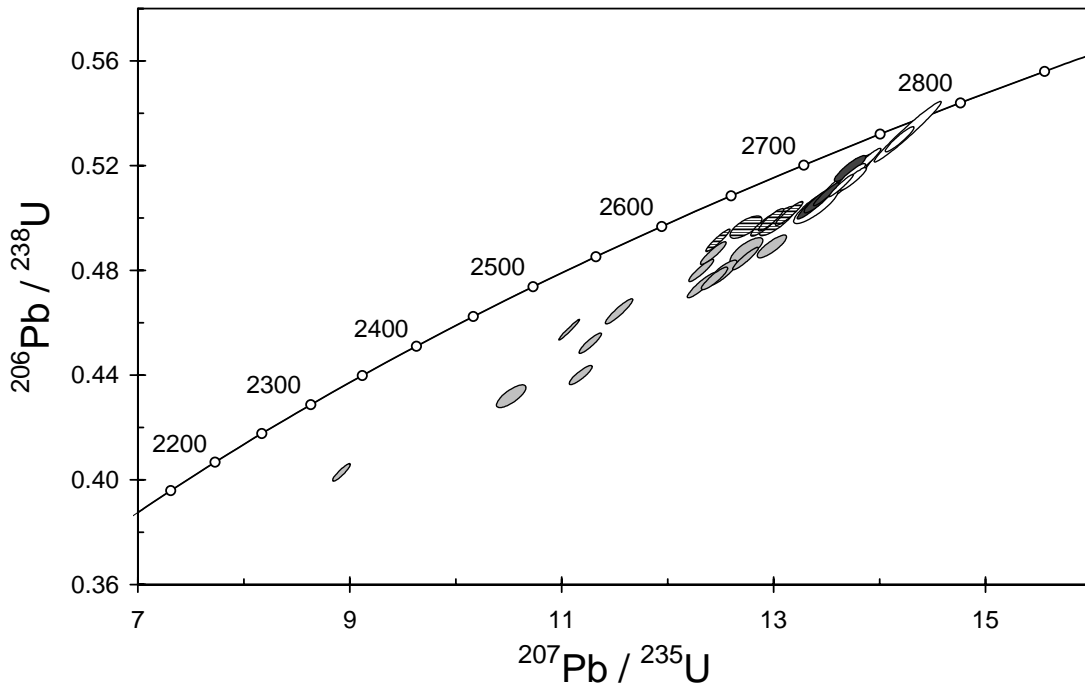


Figure 47. Concordia plot for zircons from sample 2001967053A: biotite migmatite, Mt Dennis. White filled symbols are used to define the age of the sample; young outliers are dark grey; discordant and/or high common Pb analyses are light grey; near-concordant analyses showing early Pb loss have horizontal shading.

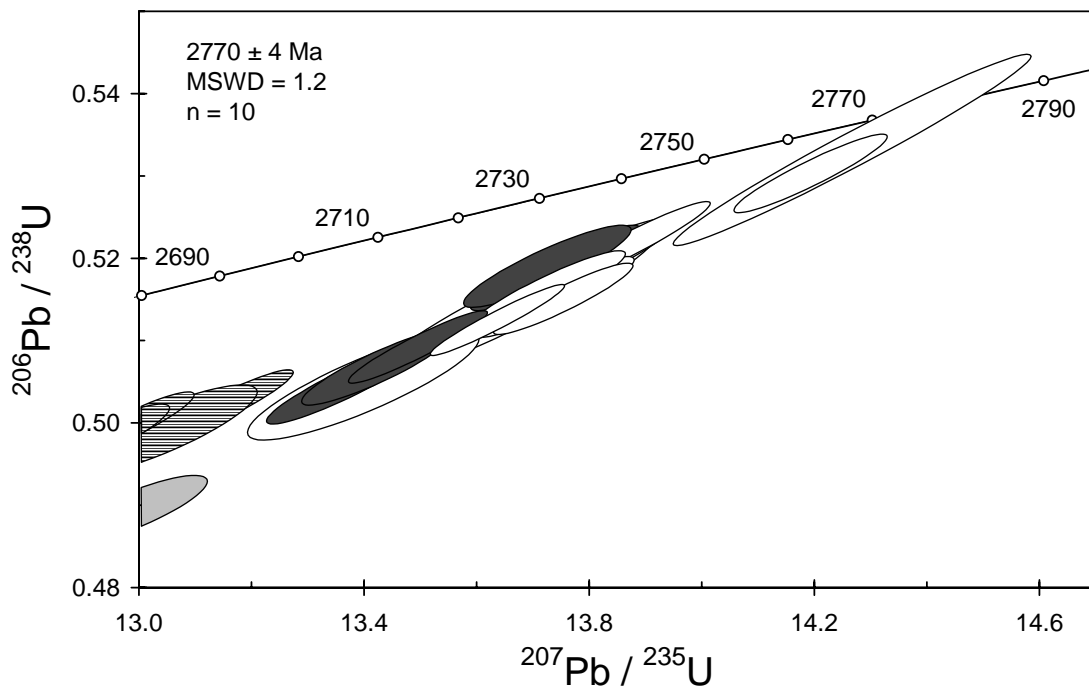


Figure 48. Concordia plot of the main data cluster for sample 2001967053A: biotite migmatite, Mt Dennis. Shading as in Figure 47.

2001967053B: biotite monzogranite, Mt Dennis

1:250,000 sheet: Laverton (SH5102)

1:100,000 sheet: Burtville (3440)

MGA: 488672mE 6793990mN

Location: The sample was taken from the northern side of a large outcrop about 250 m east of the Cogleia - Merolia Road, about 1 km north of Mt Dennis.

Description: It is a pink-grey, seriate to moderately K-feldspar porphyritic, fine-grained biotite monzogranite that occurs as small intrusions and is the last major phase of the granitoid complex. It ranges from a biotite quartzofeldspathic migmatite (sample 2001967053A), through biotite-rich and biotite-poor granodiorite, to biotite-poor monzogranite. Several generations of pegmatite veins cut the major granitic phases. The monzogranite contains minor biotite-rich clots and schlieren and displays a weak foliation defined by biotite and elongate quartz and feldspar.

The rock has a granular to granoblastic texture. Principal minerals are K-feldspar (32–37%), quartz (30–35%), plagioclase (25–30%), and biotite (5–6%), with K-feldspar > plagioclase. K-feldspar is subhedral to anhedral, and displays common well-developed tartan twinning, and minor to locally moderate perthite. Plagioclase is present as subhedral to anhedral grains that are generally unzoned or have locally developed patchy normal or oscillatory zoning in grain cores. The plagioclase is commonly twinned, particularly at grain rims. Minor myrmekite is present. Plagioclase cores are locally replaced by coarse-grained muscovite and/or minor to moderate white mica, epidote/clinozoisite and carbonate. Quartz is anhedral, and generally has moderate undulose extinction. Biotite occurs as light yellow to medium-dark red-brown, subhedral to anhedral ragged flakes that are locally variably altered to chlorite, epidote/clinozoisite, rutile, fluorite and/or white mica. Accessory phases include apatite, zircon, and opaque minerals. Secondary minerals include minor coarse-grained muscovite, chlorite, white mica, epidote/clinozoisite, carbonate, hematite and trace fluorite and rutile.

Mount, pop: 3881B

Description of zircons

The fragments and crystals of euhedral to subhedral zircon have slightly rounded crystal faces. Grain size varies widely, from small equant and stubby grains, as little as 45 μm in size, to large stubby (up to 220 μm long, aspect ratio 2:1) and elongate grains (maximum length of 300 μm ; aspect ratio 6:1). The zircon is colourless to pale grey, and many grains have a slight reddish-yellow stain. Continuous, euhedral, oscillatory zoning is visible in many grains in transmitted light. Locally this zoning appears patchy in CL, being disrupted by irregular zones of recrystallised zircon (Fig.49). A few grains (e.g., 20) have very bright CL, and some cores are visible.

Concurrent standard data

The apparent calibration slope for QGNG was 1.93. Neither of the concurrent samples was sufficiently single-aged to provide an alternate estimate and the default slope of 2.0 was used. The calibration is highly precise with 36 points giving a 1σ scatter in Pb/U of 0.49% (MSWD = 2.15). The standardised assessment of $^{207}\text{Pb}/^{206}\text{Pb}$ data results in a weighted mean age of 1847.9 ± 2.4 (n = 35; MSWD = 1.11).

Element abundance calibration was based on CZ3 (n = 3).

Sample data

Thirty five analyses of separate grains were made. The data (Table 21, Fig. 50) scatter widely, most likely due to a mixture of original ages and variable Pb loss, both in the Archaean and more

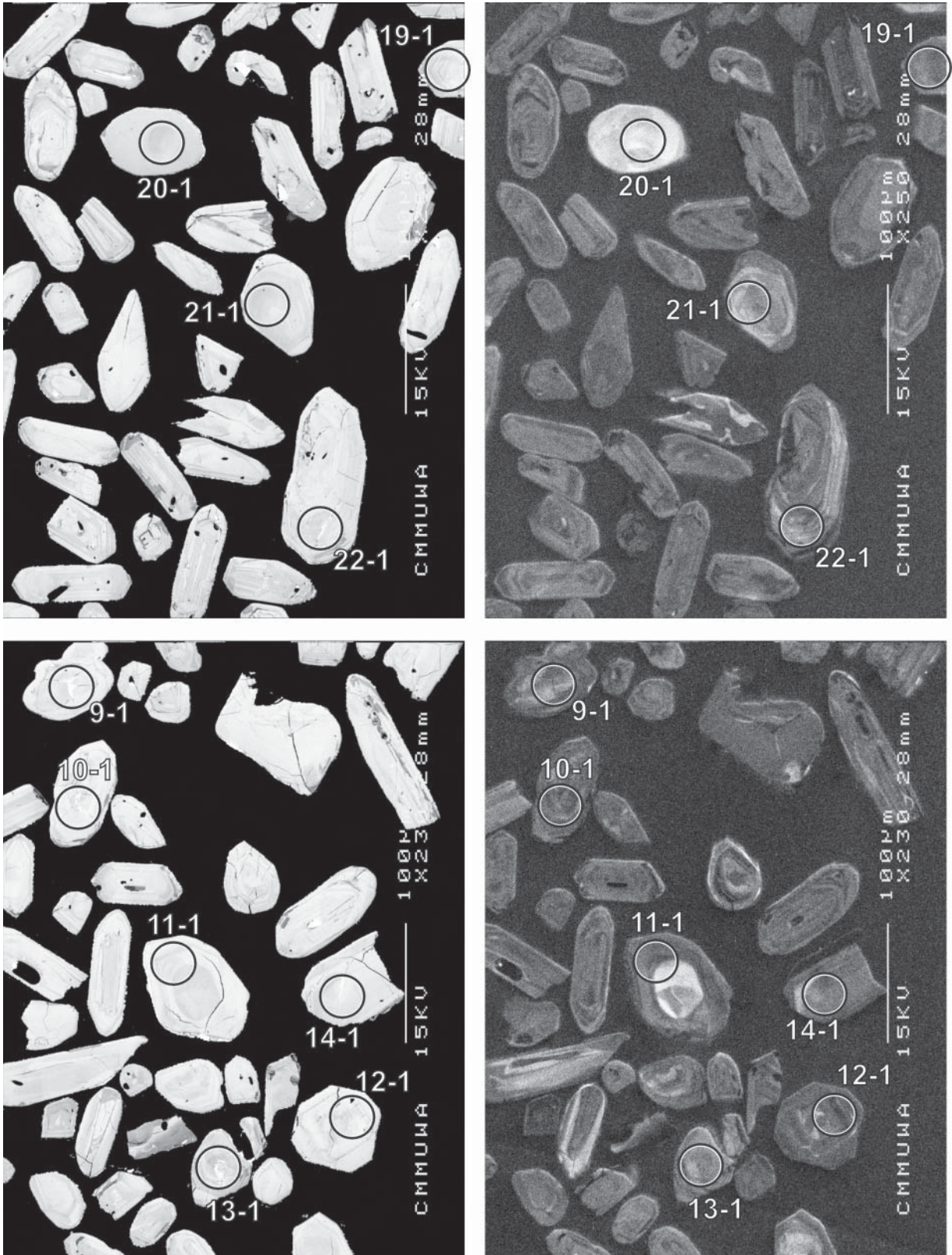


Figure 49. Representative SEM images (BSE on left, CL on right) for sample 2001967053B: biotite monzogranite, Mt Dennis. SHRIMP analysis spots are labelled. Remnant pits from the ion microprobe analyses are faintly visible in some grains. Scale bar is 100 μ m.

recently. Many of the data are >5% discordant, and not considered reliable for geochronology. Some concordant data are also considered to be unreliable (10-1 with high common Pb, and 3-1 and 27-1 which have high U and Th), even though one of them (27-1) falls amongst a cluster of concordant data. The $^{207}\text{Pb}/^{206}\text{Pb}$ dates from the remaining 19 concordant data range from ~2770 Ma to ~2550 Ma (Fig. 51), with peaks close to each end of the range. The oldest seven analyses give a weighted mean $^{207}\text{Pb}/^{206}\text{Pb}$ age of 2763 ± 8 Ma (MSWD = 1.8); the youngest eight give 2650 ± 8 Ma (MSWD = 1.5). Neither of these is expected to be totally reliable.

Geochronological interpretation

The intrusive age of this rock is probably ~2650 Ma, but the strong inheritance pattern prevents the application of a strict uncertainty to this age. The majority of the inherited grains appear to come from rocks of similar age to 2001967053A, which this monzogranite intrudes.

Table 21. SHRIMP analytical results for zircon from sample 2001967053B: biotite monzogranite, Mt Dennis.

grain-spot	U (ppm)	Th (ppm)	4f206 (%)	$^{207}\text{Pb}/^{206}\text{Pb}$	\pm	$^{206}\text{Pb}/^{238}\text{U}$	\pm	$^{207}\text{Pb}/^{235}\text{U}$	\pm	$^{208}\text{Pb}/^{232}\text{Th}$	conc. (%)	$^{207}\text{Pb}/^{206}\text{Pb}$ Age (Ma)	\pm
Concordant data, in order of $^{207}\text{Pb}/^{206}\text{Pb}$ age													
20-1	26	16	0.132	0.1776	0.0020	0.511	0.007	12.51	0.22	0.140	101	2631	19
14-1	146	159	0.303	0.1786	0.0007	0.485	0.004	11.95	0.12	0.137	96	2640	6
11-1	275	225	0.157	0.1791	0.0005	0.478	0.003	11.80	0.08	0.130	95	2645	5
21-1	78	48	0.136	0.1793	0.0009	0.505	0.004	12.50	0.13	0.139	100	2646	9
24-1	66	78	0.239	0.1800	0.0011	0.508	0.005	12.61	0.14	0.139	100	2653	10
35-1	71	229	0.578	0.1802	0.0013	0.484	0.005	12.01	0.14	0.060	96	2655	12
26-1	32	51	-0.024	0.1803	0.0013	0.510	0.007	12.67	0.19	0.139	100	2656	12
28-1	323	24	0.237	0.1808	0.0005	0.486	0.003	12.11	0.08	0.172	96	2661	5
29-1	44	38	0.077	0.1822	0.0013	0.503	0.006	12.63	0.17	0.138	98	2673	12
30-1	195	147	0.104	0.1828	0.0006	0.502	0.003	12.65	0.10	0.130	98	2678	5
34-1	36	35	0.149	0.1865	0.0014	0.517	0.007	13.30	0.20	0.142	99	2711	12
12-1	394	134	0.258	0.1872	0.0004	0.503	0.003	13.00	0.08	0.145	97	2718	4
4-1	335	114	0.907	0.1914	0.0017	0.513	0.003	13.53	0.15	0.145	97	2754	15
5-1	312	101	0.126	0.1917	0.0006	0.508	0.003	13.41	0.09	0.142	96	2757	5
32-1	260	66	0.038	0.1920	0.0005	0.527	0.003	13.96	0.10	0.136	99	2759	4
18-1	130	91	-0.004	0.1923	0.0006	0.533	0.004	14.13	0.12	0.144	100	2762	5
22-1	159	130	0.240	0.1926	0.0007	0.505	0.004	13.41	0.11	0.143	95	2764	6
33-1	204	74	0.186	0.1933	0.0006	0.521	0.004	13.88	0.11	0.146	97	2771	5
7-1	191	174	0.126	0.1946	0.0009	0.522	0.003	14.02	0.11	0.148	97	2781	8
Discordant, high common Pb or U+Th													
1-1	194	122	0.395	0.1915	0.0008	0.418	0.003	11.03	0.09	0.150	82	2755	7
2-1	603	204	0.398	0.1771	0.0006	0.451	0.003	11.02	0.07	0.123	91	2626	6
3-1	751	28	0.601	0.1439	0.0010	0.398	0.002	7.90	0.07	0.109	95	2275	11
6-1	663	89	0.404	0.1662	0.0011	0.398	0.002	9.11	0.08	0.118	86	2520	11
8-1	139	144	0.829	0.1796	0.0011	0.455	0.003	11.26	0.11	0.149	91	2649	10
9-1	116	77	0.626	0.1920	0.0009	0.470	0.003	12.45	0.11	0.152	90	2759	8
10-1	223	92	1.566	0.1918	0.0008	0.504	0.003	13.32	0.10	0.154	95	2757	7
13-1	932	73	0.488	0.1684	0.0004	0.414	0.002	9.62	0.06	1.281	88	2542	4
15-1	401	77	0.584	0.1724	0.0005	0.430	0.003	10.23	0.07	0.118	89	2581	5
16-1	111	100	3.092	0.1807	0.0016	0.400	0.003	9.97	0.12	0.091	82	2659	15
17-1	319	100	0.989	0.1905	0.0006	0.484	0.003	12.71	0.08	0.161	93	2747	5
19-1	513	884	0.917	0.1660	0.0005	0.414	0.002	9.46	0.06	0.114	89	2517	5
23-1	207	289	0.731	0.1807	0.0007	0.459	0.003	11.43	0.09	0.017	92	2659	7
25-1	421	12	0.215	0.1730	0.0006	0.440	0.003	10.51	0.07	0.149	91	2587	6
27-1	541	1028	0.099	0.1820	0.0004	0.497	0.003	12.48	0.08	0.139	97	2671	3
31-1	354	132	0.351	0.1699	0.0006	0.440	0.003	10.31	0.07	0.128	92	2557	6

Data are at 1σ precision. All Pb data are common-Pb corrected (based on ^{204}Pb and Broken Hill Pb composition). Analysis date: 26/04/02; session Z3881i.

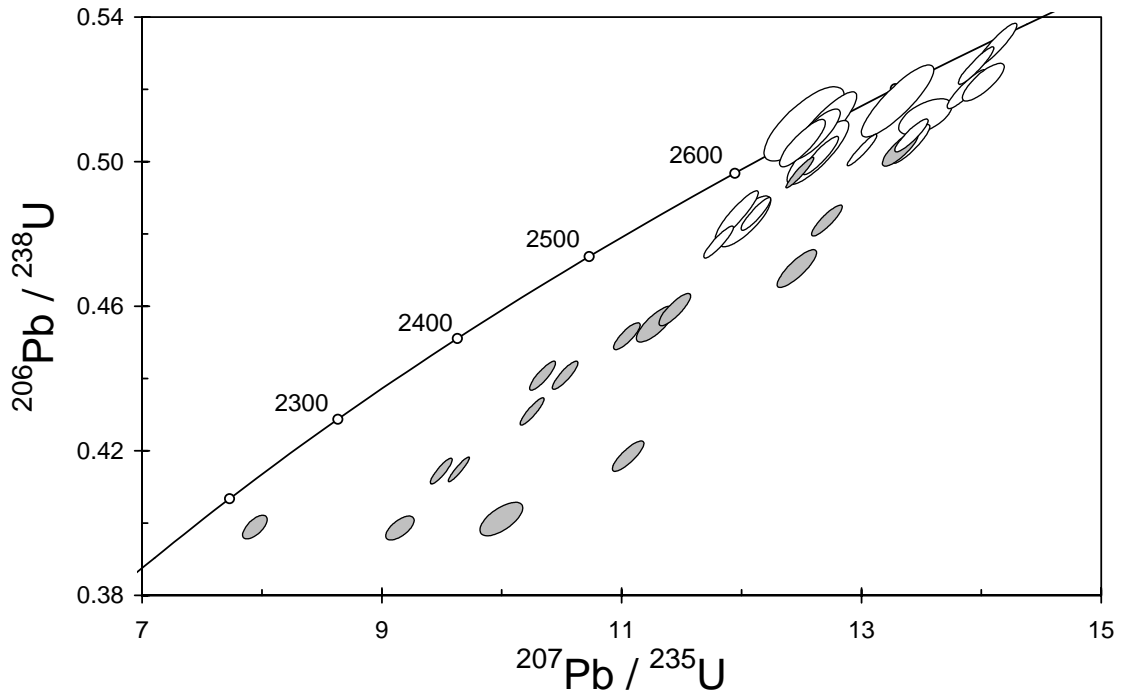


Figure 50. Concordia plot of all data for zircons from sample 2001967053B: biotite monzogranite, Mt Dennis. White filled symbols are used to define the history of the sample; discordant and/or high common Pb analyses are light grey.

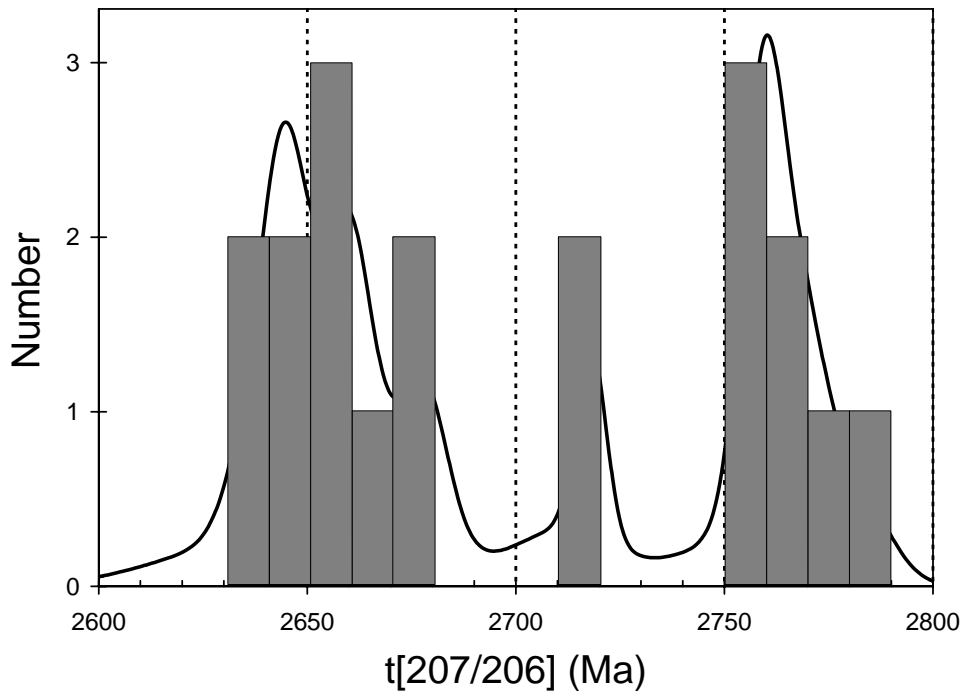


Figure 51. Cumulative probability plot for concordant data for zircons from sample 2001967053B: biotite monzogranite, Mt Dennis.

2001967056: deformed pebble meta-conglomerate, Hurleys Reward

1:250,000 sheet: Sir Samuel (SG5113)

1:100,000 sheet: Wanggannoo (3143)

MGA: 347735mE 6969499mN

Location: The sample was collected from a small rocky hill, on the south side of a track, about 300 m west of Hurleys Reward.

Description: This is a strongly deformed pebble meta-conglomerate that contains extensively recrystallised quartz and chert clasts which vary from 1 mm to 5 cm in width and 5 mm to 25 cm in length. All clasts are strongly deformed and elongate, with length:width ratios ranging from 3 to 7 and generally being greater than 5.

Quartz is dominant (>95 %), with minor white mica (2–3%), opaque minerals (~2%) and trace quantities of zircon and chlorite. The sample consists of strongly recrystallised quartz and chert clasts, ranging from <1 mm to > 1 cm, and some individual quartz grains (up to >0.5 mm) within a strongly recrystallised, quartz-rich mosaic. The latter consists of fine-grained quartz, with a typical grain size of <0.1 mm, and minor white mica flakes and opaque minerals. Original grain size is indicated by the distribution of the quartz-rich mosaic, in particular the interstitial decussate white mica and disseminated opaque minerals. Individual quartz grains, particularly the larger single quartz clasts, exhibit moderate undulose extinction, and are moderately to strongly aligned and variably elongated. The alignment of the quartz grains, and the white mica and opaque minerals, defines a strong foliation. Opaque minerals occur as subeuhedral to anhedral crystals up to 0.1 mm in size, and are generally confined to the quartz-rich mosaic, as well as some recrystallised chert clasts. Accessory phases include zircon and chlorite.

Mount, pop: Z3813A

Description of zircons

A moderately uniform size population of predominantly pale brown-grey zircon crystals (with lesser fragments) is present. Most grains are subhedral to euhedral, with variable rounding of crystal faces. Grains vary from about 50 μm to 180 μm in length, with aspect ratios up to 3:1. Small rounded inclusions are present in many grains. Well-defined continuous euhedral oscillatory zoning is clearly visible in many grains in transmitted and reflected light, although a few grains are uniform and lack visible internal features. However, all grains appear well-zoned in CL (Fig. 52), with numerous grains having visually distinct cores in which zoning is truncated by an overgrowth of zircon. In some grains, zoning of the core is irregular or disrupted, indicative of recrystallisation.

Concurrent standard data

This three-day session, analysing detrital zircon grains, used a shortened runtable (five scans instead of the standard seven). The session was interrupted twice: it was necessary to re-tune the primary ion column after eight analyses, and the duoplasmatron arc “dropped out” about 12 hours later. Both these interruptions caused a distinct shift in Pb/U calibration. The early analyses could not be properly assessed or recombined with later data, and were deleted. The second data block was also too small ($n = 7$ for QGNG) for a robust calibration. However, this calibration shift was smaller than the first, and as the second block of data overlaps with others towards the end of the session, the data were all retained in a single block for processing. The resulting calibration is less precise than usual, but acceptable. The data produce a 1σ Pb/U scatter of 1.5% with MSWD = 10.4. The observed calibration slope is 1.95, and the default value of 2.0 was used. Omitting one $\sim 3\sigma$ (low) outlier and two other points leaves 41 analyses with a weighted mean $^{207}\text{Pb}/^{206}\text{Pb}$ age of 1851.1 ± 2.5 Ma (MSWD = 1.01).

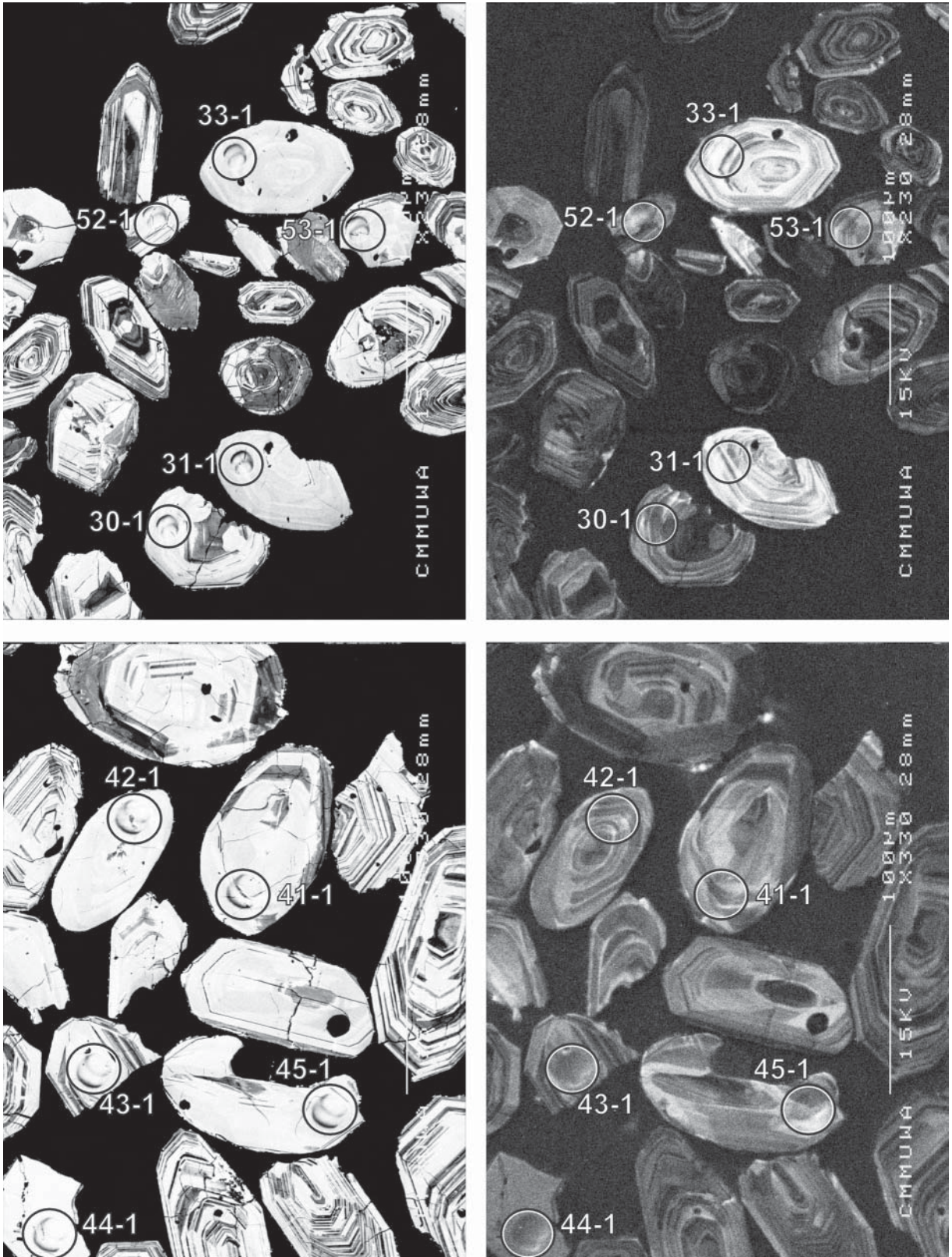


Figure 52. Representative SEM images (BSE on left, CL on right) for sample 2001967056: deformed pebble meta-conglomerate, Hurleys Reward. SHRIMP analysis spots are labelled. Remnant pits from the ion microprobe analyses are faintly visible in some grains. Scale bar is 100 µm.

Element abundance calibration was based on CZ3 (n = 3).

Sample data

About 30% of the 53 analyses of individual grains are discordant (Table 22, Fig. 53). The data are dominated by a strong $^{207}\text{Pb}/^{206}\text{Pb}$ age peak at ~2955 Ma (Fig. 54). The few younger analyses suggest an age of sedimentation ≤ 2870 Ma.

Geochronological interpretation

The maximum age of sedimentation is interpreted to be ~2870 Ma, with a significant contribution from a ca. 2955 Ma source.

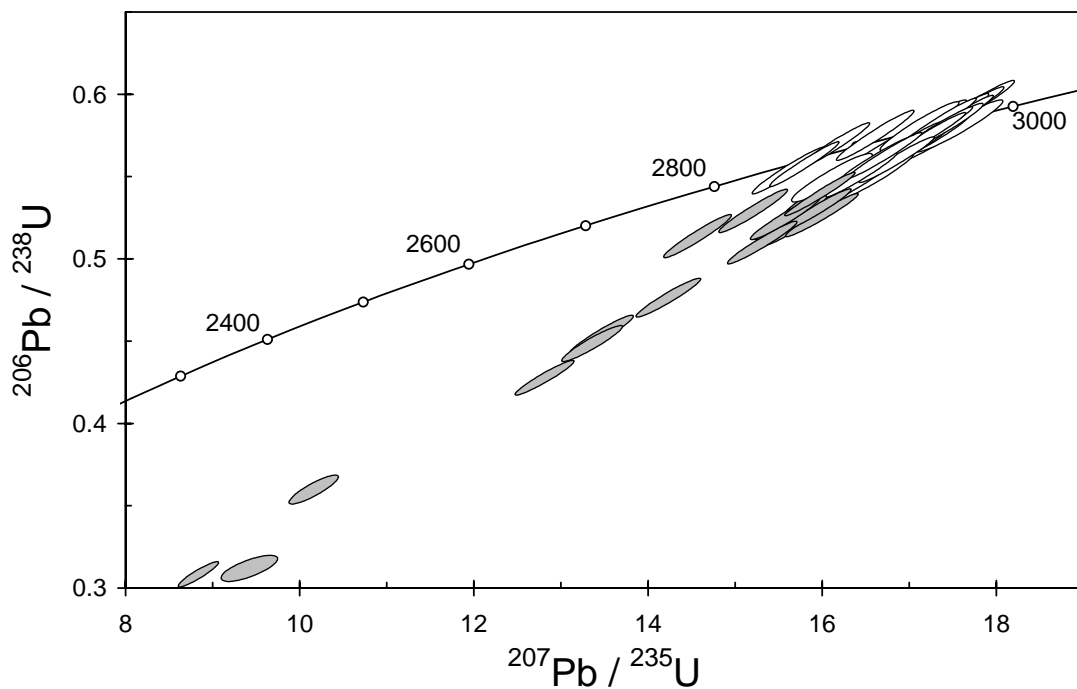


Figure 53. Concordia plot for zircons from sample 2001967056: deformed pebble meta-conglomerate, Hurleys Reward. White filled symbols are used to define the age of the sample; discordant and/or high common Pb analyses are light grey.

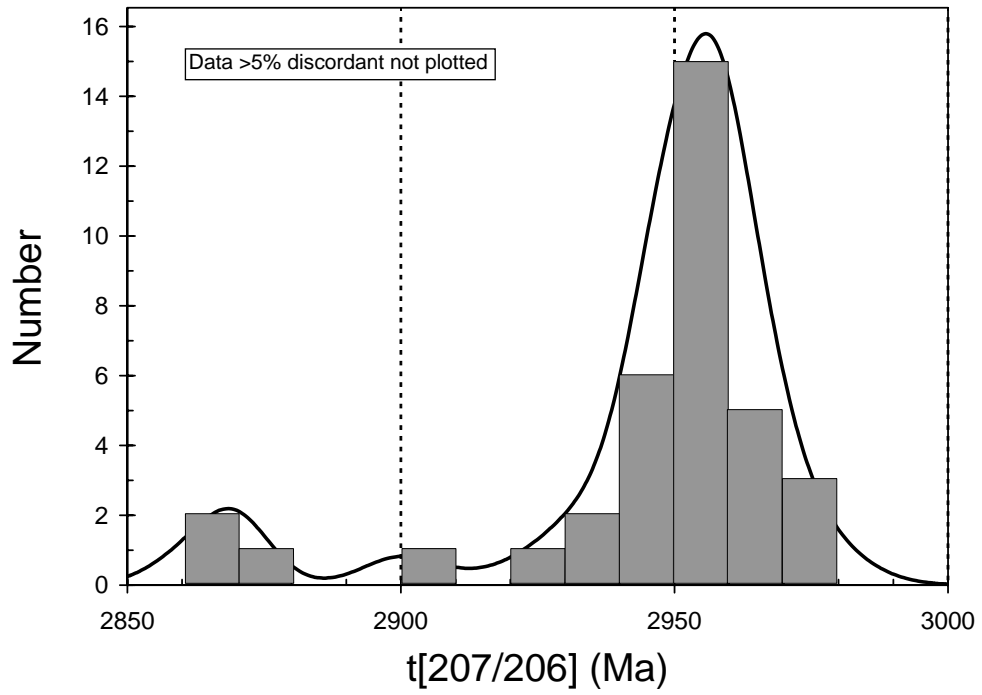


Figure 54. Cumulative probability plot of concordant $^{207}\text{Pb}/^{206}\text{Pb}$ data for zircon from sample 2001967056: deformed pebble meta-conglomerate, Hurleys Reward.

Table 22. SHRIMP analytical results for zircon from sample 2001967056: deformed pebble meta-conglomerate, Hurleys Reward, in order of $^{207}\text{Pb}/^{206}\text{Pb}$ age.

grain-spot	U (ppm)	Th (ppm)	4f206 (%)	$^{207}\text{Pb}/^{206}\text{Pb}$		$^{206}\text{Pb}/^{238}\text{U}$		$^{207}\text{Pb}/^{235}\text{U}$		$^{208}\text{Pb}/^{232}\text{Th}$	conc. (%)	$^{207}\text{Pb}/^{206}\text{Pb}$ Age (Ma)	
					±		±		±				±
34-1	93	66	0.040	0.2043	0.0009	0.554	0.009	15.61	0.27	0.149	99	2861	7
40-1	146	113	0.025	0.2053	0.0007	0.558	0.009	15.79	0.27	0.152	100	2869	6
48-1	110	43	-0.057	0.2056	0.0008	0.569	0.009	16.13	0.28	0.156	101	2872	6
6-1	105	77	0.061	0.2093	0.0009	0.576	0.010	16.61	0.30	0.153	101	2900	7
10-1	66	30	0.163	0.2126	0.0015	0.549	0.010	16.11	0.31	0.142	96	2926	11
27-1	92	64	0.103	0.2136	0.0011	0.581	0.010	17.12	0.30	0.144	101	2933	8
36-1	65	26	-0.004	0.2143	0.0011	0.582	0.010	17.19	0.32	0.159	101	2938	8
33-1	33	13	0.067	0.2147	0.0017	0.568	0.011	16.80	0.36	0.154	99	2941	12
14-1	141	57	0.063	0.2149	0.0007	0.560	0.009	16.61	0.28	0.154	97	2943	6
30-1	137	65	0.016	0.2153	0.0007	0.563	0.009	16.72	0.28	0.136	98	2946	6
29-1	87	29	-0.018	0.2154	0.0010	0.579	0.010	17.19	0.30	0.163	100	2946	7
44-1	140	215	0.099	0.2155	0.0008	0.584	0.010	17.34	0.29	0.155	101	2947	6
54-1	138	54	0.000	0.2157	0.0007	0.569	0.010	16.94	0.29	0.151	99	2949	5
39-1	97	34	-0.040	0.2161	0.0009	0.586	0.010	17.46	0.31	0.158	101	2952	7
45-1	89	59	0.068	0.2162	0.0010	0.560	0.010	16.70	0.30	0.126	97	2952	8
11-1	56	184	-0.036	0.2162	0.0012	0.563	0.010	16.78	0.31	0.150	97	2952	9
49-1	112	44	0.192	0.2162	0.0009	0.551	0.009	16.43	0.28	0.133	96	2953	7
20-1	86	39	0.110	0.2164	0.0010	0.577	0.010	17.21	0.31	0.153	99	2954	7
37-1	90	55	-0.040	0.2164	0.0010	0.573	0.010	17.11	0.30	0.151	99	2954	7
25-1	89	56	0.021	0.2165	0.0010	0.568	0.010	16.95	0.30	0.152	98	2955	7
35-1	115	54	-0.024	0.2166	0.0008	0.576	0.010	17.19	0.29	0.155	99	2956	6
8-1	87	30	-0.037	0.2166	0.0009	0.594	0.010	17.74	0.31	0.163	102	2956	7
38-1	103	46	0.005	0.2167	0.0009	0.590	0.010	17.64	0.31	0.160	101	2956	7
26-1	68	35	0.039	0.2167	0.0011	0.563	0.010	16.84	0.31	0.144	97	2957	8
23-1	157	60	0.031	0.2168	0.0007	0.579	0.009	17.30	0.29	0.149	100	2957	6
4-1	76	32	0.041	0.2169	0.0011	0.577	0.010	17.24	0.31	0.157	99	2958	8
24-1	143	101	-0.012	0.2170	0.0008	0.575	0.009	17.21	0.29	0.157	99	2958	6
42-1	123	43	0.048	0.2171	0.0008	0.585	0.010	17.52	0.30	0.156	100	2959	6
22-1	155	55	0.002	0.2173	0.0010	0.581	0.010	17.40	0.30	0.159	100	2961	7
12-1	98	57	0.079	0.2176	0.0009	0.547	0.010	16.40	0.29	0.134	95	2963	7
32-1	91	43	-0.033	0.2177	0.0009	0.567	0.010	17.01	0.30	0.158	98	2964	7
21-1	123	50	0.037	0.2180	0.0009	0.574	0.010	17.25	0.30	0.157	99	2966	7
41-1	118	68	0.034	0.2181	0.0008	0.560	0.009	16.85	0.29	0.105	97	2967	6
28-1	48	14	0.134	0.2185	0.0014	0.573	0.011	17.28	0.34	0.154	98	2970	10
13-1	55	30	-0.104	0.2187	0.0012	0.550	0.010	16.59	0.31	0.150	95	2971	9
46-1	50	24	0.128	0.2192	0.0013	0.581	0.011	17.58	0.33	0.154	99	2975	9
>5% discordant													
3-1	100	58	0.170	0.2158	0.0012	0.525	0.009	15.63	0.28	0.090	92	2949	9
5-1	128	116	0.069	0.2182	0.0009	0.529	0.009	15.92	0.27	0.108	92	2967	7
7-1	137	128	0.548	0.2152	0.0012	0.454	0.008	13.46	0.24	0.065	82	2945	9
9-1	129	134	0.356	0.2173	0.0011	0.427	0.007	12.79	0.22	0.069	77	2961	8
15-1	111	82	0.051	0.2202	0.0009	0.527	0.009	15.99	0.27	0.089	91	2982	6
16-1	146	97	0.244	0.2152	0.0011	0.525	0.009	15.57	0.27	0.089	92	2945	8
17-1	181	201	0.704	0.2084	0.0014	0.306	0.005	8.80	0.16	0.031	60	2893	11
18-1	167	229	1.341	0.2196	0.0034	0.310	0.005	9.39	0.22	0.031	58	2978	25
19-1	159	293	0.737	0.2050	0.0018	0.358	0.006	10.13	0.19	0.024	69	2867	15
31-1	53	29	0.039	0.2149	0.0012	0.541	0.010	16.03	0.30	0.137	94	2943	9
43-1	153	129	0.068	0.2147	0.0008	0.540	0.009	15.97	0.27	0.137	94	2941	6
47-1	84	47	0.088	0.2056	0.0010	0.514	0.009	14.56	0.26	0.084	93	2871	8
50-1	140	157	0.635	0.2162	0.0012	0.448	0.007	13.35	0.23	0.040	81	2952	9
51-1	109	104	0.290	0.2168	0.0011	0.476	0.008	14.23	0.25	0.073	85	2957	8
52-1	89	66	0.092	0.2178	0.0010	0.510	0.009	15.31	0.27	0.060	90	2964	7
53-1	95	51	0.323	0.2185	0.0011	0.520	0.009	15.68	0.27	0.106	91	2970	8
55-1	122	41	0.042	0.2083	0.0010	0.529	0.009	15.20	0.26	0.128	94	2893	8

Data are at 1σ precision. All Pb data are common-Pb corrected (based on ^{204}Pb and Broken Hill Pb composition). Analysis date: 28/01/02; session Z3813i.

2001969001: Juglah Monzogranite

- 1:250,000 sheet:** Kurnalpi (SH5110)
- 1:100,000 sheet:** Kanowna (3236)
- MGA:** 403198mE 6586119mN
- Location:** The sample is from a flat pavement, about 4.8 km along the road from Boundary Dam and approximately 70 m north of a fence line.
- Description:** This is a white, equigranular to very sparsely feldspar porphyritic, medium-grained homogeneous biotite monzogranite. The rock has no obvious fabric, contains no enclaves, and is cut by minor to rare aplite and pegmatite.
- The unit has a granular texture. Principal minerals are equal proportions of K-feldspar and plagioclase, and lesser quartz and biotite. K-feldspar grains are subhedral to anhedral, locally to 6 mm, with common tartan twinning and minor perthite. Plagioclase is subhedral and well twinned, with some normal and/or oscillatory zoning, and minor myrmekitic outgrowths. Also present is minor, but pervasive, coarse white mica, relatively common fine white mica, epidote (particularly dusting plagioclase cores), and minor to uncommon carbonate. Quartz is anhedral, with minor to moderately undulose extinction. Biotite (5–6%) is light yellow to medium-dark brown, and commonly chloritised, with minor to moderate epidote. Accessory phases include zircon, apatite, relatively common opaque minerals and minor allanite.
- Mount, pop:** Z3739A

Description of zircons

The zircon mainly occurs as euhedral to subhedral crystals and fragments which are stubby to elongate, and vary in size from 65 μm to 320 μm in length. A smaller proportion of the grains are anhedral fragments. Some of the crystals and fragments are well-rounded, but many have sharp crystal faces and/or only slightly abraded faces. The grains are colourless to pale grey-brown and vary from clear to turbid. Fractures are common, particularly in the darker grains. Several grains have discrete cores and rims, visible in both transmitted and reflected light, and in CL. Many grains have well-defined continuous euhedral concentric zoning, but a number appear more uniform in CL (Fig. 55). Recrystallisation is present in a number of grains.

Concurrent standard data

There was a calibration shift after re-tuning half-way through this session, and the data were therefore processed in two blocks. In the first block, the apparent calibration slope for all QGNG ($n = 16$) data is ~ 2.3 . Omitting one outlier identified by SQUID reduces this to 2.2, for a highly linear array with 1σ scatter in Pb/U of 0.5% (MSWD = 1.7). For the second block ($n = 18$) the slope is even higher (2.5) but not as well defined (1σ scatter in Pb/U = 1.05%; MSWD = 3.9). A value of 2.2 was used for the calibration exponent in both cases. The $^{207}\text{Pb}/^{206}\text{Pb}$ data form a single population. Omitting only the one calibration outlier leaves 33 points with a weighted mean $^{207}\text{Pb}/^{206}\text{Pb}$ age of 1850.8 ± 2.6 Ma (MSWD = 1.03).

Element abundance calibration was based on CZ3 ($n = 1$ in each block).

Sample data

Thirty three analyses from 33 grains (Table 23) are all concordant, but three (1-1, 9-1, 10-1) are discounted because of significant common Pb. The data fall into two clusters (Fig. 56). The older of these may be a collection of inherited grains from multiple sources, reflected in a MSWD of 4.4 for $^{207}\text{Pb}/^{206}\text{Pb}$. However, the oldest 11 analyses, with a weighted mean $^{207}\text{Pb}/^{206}\text{Pb}$ age of 2710.6 ± 4.9 Ma (MSWD = 0.93) could be derived from a single source. The younger cluster,

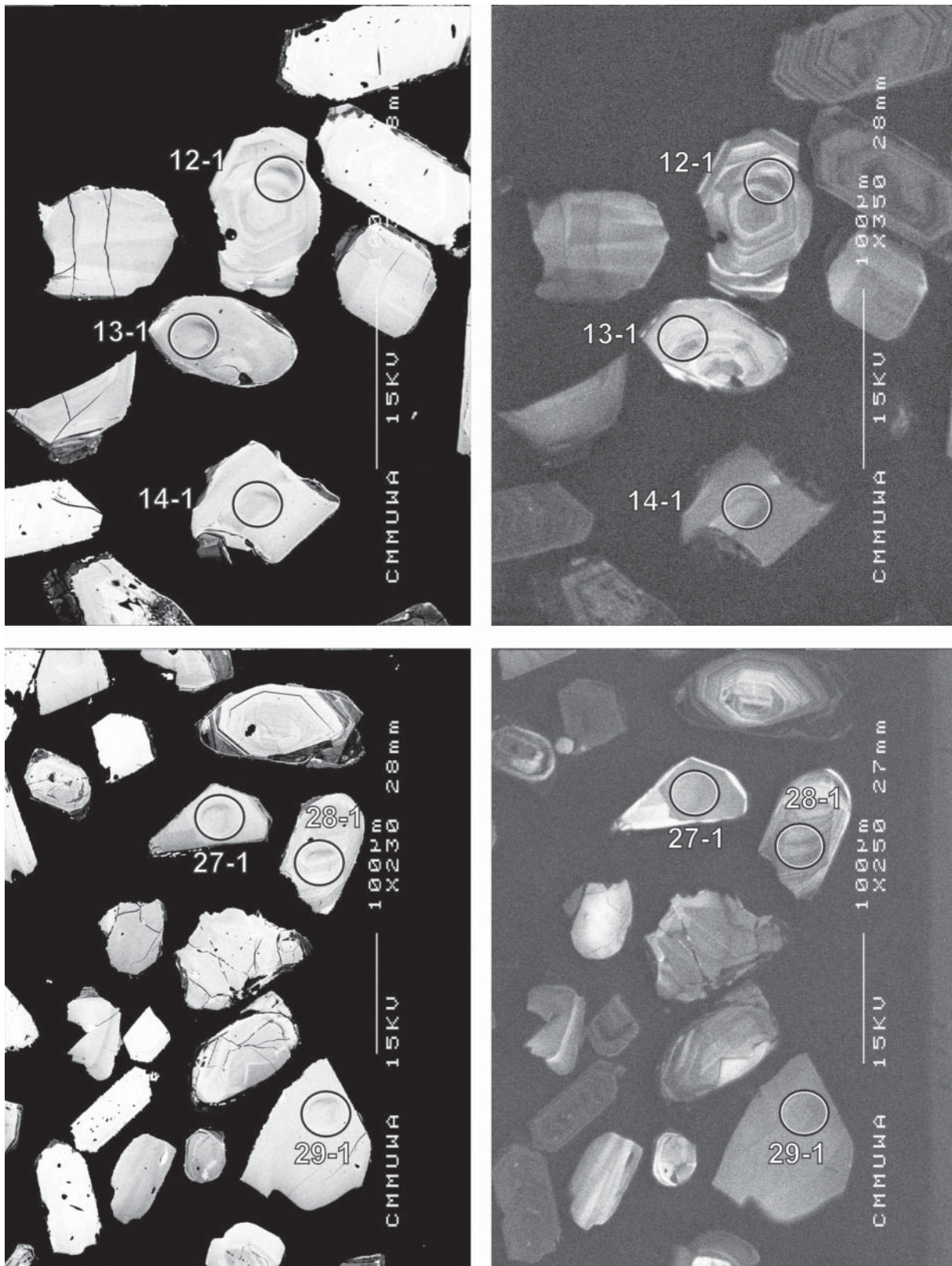


Figure 55. Representative SEM images (BSE on left, CL on right) for sample 2001969001: Juglah Monzogranite. SHRIMP analysis spots are labelled. Remnant pits from the ion microprobe analyses are faintly visible in some grains. Scale bar is 100 µm.

of 16 analyses, has a weighted mean $^{207}\text{Pb}/^{206}\text{Pb}$ age of 2632.0 ± 3.2 Ma with $\text{MSWD} = 1.12$. The older analyses are predominantly from grains with well-defined zoning, whereas the younger grains are generally clear, but there are some exceptions.

Geochronological interpretation

The intrusive age of the monzogranite is considered to be 2632 ± 4 Ma, with a large proportion of the monzogranite derived from ~ 2710 Ma precursors.

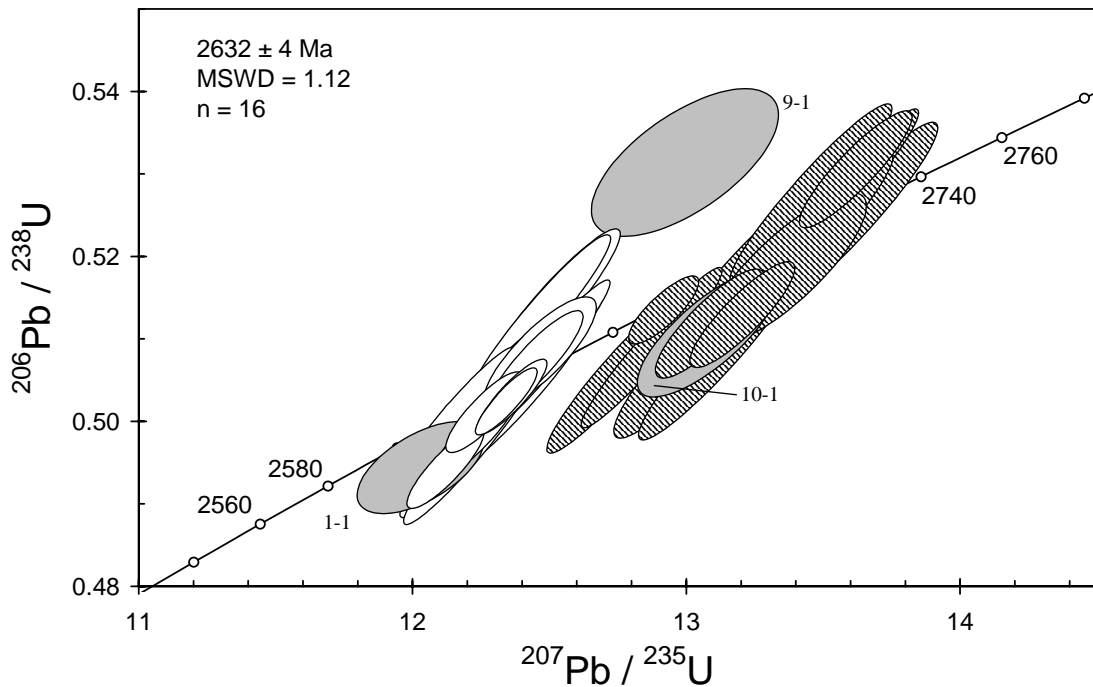


Figure 56. Concordia plot for zircons from sample 2001969001: Juglah Monzogranite. White filled symbols are used to define the age of the sample; inherited grains have diagonal shading; high common Pb analyses are light grey.

Table 23. SHRIMP analytical results for zircon from sample 2001969001: Juglah Monzogranite.

grain-spot	U (ppm)	Th (ppm)	4f206 (%)	$^{207}\text{Pb}/^{206}\text{Pb}$		$^{206}\text{Pb}/^{238}\text{U}$		$^{207}\text{Pb}/^{235}\text{U}$		$^{208}\text{Pb}/^{232}\text{Th}$	conc. (%)	$^{207}\text{Pb}/^{206}\text{Pb}$ Age (Ma)	
					±		±		±				±
Young group													
4-1	174	197	-0.013	0.1782	0.0005	0.502	0.003	12.33	0.08	0.139	99	2636	5
5-1	109	142	-0.004	0.1778	0.0007	0.494	0.003	12.11	0.09	0.136	98	2633	6
7-1	129	161	0.013	0.1780	0.0008	0.507	0.004	12.44	0.11	0.141	100	2634	7
8-1	197	178	0.166	0.1775	0.0007	0.501	0.003	12.25	0.09	0.119	100	2630	7
11-1	241	116	0.033	0.1783	0.0006	0.503	0.003	12.35	0.08	0.139	100	2637	5
15-1	112	65	0.006	0.1778	0.0011	0.508	0.005	12.46	0.14	0.143	101	2633	10
16-1	149	139	0.003	0.1779	0.0007	0.498	0.004	12.23	0.11	0.138	99	2634	7
17-1	117	77	-0.042	0.1786	0.0007	0.504	0.007	12.40	0.17	0.142	100	2640	7
18-1	157	284	0.105	0.1762	0.0007	0.499	0.006	12.13	0.16	0.137	100	2617	6
19-1	97	115	0.041	0.1778	0.0008	0.500	0.008	12.25	0.20	0.138	99	2632	7
23-1	171	208	0.109	0.1783	0.0007	0.496	0.006	12.20	0.16	0.138	99	2637	6
26-1	114	148	0.085	0.1770	0.0008	0.502	0.007	12.24	0.17	0.137	100	2625	8
29-1	114	119	0.085	0.1766	0.0009	0.513	0.007	12.49	0.17	0.140	102	2621	8
31-1	142	141	-0.040	0.1783	0.0006	0.507	0.006	12.47	0.16	0.141	100	2637	6
32-1	122	142	0.043	0.1782	0.0007	0.506	0.006	12.45	0.17	0.141	100	2637	7
34-1	114	118	0.051	0.1763	0.0007	0.512	0.007	12.46	0.17	0.140	102	2619	7
Old group													
2-1	176	97	0.265	0.1824	0.0007	0.513	0.003	12.91	0.08	0.125	100	2675	6
5-1	82	54	0.026	0.1861	0.0008	0.531	0.005	13.62	0.14	0.146	101	2708	7
12-1	122	67	0.159	0.1867	0.0009	0.513	0.004	13.20	0.13	0.144	98	2714	8
13-1	63	31	0.262	0.1869	0.0015	0.518	0.006	13.36	0.19	0.139	99	2715	14
14-1	121	133	0.110	0.1854	0.0010	0.512	0.004	13.08	0.13	0.141	99	2702	9
20-1	68	37	-0.091	0.1879	0.0010	0.525	0.008	13.60	0.21	0.147	100	2724	9
21-1	60	49	0.100	0.1858	0.0011	0.509	0.008	13.05	0.21	0.139	98	2706	10
22-1	64	55	0.164	0.1853	0.0011	0.517	0.008	13.22	0.21	0.141	99	2701	10
24-1	97	99	-0.082	0.1871	0.0008	0.522	0.007	13.47	0.19	0.145	100	2717	7
25-1	101	86	-0.021	0.1865	0.0008	0.527	0.007	13.56	0.19	0.146	101	2712	7
27-1	80	1	0.077	0.1872	0.0009	0.508	0.007	13.11	0.19	0.115	97	2717	8
28-1	129	60	-0.005	0.1835	0.0007	0.509	0.006	12.87	0.17	0.139	99	2684	6
30-1	118	102	0.206	0.1828	0.0008	0.506	0.007	12.75	0.17	0.128	98	2679	7
33-1	80	77	0.114	0.1850	0.0009	0.527	0.007	13.45	0.20	0.140	101	2698	8
High common Pb													
1-1	107	234	3.411	0.1765	0.0018	0.494	0.004	12.02	0.15	0.065	99	2620	17
9-1	71	27	2.958	0.1773	0.0024	0.531	0.006	12.99	0.23	0.172	105	2628	22
10-1	89	76	1.114	0.1858	0.0016	0.510	0.005	13.07	0.17	0.142	98	2705	14

Data are at 1 σ precision. All Pb data are common-Pb corrected (based on ^{204}Pb and Broken Hill Pb composition). Analysis date: 16/11/01; session Z3739i.

2001969013A: biotite granodiorite enclave, Ivor Rocks

1:250,000 sheet: Laverton (SH5102)

1:100,000 sheet: McMillan (3441)

MGA: 493287mE 6856695mN

Location: The sample was collected from the north-east side of large, low granite dome at Ivor Rocks, just south of the White Cliffs – Yamarna Road and 2.5 km north-west of White Cliffs Homestead.

Description: This foliated, dark grey, equigranular, fine- to medium-grained (<1–2 mm) biotite granodiorite occurs as pods, up to 10 m in length. The pods are all approximately elongated in roughly the same direction within the host porphyritic monzogranite (sample 2001969013B). Foliation is defined by elongated quartz and well-aligned biotite.

The rock has a granoblastic texture. Principal minerals are plagioclase, K-feldspar, quartz and biotite, with plagioclase >> K-feldspar. Plagioclase is subhedral to anhedral, with faint to very faint twinning. Minor amounts of myrmekite are developed. The plagioclase is locally altered to white mica and carbonate. Quartz is anhedral to elongate, weakly to strongly undulose, and aligned. K-feldspar is anhedral to interstitial; tartan twinning is common, minor perthite is present. Biotite (6–9%) occurs as well-aligned, light-yellow to medium (-dark) brown, elongated grains, with minor chloritisation. Accessory phases include zircon, relatively common, large apatite, minor allanite (<1%, subhedral), and opaque minerals.

Mount, pop: Z3805A

Description of zircons

The fragments and crystals of zircon range from anhedral, well-rounded, grains, to subhedral grains with slight rounding of crystals faces. Grain size is mostly from 70 μm to 300 μm (aspect ratio 1:1 to 4:1), although a few larger grains are present. Most grains are colourless and many contain small inclusions and internal features that make the grains appear slightly turbid in transmitted light. These grains show well-defined zoning in CL (Fig. 57). However, there is evidence of local recrystallisation, and numerous grains contain cores that are overgrown by rims of variable thickness. A minority of grains that are clear and featureless in transmitted and reflected light, appear bright and display faint zoning in CL.

Concurrent standard data

The main analytical session was interrupted by a period of duoplasmatron instability and communication problems. Data were therefore processed in two blocks. For the first of these, omission of one outlier identified by SQUID yields an apparent calibration slope for QGNG of 1.9 ($n = 19$), but the scatter is relatively large (1σ in Pb/U = 1.4%; MSWD = 9.8). For the second block ($n = 11$) there is also one obvious outlier, but the slope is better defined and closer to the ~2.2 long-term average (slope = 2.3; 1σ in Pb/U = 0.95%; MSWD = 3.7). A value of 2.2 was used for the calibration exponent in both cases. The $^{207}\text{Pb}/^{206}\text{Pb}$ data form a single population. Using the standard culling procedure (refer to chapter on "Data compilation for the QGNG standard") two calibration outliers and one 3σ (high) outlier were excluded leaving 28 points with a weighted mean $^{207}\text{Pb}/^{206}\text{Pb}$ age of 1850.5 ± 2.7 Ma (MSWD = 0.98). Element abundance calibration was based on CZ3 ($n = 2$ in each block).

Additional analyses were made on this sample and on 2001969019A (analysed in 2001; Fletcher et al., 2001) as part of session Z3963j, concentrating on possible inherited grain cores. Over 11 hours, a total of 11 analyses of QGNG were taken from mounts Z3805 and Z3734. These were treated as an independent data set, though they are entirely compatible with the QGNG data from Z3963. The 1σ scatter in Pb/U is 0.53% (MSWD = 1.80) and the calibration factor is <1%

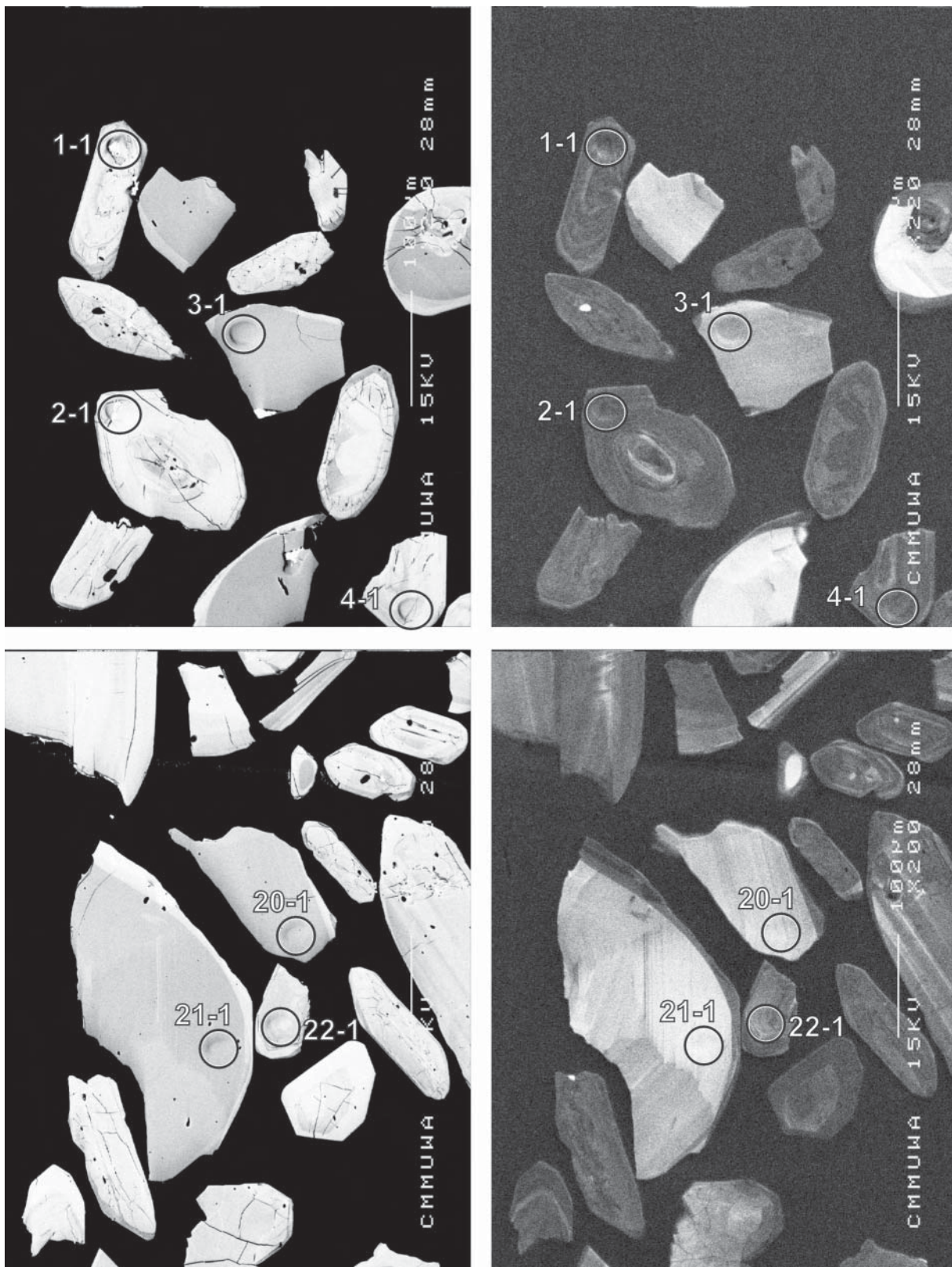


Figure 57. Representative SEM images (BSE on left, CL on right) for sample 2001969013A: biotite granodiorite enclave, Ivor Rocks. SHRIMP analysis spots are labelled. Remnant pits from the ion microprobe analyses are faintly visible in some grains. Scale bar is 100 μ m.

different from that for Z3963j. The weighted mean $^{207}\text{Pb}/^{206}\text{Pb}$ age for the 11 analyses is 1852.4 ± 6.3 Ma (MSWD = 1.4). Element abundance calibration was based on CZ3 (n = 1).

Sample data

Nine of the 39 analyses (from 38 grains; Table 24, Fig. 52) are >5% discordant or have >1% common ^{206}Pb and are here considered unreliable. The remaining data define a wide range of $^{207}\text{Pb}/^{206}\text{Pb}$ (Fig. 59). They are mostly low in U and Th, suggesting metamorphic recrystallisation. However, there is no correlation between U and $^{207}\text{Pb}/^{206}\text{Pb}$.

Geochronological interpretation

These data must be considered with those for the enclosing porphyritic granite 2001969013B. Both appear to include a complex array of reset, or partially reset, grains. Even though there are no obvious extremely old cores, it is possible that the majority of grains are xenocrysts in both samples, and that the different age spectra reflect different degrees of resetting. Note that the enclaves of this sample have a higher proportion of older grains than the enclosing granite. If this is the case, both rocks might have crystallised at ~2640 Ma. However, it is also possible that this sample is ~2700 Ma old, includes xenocrysts >2750 Ma, and had its zircon U–Pb systems partially reset when disrupted and incorporated into the porphyritic granite at ~2670 Ma. The isotopic array is difficult to interpret.

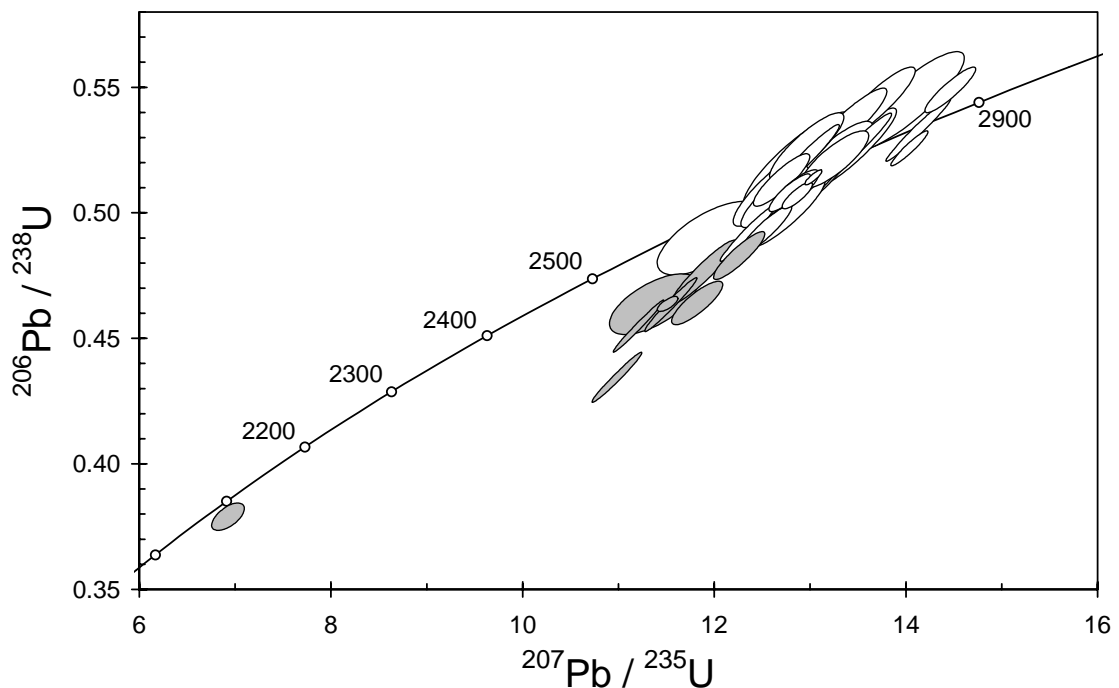


Figure 58. Concordia plot for zircons from sample 2001969013A: biotite granodiorite enclave, Ivor Rocks. White filled symbols include both inherited and reset grains, and possibly magmatic grains; discordant and/or high common Pb analyses are grey.

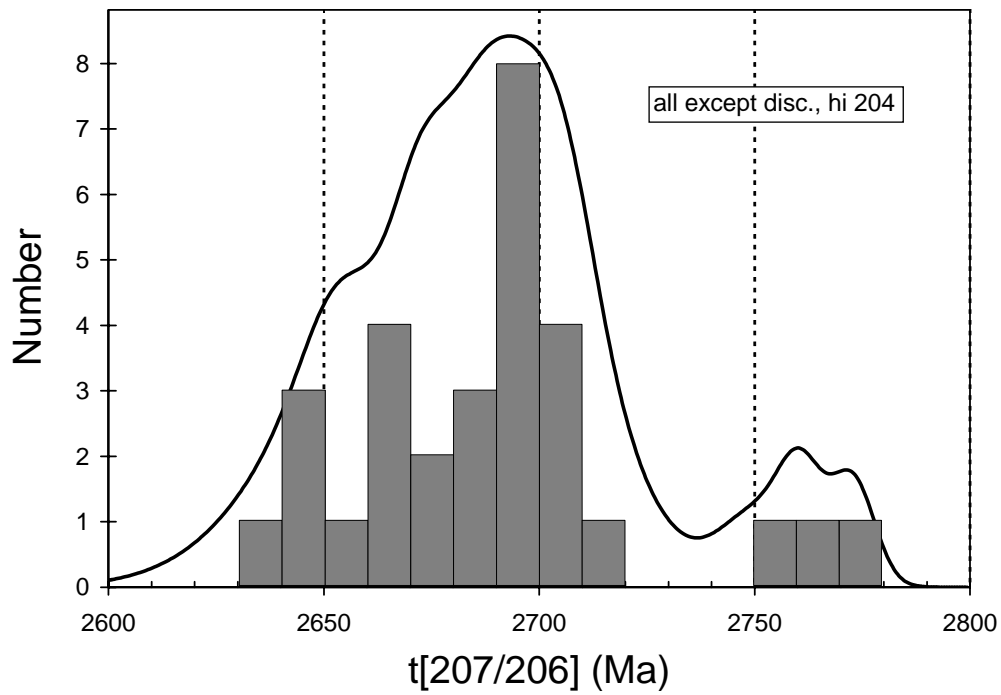


Figure 59. Cumulative probability plot of concordant $^{207}\text{Pb}/^{206}\text{Pb}$ data for sample 2001969013A: biotite granodiorite enclave, Ivor Rocks (white filled symbols in Fig. 58).

Table 24. SHRIMP analytical results for zircon from sample 2001969013A: biotite granodiorite enclave, Ivor Rocks.

grain-spot	U (ppm)	Th (ppm)	4f206 (%)	$^{207}\text{Pb}/^{206}\text{Pb}$		$^{206}\text{Pb}/^{238}\text{U}$		$^{207}\text{Pb}/^{235}\text{U}$		$^{208}\text{Pb}/^{232}\text{Th}$	conc. (%)	$^{207}\text{Pb}/^{206}\text{Pb}$	
					\pm		\pm		\pm			Age (Ma)	\pm
2-2	481	470	0.472	0.1843	0.0011	0.493	0.007	12.52	0.18	0.183	96	2692	10
3-1	44	20	0.030	0.1834	0.0010	0.508	0.009	12.85	0.24	0.140	99	2684	9
5-1	50	34	0.141	0.1837	0.0011	0.517	0.009	13.11	0.25	0.142	100	2687	10
6-1	35	16	0.271	0.1818	0.0015	0.510	0.010	12.78	0.26	0.137	99	2670	13
7-1	31	12	-0.065	0.1852	0.0012	0.512	0.010	13.07	0.27	0.148	99	2700	11
8-1	53	21	-0.087	0.1826	0.0016	0.544	0.010	13.69	0.27	0.155	104	2676	14
9-1	35	22	-0.110	0.1849	0.0012	0.510	0.010	13.00	0.26	0.145	98	2697	11
10-1	87	49	0.082	0.1859	0.0008	0.527	0.009	13.51	0.23	0.143	101	2707	7
11-1	61	17	0.007	0.1800	0.0008	0.522	0.009	12.94	0.23	0.142	102	2653	8
13-1	42	78	0.639	0.1849	0.0017	0.500	0.009	12.74	0.27	0.145	97	2697	15
14-1	24	8	0.469	0.1796	0.0021	0.510	0.011	12.64	0.31	0.129	100	2650	20
15-1	26	9	0.111	0.1855	0.0016	0.526	0.011	13.45	0.30	0.146	101	2703	14
16-1	249	132	0.303	0.1821	0.0007	0.491	0.007	12.34	0.19	0.113	96	2672	6
17-1	14	16	0.388	0.1866	0.0026	0.545	0.013	14.02	0.39	0.149	103	2712	23
19-1	150	65	0.099	0.1922	0.0006	0.533	0.008	14.13	0.23	0.148	100	2761	5
20-1	33	10	0.283	0.1813	0.0023	0.517	0.010	12.91	0.30	0.134	101	2665	21
21-1	18	5	0.437	0.1793	0.0027	0.520	0.013	12.86	0.38	0.131	102	2647	25
22-1	74	70	0.213	0.1794	0.0013	0.513	0.007	12.69	0.20	0.140	101	2647	12
23-1	52	59	0.215	0.1808	0.0017	0.506	0.008	12.62	0.23	0.139	99	2661	15
24-1	323	226	0.163	0.1936	0.0006	0.526	0.005	14.03	0.13	0.133	98	2773	5
25-1	45	1	0.502	0.1785	0.0018	0.526	0.009	12.96	0.26	—	103	2639	17
28-1	132	63	0.157	0.1909	0.0009	0.549	0.006	14.46	0.17	0.150	103	2750	8
29-1	41	13	0.190	0.1814	0.0015	0.536	0.009	13.39	0.26	0.145	104	2665	14
30-1	62	46	0.285	0.1844	0.0018	0.521	0.008	13.25	0.23	0.141	100	2693	16
31-1	41	29	0.502	0.1837	0.0020	0.523	0.009	13.24	0.27	0.138	101	2686	18
33-1	74	24	-0.014	0.1825	0.0010	0.508	0.005	12.78	0.14	0.181	99	2676	9
34-1	129	89	0.109	0.1840	0.0008	0.507	0.003	12.85	0.10	0.177	98	2689	7
35-1	14	2	1.312	0.1766	0.0039	0.490	0.010	11.92	0.36	0.236	98	2621	37
36-1	411	51	0.018	0.1837	0.0004	0.514	0.002	13.02	0.06	0.182	100	2687	4
38-1	53	21	0.019	0.1830	0.0013	0.509	0.005	12.84	0.16	0.181	99	2680	12
>5% discordant or high common Pb													
1-1	377	206	0.689	0.1835	0.0006	0.433	0.007	10.97	0.17	0.104	86	2685	5
2-1	307	221	0.310	0.1788	0.0005	0.454	0.007	11.19	0.17	0.088	91	2642	4
4-1	226	103	0.313	0.1808	0.0006	0.463	0.007	11.53	0.18	0.141	92	2660	5
12-1	83	46	0.071	0.1777	0.0036	0.463	0.008	11.35	0.30	0.063	93	2632	34
18-1	49	10	0.085	0.1809	0.0012	0.476	0.008	11.87	0.22	0.144	94	2661	11
26-1	98	54	0.308	0.1848	0.0015	0.463	0.006	11.81	0.18	0.061	91	2696	13
27-1	81	49	0.047	0.1840	0.0012	0.482	0.006	12.24	0.18	0.131	94	2690	11
32-1	549	150	2.478	0.1324	0.0017	0.377	0.004	6.89	0.11	0.167	97	2130	23
37-1	301	287	0.087	0.1801	0.0008	0.463	0.002	11.50	0.07	0.161	92	2654	7

Data are at 1σ precision. All Pb data are common-Pb corrected (based on ^{204}Pb and Broken Hill Pb composition). Analysis date: 20/11/01; session Z3805i and 8/06/02; part of session Z3963j (spots 2-2 and 32-1 to 38-1).

2001969013B: K-feldspar porphyritic monzogranite, Ivor Rocks

1:250,000 sheet: Laverton (SH5102)

1:100,000 sheet: McMillan (3441)

MGA: 493287mE 6856695mN

Location: The sample was collected from the north-east side of a large, low granite dome at Ivor Rocks, just south of the White Cliffs – Yamarna Road and 2.5 km north-west of White Cliffs Homestead.

Description: This is a grey-pink, variably (mostly moderately-) K-feldspar porphyritic, medium-grained allanite-biotite monzogranite. Potassium-feldspar phenocrysts are pinkish, and to 1–3 cm in length. The unit contains elongated enclaves of foliated finer-grained granodiorite (sample 2001969013A), and biotite-rich schlieren and bands that are sub-parallel to the margins of the enclaves.

Principal minerals of the granoblastic texture are plagioclase, K-feldspar, quartz and biotite, with plagioclase~K-feldspar. Plagioclase occurs as anhedral to subhedral grains with faint to very faint twinning, minor zoning, relatively common myrmekitic outgrowths, and weak white mica alteration. K-feldspar forms as subhedral to anhedral poikilitic phenocrysts to anhedral smaller grains, with well-developed tartan twinning, and common perthite. Quartz is anhedral and elongated, and displays moderately to locally strongly undulose extinction, with subgrain development and some recrystallisation. Biotite (5–6%) occurs as light yellow to medium red-brown flakes to 3–4 mm, that are partly chloritic, with secondary rutile. Accessory phases include euhedral zircon and apatite, irregular opaque minerals, and minor allanite (<3mm).

Mount, pop: Z3805B

Description of zircons

Most zircon grains are elongate (aspect ratios up to 5:1), ranging in length from 50 μm to >250 μm , with subhedral to euhedral morphologies. The grains are colourless to pale yellow, with some Fe-oxide staining. They are generally clear to slightly turbid, the latter feature being due to the presence of small inclusions and zoning. Well-defined zoning is visible in many grains in both transmitted and reflected light and in CL (Fig. 60). A small number of grains have visible cores. Many display evidence of recrystallisation, as indicated by the complex internal features seen in CL.

Concurrent standard data

This analytical session was interrupted by a period of duoplasmatron instability and communication problems. Data were therefore processed in two blocks. In the first block, omission of one outlier identified by SQUID yields an apparent calibration slope for QGNG of 1.9 ($n = 19$), but the scatter is relatively large (1σ in Pb/U = 1.4%; MSWD = 9.8). For the second block ($n = 11$) there is also one obvious outlier, but the slope is better defined and closer to the ~2.2 long-term average (slope = 2.3; 1σ in Pb/U = 0.95%; MSWD = 3.7). A value of 2.2 was used for the calibration exponent in both cases. The $^{207}\text{Pb}/^{206}\text{Pb}$ data form a single population. Using the standard culling procedures (refer to chapter on "Data compilation for the QGNG standard"), two calibration outliers and one 3σ (high) outlier were excluded leaving 28 points with a weighted mean $^{207}\text{Pb}/^{206}\text{Pb}$ age of 1850.5 ± 2.7 Ma (MSWD = 0.98).

Element abundance calibration was based on CZ3 ($n = 2$ in each block).

Sample data

About 25% of the 30 analyses from individual grains (Table 25, Fig. 61) are too discordant to be useful, even though the dominant Pb-loss trend appears to be recent. The concordant data give a

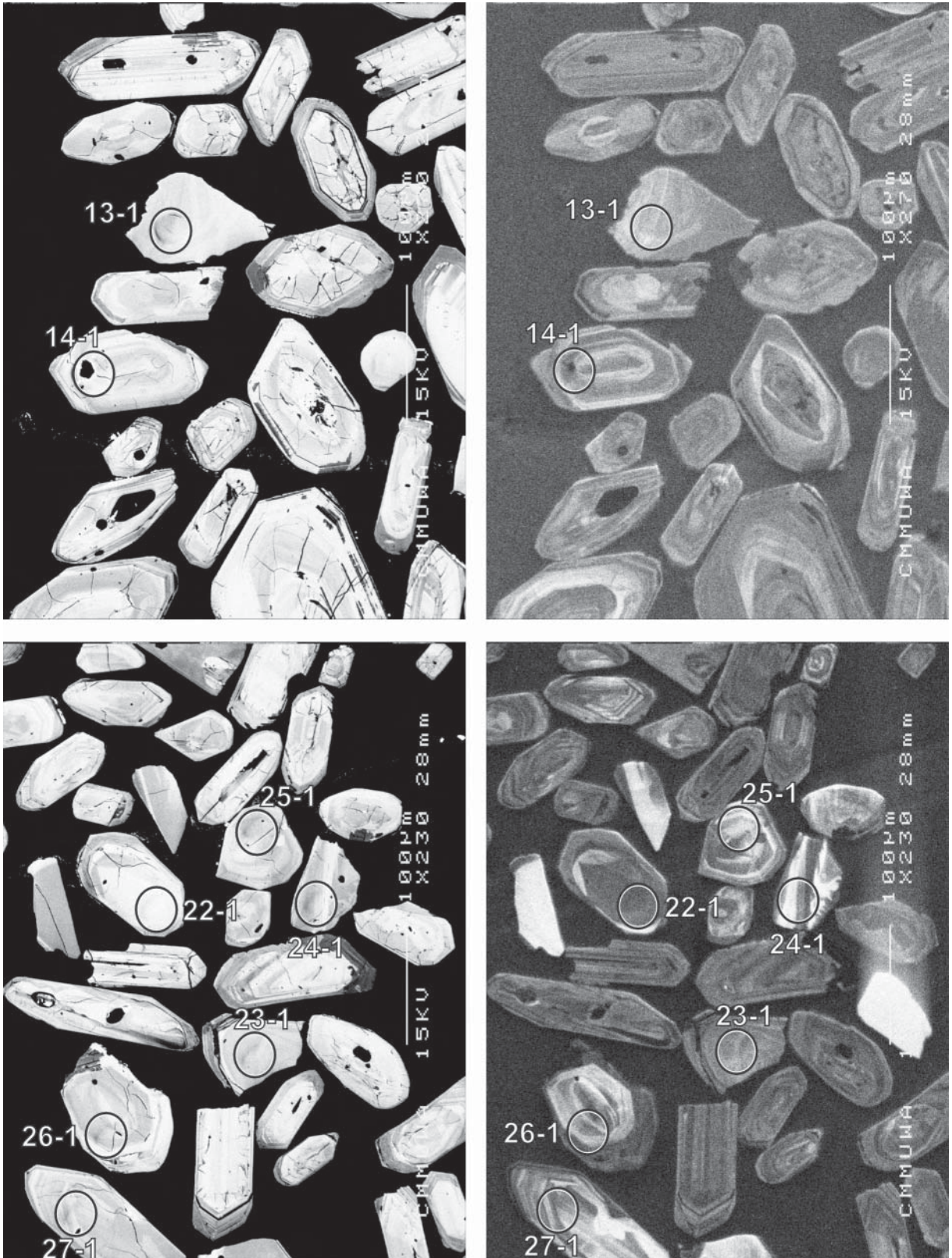


Figure 60. Representative SEM images (BSE on left, CL on right) for sample 2001969013B: K-feldspar porphyritic monzogranite, Ivor Rocks. SHRIMP analysis spots are labelled. Remnant pits from the ion microprobe analyses are faintly visible in some grains. Scale bar is 100 µm.

wide range of $^{207}\text{Pb}/^{206}\text{Pb}$ dates with a peak at ~ 2670 Ma (Fig. 56). One concordant analysis (26-1) contains relatively high common-Pb and is a younger outlier; this grain may have undergone Pb-loss and hence is not considered reliable. Many analyses have low U and Th, but there is no correlation between these abundances and $^{207}\text{Pb}/^{206}\text{Pb}$ dates, as might be expected if the array was solely due to (?remelting) resetting.

Geochronological interpretation

These data must be considered with those for the enclaves of foliated granite 2001969013A. Both samples appear to include a complex array of reset, or partially reset, grains. There are no dramatically old ages, but it is possible that the majority of grains in both samples are xenocrysts, and that the different age spectra reflect different degrees of resetting. This sample has a smaller proportion of older grains than the enclaves of 2001969013A. Although there is no well-defined data subset, it is likely that the data peak at ~ 2670 Ma (Fig. 62) records magmatism and the minor ~ 2640 Ma peak is due to a later (unidentified) magmatic event.

Table 25. SHRIMP analytical results for zircon from sample 2001969013B: K-feldspar porphyritic monzogranite, Ivor Rocks.

grain-spot	U (ppm)	Th (ppm)	4f206 (%)	$^{207}\text{Pb}/^{206}\text{Pb}$		^{206}Pb		^{207}Pb		$^{208}\text{Pb}/^{232}\text{Th}$	conc. (%)	$^{207}\text{Pb}/^{206}\text{Pb}$	
				\pm	\pm	^{235}U	\pm	Age (Ma)	\pm				
Main group													
1-1	118	66	0.054	0.1817	0.0007	0.525	0.008	13.14	0.22	0.144	102	2668	7
3-1	162	82	0.128	0.1841	0.0006	0.508	0.008	12.89	0.20	0.140	98	2690	5
5-1	54	45	0.410	0.1791	0.0012	0.514	0.009	12.69	0.24	0.137	101	2645	11
6-1	29	26	0.046	0.1820	0.0016	0.492	0.010	12.35	0.27	0.140	96	2672	14
7-1	48	34	0.082	0.1813	0.0011	0.538	0.010	13.44	0.25	0.146	104	2665	10
8-1	89	59	-0.029	0.1858	0.0007	0.507	0.008	13.00	0.22	0.143	98	2706	6
9-1	55	59	0.124	0.1813	0.0014	0.484	0.008	12.10	0.23	0.143	95	2665	13
10-1	88	91	0.118	0.1822	0.0008	0.508	0.008	12.77	0.22	0.142	99	2673	7
11-1	90	54	0.203	0.1814	0.0009	0.501	0.009	12.54	0.24	0.137	98	2666	8
12-1	28	23	0.207	0.1833	0.0013	0.500	0.010	12.64	0.26	0.139	97	2683	12
13-1	87	32	0.084	0.1820	0.0008	0.504	0.008	12.65	0.22	0.137	99	2671	7
15-1	59	63	0.069	0.1814	0.0010	0.502	0.009	12.56	0.23	0.139	98	2666	9
18-1	24	19	0.397	0.1783	0.0015	0.508	0.011	12.49	0.28	0.136	100	2637	14
21-1	34	26	0.137	0.1825	0.0017	0.494	0.010	12.43	0.28	0.148	97	2675	15
22-1	210	157	0.066	0.1846	0.0007	0.515	0.005	13.11	0.14	0.139	99	2695	6
23-1	41	45	0.064	0.1826	0.0019	0.522	0.009	13.14	0.27	0.144	101	2676	17
24-1	78	79	0.221	0.1795	0.0016	0.515	0.007	12.76	0.21	0.143	101	2649	14
25-1	73	38	0.001	0.1890	0.0011	0.527	0.007	13.73	0.20	0.146	100	2734	10
27-1	72	88	0.207	0.1818	0.0012	0.514	0.007	12.88	0.20	0.139	100	2669	11
28-1	592	445	0.189	0.1871	0.0005	0.498	0.004	12.86	0.11	0.131	96	2717	4
31-1	116	128	0.112	0.1807	0.0010	0.517	0.006	12.88	0.17	0.141	101	2659	9
>5% discordant and/or high common Pb													
4-1	222	68	2.067	0.1802	0.0009	0.416	0.006	10.34	0.17	0.166	84	2655	8
14-1	195	354	1.573	0.1801	0.0009	0.392	0.006	9.74	0.16	0.036	80	2654	9
16-1	71	89	0.174	0.1826	0.0010	0.421	0.007	10.60	0.19	0.098	85	2677	10
17-1	244	338	0.616	0.1822	0.0009	0.445	0.007	11.17	0.18	0.099	89	2673	8
19-1	90	71	0.361	0.1806	0.0013	0.461	0.008	11.47	0.21	0.137	92	2658	12
26-1	86	64	0.946	0.1760	0.0016	0.513	0.012	12.44	0.31	0.213	102	2616	15
29-1	168	123	0.515	0.1819	0.0010	0.425	0.006	10.66	0.17	0.135	85	2671	10
30-1	94	190	0.552	0.1816	0.0014	0.462	0.006	11.57	0.17	0.078	92	2668	13
32-1	124	115	0.582	0.1799	0.0014	0.471	0.005	11.68	0.16	0.144	94	2652	13

Data are at 1σ precision. All Pb data are common-Pb corrected (based on ^{204}Pb and Broken Hill Pb composition). Analysis date: 20/11/01; session Z3805i. Analysis 2-1 was aborted when high ^{204}Pb counts were observed; 20-1 was lost due to failure of the duoplasmatron arc.

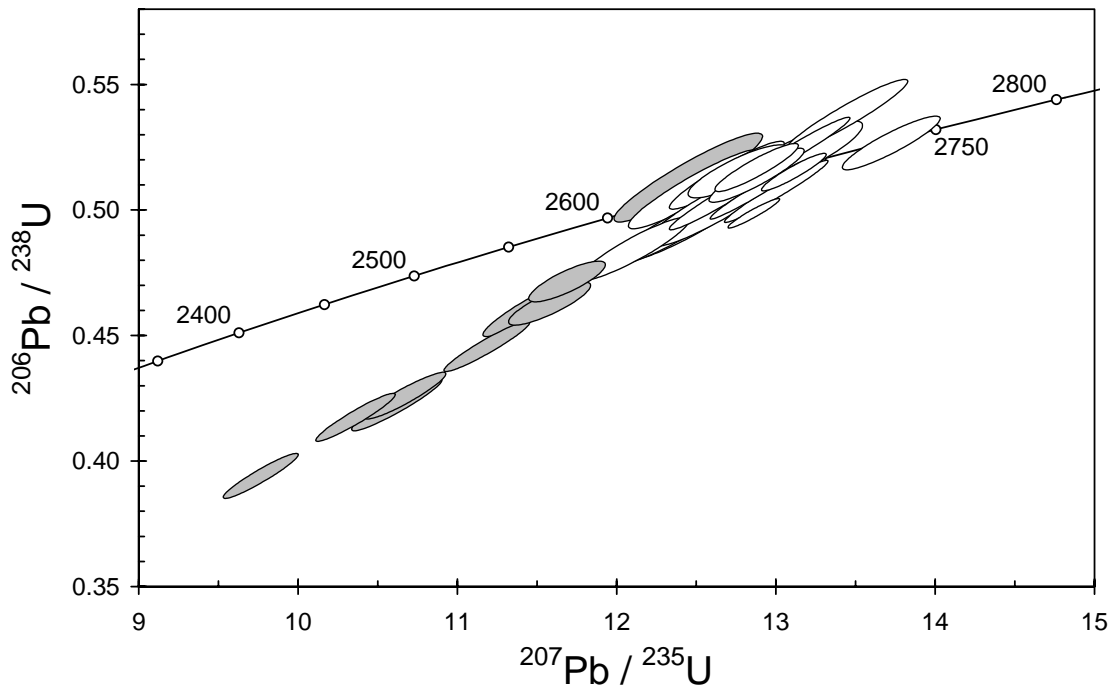


Figure 61. Concordia plot for zircons from sample 2001969013B: K-feldspar porphyritic monzogranite, Ivor Rocks. White filled symbols possibly include inherited and magnetic grains; discordant analyses are grey.

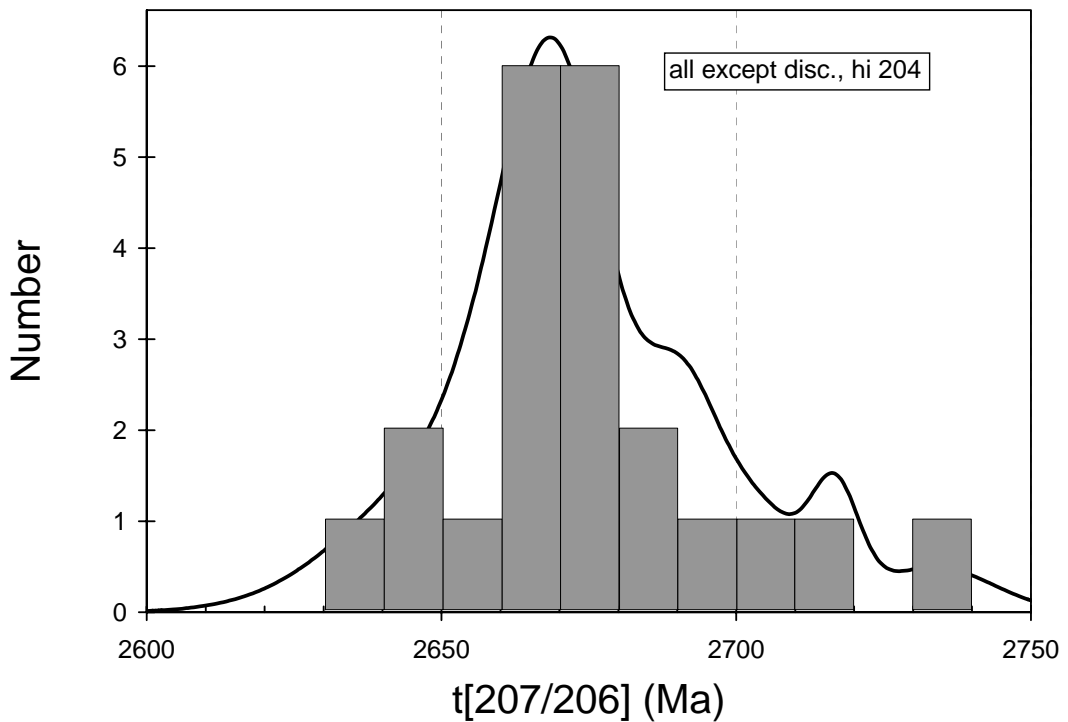


Figure 62. Cumulative probability plot of concordant data for sample 2001969013B: K-feldspar porphyritic monzogranite, Ivor Rocks (white filled symbols in Fig. 61).

2001969019A: biotite granodiorite, Ironstone Point

1:250,000 sheet: Laverton (SH5102)

1:100,000 sheet: Burtville (3440)

MGA: 493149mE 6801680mN

Location: The sample comes from a large boulder on the northeast side of a bouldery hill, immediately south of the track, about 9 km east of the Coglia-Merolia Road, and approximately 9 km south of Ironstone Point.

Description: This sample is a grey fine- to medium-grained equigranular biotite granodiorite. It forms one of a number of bands that vary in thickness from <1 cm to >80 cm within a banded granitoid complex; other bands comprise pegmatite, felsic granitoid, medium- to coarse-grained granodiorite, and thin biotite-rich layers and schlieren. The sampled layer is interpreted to have been a thin dyke in coarser-grained granodiorite. Moderate foliation in the banded granitoid complex is defined by aligned minerals and elongate quartz grains. The unit is cut by a swarm of late syenogranite dykes, of which sample 200196 9019B is representative.

The unit is characterised by a granoblastic assemblage of plagioclase (50–60%), quartz (20–30%), biotite (10%), and lesser (mostly interstitial) K-feldspar (<10%). Accessory minerals include Fe oxides, zircon and (acicular and more equant) apatite. Secondary phases include minor white mica, and lesser chlorite and carbonate.

Mount, pop: Z3734B

Introduction

Zircon from this sample was originally analysed in 2001 during the first year of the project (Fletcher et al., 2001). Subsequently, additional zircon analyses were made and rutile was analysed for the first time, as reported below (zircon) and in the next chapter (rutile). Zircon descriptions and representative SEM images were presented in Fletcher et al. (2001).

Concurrent standard data

Additional analyses were made on this sample and on 2001969013A (mount Z3805A) as part of session Z3963j, concentrating on possible inherited grain cores. Over 11 hours, a total of 11 analyses of QGNG were taken from mounts Z3805 and Z3734. These were treated as an independent data set, though they are entirely compatible with the QGNG data from Z3963. The 1σ scatter in Pb/U is 0.53% (MSWD = 1.80) and the calibration factor is <1% different from that for Z3963j. The weighted mean $^{207}\text{Pb}/^{206}\text{Pb}$ age for the 11 analyses is 1852.4 ± 6.3 Ma (MSWD = 1.4). Element abundance calibration was based on CZ3 (n = 1).

Sample data

Eight zircon analyses were obtained (Table 26, Fig. 63). Four of these are >5% discordant (34-1, 37-1, 38-1, 39-1) and are unsuitable for accurate dating, although one of them (39-1) is clearly older than the 2668 ± 4 Ma age obtained for the main data group (Fig. 64) during the original analysis of this sample (Fletcher et al., 2001). Three of the analyses (22-2, 35-1, 36-1) fall amongst the main data group from the original analyses, and one (18-2) is distinctly younger. The low U and Th for this analysis suggest that it might be from a recrystallised zone.

Geochronological interpretation

When these data are combined with those obtained previously by Fletcher et al. (2001), the weighted mean $^{207}\text{Pb}/^{206}\text{Pb}$ age changes only very slightly, to 2669 ± 4 Ma (MSWD = 1.20; n = 29). The one distinct xenocryst analysed during this session supports the meagre evidence in the

original data set for inheritance. However, there are insufficient xenocryst dates to determine inheritance patterns or identify likely precursor rocks.

Table 26. Supplementary SHRIMP analytical results for zircon from sample 200196 9019A: biotite granodiorite, Ironstone Point.

grain-spot	U (ppm)	Th (ppm)	4f206 (%)	$\frac{^{207}\text{Pb}}{^{206}\text{Pb}}$	\pm	$\frac{^{206}\text{Pb}}{^{238}\text{U}}$	\pm	$\frac{^{207}\text{Pb}}{^{235}\text{U}}$	\pm	$\frac{^{208}\text{Pb}}{^{232}\text{Th}}$	conc. (%)	$\frac{^{207}\text{Pb}}{^{206}\text{Pb}}$	Age (Ma)	\pm
Main group														
B.22-2	202	126	0.372	0.1809	0.0012	0.490	0.002	12.24	0.10	0.176	97	2662	11	
B.35-1	176	177	0.068	0.1824	0.0008	0.509	0.003	12.82	0.09	0.181	99	2674	7	
B.36-1	99	59	-0.002	0.1838	0.0008	0.499	0.004	12.66	0.11	0.181	97	2687	8	
>5% discordant														
B.34-1	57	47	0.347	0.1784	0.0015	0.465	0.005	11.46	0.15	0.172	93	2638	14	
B.37-1	162	113	2.082	0.1809	0.0014	0.352	0.002	8.76	0.09	0.162	73	2661	13	
B.38-1	515	307	0.483	0.1603	0.0006	0.415	0.001	9.19	0.04	0.157	91	2459	6	
Xenocrystic core														
B.39-1	38	23	1.684	0.1867	0.0026	0.481	0.006	12.39	0.23	0.198	93	2713	23	
Young outlier														
B.18-2	22	8	0.899	0.1759	0.0026	0.484	0.008	11.74	0.26	0.160	97	2614	24	

Data are at 1σ precision. All Pb data are common-Pb corrected (based on ^{204}Pb and Broken Hill Pb composition). Analysis date: 8/06/02; session Z3963j.

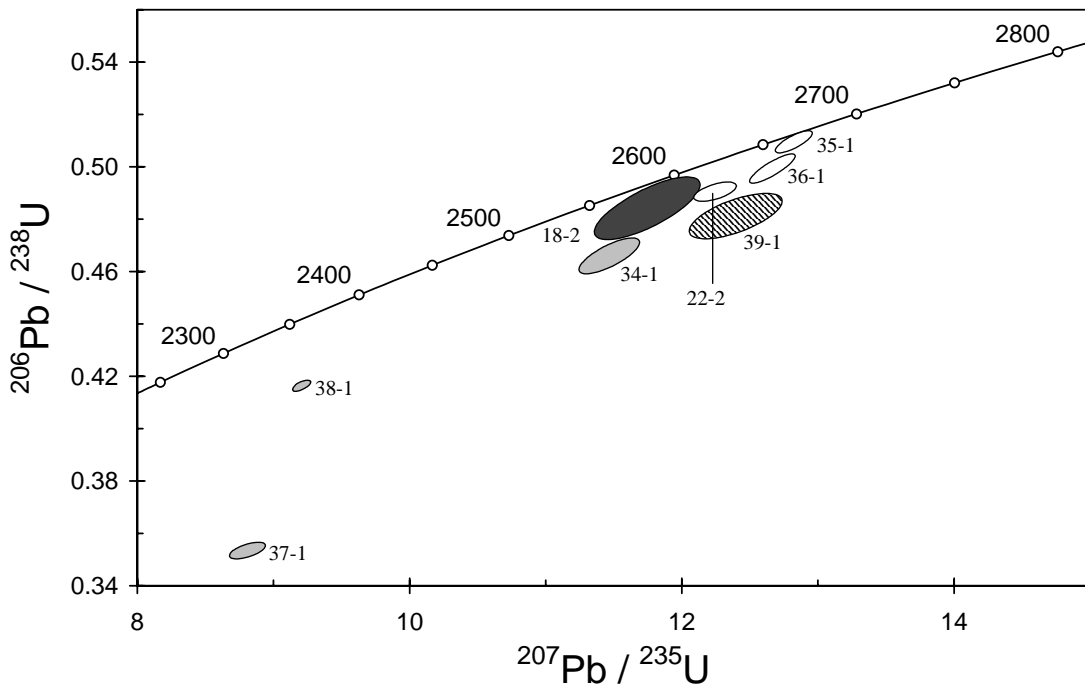


Figure 63. Concordia plot for supplementary analyses of zircon from sample 2001969019A: biotite granodiorite, Ironstone Point. White filled symbols are consistent with those used previously to define the age of the sample; inherited grain has diagonal shading; younger outlier is dark grey; discordant and/or high common Pb analyses are light grey.

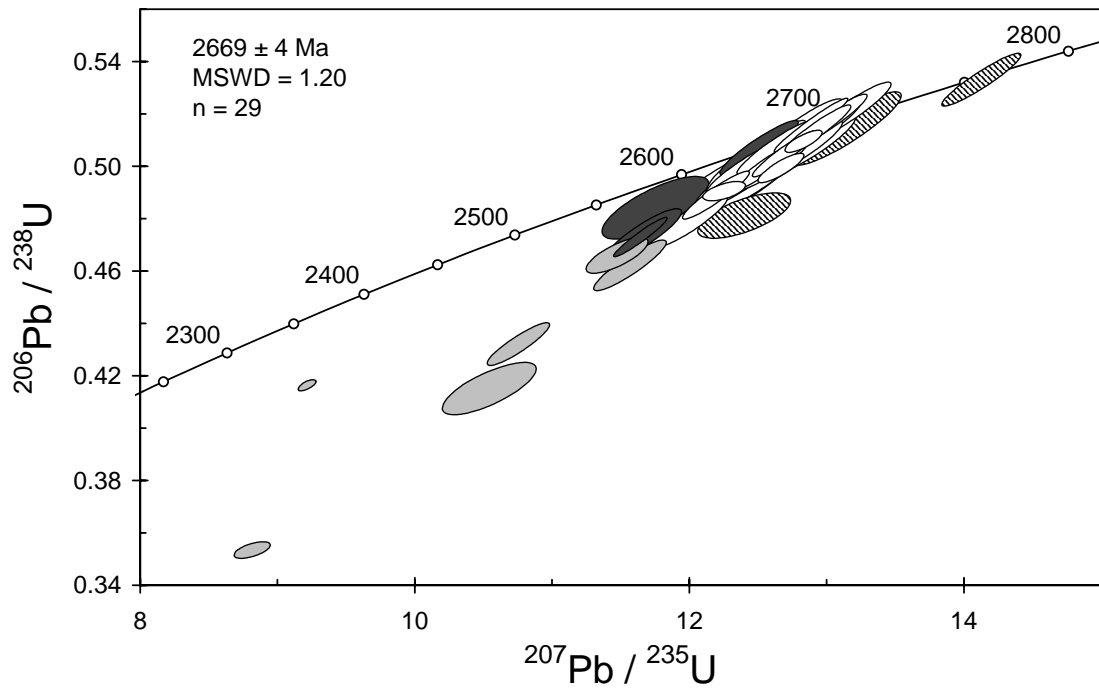


Figure 64. Concordia plot for all zircon data from sample 2001969019A: biotite granodiorite, Ironstone Point. Both the new supplementary analyses as well as data from Fletcher et al. (2001) are plotted. Shading as in Fig. 63.

2001969019A: biotite granodiorite, Ironstone Point

1:250,000 sheet: Laverton (SH5102)

1:100,000 sheet: Burtville (3440)

MGA: 493149mE 6801680mN

Location: The sample comes from a large boulder on the northeast side of a bouldery hill, immediately south of the track, about 9 km east of the Coglia-Merolia Road, and approximately 9 km south of Ironstone Point.

Description: This is a grey fine- to medium-grained equigranular biotite granodiorite. It forms one of a number of bands that vary in thickness from <1 cm to >80 cm within a banded granitoid complex; other bands comprise pegmatite, felsic granitoid, medium- to coarse-grained granodiorite, and thin biotite-rich layers and schlieren. The sampled layer is interpreted to have been a thin dyke in coarser-grained granodiorite. Moderate foliation in the banded granitoid complex is defined by aligned minerals and elongate quartz grains. The unit is cut by a swarm of late syenogranite dykes, of which sample 2001969019B is representative.

The unit is characterised by a granoblastic assemblage of plagioclase (50–60%), quartz (20–30%), biotite (10%), and lesser (mostly interstitial) K-feldspar (<10%). Accessory minerals include Fe oxides, zircon and (acicular and more equant) apatite. Secondary phases include minor white mica, and lesser chlorite and carbonate.

Mount, pop: Z3734

Introduction

Both rutile and zircon were recovered from this sample. Zircon from this sample was originally analysed in 2001 during the first year of the project (Fletcher et al., 2001). Subsequently, new rutile was analysed and additional zircon analyses were made, as reported below (rutile) and in the previous chapter (zircon). Details of the analytical procedures for rutile are presented in the Analytical Procedures chapter.

Description of rutile

A small number of light yellow-brown to dark honey brown rutile grains were obtained from the sample. They are generally clear, subhedral grains, with some rounding of crystal faces. They are mostly less than 60 μm in size. Small inclusions and fractures are present in some grains.

Concurrent standard data

Data for the WH-1 standard are listed below with the sample data (Table 27). For the early analyses, before data collection began for sample 2001969019A, the mass-204 position was set too low, causing some spurious counts to be recorded from a nearby interference peak. The corresponding data are not shown. The data scatter is more than expected in $^{206}\text{Pb}/^{238}\text{U}$, with a 1σ reproducibility of ~7%, resulting in the propagation of a large uncertainty in $^{206}\text{Pb}/^{238}\text{U}$ to the sample data.

To assess the accuracy of $^{207}\text{Pb}/^{206}\text{Pb}$, ^{208}Pb is used as a monitor of initial (common) Pb. Figure 65 shows all $^{207}\text{Pb}/^{206}\text{Pb}$ data plotted against $^{208}\text{Pb}/^{206}\text{Pb}$. There is a distinct correlation, though the best-fit line has a higher slope than expected for model common-Pb compositions. In principle, this approach could be complicated by small amounts of ^{208}Pb derived from trace Th in the sample. However, this would move data laterally and would be unlikely to generate a high slope, but it would cause additional scatter in this plot. The trend projects to an intercept (no common Pb) $^{207}\text{Pb}/^{206}\text{Pb}$ date of 2632 ± 7 Ma, indistinguishable from the TIMS reference age (2625 Ma). There are two possible outliers in these data: point 1-7 is clearly above the trend and point 1-2 is extreme in $^{208}\text{Pb}/^{206}\text{Pb}$. Omitting either of these improves agreement with the TIMS $^{207}\text{Pb}/^{206}\text{Pb}$ age. Using a conventional ^{204}Pb -based common Pb correction on the samples for which this is valid (and omitting 1-7) gives an almost identical result.

Table 27. SHRIMP analytical results for rutile WH-1 standard.

grain-spot	U (ppm)	Raw ratios		4f206 (%)	Common Pb corrected				207Pb*/206Pb* conc. (%)	Age (Ma)	±				
		207Pb/206Pb	208Pb/206Pb		207Pb*/206Pb*	208Pb*/206Pb*	209Pb*/238U	207Pb*/235U							
WH-1 reference rutile															
WH.1-1	69	0.1802	0.0008	0.00172	0.00010	0.1775	0.0009	0.0004	0.500	0.035	12.24	0.86	99	2629	8
WH.1-2	38	0.1811	0.0012	0.00498	0.00024	0.1801	0.0006	0.0004	0.474	0.033	11.76	0.82	94	2654	5
WH.1-3	58	0.1789	0.0010	0.00124	0.00006	0.1775	0.0007	0.0003	0.602	0.042	14.74	1.04	116	2630	7
WH.1-4	103	0.1789	0.0007	0.00078	0.00005	0.1779	0.0004	0.0000	0.491	0.034	12.04	0.84	98	2633	4
WH.1-5	265	0.1778	0.0005	0.00033	0.00003	0.1775	0.0009	0.0006	0.500	0.035	12.24	0.86	99	2629	8
WH.1-6	74	0.1779	0.0009	0.00052	0.00004	0.1779	0.0005	0.0004	0.498	0.035	12.22	0.85	99	2633	5
WH.1-7	270	0.1806	0.0005	0.00145	0.00006	0.1801	0.0006	0.0004	0.474	0.033	11.76	0.82	94	2654	5
WH.2-5	105	0.1777	0.0007	0.00070	0.00006	0.1775	0.0007	0.0003	0.602	0.042	14.74	1.04	116	2630	7
WH.3-2	247	0.1779	0.0004	0.00042	0.00003	0.1779	0.0004	0.0000	0.491	0.034	12.04	0.84	98	2633	4
WH.3-3	155	0.1783	0.0005	0.00079	0.00004	0.1779	0.0005	0.0004	0.498	0.035	12.22	0.85	99	2633	5
WH.3-4	421	0.1777	0.0004	0.00061	0.00004	0.1776	0.0004	0.0003	0.501	0.035	12.27	0.86	99	2631	4

Data are at 1σ precision. Common-Pb corrections are based on ²⁰⁴Pb and Broken Hill Pb composition. Analysis date: 11/05/02.

Table 28. SHRIMP analytical results for rutile from sample 2001969019A: biotite granodiorite, Ironstone Point.

grain-spot	U (ppm)	Raw ratios		4f206 (%)	Common Pb corrected				207Pb*/206Pb* conc. (%)	Age (Ma)	±				
		207Pb/206Pb	208Pb/206Pb		207Pb*/206Pb*	208Pb*/206Pb*	209Pb*/238U	207Pb*/235U							
2001969019A rutile															
1-1	463	0.1778	0.0003	0.00017	0.00002	0.1778	0.0003	0.0001	0.491	0.034	12.04	0.84	98	2632	3
2-1	120	0.1779	0.0007	0.00137	0.00009	0.1773	0.0008	0.0010	0.462	0.032	11.31	0.80	93	2628	8
3-1	177	0.1770	0.0005	0.00030	0.00003	0.1770	0.0005	0.0000	0.503	0.035	12.28	0.86	100	2625	5
4-1	133	0.1777	0.0006	0.00040	0.00003	0.1775	0.0006	0.0003	0.502	0.035	12.29	0.86	100	2630	6
5-1	34	0.1774	0.0012	0.00076	0.00007	0.1774	0.0012	0.0008	0.503	0.035	12.29	0.87	100	2628	11
6-1	117	0.1784	0.0007	0.00083	0.00007	0.1784	0.0007	0.0001	0.475	0.033	11.69	0.82	95	2638	6
7-1	335	0.1774	0.0004	0.00028	0.00003	0.1773	0.0004	0.0001	0.467	0.033	11.42	0.80	94	2628	4
8-1	384	0.1769	0.0004	0.00030	0.00022	0.1768	0.0004	0.0027	0.477	0.033	11.64	0.81	96	2623	4
9-1	116	0.1796	0.0006	0.00080	0.00008	0.1795	0.0006	0.0006	0.479	0.033	11.85	0.83	95	2649	6
10-1	61	0.1779	0.0009	0.000323	0.00008	0.1773	0.0009	0.0016	0.540	0.037	13.19	0.93	106	2628	9
11-1	183	0.1785	0.0006	0.00062	0.00005	0.1783	0.0006	0.0001	0.478	0.033	11.76	0.83	96	2637	6

Data are at 1σ precision. Common-Pb corrections are based on ²⁰⁴Pb and Broken Hill Pb composition. Analysis date: 11/05/02.

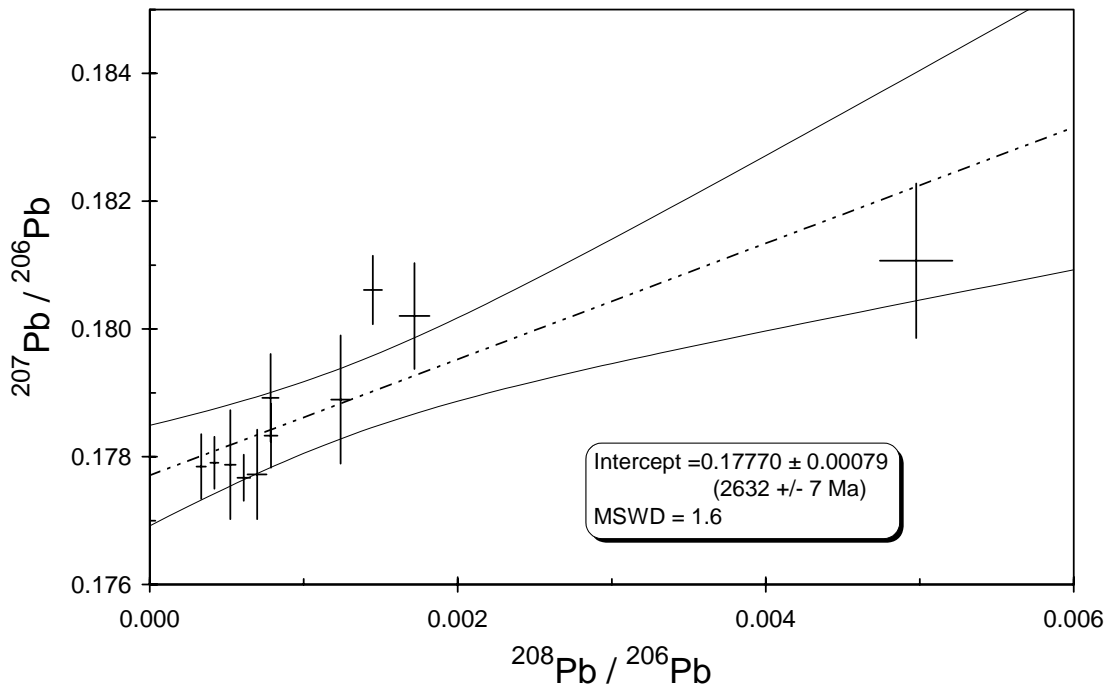


Figure 65. SHRIMP Pb/Pb data for rutile standard WH-1. Best-fit line (dashed) using York Model 1, with 95% confidence error envelope (solid lines).

Sample data

Data are listed in Table 28. A concordia plot (Fig. 66) shows the data to be generally concordant, but the scatter in $^{206}\text{Pb}/^{238}\text{U}$ for WH-1, which is propagated to Pb/U for the data, makes this an imprecise test of data quality. These data are actually better grouped in $^{206}\text{Pb}/^{238}\text{U}$ than WH-1 (MSWD = 0.39), this grouping being a stronger argument for a closed system history for these grains than the apparent concordance values.

There is no significant correlation between measured $^{207}\text{Pb}/^{206}\text{Pb}$ and $^{208}\text{Pb}/^{206}\text{Pb}$ (Fig. 67), suggesting that there are spurious mass-208 counts. These counts might represent ^{208}Pb from the decay of trace Th, but their actual origin is unknown. If the data are forced to fit a line through a likely common-Pb composition (Fig. 67) the resulting $^{207}\text{Pb}/^{206}\text{Pb}$ date is 2628 ± 6 Ma (MSWD = 3.3.) An alternative approach is to simply apply a conventional common Pb correction from the recorded ^{204}Pb . This gives a weighted mean $^{207}\text{Pb}/^{206}\text{Pb}$ age of 2630.8 ± 4.6 Ma (MSWD = 1.8). Omitting one $\sim 3\sigma$ outlier (9-1) would change this to 2629.5 ± 3.1 (MSWD = 0.88). Clearly, the result is only marginally affected by any choice of common-Pb correction procedure or by possible data exclusions. Given the relatively small number of analyses, we prefer to use an age of 2630 Ma with a conservative uncertainty of ± 7 Ma.

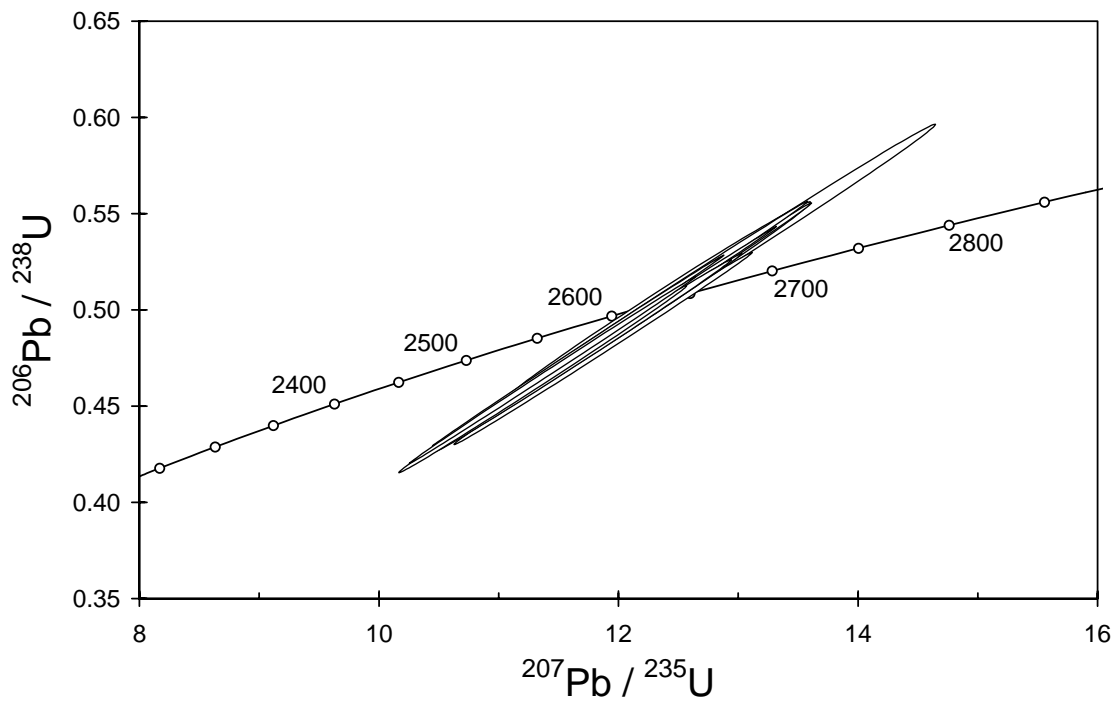


Figure 66. Concordia plot of rutile data from sample 2001969019A: biotite granodiorite, Ironstone Point.

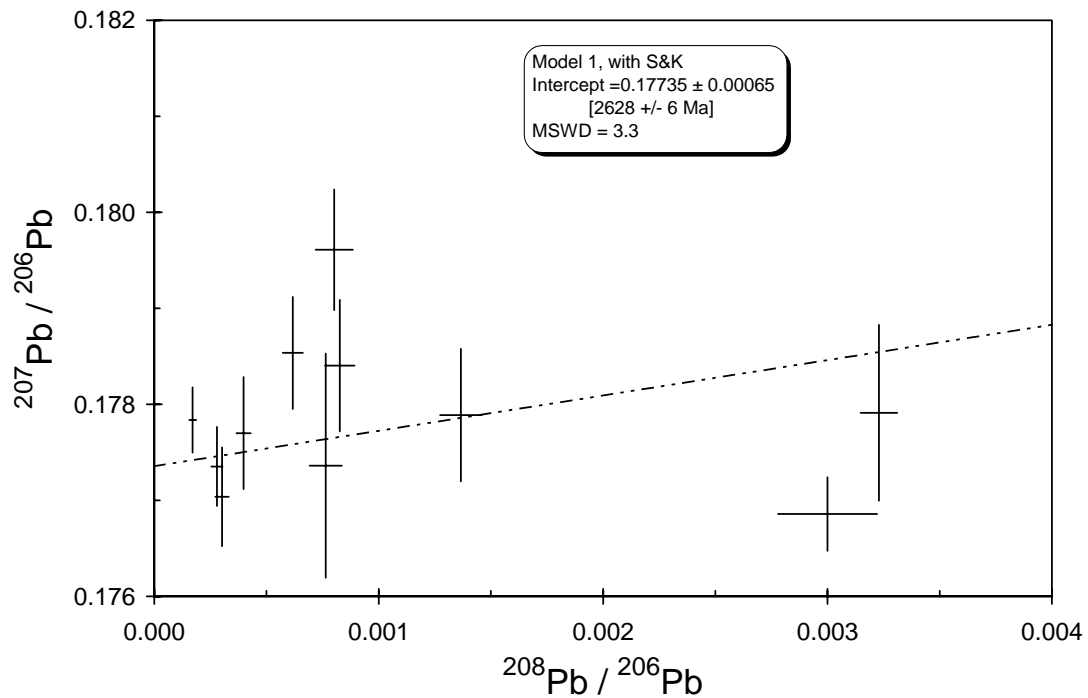


Figure 67. SHRIMP Pb/Pb data for rutile from sample 2001969019A: biotite granodiorite, Ironstone Point, with a York Model 1 linefit, projected to a common Pb composition (Stacey and Kramers, 1975) at sample age.

Geochronological interpretation

The 2630 Ma date obtained from rutile is much younger than the 2668 ± 4 Ma age for the zircons from this rock (Fletcher et al., 2001), but close to the 2638 ± 2 Ma zircon age for the crosscutting syenogranite dyke 2001969019B (Fletcher et al., 2001). Given the lower closure temperature for rutile, relative to zircon ($\sim 400^\circ\text{C}$ vs $\sim 750^\circ\text{C}$), 2630 ± 7 Ma could record cooling through the closure temperature of rutile.

2001969033A: Burtville granodiorite

- 1:250,000 sheet:** Laverton (SH5102)
1:100,000 sheet: Burtville (3440)
MGA: 464917mE 6817670mN
Location: The sample comes from mine dump material from the Burtville open-pit, and stockpiled just west of the it.
Description: This is a grey, seriate medium-grained biotite granodiorite that contains mafic (?greenstone) enclaves (10–30 cm), biotite-clots (<6 mm), and microdiorite enclaves.
Principal minerals in the granoblastic rock are plagioclase, quartz, K-feldspar and biotite, with plagioclase>>K-feldspar. Plagioclase occurs as subhedral to euhedral grains that are either zoned or display broad oscillatory to complex zoning. The plagioclase is variably altered to fine- to coarse-grained white mica and lesser biotite, with minor epidote/clinozoisite and carbonate. Quartz is present as minor to moderately undulose, anhedral grains. K-feldspar is anhedral to interstitial, and locally perthitic. Biotite (6–9%) occurs as medium brown to light yellow, ragged flakes, and commonly displays minor chlorite alteration, with relatively common fine epidote, rutile and Fe-oxides. Accessory phases include zircon, apatite and opaque minerals.
Mount, pop: Z3963A

Description of zircons

Zircon from this sample consists of colourless to pale grey-brown fragments and crystals, most of which are slightly rounded to subhedral (in some crystals, very sharp prismatic terminations are preserved). Grains range from equant to elongated (60 μm to 240 μm long; aspect ratios up to 4:1). Inclusions and zoning are locally visible in transmitted and reflected light; other grains are clear. Oscillatory zoning is variably developed, as shown by CL (Fig. 68). A number of grains have patchy or irregular zoning patterns, consistent with recrystallisation. Some grains appear to contain xenocrystic cores.

Concurrent standard data

The primary beam became unstable in the latter part of this session. Following subsequent assessment, the data file was truncated after 38 hours, but this makes no significant difference to the data structures of either QGNG or the samples. Two of the 31 QGNG analyses that were retained are distinctly low in both $^{206}\text{Pb}/^{238}\text{U}$ and $^{207}\text{Pb}/^{206}\text{Pb}$, and were omitted from the calibration. The apparent calibration slope for QGNG is ~ 2.1 ; one of the concurrent samples indicates a value ~ 2.4 . The long-term average value of 2.2 was used for data processing. The 29 analyses give a $^{206}\text{Pb}/^{238}\text{U}$ calibration with a 1σ scatter of 0.68% (MSWD = 2.47). Corresponding $^{207}\text{Pb}/^{206}\text{Pb}$ data have an unusually wide spread, and the preferred low-side culling procedure results in excessive deletion if MSWD is forced to 1.0. Culling was therefore stopped at MSWD ≥ 1.3 (refer to chapter on “Data compilation for the QGNG standard”), resulting in a weighted mean $^{207}\text{Pb}/^{206}\text{Pb}$ age of 1849.2 ± 3.3 Ma (MSWD = 1.3; $n = 25$). Alternate data treatments, such as deleting the most extreme outliers (several at $\sim 2\sigma$, both high and low) give a similar average.

Element abundance calibration was based on CZ3 ($n = 3$).

Sample data

There are thirty analyses from individual grains in the truncated data file (Table 29). Three of these are discordant (12-1, 21-1, 27-1; Fig. 69) and are not considered for geochronological interpretation. The remainder form a single population (Fig. 70) that has a weighted mean $^{207}\text{Pb}/^{206}\text{Pb}$ age of 2715.6 ± 2.8 Ma (MSWD = 0.91).

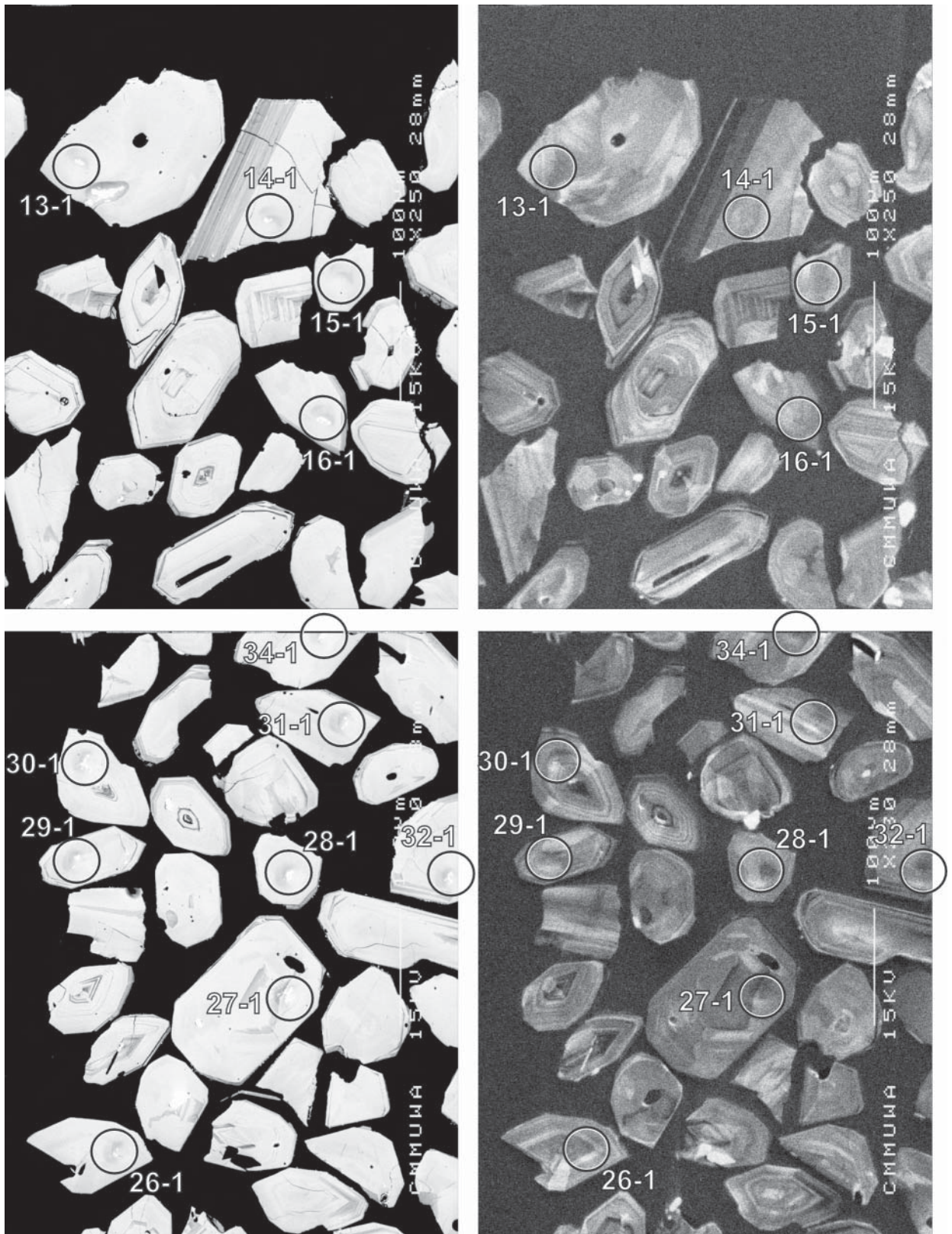


Figure 68. Representative SEM images (BSE on left, CL on right) for sample 2001969033A: Burtville granodiorite. SHRIMP analysis spots are labelled. Remnant pits from the ion microprobe analyses are faintly visible in some grains. Scale bar is 100 μm.

Geochronological interpretation

The crystallization age of the granodiorite is considered to be 2716 ± 4 Ma.

Table 29. SHRIMP analytical results for zircon from sample 2001969033A: Burtville granodiorite.

grain-spot	U (ppm)	Th (ppm)	4f206 (%)	$^{207}\text{Pb}/^{206}\text{Pb}$		$^{206}\text{Pb}/^{238}\text{U}$		$^{207}\text{Pb}/^{235}\text{U}$		$^{208}\text{Pb}/^{232}\text{Th}$	conc. (%)	$^{207}\text{Pb}/^{206}\text{Pb}$ Age (Ma)	
					\pm		\pm		\pm				\pm
Main group													
1-1	88	62	0.103	0.1863	0.0010	0.524	0.005	13.47	0.16	0.139	100	2710	9
2-1	99	46	0.009	0.1868	0.0007	0.525	0.008	13.51	0.20	0.144	100	2714	6
3-1	117	77	0.123	0.1860	0.0007	0.521	0.005	13.36	0.14	0.140	100	2707	6
4-1	113	54	0.206	0.1866	0.0008	0.515	0.005	13.24	0.14	0.141	99	2713	7
5-1	77	49	0.048	0.1878	0.0009	0.520	0.006	13.47	0.16	0.143	99	2723	8
6-1	80	28	0.172	0.1858	0.0009	0.525	0.006	13.45	0.16	0.139	101	2706	8
7-1	81	57	-0.015	0.1876	0.0008	0.526	0.006	13.61	0.16	0.145	100	2721	7
8-1	84	64	0.124	0.1871	0.0008	0.530	0.006	13.68	0.16	0.144	101	2717	7
9-1	139	143	0.405	0.1873	0.0008	0.513	0.005	13.24	0.14	0.138	98	2718	7
10-1	129	148	0.032	0.1881	0.0007	0.518	0.005	13.43	0.14	0.144	99	2726	6
11-1	75	64	0.249	0.1878	0.0012	0.498	0.005	12.90	0.16	0.117	96	2723	10
13-1	101	99	-0.020	0.1878	0.0010	0.522	0.005	13.51	0.15	0.145	99	2723	9
14-1	92	55	0.033	0.1869	0.0008	0.526	0.005	13.56	0.15	0.144	100	2715	7
15-1	116	102	-0.056	0.1874	0.0007	0.520	0.005	13.43	0.14	0.143	99	2720	6
16-1	123	42	0.096	0.1840	0.0022	0.526	0.005	13.35	0.21	0.142	101	2689	20
17-1	88	29	0.112	0.1863	0.0008	0.526	0.005	13.52	0.15	0.146	101	2709	7
18-1	86	61	0.252	0.1872	0.0009	0.518	0.005	13.37	0.16	0.139	99	2717	8
19-1	104	73	-0.036	0.1880	0.0011	0.536	0.005	13.89	0.16	0.148	101	2725	9
20-1	88	89	0.263	0.1860	0.0011	0.495	0.005	12.70	0.15	0.121	96	2707	10
22-1	85	75	0.103	0.1850	0.0008	0.528	0.005	13.47	0.15	0.143	101	2699	7
23-1	92	80	0.007	0.1877	0.0007	0.520	0.005	13.47	0.14	0.143	99	2722	6
24-1	71	30	0.021	0.1873	0.0009	0.527	0.006	13.62	0.16	0.146	100	2719	8
25-1	114	51	0.721	0.1863	0.0009	0.509	0.005	13.07	0.14	0.134	98	2710	8
26-1	91	33	-0.020	0.1874	0.0007	0.531	0.005	13.71	0.14	0.147	101	2719	6
28-1	104	94	-0.036	0.1870	0.0007	0.530	0.005	13.66	0.14	0.146	101	2716	6
29-1	84	61	0.000	0.1870	0.0009	0.525	0.005	13.55	0.15	0.143	100	2716	8
30-1	89	61	0.259	0.1862	0.0009	0.505	0.005	12.96	0.14	0.074	97	2709	8
>5% discordant													
12-1	103	64	0.485	0.1864	0.0009	0.488	0.005	12.55	0.14	0.135	94	2711	8
21-1	162	67	2.893	0.1877	0.0014	0.458	0.006	11.85	0.17	0.129	89	2722	13
27-1	169	225	7.705	0.1877	0.0037	0.354	0.004	9.17	0.21	0.083	72	2722	33

Data are at 1σ precision. All Pb data are common-Pb corrected (based on ^{204}Pb and Broken Hill Pb composition). Analysis date: 27/05/02; session Z3963i.

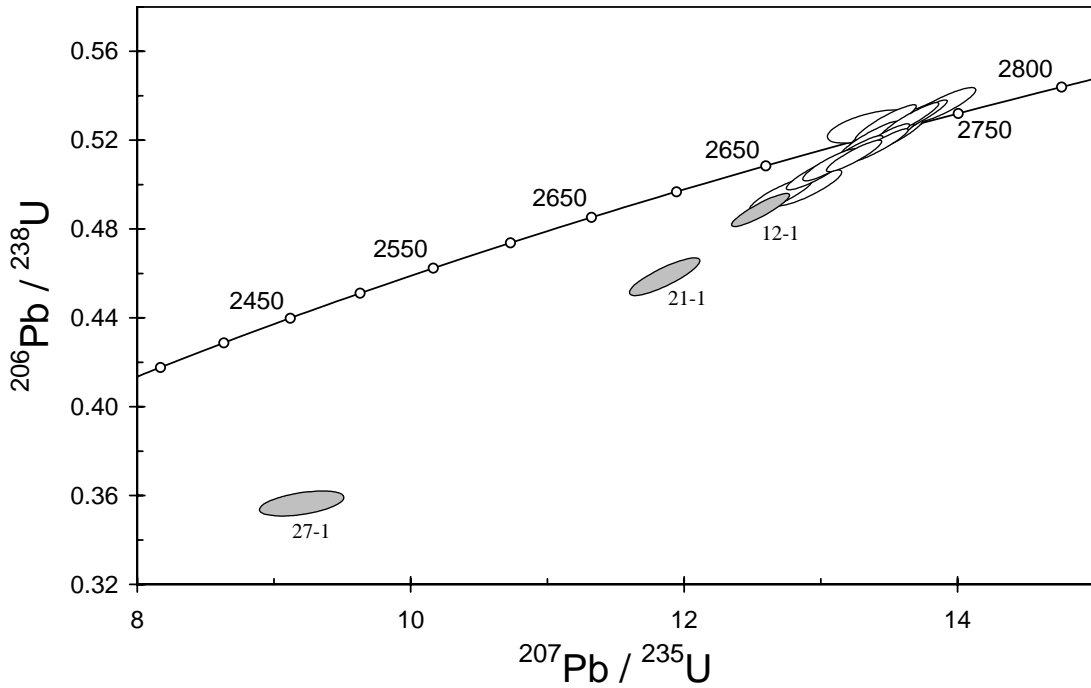


Figure 69. Concordia plot for zircons from sample 2001969033A: Burtville granodiorite. White filled symbols are used to define the age of the sample; discordant and/or high common Pb analyses are light grey.

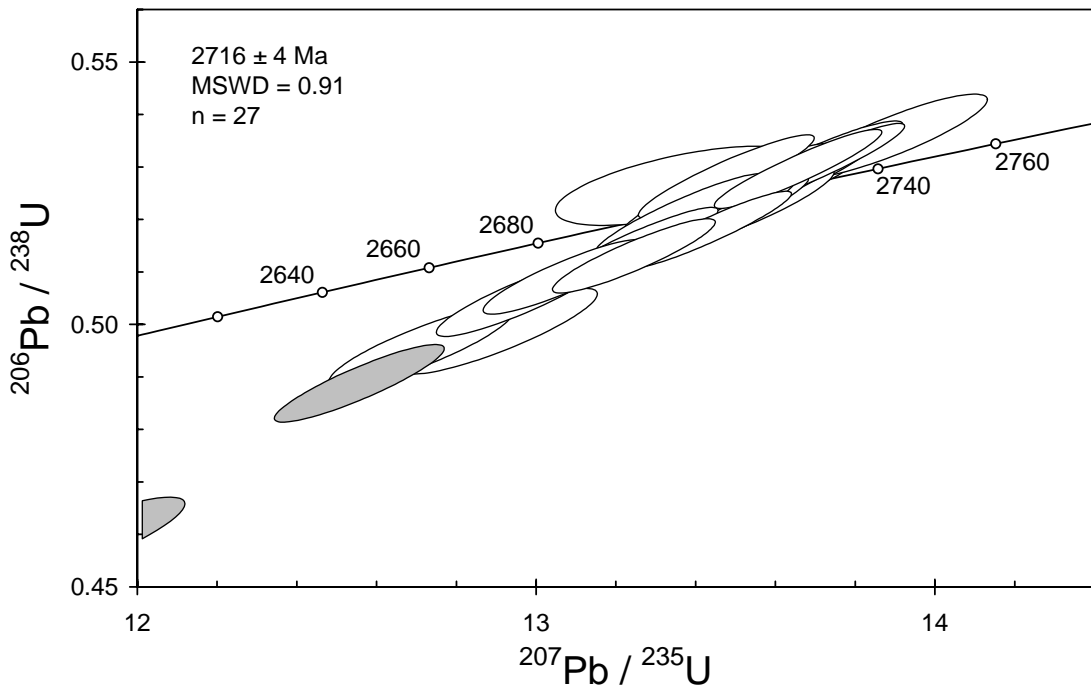


Figure 70. Concordia plot for the main data group for sample 2001969033A: Burtville granodiorite. Shading as in Figure 69.

2001969035: Menangina monzogranite

1:250,000 sheet: Edjudina (SH5106)

1:100,000 sheet: Boyce (3238)

MGA: 397629mE 6698658mN

Location: This sample was collected from a low whaleback, in a region of good outcrop, that forms part of Menangina Rocks, about 600 m west of Yarri Road.

Description: The sample is from a white-pink, sparsely (quartz-)feldspar porphyritic, medium-grained titanite-biotite monzogranite. Phenocrysts comprise pinkish K-feldspar (1 to >2 cm), subhedral plagioclase (to >5 mm), and anhedral quartz (5 to 7 mm).

The rock has a granular to granoblastic texture. Principal minerals are plagioclase, K-feldspar, quartz and biotite, with plagioclase>K-feldspar. Plagioclase forms subhedral laths that are unzoned to variably zoned (including broad oscillatory zoning), complexly zoned cores, and normally zoned rims. The plagioclase grains are weakly to moderately altered to fine- to medium-grained white mica and minor carbonate. Myrmekitic outgrowths are common. K-feldspar largely occurs as anhedral to subhedral poikilitic phenocrysts and anhedral to interstitial smaller grains. It displays variably-developed tartan twinning. Perthite is rare to absent. Quartz is present as anhedral grains with mild to locally moderately undulose extinction. Biotite (~5%) occurs as ragged to irregular, light yellow to medium red-brown, flakes, to 3–4 mm, that are moderately altered to chlorite with minor rutile. Accessory phases include altered subhedral titanite (<1–2 mm), zircon, apatite, and relatively common irregular to subhedral opaque minerals.

Mount, pop: Z3877B

Description of zircons

This sample contains colourless or pale grey to dark brown zircon fragments and whole crystals which vary from clear to turbid (the latter due to the presence of fine inclusions and/or extensive metamictisation). Cracks and highly corroded patches (mainly along growth planes) are pervasive in some grains. The grains are predominantly subhedral, with slightly rounded crystal faces; a small proportion of anhedral and/or moderately to well-rounded grains are also present. Grain size ranges from 45 μm to 250 μm in length, with aspect ratios extending from 1:1 to 4:1. Well-defined continuous core to rim oscillatory zoning is visible in most grains in CL, although a small number only have faint zoning, or are partially to completely recrystallised (Fig. 71). Cores and rims are visible in some grains in BSE; some rims appear very dark in CL.

Concurrent standard data

This three-day session was interrupted mid-way by several arc ‘drop-outs’ and related instabilities. There was a calibration change across this period but it is considered too minor to justify splitting the data into two blocks. Using all data (including several of poor precision, which have little bearing on the result), the Pb/U calibration has a 1σ scatter of 1.16% (MSWD = 7.82; $n = 41$). The observed calibration slope is 2.16, with the corresponding sample data suggest values >2.3. A value of 2.2 was used for data reduction. The $^{207}\text{Pb}/^{206}\text{Pb}$ data display a small amount of excess scatter that is difficult to characterise. Omitting two 3σ outliers and three points with internal precision >15 Ma gives a weighted mean $^{207}\text{Pb}/^{206}\text{Pb}$ age of 1849.9 ± 2.4 Ma, with MSWD = 1.4 ($n = 36$). Further omitting three $\geq 2\sigma$ outliers (two low, one high) gives 1850 ± 2 Ma (MSWD = 1.10), while the preferred “standard” low-side culling procedure gives 1851.4 ± 2.1 Ma (MSWD = 1.04; $n = 30$).

Element abundance calibration was based on CZ3 ($n = 3$).

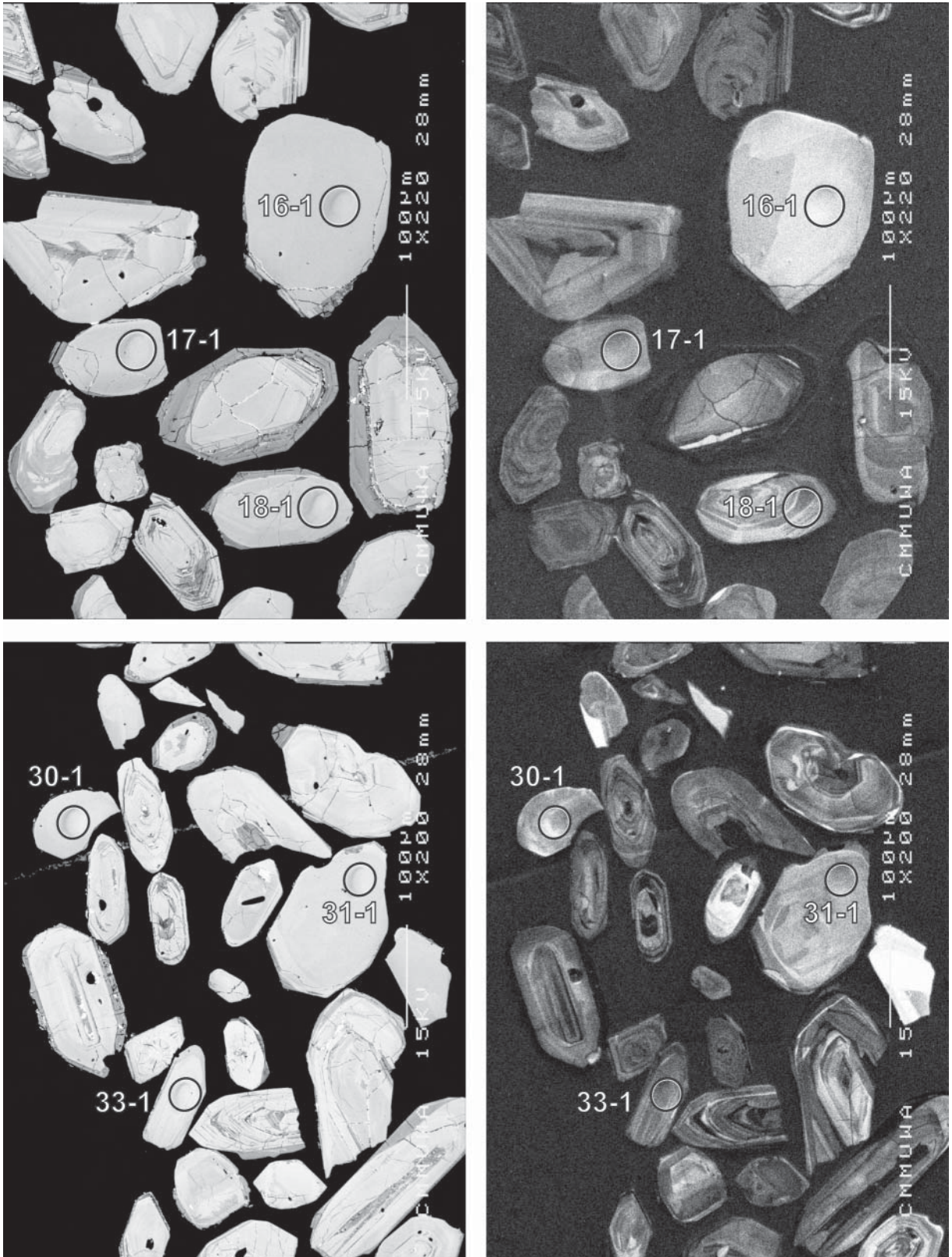


Figure 71. Representative SEM images (BSE on left, CL on right) for sample 2001969035: *Menangina monzogranite*. SHRIMP analysis spots are labelled. Remnant pits from the ion microprobe analyses are faintly visible in some grains. Scale bar is 100 μm.

Sample data

Only one of the 39 analyses (19-1), each from a separate grain, is >5% discordant (Table 30; Fig. 72). The others plot on concordia but are significantly scattered. Two analyses (2-1, 18-1) are old $^{207}\text{Pb}/^{206}\text{Pb}$ outliers, and four others (3-1, 8-1, 11-1, 17-1) are approximately 2σ outliers, although this depends somewhat on the definition of the main group. Omitting these seven analyses leaves 32 with a weighted mean $^{207}\text{Pb}/^{206}\text{Pb}$ age of 2671 ± 4 Ma, but with MSWD = 2.8. The excess scatter cannot be attributed to systematic factors, since the concurrent data for sample 2001967017A have a simple “main group” of data with MSWD <1.0.

There is no apparent structure in the $^{207}\text{Pb}/^{206}\text{Pb}$ distribution with dates ranging from about 2690 Ma to 2645 Ma. There is no statistical justification in choosing any age group over another. An internally consistent youngest group (n = 12) gives 2659.9 ± 3.6 Ma (MSWD = 1.08). Conversely, an oldest group (n = 21) gives 2677 ± 2.8 Ma (MSWD = 1.05).

Geochronological interpretation

Given the obvious existence of some old outliers, one possible interpretation is that all grains are reset xenocrysts. This is supported by generally low U, and in some cases very low Th, contents, such as are commonly seen in metamorphic grains. In this interpretation, the age of the monzogranite is 2660 ± 4 Ma.

However, it is possible that the younger dates come from grains that have lost radiogenic Pb since the crystallisation of the granite. Given that all grains are relatively low-U and low-Th, and the rock is not highly metamorphosed, this seems unlikely, but it might result from very slow cooling. In this case, the monzogranite age could be ~2680 Ma, but not precisely defined.

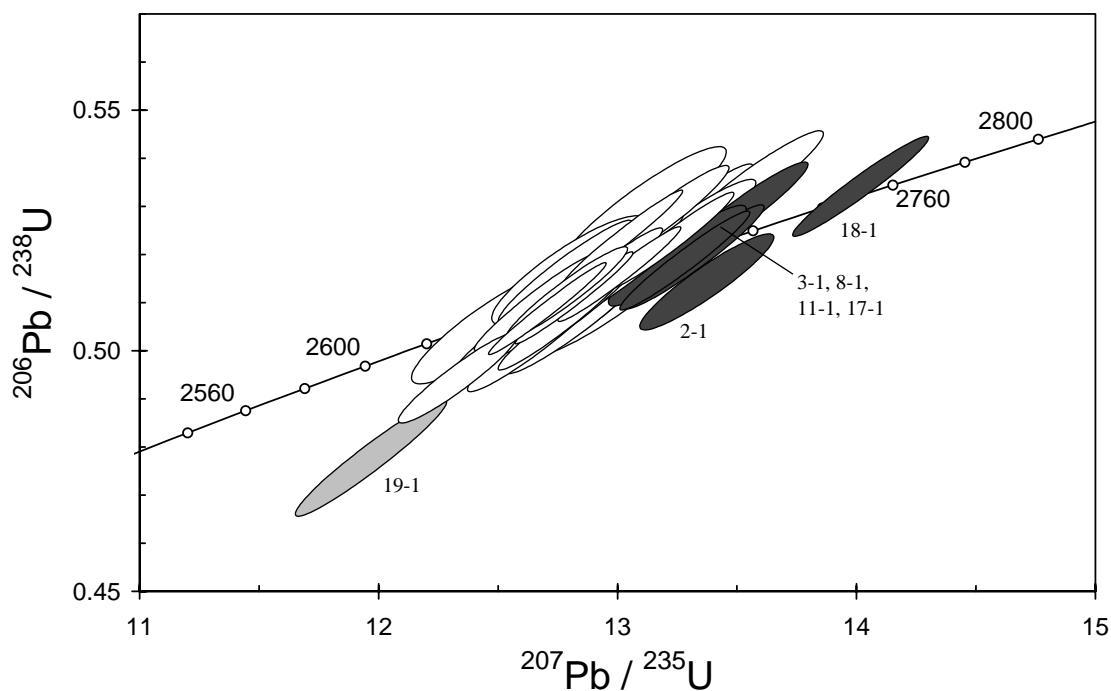


Figure 72. Concordia plot for zircon data from sample 2001969035: Menangina monzogranite. White filled symbols might define the age of the sample; one discordant analysis is light grey; old outliers are dark grey.

Table 30. SHRIMP analytical results for zircon from sample 2001969035: Menangina monzogranite, in order of $^{207}\text{Pb}/^{206}\text{Pb}$ age.

grain-spot	U (ppm)	Th (ppm)	4f206 (%)	$^{207}\text{Pb}/^{206}\text{Pb}$		$^{206}\text{Pb}/^{238}\text{U}$		$^{207}\text{Pb}/^{235}\text{U}$		$^{208}\text{Pb}/^{232}\text{Th}$	conc. (%)	$^{207}\text{Pb}/^{206}\text{Pb}$ Age (Ma)	
					±		±		±				±
Main group													
16-1	33	2	0.165	0.1791	0.0014	0.505	0.008	12.46	0.22	---	100	2645	13
22-1	28	9	0.052	0.1795	0.0013	0.530	0.008	13.11	0.23	0.150	103	2648	12
30-1	60	19	0.120	0.1795	0.0009	0.516	0.007	12.78	0.19	0.144	101	2649	8
34-1	45	7	0.586	0.1796	0.0015	0.516	0.008	12.79	0.21	0.153	101	2649	14
39-1	98	59	0.030	0.1800	0.0006	0.510	0.007	12.65	0.17	0.142	100	2653	6
37-1	180	66	0.051	0.1804	0.0005	0.523	0.007	13.02	0.17	0.142	102	2656	4
12-1	71	39	-0.063	0.1807	0.0007	0.505	0.007	12.57	0.18	0.140	99	2659	7
35-1	129	99	0.264	0.1810	0.0008	0.494	0.006	12.32	0.17	0.138	97	2662	8
23-1	214	158	0.232	0.1812	0.0007	0.512	0.006	12.78	0.17	0.144	100	2664	7
40-1	74	27	0.118	0.1812	0.0008	0.528	0.007	13.18	0.19	0.144	102	2664	7
35-1	159	19	-0.002	0.1812	0.0005	0.508	0.006	12.70	0.16	0.142	99	2664	4
20-1	140	73	0.014	0.1817	0.0005	0.510	0.007	12.78	0.18	0.144	100	2668	4
38-1	86	28	0.064	0.1818	0.0007	0.509	0.007	12.76	0.18	0.140	99	2669	7
6-1	106	31	0.056	0.1819	0.0007	0.515	0.007	12.92	0.17	0.141	100	2670	6
31-1	60	47	-0.018	0.1819	0.0008	0.518	0.007	12.98	0.19	0.144	101	2671	7
33-1	156	52	-0.023	0.1819	0.0005	0.511	0.006	12.81	0.16	0.145	100	2671	4
25-1	29	7	0.072	0.1820	0.0012	0.524	0.008	13.16	0.23	0.150	102	2671	11
28-1	96	45	-0.009	0.1824	0.0008	0.526	0.008	13.24	0.22	0.145	102	2675	7
14-1	53	19	-0.050	0.1828	0.0008	0.507	0.007	12.79	0.19	0.142	99	2679	8
21-1	59	22	0.035	0.1828	0.0008	0.501	0.007	12.64	0.18	0.139	98	2679	7
4-1	132	57	-0.029	0.1829	0.0005	0.516	0.007	13.00	0.17	0.145	100	2679	5
15-1	81	77	-0.056	0.1829	0.0007	0.507	0.007	12.79	0.18	0.143	99	2680	7
1-1	98	36	0.052	0.1830	0.0007	0.506	0.007	12.75	0.17	0.140	98	2680	6
5-1	58	20	0.062	0.1831	0.0009	0.508	0.007	12.83	0.19	0.144	99	2681	8
13-1	96	37	-0.027	0.1833	0.0006	0.517	0.007	13.06	0.18	0.143	100	2683	6
7-1	57	24	0.325	0.1834	0.0011	0.506	0.007	12.81	0.20	0.139	98	2684	10
27-1	111	79	0.131	0.1834	0.0006	0.523	0.007	13.22	0.18	0.150	101	2684	5
29-1	18	7	-0.041	0.1835	0.0014	0.518	0.010	13.11	0.26	0.148	100	2684	12
26-1	52	20	0.036	0.1836	0.0010	0.524	0.007	13.27	0.20	0.149	101	2685	9
9-1	61	23	-0.023	0.1839	0.0008	0.506	0.007	12.82	0.19	0.143	98	2688	7
10-1	28	1	-0.260	0.1839	0.0014	0.511	0.008	12.95	0.23	---	99	2688	12
24-1	56	33	0.024	0.1840	0.0009	0.534	0.008	13.55	0.21	0.150	103	2689	8
>5% discordant													
19-1	108	42	0.429	0.1818	0.0009	0.477	0.008	11.96	0.21	0.168	94	2670	8
Old outliers													
17-1	81	33	0.094	0.1850	0.0010	0.519	0.007	13.25	0.19	0.145	100	2698	9
11-1	56	23	-0.044	0.1854	0.0008	0.528	0.008	13.49	0.20	0.148	101	2702	7
8-1	95	70	-0.049	0.1857	0.0007	0.518	0.007	13.28	0.18	0.144	100	2705	6
3-1	69	26	-0.047	0.1860	0.0008	0.519	0.007	13.32	0.19	0.148	100	2707	7
2-1	106	61	0.440	0.1887	0.0010	0.514	0.007	13.37	0.19	0.148	98	2731	9
18-1	102	37	0.074	0.1904	0.0006	0.534	0.007	14.02	0.19	0.148	100	2745	6

Data are at 1σ precision. All Pb data are common-Pb corrected (based on ^{204}Pb and Broken Hill Pb composition). Analysis date: 26/02/02; session Z3877i. Th/Pb data are considered unreliable for Th < 5 ppm, hence no ratios are given for such analyses.

2001969039: Donkey Rocks monzogranite

1:250,000 sheet: Edjudina (SH5106)

1:100,000 sheet: Boyce (3238)

MGA: 377114mE 6699755mN

Location: The sample was taken from outcrop at Donkey Rocks, approximately 200 m north of a track about 800 m northwest of Donkey Rocks Well.

Description: This grey-pink, seriate to quartz-feldspar porphyritic, medium-grained biotite monzogranite contains phenocrysts of pinkish K-feldspar (<1 cm), plagioclase (<5–6 mm) and dark/smokey quartz (<5–8 mm). Minor uncommon biotite-rich schlieren, up to 10 cm in length, are present.

Principal minerals in this granoblastic rock are K-feldspar, plagioclase, quartz and biotite, with K-feldspar > plagioclase. K-feldspar is subhedral to anhedral. Larger grains are commonly poikilitic. Tartan twinning is variably developed, as is perthite. Plagioclase forms subhedral to anhedral grains that are unzoned to variably zoned. These grains include normally zoned rims, patchy-zoned cores, broad oscillatory zoning, and locally bent twins. Minor myrmekite is present. The plagioclase is characterised by minor to locally moderate replacement by white mica and minor carbonate. Quartz is anhedral, moderately to locally strongly undulose, with common, locally well-developed, sub-grain development. Biotite (<5%) forms anhedral to ragged, light yellow to medium-dark brown flakes that are locally deformed. It is mostly chloritised, with secondary rutile and minor epidote/clinozoisite or white mica. Accessory phases include zircon, apatite and anhedral opaque minerals.

Mount, pop: Z3877A

Description of zircons

The zircon consists of euhedral whole crystals and fragments, with only slight rounding of crystal faces. It varies from small (~35 µm), equant grains, to stubby prismatic grains, to elongate grains up to 170 µm in length (aspect ratios to 4:1). Subhedral to anhedral rounded grains also vary in size, from about 35 µm to 100 µm. The zircon is colourless to pale yellow-brown and mostly fractured to highly fractured. Continuous concentric oscillatory zoning is present in most grains (Fig. 73), but chaotic patches and/or irregular zones indicative of recrystallisation/metamictisation are often present. Some grains contain cores.

Concurrent standard data

This three-day session was interrupted mid-way by several arc ‘drop-outs’ and related instabilities. There was a calibration change across this period but it is considered too minor to justify splitting the data into two blocks. Using all data (including several of poor precision, which have little bearing on the result), the Pb/U calibration has a 1σ scatter of 1.16% (MSWD = 7.82; n = 41). The observed calibration slope is 2.16, with the corresponding sample data suggest values >2.3. A value of 2.2 was used for data reduction. The $^{207}\text{Pb}/^{206}\text{Pb}$ data display a small amount of excess scatter that is difficult to characterise. Omitting two 3σ outliers and three points with internal precision >15 Ma gives a weighted mean $^{207}\text{Pb}/^{206}\text{Pb}$ age of 1849.9 ± 2.4 Ma with MSWD = 1.4 (n = 36). Further omitting three $\geq 2\sigma$ outliers (two low, one high) gives 1850 ± 2 Ma (MSWD = 1.10), while the preferred “standard” low-side culling procedure gives 1851.4 ± 2.1 Ma (MSWD = 1.04; n = 30).

Element abundance calibration was based on CZ3 (n = 3).

Sample data

Forty analyses were obtained from individual grains (Table 31). Three low-precision analyses taken during periods of primary beam instability mid-way through the session were deleted from

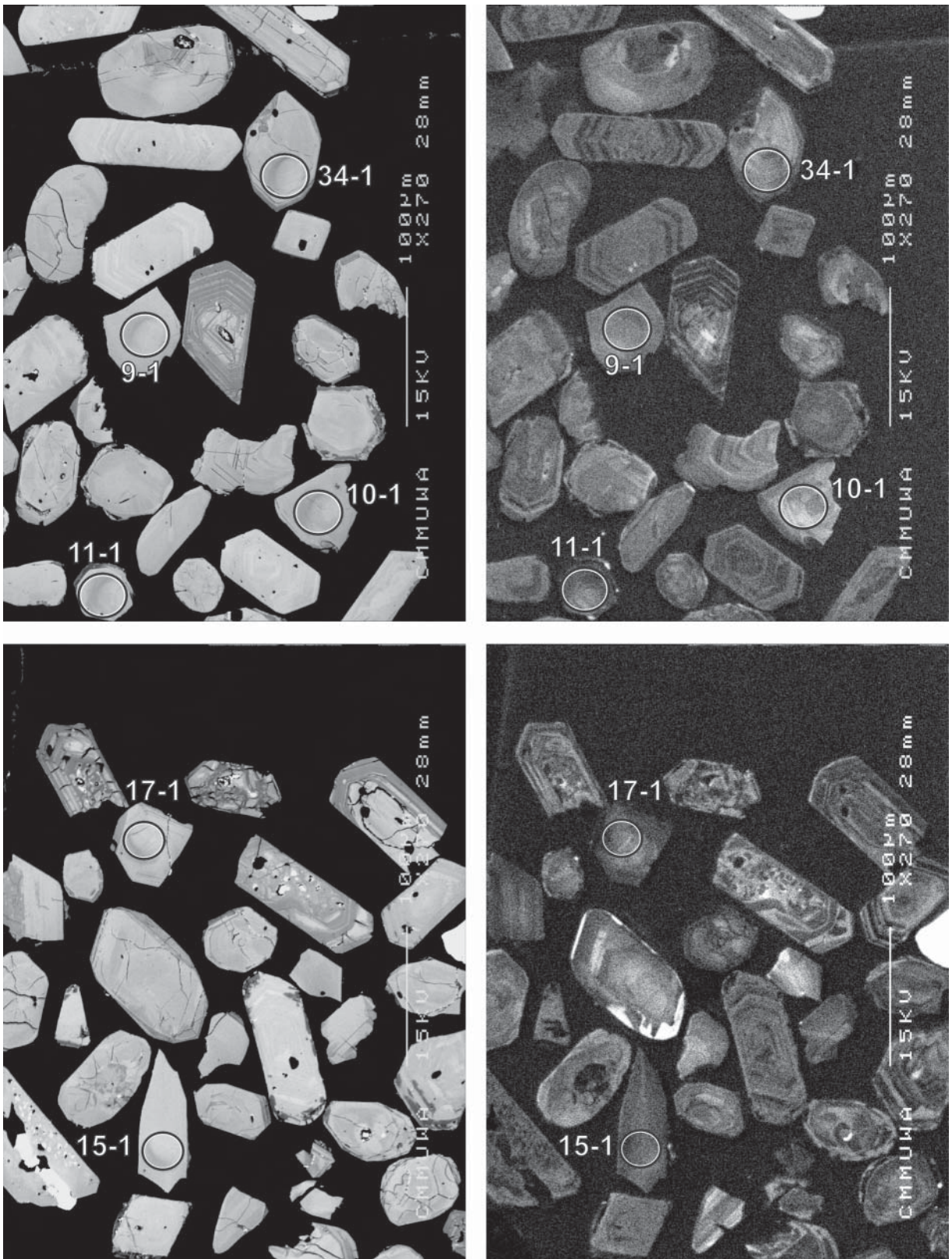


Figure 73. Representative SEM images (BSE on left, CL on right) for sample 2001969039: Donkey Rocks monzogranite. SHRIMP analysis spots are labelled. Remnant pits from the ion microprobe analyses are faintly visible in some grains. Scale bar is 100 µm.

files. One discordant analysis (4-1), one other with >2% common Pb (41-1) and four with U > 1000 ppm (2-1, 3-1, 18-1, 26-1) are not considered reliable for chronology, although two of the high-U points are consistent with the main data group. The remaining data group fairly well, but tail towards higher dates, with an apparent break at ~2665 Ma (Fig. 74). Omitting dates > 2665 Ma and one 3 σ young outlier (39-1) leaves 24 with a weighted mean $^{207}\text{Pb}/^{206}\text{Pb}$ age of 2650.2 ± 2.8 Ma (Fig. 75). This group has some excess scatter (MSWD = 1.4), but additional data deletions are difficult to justify.

Geochronological interpretation

The 2650 ± 3 Ma age is considered to date the crystallisation of the monzogranite.

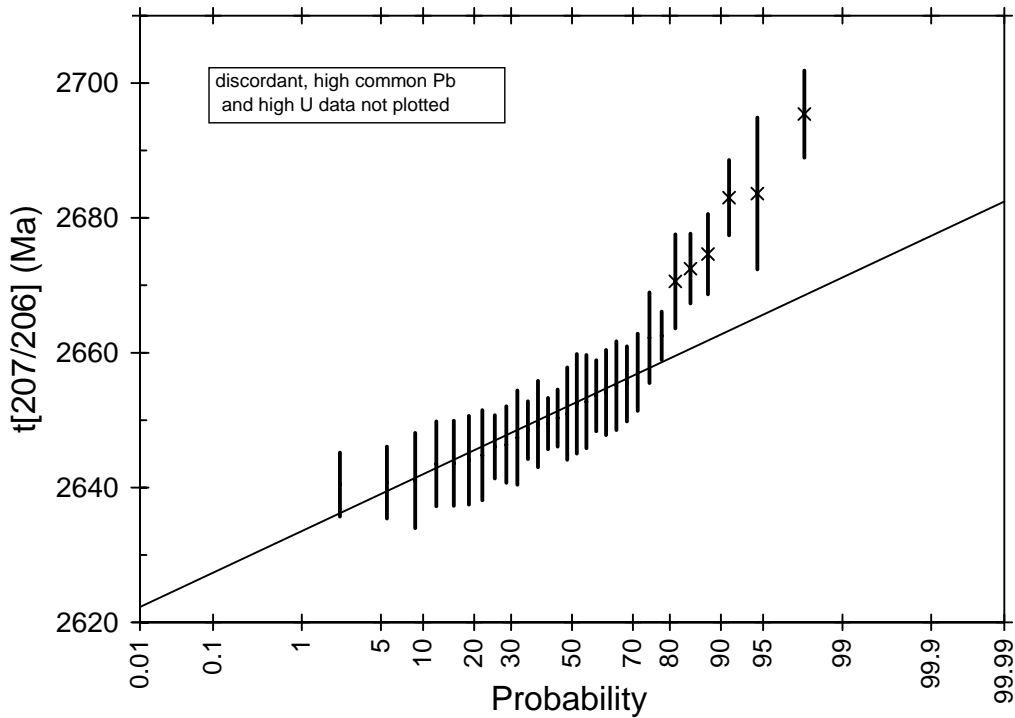


Figure 74. Probability plot for data from sample 2001969039: Donkey Rocks monzogranite. There is an apparent break in the data at 2665 Ma; these older analyses (marked with "x") are excluded from the final weighted mean calculation.

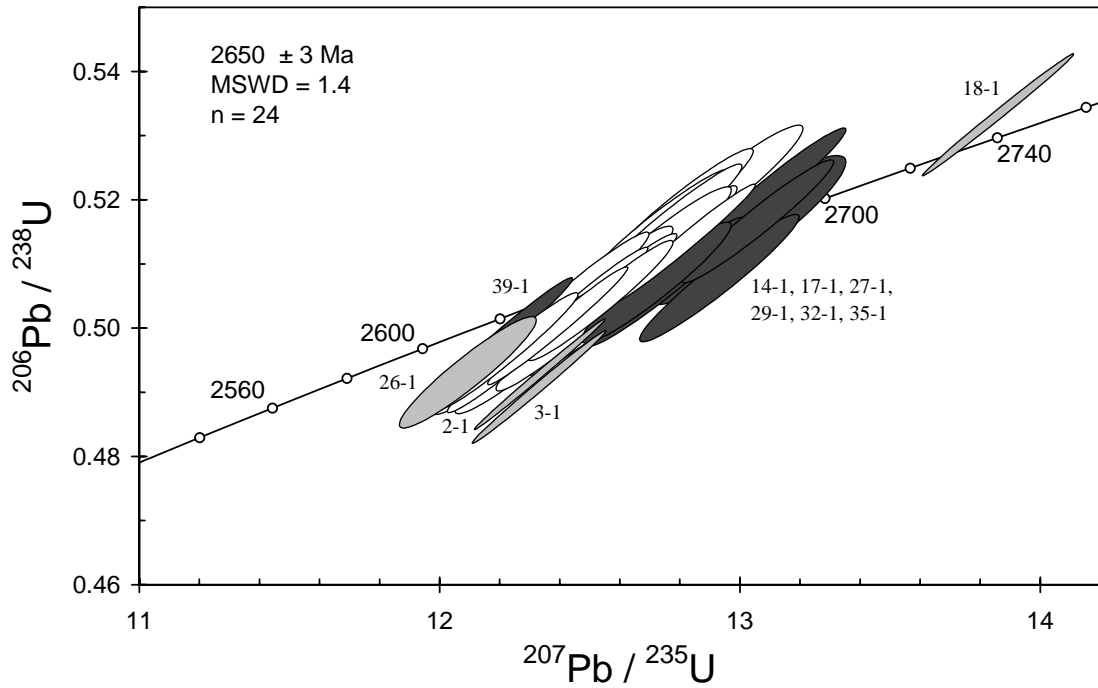


Figure 75. Concordia plot for zircons from 2001969039: Donkey Rocks monzogranite. White filled symbols are used to define the age of the sample; data for older outliers (inherited grains?), and one young outlier, are dark grey; high-U analyses are light grey. Two low-precision analyses from spots with high common Pb (4-1, 41-1) are not plotted.

Table 31. SHRIMP analytical results for zircon from sample 2001969039: Donkey Rocks monzogranite.

grain-spot	U (ppm)	Th (ppm)	4f206 (%)	²⁰⁷ Pb/ ²⁰⁶ Pb		²⁰⁶ Pb/ ²³⁸ U		²⁰⁷ Pb/ ²³⁵ U		²⁰⁸ Pb/ ²³² Th	conc. (%)	²⁰⁷ Pb/ ²⁰⁶ Pb Age (Ma)	
				±	±	±	±	±	±				
Main group													
5-1	171	131	0.013	0.1795	0.0005	0.503	0.006	12.45	0.16	0.141	99	2649	4
6-1	133	97	0.035	0.1794	0.0008	0.506	0.006	12.52	0.17	0.141	100	2647	7
7-1	105	130	0.112	0.1801	0.0007	0.501	0.007	12.45	0.17	0.140	99	2654	6
8-1	104	131	-0.015	0.1810	0.0007	0.502	0.007	12.53	0.17	0.141	99	2662	7
9-1	183	178	0.021	0.1787	0.0006	0.505	0.006	12.45	0.16	0.139	100	2641	5
10-1	96	124	-0.031	0.1805	0.0006	0.500	0.007	12.43	0.17	0.142	98	2657	6
11-1	194	167	0.055	0.1797	0.0005	0.499	0.007	12.36	0.18	0.140	98	2650	4
12-1	162	204	0.065	0.1793	0.0005	0.496	0.006	12.25	0.16	0.139	98	2646	5
13-1	79	80	0.109	0.1791	0.0007	0.504	0.007	12.45	0.18	0.139	99	2645	7
15-1	239	244	0.021	0.1787	0.0005	0.496	0.006	12.22	0.15	0.138	98	2640	5
16-1	92	119	0.011	0.1798	0.0007	0.496	0.007	12.30	0.17	0.139	98	2651	7
19-1	241	212	0.036	0.1796	0.0004	0.500	0.006	12.39	0.15	0.139	99	2649	4
20-1	197	122	0.006	0.1810	0.0004	0.513	0.006	12.80	0.16	0.144	100	2662	4
24-1	114	142	0.067	0.1790	0.0007	0.515	0.007	12.70	0.17	0.143	101	2644	7
25-1	130	119	0.142	0.1793	0.0006	0.516	0.007	12.75	0.17	0.144	101	2646	6
28-1	85	93	0.091	0.1796	0.0007	0.519	0.007	12.86	0.18	0.142	102	2649	6
30-1	188	149	-0.027	0.1803	0.0006	0.504	0.006	12.53	0.16	0.141	99	2655	6
31-1	72	75	0.099	0.1787	0.0008	0.496	0.007	12.23	0.17	0.138	98	2641	7
33-1	166	136	0.124	0.1801	0.0006	0.505	0.006	12.54	0.16	0.144	99	2654	5
34-1	121	144	0.347	0.1800	0.0008	0.521	0.007	12.94	0.18	0.145	102	2652	7
36-1	131	196	0.098	0.1800	0.0008	0.512	0.007	12.71	0.17	0.143	100	2653	7
37-1	86	82	0.041	0.1802	0.0007	0.512	0.007	12.72	0.18	0.141	100	2655	7
38-1	108	98	0.205	0.1790	0.0007	0.503	0.007	12.41	0.17	0.139	99	2644	6
40-1	94	118	0.142	0.1790	0.0007	0.518	0.007	12.78	0.17	0.144	102	2644	6
Young outlier													
39-1	306	187	0.065	0.1776	0.0004	0.498	0.006	12.20	0.16	0.139	99	2631	4
Old outliers													
14-1	105	47	0.006	0.1847	0.0007	0.508	0.007	12.92	0.18	0.142	98	2695	6
17-1	207	87	0.476	0.1819	0.0008	0.507	0.006	12.71	0.17	0.122	99	2671	7
27-1	39	23	0.229	0.1834	0.0012	0.515	0.008	13.02	0.22	0.143	100	2684	11
29-1	112	57	0.027	0.1821	0.0006	0.521	0.007	13.09	0.17	0.144	101	2672	5
32-1	87	105	-0.121	0.1824	0.0007	0.507	0.007	12.75	0.18	0.141	99	2675	6
35-1	183	81	0.285	0.1833	0.0006	0.516	0.006	13.05	0.17	0.145	100	2683	6
>5% discordant or >2% 4f206													
4-1	177	229	2.032	0.1795	0.0024	0.598	0.008	14.79	0.27	0.157	114	2648	23
41-1	183	159	3.688	0.1815	0.0063	0.516	0.016	12.92	0.60	0.149	101	2667	57
U >1000 ppm													
2-1	1552	349	0.004	0.1816	0.0002	0.492	0.006	12.32	0.14	0.135	97	2667	2
3-1	1156	324	0.015	0.1823	0.0002	0.490	0.006	12.32	0.15	0.140	96	2674	2
18-1	1323	55	0.017	0.1885	0.0002	0.533	0.006	13.86	0.17	0.164	101	2729	2
26-1	5400	2384	0.015	0.1779	0.0008	0.493	0.006	12.09	0.15	0.148	98	2634	7

Data are at 1σ precision. All Pb data are common-Pb corrected (based on ²⁰⁴Pb and Broken Hill Pb composition). Analysis date: 26/02/02; session Z3877i. Analyses 21-1, 22-1 and 23-1 were recorded during periods of primary beam instability, resulting in imprecise data; these were deleted from files.

2001969043A: foliated biotite monzogranite, Blueys Well

- 1:250,000 sheet:** Leonora (SH5101)
- 1:100,000 sheet:** Wilbah (3040)
- MGA:** 258698mE 6805799mN
- Location:** The sample was collected from a large outcrop located about 350 m east of the Lawlers – Mt Ida Road, and about 3 km west of Blueys Well.
- Description:** It is a foliated, grey-white, moderately feldspar porphyritic, medium-grained biotite monzogranite. Phenocrysts comprise grey-pink and grey K-feldspar (and minor plagioclase) to 1.5 cm in length. The monzogranite contains a moderate foliation defined by elongate quartz grains, aligned biotite trails, and aligned phenocrysts. The unit is intruded by dykes and pods of unfoliated equigranular biotite granite, of which sample 2001969044 is representative.
- This rock has a granoblastic texture. Principal minerals are K-feldspar, plagioclase, quartz and biotite, with K-feldspar > plagioclase. K-feldspar is present as subhedral to anhedral grains. Larger grains are poikilitic, and have moderate tartan twinning and variable perthite. Plagioclase is subhedral, and is variably zoned. Minor myrmekite is developed. The plagioclase is weakly to moderately altered to white mica and carbonate. Quartz occurs as anhedral to markedly elongate grains, with moderately to strongly undulose extinction. Biotite (5–7%) occurs as aligned, light yellow to red-brown, elongate subhedral flakes that are commonly altered to chlorite, rutile, epidote and/or coarse white mica. Accessory phases include zircon, apatite, opaque minerals and minor, mostly altered, titanite (possibly partly secondary).
- Mount, pop:** Z3878B

Description of zircons

Most zircon grains are pale grey-brown to colourless, and have pervasive fractures and contain small inclusions. The grains are generally subhedral to euhedral, with slightly rounded faces. Relatively small, equant grains (~40 µm), stubby, prismatic grains (aspect ratios from 2:1 to 3:1, up to >300 µm), and long, thin, elongate grains (>200 µm, aspect ratios up to 5:1) are present. Most grains display continuous core to rim euhedral zoning in CL, but features consistent with recrystallisation (patches of unzoned or irregular zoned zircon disrupting the regular zoning) are also present (Fig. 76). Some cores are present.

Concurrent standard data

The apparent calibration slope for QGNG was ~2.1, and that for each of the two concurrent samples was > 2.2; a value of 2.2 was used for data reduction. Omitting two outliers identified by SQUID and two with extreme UO^+/U^+ leaves 33 analyses with a 1σ scatter in Pb/U of 0.63% (MSWD = 2.12). Deleting two additional points that are 3σ (low) outliers in $^{207}Pb/^{206}Pb$ gives a weighted mean $^{207}Pb/^{206}Pb$ age of 1847.5 ± 2.7 Ma (MSWD = 0.89).

Element abundance calibration was based on CZ3 (n = 3).

Sample data

Thirty six analyses were obtained from 36 grains (Table 32). Only three of these (20-1, 22-1, 29-1) were >5% discordant (Fig. 77). Several grains are presumably xenocrysts (analyses 1-1, 2-1 and 31-1). One high-U analysis (8-1) is a young outlier and plots above concordia, and is interpreted to have suffered open system behaviour. In general, there is no correlation between U content and $^{207}Pb/^{206}Pb$ dates. The remaining analyses group relatively well, but there is excess scatter. Given the clear evidence for inheritance and the preservation of ~2800 Ma dates in at least one high-U grain (1-1), it has been assumed that the spread in the main data represents

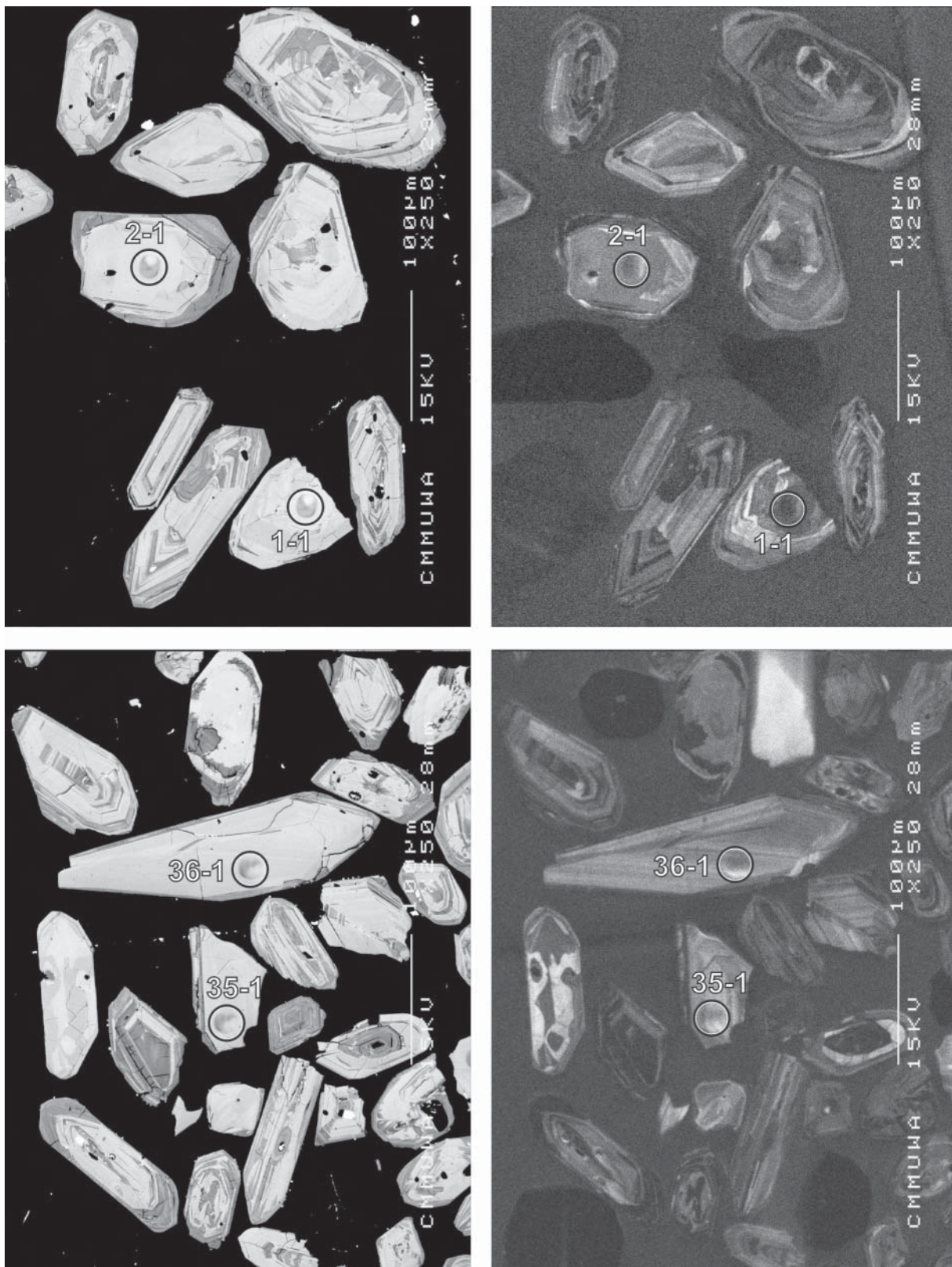


Figure 76. Representative SEM images (BSE on left, CL on right) for sample 2001969043A: foliated biotite monzogranite, Blueys Well. SHRIMP analysis spots are labelled. Remnant pits from the ion microprobe analyses are faintly visible in some grains. Scale bar is 100 μ m.

inheritance (possibly with variable resetting), and culling has been from the high-age side. This gives a weighted mean $^{207}\text{Pb}/^{206}\text{Pb}$ age of 2674.4 ± 2.5 Ma (MSWD = 1.3) from 25 analyses. Any additional culling gives MSWD <1.

Geochronological interpretation

The 2674 ± 3 Ma date is interpreted to be the magmatic age of the granite. This date is indistinguishable from the 2670 Ma date, interpreted as a metamorphic age, for the banded gneiss 2001969053C intruded by this granite. However, this sample shows none of the low-U, Th characteristics of the banded gneiss zircons.

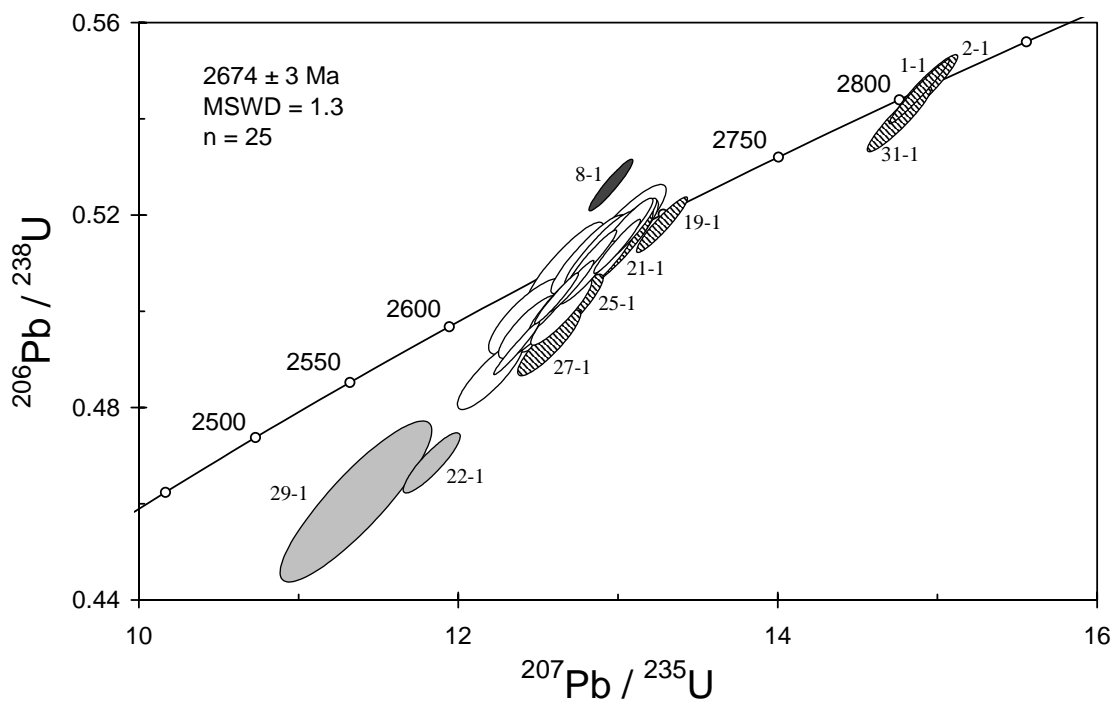


Figure 77. Concordia plot for zircons from sample 2001969043A: foliated biotite monzogranite, Blueys Well. White filled symbols are used to define the age of the sample; inherited grains have diagonal shading; younger outlier is dark grey; discordant and/or high common Pb analyses are light grey. One very imprecise, discordant analysis (20-1) is not shown.

Table 32. SHRIMP analytical results for zircon from sample 200196 9043A: foliated biotite monzogranite, Blueys Well.

grain-spot	U (ppm)	Th (ppm)	4f206 (%)	$^{207}\text{Pb}/^{206}\text{Pb}$		$^{206}\text{Pb}/^{238}\text{U}$		$^{207}\text{Pb}/^{235}\text{U}$		$^{208}\text{Pb}/^{232}\text{Th}$	conc. (%)	$^{207}\text{Pb}/^{206}\text{Pb}$ Age (Ma)	
					±		±		±				±
Main group													
3-1	397	73	0.019	0.1821	0.0004	0.511	0.004	12.83	0.10	0.150	100	2672	4
4-1	141	133	0.115	0.1835	0.0007	0.499	0.005	12.63	0.13	0.126	97	2684	7
5-1	176	166	0.035	0.1827	0.0006	0.508	0.004	12.79	0.12	0.140	99	2678	6
6-1	140	145	0.076	0.1832	0.0009	0.510	0.005	12.88	0.14	0.141	99	2682	8
7-1	113	103	0.586	0.1818	0.0010	0.486	0.005	12.19	0.14	0.076	95	2670	9
9-1	133	84	0.021	0.1831	0.0007	0.516	0.005	13.03	0.13	0.141	100	2681	6
10-1	189	164	0.062	0.1829	0.0006	0.517	0.004	13.03	0.12	0.143	100	2679	6
11-1	82	97	0.076	0.1832	0.0011	0.515	0.005	13.00	0.16	0.142	100	2682	10
12-1	90	139	0.936	0.1806	0.0013	0.499	0.005	12.42	0.16	0.080	98	2659	12
13-1	88	78	0.281	0.1810	0.0012	0.504	0.006	12.59	0.16	0.139	99	2662	11
14-1	453	646	0.178	0.1820	0.0004	0.501	0.004	12.57	0.10	0.149	98	2671	4
15-1	683	219	0.045	0.1819	0.0003	0.502	0.004	12.60	0.09	0.138	98	2671	3
16-1	57	37	0.087	0.1827	0.0012	0.517	0.006	13.02	0.18	0.142	100	2677	11
17-1	584	91	0.074	0.1823	0.0003	0.505	0.004	12.69	0.09	0.138	99	2674	3
18-1	82	110	0.071	0.1814	0.0009	0.512	0.005	12.79	0.15	0.139	100	2665	8
23-1	86	65	0.040	0.1832	0.0009	0.514	0.006	12.98	0.15	0.142	100	2682	8
24.1	664	270	0.028	0.1821	0.0003	0.492	0.004	12.35	0.09	0.138	96	2672	3
26-1	87	89	0.010	0.1822	0.0009	0.512	0.005	12.87	0.15	0.142	100	2673	8
28-1	451	336	0.017	0.1834	0.0004	0.513	0.004	12.98	0.10	0.139	99	2684	3
30-1	154	196	0.426	0.1817	0.0011	0.496	0.004	12.43	0.13	0.115	97	2668	10
32-1	139	82	0.031	0.1826	0.0007	0.509	0.005	12.82	0.13	0.142	99	2676	6
33-1	84	52	-0.010	0.1816	0.0009	0.512	0.006	12.81	0.15	0.141	100	2667	8
34-1	76	42	-0.016	0.1827	0.0009	0.508	0.006	12.80	0.16	0.138	99	2677	8
35-1	62	56	0.124	0.1828	0.0013	0.500	0.006	12.60	0.18	0.138	98	2678	11
36-1	73	73	0.127	0.1801	0.0010	0.510	0.006	12.65	0.16	0.139	100	2654	9
Probably inherited													
21-1	85	45	-0.036	0.1836	0.0008	0.513	0.005	12.98	0.15	0.143	99	2686	7
25-1	112	63	0.171	0.1839	0.0009	0.500	0.005	12.68	0.14	0.140	97	2689	8
27-1	141	282	0.000	0.1847	0.0009	0.493	0.005	12.55	0.13	0.137	96	2696	8
19-1	741	253	0.036	0.1858	0.0005	0.518	0.004	13.27	0.11	0.156	99	2705	4
Inherited													
1-1	518	337	-0.009	0.1977	0.0004	0.546	0.004	14.88	0.13	0.150	100	2808	3
2-1	186	139	0.048	0.1980	0.0006	0.547	0.005	14.92	0.13	0.150	100	2810	5
31-1	208	105	0.079	0.1982	0.0006	0.540	0.005	14.76	0.13	0.147	99	2811	5
Young outlier													
8-1	872	100	0.023	0.1784	0.0004	0.526	0.004	12.94	0.09	0.141	103	2638	4
>5% discordant													
20-1	199	112	3.768	0.1850	0.0218	0.477	0.010	12.17	1.46	0.168	93	2698	195
22-1	157	221	0.390	0.1832	0.0008	0.468	0.004	11.82	0.12	0.087	92	2682	8
29-1	425	412	1.092	0.1789	0.0023	0.460	0.011	11.34	0.31	0.128	92	2643	22

Data are at 1 σ precision. All Pb data are common-Pb corrected (based on ^{204}Pb and Broken Hill Pb composition). Analysis date: 2203/02; session Z3878j.

2001969044: Mars Bore monzogranite

- 1:250,000 sheet:** Leonora (SH5101)
- 1:100,000 sheet:** Wilbah (3040)
- MGA:** 258288mE 6804422mN
- Location:** The sample is from a low, large platform about 200 m east of Lawlers - Mt Ida Road, and about 5 km northwest of Mars Bore.
- Description:** The sample is a grey-white, equigranular to seriate, medium-grained biotite monzogranite which has a weak fabric defined by aligned biotite. The unit is a late biotite monzogranite phase that intrudes banded granitic gneiss (sample 2001969053C) and foliated granitoids (sample 2001969043A).
- This rock has a granular texture. Principal minerals are K-feldspar, plagioclase, quartz and biotite, with K-feldspar > plagioclase. K-feldspar is subhedral to anhedral, with moderate to well-developed tartan twinning and minor perthite. Plagioclase is subhedral to anhedral, and is generally faintly twinned. It is generally unzoned to weakly normally zoned. Complex/patchy zoning occurs in some cores. Myrmekite is present. Plagioclase is locally altered to white mica and minor carbonate, especially in grain centres. Quartz occurs as undulose grains to 5–6 mm. Biotite (5–6%) forms light yellow to reddish brown, subhedral to anhedral flakes, that are often replaced by chlorite with rutile, and minor fluorite and epidote and/or coarse white mica. Accessory phases include common apatite, zircon and irregular opaque minerals.
- Mount, pop:** Z3878D

Description of zircons

Zircon is colourless to pale yellow-grey, with a pale yellowish red-brown stain present on numerous grains. Fractures are pervasive in some grains. Inclusions are present in numerous grains. Subhedral to euhedral morphologies are present, generally with slightly rounded crystal faces, but some grains are moderately- to well-rounded. Stubby (generally < 150 μm) and elongate (aspect ratios to 5:1, up to ~250 μm length) grains are present. Continuous euhedral zoning is present in some grains in transmitted and reflected light. Most grains have concentric zoning patterns in CL, but some also contain disrupted patches (Fig. 78). Cores are visible in some grains.

Concurrent standard data

The apparent calibration slope for QGNG was ~2.1, and that for each of the two concurrent samples was >2.2; a value of 2.2 was used for data reduction. Omitting two outliers identified by SQUID and two with extreme UO^+/U^+ leaves 33 analyses with a 1σ scatter in Pb/U of 0.63% (MSWD = 2.12). Deleting two additional points that are 3σ (low) outliers in $^{207}\text{Pb}/^{206}\text{Pb}$ gives a weighted mean $^{207}\text{Pb}/^{206}\text{Pb}$ age of 1847.5 ± 2.7 Ma (MSWD = 0.89).

Element abundance calibration was based on CZ3 (n = 3).

Sample data

Five of the 36 grains (Table 33, Fig. 79) are >5% discordant (8-1, 9-1, 11-1, 13-1, 33-1); several of these also have high common Pb. There are two distinctly older grains (16-1, 21-1), as is one of the discordant analyses (9-1). The remaining 29 analyses form a cluster, with some excess scatter in $^{207}\text{Pb}/^{206}\text{Pb}$ (MSWD = 1.7). Omitting two 3σ (old) outliers (17-1, 34-1) leaves 27 with a weighted mean $^{207}\text{Pb}/^{206}\text{Pb}$ age of 2646.5 ± 2.5 Ma (MSWD = 0.78).

Geochronological interpretation

The crystallization age of the monzogranite is 2647 ± 3 Ma.

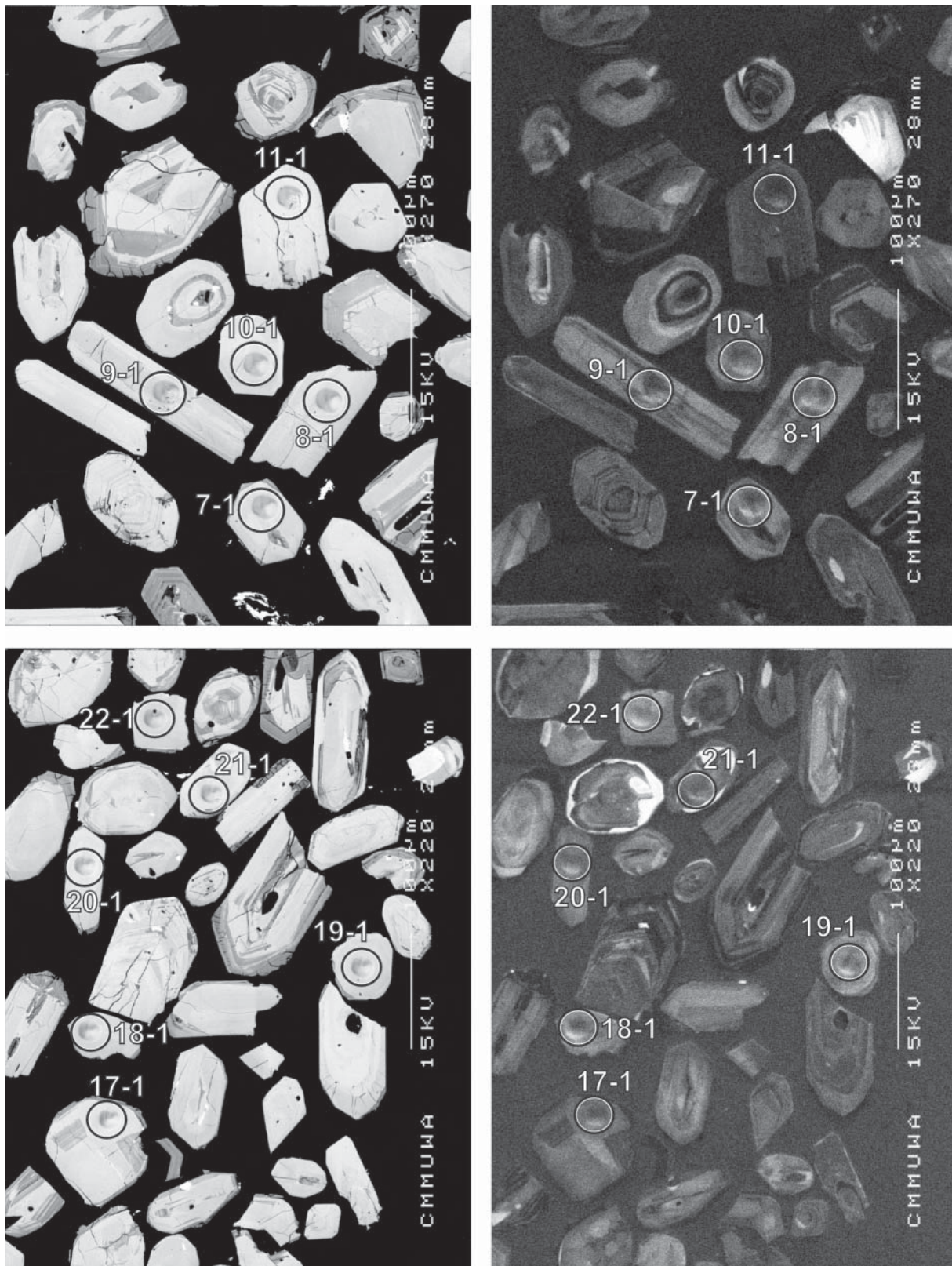


Figure 78. Representative SEM images (BSE on left, CL on right) for sample 2001969044: Mars Bore monzogranite. SHRIMP analysis spots are labelled. Remnant pits from the ion microprobe analyses are faintly visible in some grains. Scale bar is 100 μ m.

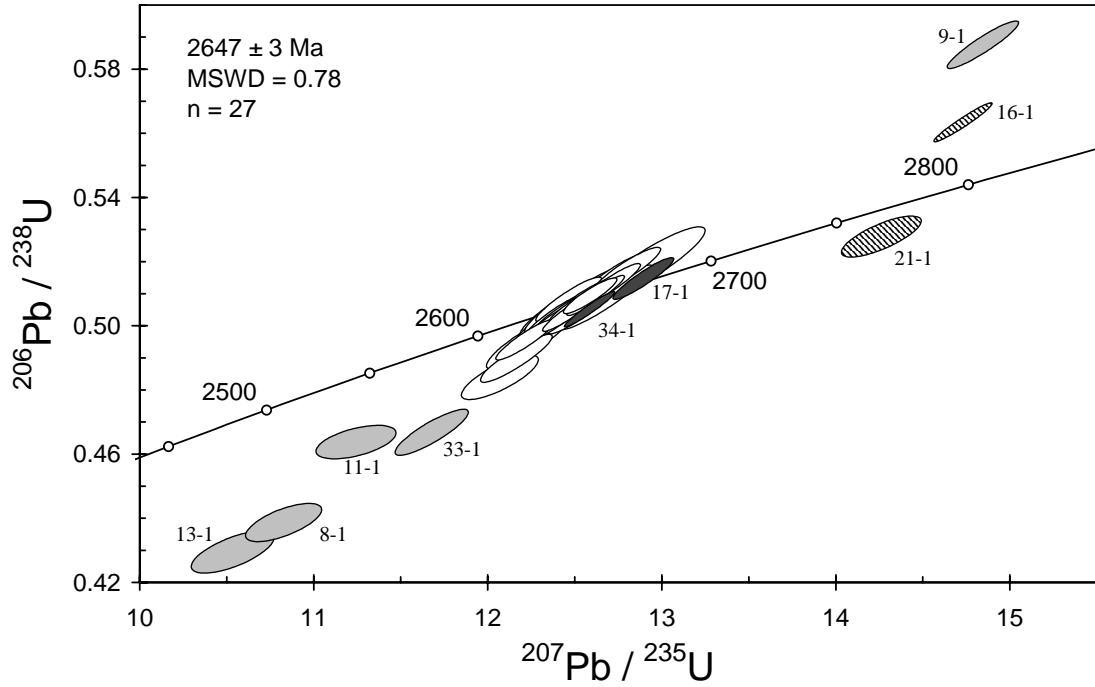


Figure 79. Concordia plot for zircons from sample 2001969044: Mars Bore monzogranite. White filled symbols are used to define the age of the sample; inherited grains have diagonal shading; old outliers are dark grey; discordant and/or high common Pb analyses are light grey.

Table 33. SHRIMP analytical results for zircon from sample 2001969044: Mars Bore monzogranite.

grain-spot	U (ppm)	Th (ppm)	4f206 (%)	$^{207}\text{Pb}/^{206}\text{Pb}$		$^{206}\text{Pb}/^{238}\text{U}$		$^{207}\text{Pb}/^{235}\text{U}$		$^{208}\text{Pb}/^{232}\text{Th}$	conc. (%)	$^{207}\text{Pb}/^{206}\text{Pb}$ Age (Ma)	
					±		±		±				±
Main group													
1-1	208	148	0.010	0.1797	0.0005	0.509	0.004	12.61	0.11	0.142	100	2650	5
2-1	233	254	0.026	0.1795	0.0005	0.504	0.004	12.46	0.11	0.139	99	2648	5
3-1	358	393	0.331	0.1793	0.0006	0.509	0.004	12.58	0.10	0.135	100	2646	5
4-1	90	94	0.008	0.1808	0.0009	0.508	0.007	12.67	0.18	0.140	100	2660	9
5-1	193	177	0.038	0.1792	0.0006	0.506	0.004	12.50	0.11	0.141	100	2646	6
6-1	172	192	0.068	0.1797	0.0006	0.512	0.004	12.69	0.12	0.141	101	2650	6
7-1	143	211	0.092	0.1795	0.0007	0.517	0.005	12.79	0.13	0.146	101	2648	7
10-1	149	177	0.141	0.1792	0.0008	0.508	0.005	12.54	0.13	0.137	100	2646	7
12-1	126	216	1.728	0.1810	0.0014	0.483	0.005	12.06	0.15	0.102	95	2662	13
14-1	94	31	0.013	0.1782	0.0009	0.504	0.005	12.39	0.15	0.132	100	2636	8
15-1	84	83	0.025	0.1786	0.0009	0.509	0.005	12.55	0.15	0.141	101	2640	8
18-1	133	150	0.015	0.1790	0.0007	0.515	0.005	12.71	0.13	0.143	101	2644	7
19-1	133	201	-0.049	0.1788	0.0007	0.503	0.005	12.40	0.12	0.137	99	2642	6
20-1	187	149	0.070	0.1798	0.0006	0.507	0.004	12.56	0.12	0.139	100	2651	6
22-1	68	80	0.055	0.1789	0.0010	0.504	0.006	12.44	0.16	0.139	100	2642	10
23-1	106	116	0.112	0.1783	0.0008	0.504	0.005	12.40	0.13	0.137	100	2637	8
24-1	184	221	0.067	0.1789	0.0007	0.503	0.004	12.42	0.12	0.139	99	2643	6
25-1	170	128	0.089	0.1792	0.0006	0.501	0.004	12.38	0.12	0.137	99	2645	6
26-1	69	78	0.146	0.1793	0.0011	0.494	0.006	12.22	0.16	0.134	98	2646	10
27-1	195	279	0.088	0.1788	0.0007	0.495	0.004	12.20	0.11	0.136	98	2642	6
28-1	175	229	0.000	0.1803	0.0006	0.503	0.004	12.51	0.12	0.139	99	2656	6
29-1	37	32	-0.150	0.1806	0.0013	0.519	0.008	12.92	0.21	0.143	101	2658	12
30-1	149	206	0.088	0.1779	0.0007	0.508	0.005	12.45	0.12	0.140	100	2634	7
31-1	92	100	0.014	0.1789	0.0009	0.501	0.005	12.36	0.15	0.136	99	2642	9
32-1	97	107	0.152	0.1802	0.0009	0.489	0.005	12.15	0.14	0.136	97	2655	8
35-1	113	121	0.077	0.1789	0.0008	0.502	0.005	12.37	0.13	0.135	99	2643	7
36-1	186	273	0.027	0.1797	0.0007	0.504	0.004	12.50	0.12	0.140	99	2650	6
3σ old outliers													
17-1	185	137	0.028	0.1817	0.0006	0.514	0.004	12.89	0.12	0.143	100	2669	6
34-1	471	93	-0.001	0.1807	0.0004	0.505	0.004	12.58	0.09	0.141	99	2660	3
Inherited													
16-1	575	548	0.023	0.1896	0.0004	0.564	0.004	14.73	0.11	0.137	105	2738	3
21-1	246	135	0.740	0.1961	0.0014	0.528	0.004	14.26	0.15	0.144	98	2794	11
Discordant													
8-1	153	203	0.997	0.1793	0.0018	0.437	0.004	10.81	0.15	0.130	88	2646	16
9-1	181	239	0.010	0.1832	0.0006	0.588	0.005	14.85	0.14	0.121	111	2682	6
11-1	383	117	1.289	0.1759	0.0020	0.463	0.003	11.22	0.15	0.134	94	2615	19
13-1	100	157	1.706	0.1781	0.0020	0.428	0.004	10.51	0.16	0.115	87	2636	18
33-1	94	92	0.195	0.1816	0.0011	0.466	0.005	11.66	0.14	0.085	92	2667	10

Data are at 1σ precision. All Pb data are common-Pb corrected (based on ^{204}Pb and Broken Hill Pb composition). Analysis date: 22/03/02; session Z3878j.

2001969053A: granodiorite leucosome, Turkey Well

1:250,000 sheet: Leonora (SH5101)

1:100,000 sheet: Wilbah (3040)

MGA: 267154mE 6800317mN

Location: The sample is from a low pavement, next to a fence line track, about 3 km west-southwest of Turkey Well.

Description: It is a foliated, white, (sparsely plagioclase porphyritic to) seriate, medium-grained biotite granodioritic leucosome in a banded gneiss, of which sample 2001969053C is representative. The leucosome contains plagioclase grains that vary in size from <4 mm to locally >7 mm. The leucosome cross-cuts banding in the host granitic gneiss, including felsic layers which are mineralogically similar to the leucosome.

The sample is characterised by a granoblastic texture. Principal minerals are plagioclase, K-feldspar, quartz and biotite, with plagioclase>>K-feldspar. Plagioclase is subhedral to anhedral/rounded. It is well-zoned, with very common irregular complex/patchy-zoned cores and/or subhedral unzoned cores, and normally or oscillatory zoned rims. Moderate myrmekite is developed. The plagioclase is variably altered to white mica and carbonate. K-feldspar occurs as anhedral to interstitial grains, which are commonly poikilitic, and have moderate tartan twinning. Quartz is anhedral, with moderately to locally strongly undulose extinction. Biotite (5–6%) occurs as aligned, light yellow to medium-dark brown, anhedral to ragged flakes that are moderately altered to chlorite, rutile, epidote and/or minor white mica. Accessory phases include zircon (with apparent cores in some of the larger grains), apatite, opaque minerals and possibly anhedral titanite (secondary?).

Mount, pop: Z3878A

Description of zircons

Zircon from this sample is predominantly colourless to pale yellow-brown and clear, but some grains contain inclusions and fractures. The grains are generally euhedral to subhedral crystals and fragments, with slightly to moderately rounded crystal faces. Grains vary from approximately 65 μm to 180 μm in length, with aspect ratios of 2:1 to 3:1. Concentric oscillatory zoning is faintly visible in many grains in CL, although irregular patches of recrystallised zircon are also present (Fig. 80). A small number of grains are very bright in CL. Cores and thin rims are present in some grains, visible in both CL and transmitted light.

Concurrent standard data

This session gave an extremely good Pb/U calibration. The omission of one outlier leaves 37 analyses with a 1σ Pb/U reproducibility of 0.59% (MSWD = 2.73). The apparent calibration slope for QGNG is 2.18 and the concurrent sample data also indicate values ~ 2.2 , which was used for calibration. The standardised assessment procedure produced a weighted mean $^{207}\text{Pb}/^{206}\text{Pb}$ age for QGNG is 1849.9 ± 2.5 Ma (MSWD = 1.07; $n = 28$).

Element abundance calibration was based on CZ3 ($n = 1$).

Sample data

One analysis was obtained from each of 37 grains (Table 34). Only one analysis (2-1) is >5% discordant, and there are two distinct young outliers (4-1, 19-1; Fig. 81). The remaining data group together, but with excess scatter in $^{207}\text{Pb}/^{206}\text{Pb}$ (MSWD = 1.7). Omitting two $>3\sigma$ outliers (20-1 and 22-1) leaves 32 analyses with a weighted mean $^{207}\text{Pb}/^{206}\text{Pb}$ age of 2809 ± 2 Ma and MSWD = 1.19.

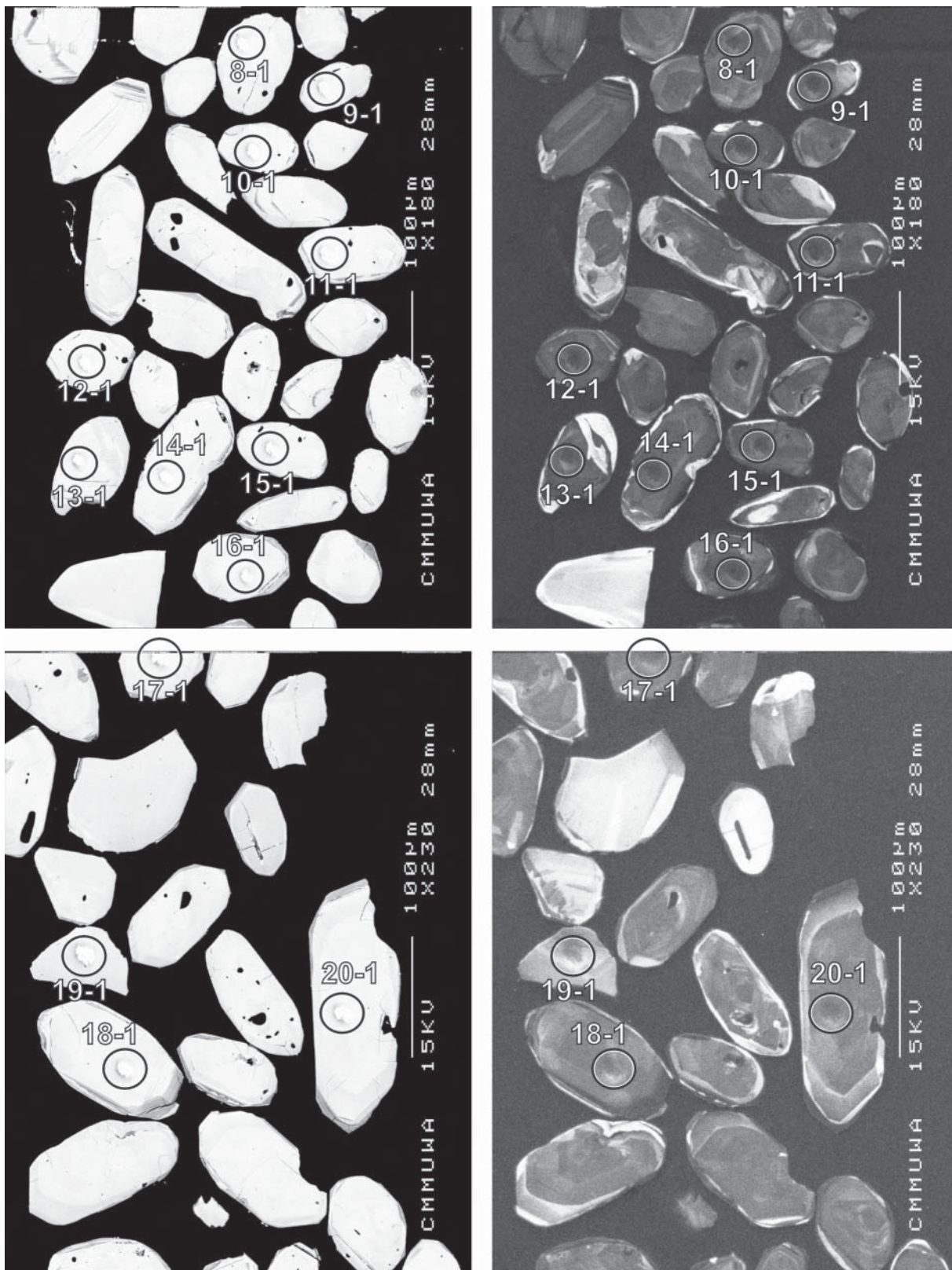


Figure 80. Representative SEM images (BSE on left, CL on right) for sample 2001969053A: granodiorite leucosome, Turkey Well. SHRIMP analysis spots are labelled. Remnant pits from the ion microprobe analyses are faintly visible in some grains. Scale bar is 100 µm.

Geochronological interpretation

The relatively tight structure of this data set suggests that it records a single crystallization event, but identifying that event is difficult, despite constraints from the ages of associated rocks. There are two main possibilities. Either this is the age of the leucosome, or the age of a pre-existing rock from which the leucosome was derived.

If 2809 ± 2 Ma is the age of the leucosome, this requires a severe metamorphic resetting of zircons in the enclosing banded gneiss (2001969053C; 2670 Ma) that has not affected those in the leucosome. The zircons in the banded gneiss do have the low-U high U/Th character of metamorphic grains. If the banded gneiss (or its protolith) are actually 2670 Ma, the 2809 ± 2 Ma date must be the age of the rock from which the leucosome was derived, and the formation of the fractionated melt and its transport and intrusion all happened with almost no interaction with other sources of zircon. The two distinct young outliers, one of them within uncertainty of 2670 Ma, is consistent with this scenario.

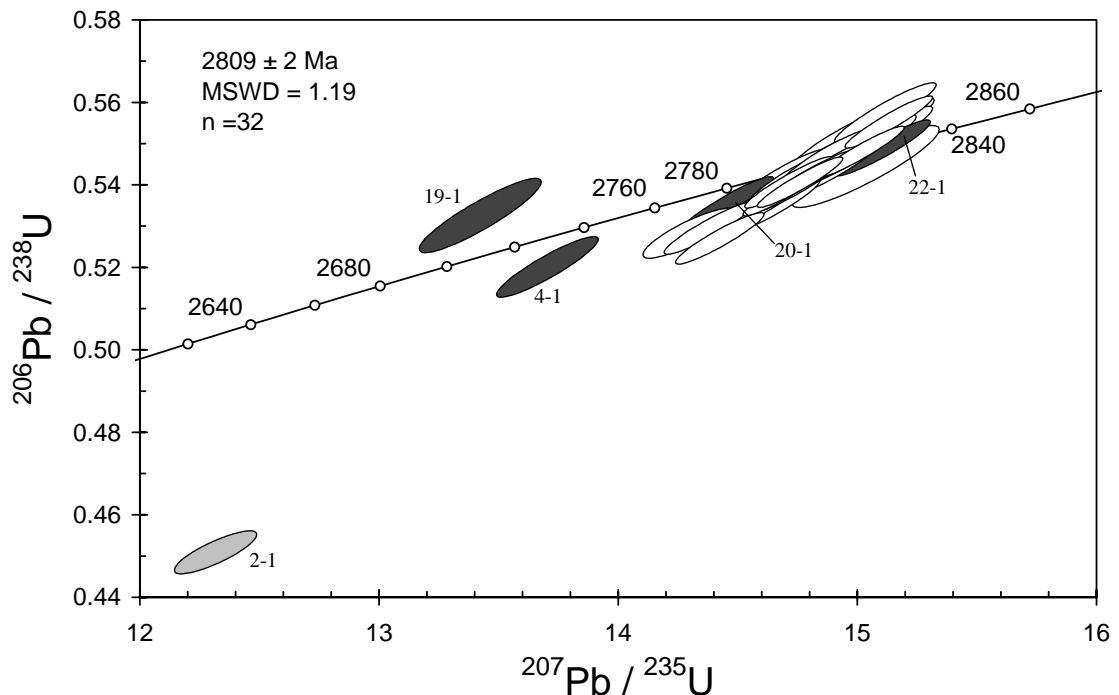


Figure 81. Concordia plot for zircons from sample 2001969053A: granodiorite leucosome, Turkey Well. White filled symbols are used to define the age of the sample; outliers are dark grey; discordant analysis is light grey.

Table 34. SHRIMP analytical results for zircon from sample 2001969053A: granodiorite leucosome, Turkey Well.

grain-spot	U (ppm)	Th (ppm)	4f206 (%)	$^{207}\text{Pb}/^{206}\text{Pb}$		$^{206}\text{Pb}/^{238}\text{U}$		$^{207}\text{Pb}/^{235}\text{U}$		$^{208}\text{Pb}/^{232}\text{Th}$	conc. (%)	$^{207}\text{Pb}/^{206}\text{Pb}$ Age (Ma)	
					±		±		±				±
Main group													
1-1	125	61	-0.025	0.1977	0.0006	0.544	0.004	14.83	0.13	0.154	100	2807	5
3-1	122	63	0.036	0.1987	0.0006	0.544	0.004	14.90	0.13	0.150	99	2815	5
5-1	81	33	0.022	0.1966	0.0007	0.551	0.005	14.94	0.14	0.151	101	2798	6
6-1	87	41	-0.012	0.1985	0.0007	0.552	0.005	15.10	0.14	0.151	101	2814	6
7-1	87	37	0.019	0.1982	0.0007	0.546	0.005	14.93	0.14	0.149	100	2811	6
8-1	125	44	0.025	0.1984	0.0006	0.544	0.004	14.88	0.13	0.145	100	2813	5
9-1	161	103	0.098	0.1976	0.0005	0.555	0.004	15.13	0.12	0.153	101	2807	4
10-1	144	83	-0.017	0.1972	0.0005	0.547	0.004	14.87	0.12	0.152	100	2803	4
11-1	168	95	0.011	0.1987	0.0005	0.548	0.004	15.01	0.12	0.152	100	2815	4
12-1	138	71	-0.009	0.1985	0.0005	0.546	0.004	14.95	0.13	0.148	100	2814	4
13-1	104	37	0.033	0.1981	0.0007	0.541	0.005	14.77	0.13	0.148	99	2811	5
14-1	151	94	0.355	0.1963	0.0009	0.528	0.004	14.29	0.13	0.144	98	2796	7
15-1	139	62	0.101	0.1985	0.0006	0.527	0.004	14.42	0.12	0.147	97	2814	5
16-1	130	79	0.284	0.1977	0.0007	0.534	0.004	14.56	0.13	0.149	98	2808	6
17-1	144	80	-0.040	0.1982	0.0005	0.545	0.004	14.90	0.12	0.154	100	2812	4
18-1	80	36	0.013	0.1978	0.0007	0.554	0.005	15.10	0.15	0.149	101	2808	6
21-1	119	68	-0.038	0.1987	0.0006	0.535	0.004	14.65	0.13	0.148	98	2816	5
23-1	112	49	0.104	0.1982	0.0007	0.533	0.004	14.56	0.13	0.144	98	2812	6
25-1	35	10	-0.118	0.2003	0.0012	0.544	0.007	15.03	0.20	0.157	99	2828	10
26-1	110	51	0.033	0.1973	0.0006	0.546	0.005	14.85	0.13	0.150	100	2804	5
27-1	147	75	0.020	0.1974	0.0005	0.541	0.004	14.71	0.12	0.148	99	2805	4
28-1	94	45	-0.014	0.1966	0.0007	0.558	0.005	15.12	0.14	0.153	102	2798	6
29-1	157	98	0.045	0.1980	0.0005	0.539	0.004	14.70	0.12	0.147	99	2810	4
30-1	132	68	-0.058	0.1981	0.0006	0.540	0.004	14.75	0.13	0.151	99	2811	5
31-1	131	77	0.179	0.1970	0.0006	0.529	0.004	14.38	0.12	0.148	98	2802	5
32-1	166	131	-0.006	0.1981	0.0005	0.542	0.004	14.80	0.12	0.149	99	2811	4
33-1	168	112	0.012	0.1980	0.0005	0.541	0.004	14.76	0.12	0.147	99	2810	4
34-1	130	58	-0.003	0.1972	0.0006	0.542	0.004	14.74	0.12	0.147	100	2803	5
35-1	94	30	0.048	0.1975	0.0007	0.545	0.005	14.83	0.14	0.147	100	2805	6
36-1	105	47	0.028	0.1976	0.0006	0.540	0.005	14.70	0.13	0.142	99	2807	5
37-1	97	46	-0.026	0.1983	0.0007	0.550	0.005	15.04	0.14	0.152	100	2812	5
38-1	122	63	-0.010	0.1966	0.0007	0.542	0.004	14.70	0.13	0.151	100	2798	6
>5% discordant													
2-1	161	83	0.383	0.1984	0.0010	0.450	0.003	12.30	0.11	0.130	85	2813	8
>3σ outliers													
4-1	68	0	0.029	0.1911	0.0008	0.520	0.005	13.70	0.14	0.190	98	2752	7
19-1	43	3	-0.063	0.1827	0.0010	0.532	0.006	13.41	0.17	0.160	103	2678	9
20-1	117	72	-0.005	0.1959	0.0006	0.535	0.004	14.46	0.13	0.147	99	2792	5
22-1	110	33	-0.051	0.1996	0.0006	0.549	0.005	15.11	0.13	0.158	100	2823	5

Data are at 1σ precision. All Pb data are common-Pb corrected (based on ^{204}Pb and Broken Hill Pb composition). Analysis date: 15/03/02; session Z3878i. Secondary ion beams were not centred correctly during analysis 24-1 and this was deleted from files.

2001969053C: banded biotite granitic gneiss, Turkey Well

1:250,000 sheet: Leonora (SH5101)

1:100,000 sheet: Wilbah (3040)

MGA: 267154mE 6800317mN

Location: The sample comes from a low pavement, next to a fence line track, about 3 km west-southwest of Turkey Well.

Description: This is a white and blue-grey, fine- to medium-grained, banded biotite granitic gneiss that is cut by leucosome (sample 2001969053A) and by late biotite monzogranite (sample 2001969044). Banding (<5 mm to >3 cm in width) is defined by variable biotite content (5–6% to >20%), variable grain size and by the presence of concordant pegmatite layers. The banding is locally isoclinally folded.

Principal minerals in the granoblastic rock are plagioclase, K-feldspar, quartz and biotite, with plagioclase >> K-feldspar. Plagioclase occurs as mostly anhedral, rounded to lesser subhedral grains with faint to no visible twinning, and no obvious zoning. Minor myrmekite is present. The plagioclase grains are variably altered, mostly minor white mica and minor carbonate, but some grains are partly to moderately pseudomorphed by coarse white mica. K-feldspar is anhedral to interstitial and locally poikilitic, with variably developed tartan twinning, and minor perthite. Quartz occurs as anhedral grains, with mild to locally moderately undulose extinction. Biotite is present as light yellow to medium red-brown, subhedral to irregular flakes, with minor to moderate chlorite, epidote, and/or white mica alteration. Accessory minerals include zircon, large hexagonal apatite, and opaque minerals.

Mount, pop: Z3878C

Description of zircons

Many zircon grains are fragments of larger crystals that range in length from ~60 μm to 250 μm (aspect ratios vary from 2:1 to 4:1), although whole crystals are also present. Approximately equal proportions of subhedral and anhedral grains are present, with most being moderately- to well-rounded. The zircon is colourless to pale brown-grey, and is commonly fractured. Some grains contain inclusions. Most of the grains have clearly-defined features in CL, with continuous layer-parallel or concentric zoning commonly present (Fig. 82). However, many grains also contain irregular patches or zones, mostly defined by very sharp angular boundaries which possibly represent recrystallisation fronts. Core-rim relationships are visible in a few grains.

Concurrent standard data

This session gave an extremely good Pb/U calibration. The omission of one outlier leaves 37 analyses with a 1σ Pb/U reproducibility of 0.59% (MSWD = 2.73). The apparent calibration slope for QGNG is 2.18 and the concurrent sample data also indicate values ~2.2, which was used for calibration. The standardised assessment procedure produced a weighted mean $^{207}\text{Pb}/^{206}\text{Pb}$ age for QGNG of 1849.9 ± 2.5 Ma (MSWD = 1.07; $n = 28$).

Element abundance calibration was based on CZ3 ($n = 1$).

Sample data

Thirty nine analyses were obtained from 38 grains (Table 35). Only one analysis (21-1) is >5% discordant (Fig. 83), but two others (1-1, 24-1) with <10 ppm U are also considered unreliable for geochronology. Amongst the remainder there are two slightly older outliers (15-1, 27-1) and two other 3σ outliers (one younger, 4-1; one older, 28-1). Omitting these leaves 32 well-grouped analyses with a weighted mean $^{207}\text{Pb}/^{206}\text{Pb}$ age of 2670.1 ± 3.2 Ma (MSWD = 1.07).



Figure 82. Representative SEM images (BSE on left, CL on right) for sample 2001969053C: banded biotite granitic gneiss, Turkey Well. SHRIMP analysis spots are labelled. Remnant pits from the ion microprobe analyses are faintly visible in some grains. Scale bar is 100 μ m.

Geochronological interpretation

These data must be reconciled with those for the crosscutting leucosome 2001969053A and foliated granite 2001969043A. The latter is 2674 ± 3 Ma (interpreted as a crystallisation age), indistinguishable from 2670 ± 4 Ma but unlikely to be younger; the former gives a zircon age of 2809 Ma, interpreted to represent the age of inherited grains from the protolith. It seems most likely that the 2670 ± 4 Ma date is a metamorphic age for this banded gneiss, even though the grains do not show complete recrystallisation. The low U and low Th/U are typical of intensely metamorphosed zircons. Although there are no distinctly earlier ages preserved, the several old outliers could be incompletely reset older grains.

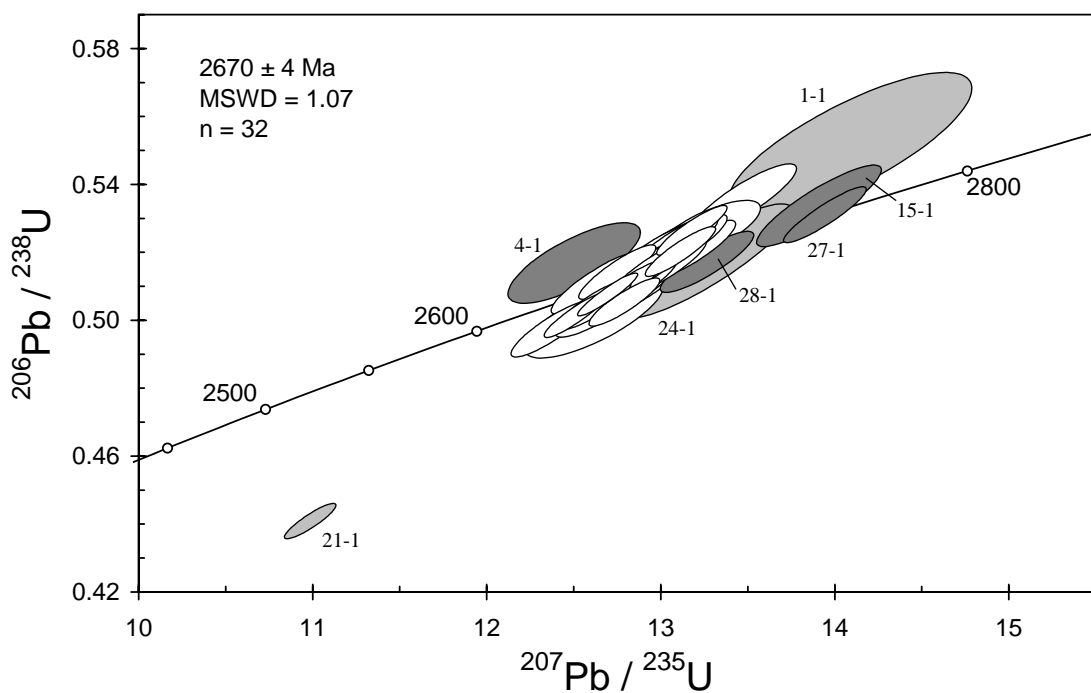


Figure 83. Concordia plot for zircons from sample 2001969053C: banded biotite granitic gneiss, Turkey Well. White filled symbols are used to define the age of the sample; older and younger outliers are dark grey; discordant or low-U analyses are light grey.

Table 35. SHRIMP analytical results for zircon from sample 2001969053C: banded biotite granitic gneiss, Turkey Well.

grain-spot	U (ppm)	Th (ppm)	4f206 (%)	$^{207}\text{Pb}/^{206}\text{Pb}$		$^{206}\text{Pb}/^{238}\text{U}$		$^{207}\text{Pb}/^{235}\text{U}$		$^{208}\text{Pb}/^{232}\text{Th}$	conc. (%)	$^{207}\text{Pb}/^{206}\text{Pb}$ Age (Ma)	
					±		±		±				±
Main group													
2-1	43	<1	0.112	0.1818	0.0013	0.522	0.006	13.09	0.17	—	101	2669	12
3-1	42	<1	0.202	0.1836	0.0012	0.520	0.006	13.17	0.17	—	101	2685	10
5-1	42	13	-0.030	0.1827	0.0010	0.519	0.008	13.06	0.21	0.146	101	2677	9
6-1	63	<1	0.020	0.1837	0.0009	0.505	0.005	12.78	0.13	—	98	2686	8
7-1	74	<1	-0.017	0.1828	0.0008	0.520	0.005	13.11	0.14	—	101	2679	7
8-1	29	<1	0.167	0.1825	0.0014	0.535	0.007	13.47	0.20	—	103	2675	12
9-1	53	25	0.126	0.1822	0.0013	0.502	0.005	12.62	0.16	0.136	98	2673	11
10-1	52	1	0.191	0.1817	0.0012	0.522	0.006	13.08	0.16	—	102	2668	11
11-1	45	<1	0.118	0.1822	0.0012	0.522	0.006	13.13	0.17	—	101	2673	11
12-1	49	<1	0.090	0.1832	0.0010	0.515	0.005	13.02	0.16	—	100	2682	9
13-1	46	<1	0.109	0.1809	0.0011	0.519	0.006	12.95	0.16	—	101	2661	10
14-1	52	16	0.061	0.1813	0.0009	0.514	0.005	12.86	0.15	0.142	100	2665	8
16-1	48	18	0.120	0.1818	0.0011	0.507	0.005	12.71	0.16	—	99	2670	10
17-1	22	<1	-0.035	0.1826	0.0014	0.520	0.008	13.08	0.21	—	101	2677	12
17-2	76	<1	0.071	0.1815	0.0008	0.526	0.005	13.17	0.13	—	102	2667	7
18-1	55	22	0.009	0.1822	0.0009	0.514	0.005	12.93	0.15	0.140	100	2673	8
19-1	51	21	-0.003	0.1831	0.0009	0.510	0.005	12.86	0.15	0.141	99	2681	8
20-1	64	<1	0.056	0.1822	0.0008	0.510	0.005	12.80	0.14	—	99	2673	7
22-1	52	21	-0.023	0.1810	0.0009	0.513	0.005	12.80	0.15	0.147	100	2662	8
23-1	45	24	0.045	0.1805	0.0011	0.497	0.005	12.36	0.15	0.137	98	2657	10
25-1	32	13	-0.072	0.1834	0.0011	0.510	0.006	12.90	0.18	0.141	99	2684	10
26-1	18	<1	0.385	0.1828	0.0025	0.500	0.008	12.61	0.27	—	98	2678	22
29-1	24	<1	-0.117	0.1814	0.0013	0.520	0.007	13.00	0.20	—	101	2666	12
30-1	36	13	-0.207	0.1828	0.0014	0.509	0.006	12.83	0.18	0.149	99	2678	12
31-1	36	<1	-0.118	0.1813	0.0012	0.520	0.006	13.00	0.18	—	101	2664	11
32-1	54	19	0.134	0.1798	0.0009	0.514	0.005	12.74	0.15	0.137	101	2651	9
33-1	50	7	0.126	0.1819	0.0012	0.502	0.005	12.60	0.16	—	98	2671	11
34-1	73	<1	0.209	0.1815	0.0010	0.504	0.005	12.61	0.14	—	99	2667	9
35-1	95	49	0.074	0.1810	0.0007	0.501	0.004	12.50	0.12	0.114	98	2662	6
36-1	114	62	-0.008	0.1814	0.0006	0.507	0.004	12.68	0.11	0.130	99	2666	5
37-1	38	15	0.094	0.1792	0.0011	0.510	0.006	12.61	0.17	0.138	100	2646	10
38-1	40	<1	0.015	0.1829	0.0019	0.526	0.006	13.26	0.20	—	102	2679	17
>3σ age outliers													
4-1	19	<1	0.741	0.1755	0.0023	0.516	0.008	12.49	0.25	—	103	2610	22
15-1	21	<1	-0.068	0.1891	0.0015	0.533	0.008	13.91	0.24	—	101	2734	13
27-1	53	<1	-0.037	0.1905	0.0009	0.531	0.006	13.94	0.16	—	100	2746	8
28-1	39	<1	0.109	0.1861	0.0012	0.517	0.006	13.26	0.18	—	99	2708	11
>5% discordant or U <10ppm													
1-1	6	<1	0.047	0.1852	0.0038	0.552	0.014	14.09	0.47	—	105	2700	34
21-1	138	49	0.369	0.1809	0.0007	0.440	0.003	10.97	0.10	0.007	88	2661	7
24-1	9	<1	-0.194	0.1860	0.0022	0.517	0.011	13.26	0.33	—	99	2707	20

Data are at 1σ precision. All Pb data are common-Pb corrected (based on ^{204}Pb and Broken Hill Pb composition). Analysis date: 15/03/02; session Z3878i. $^{208}\text{Pb}/^{232}\text{Th}$ data are not reported where Th<10ppm.

2001969111B: gneissic biotite trondhjemite, Wingora Soak

1:250,000 sheet: Duketon (SG5114)

1:100,000 sheet: Tate (3243)

MGA: 373648mE 6961614mN

Location: The sample was collected from a granite pavement, on the southern side of a low hill, about 400 m north of Wingora Soak.

Description: The foliated, white, seriate, medium-grained banded gneissic biotite (5–6%) trondhjemite is interlayered with subordinate grey, equigranular, fine- to medium-grained titanite-biotite granodiorite. The latter forms bands, locally to >1 m thick but often much thinner (<1 to >10 cm), which are characterised by significantly more mafic and biotite-rich (20–30%) compositions, than the dated host. These bands may represent original dykes or enclaves (now strung out) within the host trondhjemite. The bands are generally sub-parallel and typically parallel to the foliation. Both phases are cut by thin discordant felsic granite and pegmatite veins, and by later, essentially unfoliated, pink monzogranite dykes, up to 10 m in width, which form part of a large dyke swarm.

The principal minerals contributing to the granoblastic texture are plagioclase, K-feldspar, quartz and biotite, with plagioclase >> K-feldspar. Plagioclase occurs as subhedral to lesser anhedral grains, with faint to no visible twinning, and no obvious to minor zoning. Minor myrmekite is present. The plagioclase displays minor to moderate white mica and carbonate alteration. K-feldspar is present as anhedral to interstitial grains, with moderately- to well-developed tartan twinning, and minor perthite. Quartz is largely anhedral, with mostly moderately undulose extinction. Biotite occurs as irregular to locally subhedral flakes. It is light yellow to medium red-brown in colour, with minor alteration to chlorite, rutile, fluorite and/or minor white mica. Accessory minerals include zircon and apatite (commonly large hexagonal grains), anhedral to subhedral minor titanite (<1%), and irregular opaque minerals.

Mount, pop: Z3963B

Description of zircons

The zircon occurs as colourless and clear to pale brown and turbid crystals and fragments. It varies from stubby, equant grains, approximately 65 μm long, to large, elongate grains, greater than 400 μm in length (aspect ratios up to 7:1). There is slight to moderate rounding of crystal faces. A small proportion of anhedral, rounded grains are also present, ranging from about 60 μm to 190 μm in diameter. Fractures and inclusions are common. Zoning and cores are visible in many grains in transmitted and reflected light, although some are devoid of any features. In CL many grains display patchy, irregular zones, and/or oscillatory zoning (Fig. 84). Cores with truncated zoning are clearly visible in a number of grains.

Concurrent standard data

The primary beam became unstable in the latter part of this session. Following subsequent assessment, the data file was truncated after 38 hours, but this makes no significant difference to the data structures of either QGNG or the samples. Two of the 31 QGNG analyses that were retained are distinctly low in both $^{206}\text{Pb}/^{238}\text{U}$ and $^{207}\text{Pb}/^{206}\text{Pb}$, and were omitted from the calibration. The apparent calibration slope for QGNG is ~ 2.1 ; one of the concurrent samples indicates a value ~ 2.4 . The long-term average values of 2.2 was used for data processing. The 29 analyses give a $^{206}\text{Pb}/^{238}\text{U}$ calibration with a 1σ scatter of 0.68% (MSWD = 2.47). The corresponding $^{207}\text{Pb}/^{206}\text{Pb}$ data have an unusually wide spread, and the preferred low-side culling procedure results in excessive deletion if MSWD is forced to 1.0. Culling was therefore stopped at MSWD ≥ 1.3 (refer to chapter on “Data compilation for the QGNG standard”), resulting in a weighted mean $^{207}\text{Pb}/^{206}\text{Pb}$ age of 1849.2 ± 3.3 Ma (MSWD = 1.3; $n = 25$). Alternate data treatments,



Figure 84. Representative SEM images (BSE on left, CL on right) for sample 2001969111B: gneissic biotite trondhjemite, Wingora Soak. SHRIMP analysis spots are labelled. Remnant pits from the ion microprobe analyses are faintly visible in some grains. Scale bar is 100 μm .

such as deleting the most extreme outliers (several at $\sim 2\sigma$, both high and low) give a similar average. Element abundance calibration was based on CZ3 ($n = 3$).

A second session (Z3963j) on this sample and sample 2001969122 included 19 analyses of QGNG, which gave a Pb/U calibration with a 1σ scatter of 1.36% (MSWD = 4.97) and a weighted mean $^{207}\text{Pb}/^{206}\text{Pb}$ age of 1849.8 ± 4.3 Ma (MSWD = 0.76). Element abundance calibration was based on CZ3 ($n = 2$). See chapter on sample 2001969122 for additional details.

Sample data

Thirty four analyses were obtained from 33 grains, including four analyses from the partial supplementary session (Table 36). The data display a high degree of scatter (Fig. 85), possibly due to ancient and recent Pb loss; many of the grains are xenocrysts up to ~ 2955 Ma (cores were specifically targeted in a number of analyses). Amongst the concordant data there is only one small cluster of 13 points (Fig. 86), at ~ 2710 Ma, that is likely to retain age significance. One analysis (25-1) with very high U (>1100 ppm) is considered unreliable for chronology and is discarded, although it is consistent with the main group of data. The weighted mean $^{207}\text{Pb}/^{206}\text{Pb}$ age for these 13 analyses is 2709 ± 5 Ma, with MSWD = 2.2. There are two possible outliers to this group (16-1, 39-1) at 2689 ± 7 Ma (1σ). Omitting these is a reasonable option, given the existence of four younger, marginally discordant points (12-1, 14-1, 18-1, 20-1). The culling of either of these analyses revises the date to 2710.0 ± 4.4 Ma (MSWD = 1.6), while removing both gives 2711.1 ± 3.1 Ma (MSWD = 0.70). All these possible groupings are covered by a rounding to 2710 ± 5 Ma.

Geochronological interpretation

The very old dates obtained for some of the grains implies that these, at least, are xenocrysts. Because there is no grouping for the older dates, we interpret all these grains as xenocrysts. The 2710 Ma date could be either the magmatic age of the granitic precursor to the banded gneiss, or the time of gneiss formation. Because of the overall data scatter and the small number of analyses in the main group, the age cannot be considered to be well-determined, and using a notional age of ~ 2710 Ma is preferable to quoting a seemingly rigorous uncertainty.

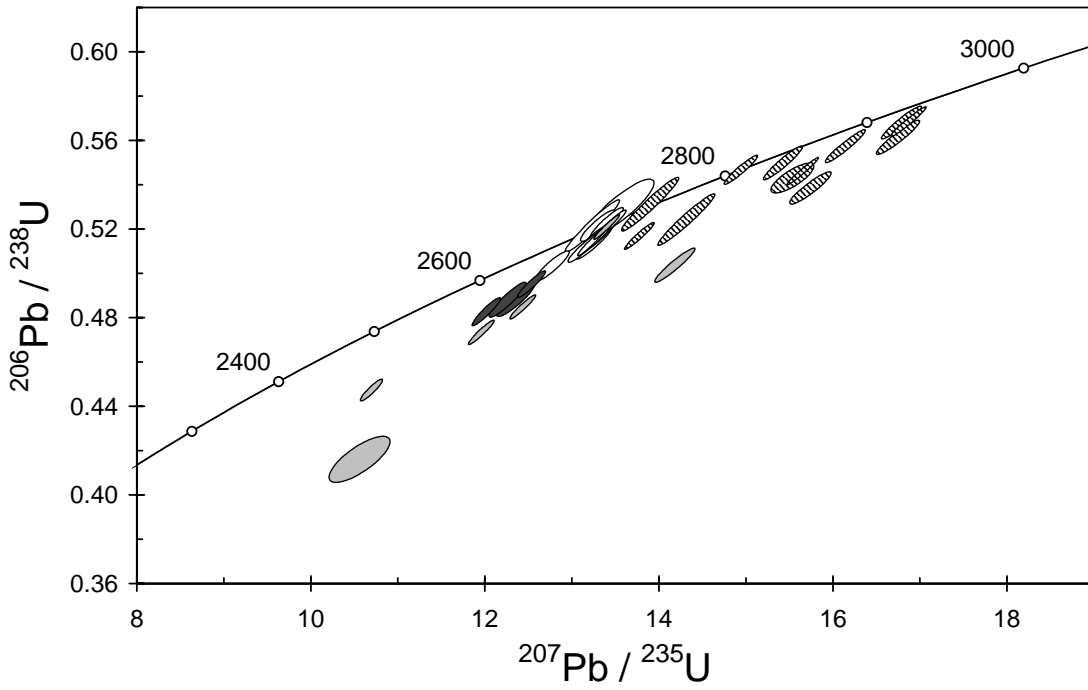


Figure 85. Concordia plot for zircons from sample 2001969111B: gneissic biotite trondhjemite, Wingora Soak. White filled symbols are used to define the age of the sample; inherited grains have diagonal shading; younger outliers are dark grey; discordant and/or high U analyses are light grey.

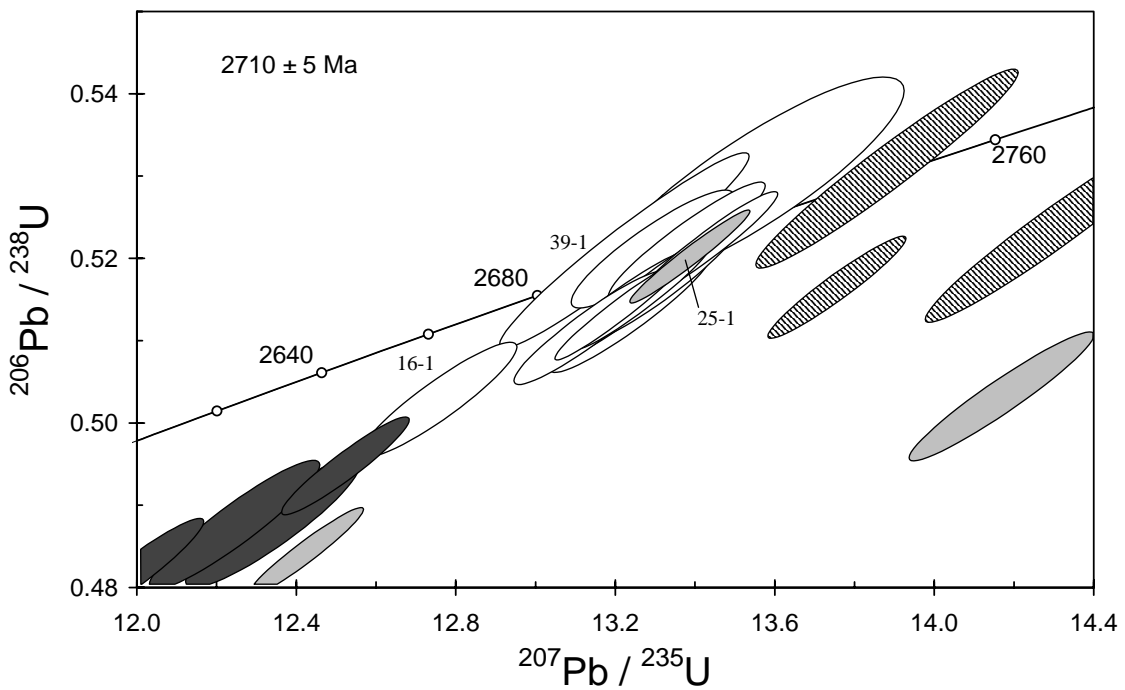


Figure 86. Concordia plot for the main data group from sample 2001969111B: gneissic biotite trondhjemite, Wingora Soak. Shading as in Figure 85.

Table 36. SHRIMP analytical results for zircon from sample 2001969111B: gneissic biotite trondhjemite, Wingora Soak.

grain-spot	U (ppm)	Th (ppm)	4f206 (%)	$^{207}\text{Pb}/^{206}\text{Pb}$		$^{206}\text{Pb}/^{238}\text{U}$		$^{207}\text{Pb}/^{235}\text{U}$		$^{208}\text{Pb}/^{232}\text{Th}$	conc. (%)	$^{207}\text{Pb}/^{206}\text{Pb}$ Age (Ma)	
					±		±		±				±
Main group													
1-1	332	24	0.001	0.1865	0.0004	0.514	0.004	13.21	0.11	0.142	99	2711	3
2-1	157	12	0.013	0.1868	0.0006	0.517	0.005	13.31	0.13	0.143	99	2714	5
3-1	287	73	-0.002	0.1867	0.0004	0.515	0.004	13.26	0.11	0.143	99	2713	4
5-1	147	13	0.047	0.1858	0.0006	0.522	0.005	13.38	0.13	0.137	100	2706	6
6-1	155	49	0.061	0.1862	0.0006	0.511	0.005	13.13	0.13	0.142	98	2709	6
15-1	123	31	-0.014	0.1870	0.0007	0.513	0.005	13.24	0.14	0.142	98	2716	6
16-1	165	6	0.344	0.1840	0.0007	0.503	0.005	12.75	0.13	0.079	98	2689	7
17-1	163	40	0.073	0.1864	0.0006	0.514	0.005	13.21	0.13	0.140	99	2711	6
22-1	22	5	0.247	0.1856	0.0017	0.530	0.008	13.55	0.25	0.129	101	2703	15
28-1	200	15	0.019	0.1867	0.0005	0.521	0.004	13.43	0.12	0.141	100	2714	4
29-1	118	5	0.470	0.1849	0.0008	0.521	0.005	13.29	0.14	0.140	100	2698	7
39-1	164	18	0.122	0.1840	0.0008	0.521	0.008	13.22	0.21	0.136	101	2689	7
Xenocrysts													
4-1	313	118	0.305	0.1932	0.0005	0.516	0.004	13.75	0.11	0.142	97	2769	4
7-1	148	107	0.091	0.2164	0.0007	0.561	0.005	16.75	0.16	0.157	97	2954	5
8-1	292	131	0.030	0.2075	0.0013	0.543	0.004	15.53	0.16	0.150	97	2886	10
9-1	182	97	0.261	0.2120	0.0008	0.538	0.005	15.74	0.16	0.142	95	2921	6
11-1	201	99	0.039	0.2142	0.0006	0.568	0.005	16.79	0.15	0.154	99	2938	4
13-1	166	47	0.000	0.2100	0.0006	0.557	0.005	16.14	0.15	0.155	98	2906	5
19-1	143	49	0.017	0.2035	0.0006	0.550	0.005	15.42	0.15	0.148	99	2854	5
21-1	527	273	0.120	0.2079	0.0003	0.546	0.004	15.65	0.12	0.151	97	2889	3
26-1	262	285	0.008	0.1982	0.0005	0.547	0.004	14.93	0.13	0.150	100	2811	4
27-1	318	95	0.039	0.2152	0.0004	0.569	0.004	16.87	0.14	0.156	99	2945	3
37-1	174	59	0.007	0.1896	0.0008	0.531	0.008	13.88	0.22	0.147	100	2739	7
38-1	215	18	0.181	0.1981	0.0008	0.524	0.008	14.31	0.22	0.162	96	2811	6
Young outliers													
12-1	82	15	0.229	0.1835	0.0009	0.487	0.005	12.33	0.14	0.123	95	2685	8
14-1	710	78	0.429	0.1836	0.0005	0.494	0.004	12.51	0.11	0.135	96	2685	5
18-1	218	10	0.125	0.1805	0.0006	0.482	0.004	11.99	0.11	0.113	95	2658	5
20-1	662	184	0.357	0.1821	0.0008	0.487	0.005	12.23	0.14	0.124	96	2672	7
>5% discordant or high U													
6-2	75	18	0.881	0.1843	0.0026	0.414	0.007	10.53	0.23	0.116	83	2692	23
10-1	416	205	0.349	0.2043	0.0007	0.503	0.005	14.17	0.15	0.145	92	2861	5
23-1	1001	160	0.991	0.1734	0.0005	0.446	0.003	10.67	0.08	0.145	92	2591	5
24-1	324	5	0.242	0.1832	0.0004	0.472	0.004	11.93	0.10	0.169	93	2682	4
25-1	1119	234	0.778	0.1866	0.0003	0.520	0.004	13.38	0.10	0.151	100	2712	3
30-1	696	371	0.309	0.1860	0.0004	0.484	0.004	12.41	0.10	0.120	94	2708	4

Data are at 1σ precision. All Pb data are common-Pb corrected (based on ^{204}Pb and Broken Hill Pb composition). Analysis date: 27/05/02; session Z3963i and four analyses (6-2 and 37-1 to 39-1) on 07/06/02; session Z3963j.

2001969122: Mt Joanna granodiorite

1:250,000 sheet: Duketon (SG5114)

1:100,000 sheet: Urarey (3343)

MGA: 396502mE 6967198mN

Location: The sample was collected from a moderate-sized whaleback in an area of good bouldery outcrop north of fence line, about 4.6 km north-northwest of Six Mile Hill.

Description: This sample is a foliated, lineated, incipiently banded, grey-white, fine- to medium-grained biotite granodiorite. The fine banding (<2 cm in width) is defined by biotite-rich and biotite-poor layers. The rock is an early granitic gneiss that is cut by late granite dykes and pegmatites.

Principal minerals in the granoblastic to granular rock are plagioclase, K-feldspar, quartz and biotite, with plagioclase >>K-feldspar. Plagioclase occurs as subhedral to anhedral grains in which twinning is faint to absent. Zoning is not obvious in these grains. Minor myrmekite is present. Plagioclase displays minor to moderate white mica and carbonate alteration. K-feldspar is anhedral to interstitial, with moderately developed tartan twinning, and minor perthite. Quartz occurs as anhedral to elongate grains that are mostly moderately to mildly undulose. Biotite is present as irregular to locally subhedral, light yellow to medium-dark brown flakes, with minor alteration to chlorite, rutile, epidote and/or minor white mica. Accessory minerals include apatite, zircon, opaque minerals and allanite.

Mount, pop: Z3963C

Description of zircons

A relatively small number of zircon grains were recovered from this sample. They consist of colourless to pale brown-grey fragments and a smaller proportion of whole crystals. Many of the grains are euhedral to subhedral prismatic fragments with aspect ratios of 2:1 to 3:1; they vary from about 65 μm to 175 μm in length. Some fragments are up to 100 μm wide. The grains contain small inclusions, and in many cases zoning and cores are visible in transmitted and reflected light. The CL images more clearly display continuous euhedral oscillatory zoning and the cores, as well as the presence of irregular or weak zoning in some grains, which suggests partial recrystallisation (Fig. 87).

Concurrent standard data

This session involved analyses on this mount over 35 hours, followed by analyses on several other mounts in search of old grain cores. This summary deals only with the analyses on mount Z3963. Nineteen analyses of QGNG give a Pb/U calibration with a 1σ scatter of 1.36% (MSWD = 4.97). Although the omission of two extreme values would reduce the scatter to 0.68%, all of the data have been retained. After omitting one $>3\sigma$ young $^{207}\text{Pb}/^{206}\text{Pb}$ outlier, the remaining 18 analyses give a weighted mean $^{207}\text{Pb}/^{206}\text{Pb}$ age of 1849.8 ± 4.3 Ma (MSWD = 0.76).

Element abundance calibration was based on CZ3 (n = 2).

Sample data

The 29 analyses (Table 37), obtained from individual grains, show a strong recent Pb-loss trend (Fig. 88), with more than half of them being $>5\%$ discordant. The 13 concordant analyses form a single $^{207}\text{Pb}/^{206}\text{Pb}$ age population (Fig. 89), with a weighted mean age of 2939.2 ± 5.4 Ma (MSWD = 0.84).

Geochronological interpretation

The 2939 ± 6 Ma age is interpreted to be the crystallisation age of the granodiorite.

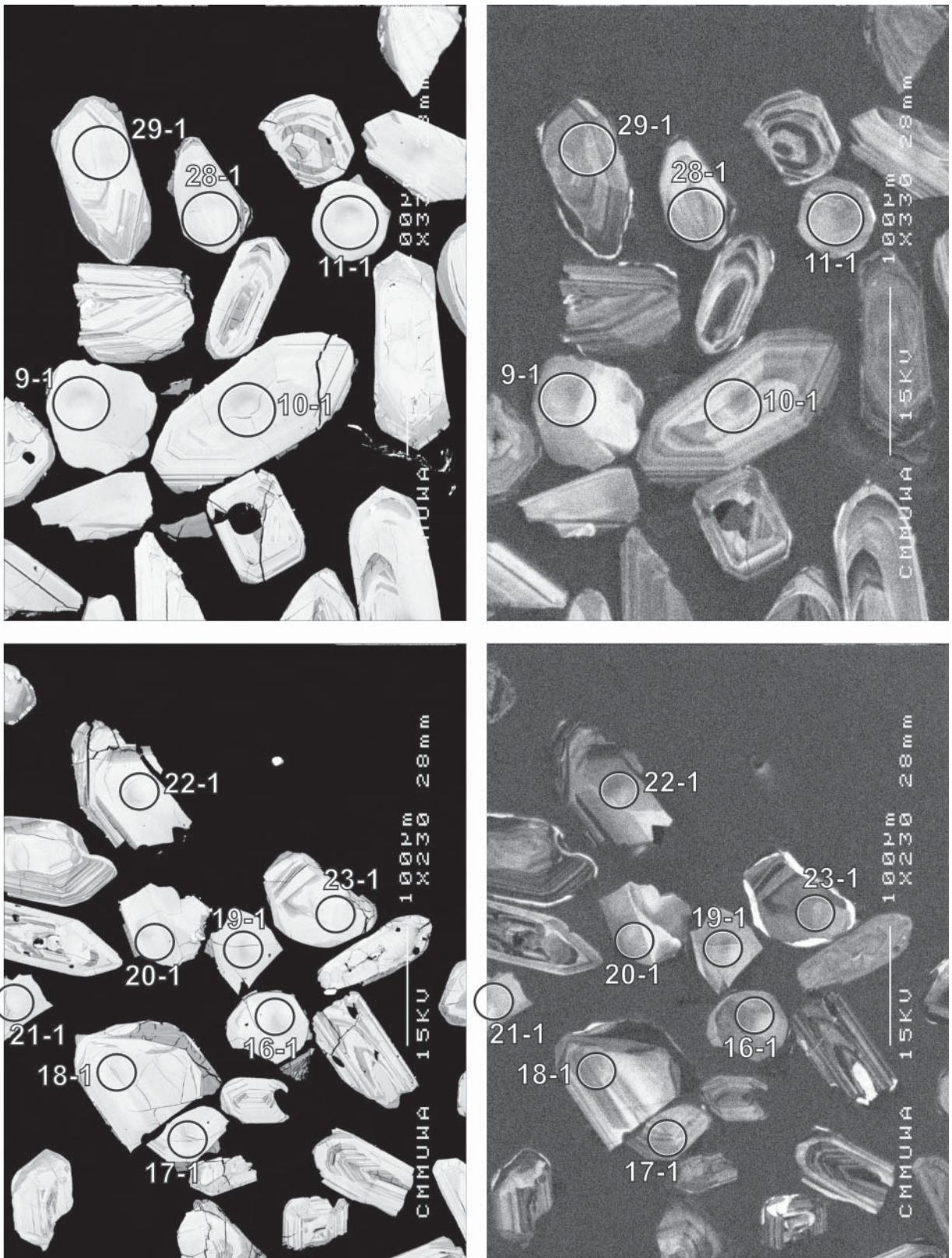


Figure 87. Representative SEM images (BSE on left, CL on right) for sample 2001969122: Mt Joanna granodiorite. SHRIMP analysis spots are labelled. Remnant pits from the ion microprobe analyses are faintly visible in some grains. Scale bar is 100 µm.

Table 37. SHRIMP analytical results for zircon from sample 2001969122: Mt Joanna granodiorite

grain-spot	U (ppm)	Th (ppm)	4f206 (%)	$^{207}\text{Pb}/^{206}\text{Pb}$		$^{206}\text{Pb}/^{238}\text{U}$		$^{207}\text{Pb}/^{235}\text{U}$		$^{208}\text{Pb}/^{232}\text{Th}$	conc. (%)	$^{207}\text{Pb}/^{206}\text{Pb}$ Age (Ma)	
					±		±		±				±
Concordant subgroup													
1-1	157	47	0.421	0.2151	0.0012	0.542	0.008	16.09	0.26	0.166	95	2945	9
3-1	152	28	0.052	0.2137	0.0022	0.574	0.009	16.91	0.31	0.164	100	2934	17
9-1	97	55	0.202	0.2143	0.0013	0.577	0.012	17.05	0.38	0.152	100	2938	10
11-1	130	39	0.196	0.2147	0.0009	0.572	0.009	16.93	0.27	0.156	99	2941	6
12-1	87	28	0.262	0.2138	0.0018	0.566	0.009	16.68	0.31	0.149	98	2935	14
14-1	48	19	0.119	0.2174	0.0017	0.559	0.010	16.76	0.33	0.152	97	2962	13
16-1	83	24	-0.040	0.2132	0.0011	0.578	0.009	16.98	0.29	0.157	100	2930	8
20-1	107	62	0.334	0.2136	0.0011	0.569	0.010	16.77	0.32	0.145	99	2933	8
22-1	106	62	0.140	0.2138	0.0014	0.574	0.009	16.91	0.29	0.147	100	2934	11
26-1	101	42	0.726	0.2162	0.0018	0.549	0.010	16.37	0.31	0.114	95	2953	13
28-1	124	47	0.233	0.2132	0.0011	0.574	0.009	16.88	0.29	0.151	100	2930	8
30-1	112	45	0.482	0.2158	0.0014	0.560	0.009	16.67	0.30	0.160	97	2950	10
Discordant													
2-1	151	40	1.685	0.2134	0.0014	0.530	0.008	15.59	0.26	0.181	93	2932	11
4-1	76	20	0.619	0.2129	0.0014	0.526	0.009	15.44	0.27	0.143	93	2928	11
5-1	159	52	1.362	0.2125	0.0037	0.424	0.008	12.43	0.31	0.162	78	2925	28
6-1	110	30	2.033	0.2080	0.0022	0.496	0.009	14.23	0.30	0.151	90	2890	17
7-1	157	45	0.814	0.2134	0.0015	0.440	0.011	12.95	0.34	0.155	80	2931	11
8-1	111	42	0.633	0.2108	0.0013	0.530	0.008	15.42	0.26	0.150	94	2912	10
10-1	84	28	0.309	0.2143	0.0012	0.517	0.008	15.27	0.26	0.151	91	2939	9
13-1	118	98	0.757	0.2136	0.0014	0.411	0.007	12.11	0.21	0.051	76	2933	11
15-1	94	37	0.618	0.2156	0.0017	0.487	0.008	14.47	0.26	0.145	87	2948	13
17-1	87	33	1.609	0.2131	0.0019	0.498	0.008	14.64	0.27	0.163	89	2929	14
18-1	90	28	0.452	0.2152	0.0045	0.522	0.032	15.50	1.01	0.154	92	2945	34
19-1	86	23	1.075	0.2106	0.0015	0.466	0.008	13.55	0.25	0.156	85	2910	12
21-1	81	37	2.366	0.2080	0.0021	0.387	0.008	11.09	0.26	0.099	73	2890	17
27-1	626	136	13.988	0.1994	0.0039	0.133	0.002	3.64	0.09	0.175	28	2822	32
29-1	161	79	0.628	0.2167	0.0013	0.439	0.007	13.11	0.22	0.124	79	2957	10
31-1	301	126	7.032	0.2070	0.0024	0.355	0.005	10.14	0.19	0.143	68	2882	19
32-1	131	126	0.252	0.2125	0.0012	0.505	0.008	14.81	0.25	0.058	90	2925	9

Data are at 1 σ precision. All Pb data are common-Pb corrected (based on ^{204}Pb and Broken Hill Pb composition). Analysis date: 7/06/02; session Z3963j. Analyses on grains 23–25 were lost due to computer and primary beam problems.

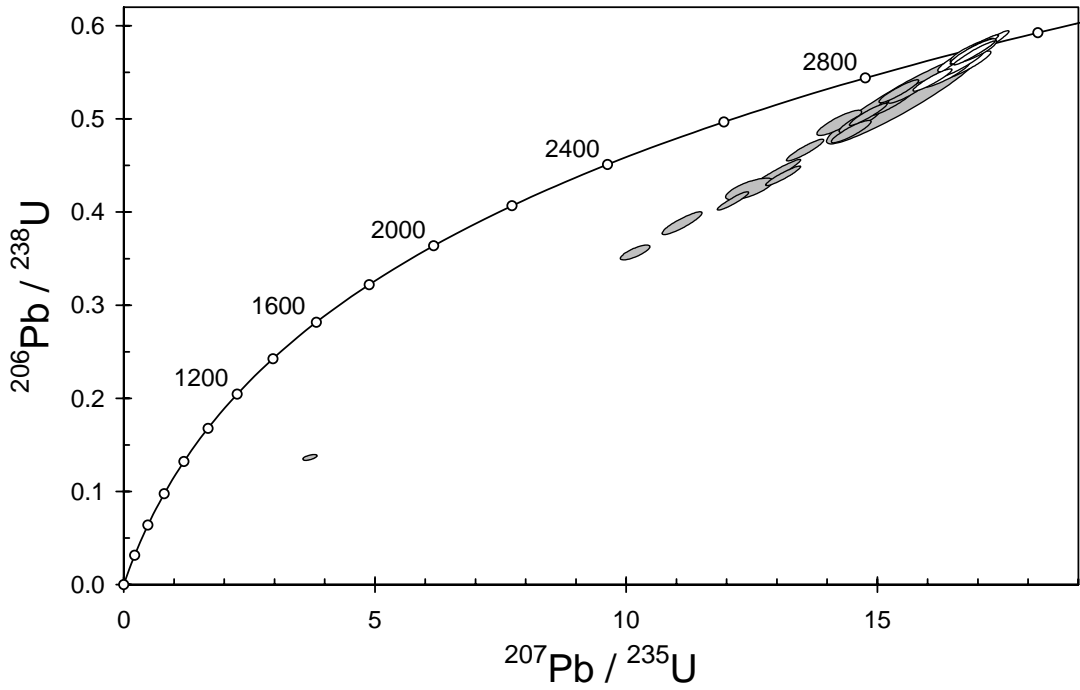


Figure 88. Concordia plot for zircons from sample 2001969122: Mt Joanna granodiorite. White filled symbols are used to define the age of the sample; discordant analyses are light grey.

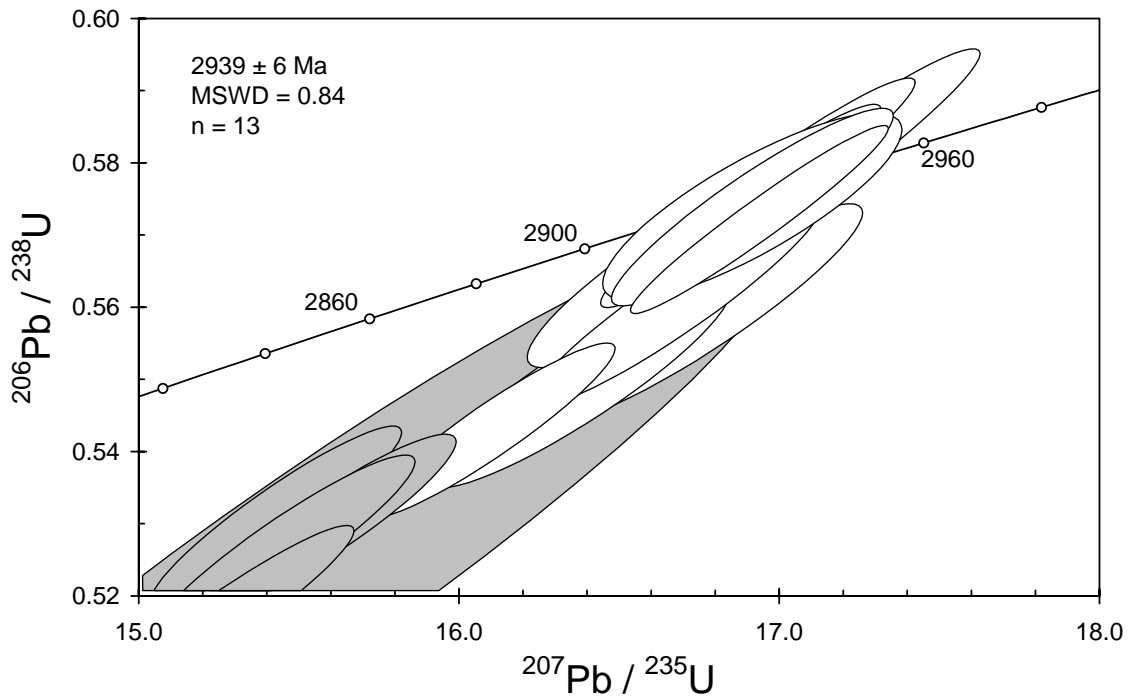


Figure 89. Concordant data from sample 2001969122: Mt Joanna granodiorite. Shading as in Figure 88.

Acknowledgements

The Curtin University-Geoscience Australia collaborative research agreement was coordinated by Neal McNaughton. Special thanks go to John de Laeter and Barney Glover (Curtin University) and Chris Pigram and Russell Korsch (Geoscience Australia) for their assistance in establishing and maintaining the agreement.

We acknowledge the technical assistance of Peter Taylor in the collection of field samples. Sample preparation was undertaken by Tas Armstrong, Stephen Ridgway and Gerald Kuehlich, and the preparation, photography and SEM imaging of mineral mounts was undertaken by Chris Foudoulis at the mineral separation laboratories at Geoscience Australia.

SHRIMP analyses were undertaken by the Curtin authors with assistance from Matt Godfrey, April Pickard, Brock Salier, Natalie Kositcin and J-P Pigois. SEM imaging for this report was performed by one of the authors (JMD) at the Centre for Microscopy and Microanalysis, UWA.

Constructive comments by Lance Black and Andrew Cross during internal review improved this report.

The SHRIMP II is maintained by Allen Kennedy (Curtin University) and operated by a consortium consisting of Curtin University of Technology, the Geological Survey of Western Australia and the University of Western Australia with the support of the Australian Research Council.

References

- Black, L.P., Champion, D.C. and Cassidy, K.F., 2003, Compilation of SHRIMP U–Pb geochronology data, Yilgarn Craton, Western Australia, 1997-2000: Geoscience Australia Record, in press.
- Clark, D.J., Hensen, B.J. and Kinney, P.D., 2000, Geochronological constraints for a two-stage history of the Albany-Fraser Orogen, Western Australia: *Precambrian Research*, **102**, 155-183.
- Compston, W., Williams, I.S. and Meyer, C., 1984, U–Pb geochronology of zircons from lunar breccia 73217 using a sensitive high-resolution ion microprobe: *Journal of Geophysical Research*, **98**, B525–B534.
- Daly, S.J., Fanning, C.M. and Fairclough, M.C., 1998, Tectonic evolution and exploration potential of the Gawler Craton, South Australia: *AGSO Journal of Australian Geology and Geophysics*, **17**, 145-168.
- Fletcher, I.R., Dunphy, J.M., Cassidy, K.F. and Champion, D.C., 2001, Compilation of SHRIMP U–Pb geochronological data, Yilgarn Craton, Western Australia, 2000-2001: Geoscience Australia, Record **2001/47**.
- Kinny, P.D., 1997, Krill (computer program): Curtin University of Technology, Perth, WA.
- Ludwig, K.R., 2001, SQUID 1.00: Berkley Geochronology Centre, Special Publication **2**.
- Nelson, D.R., 1997, Compilation of SHRIMP U–Pb zircon geochronology data, 1996: Western Australia Geological Survey, Record **1997/2**.
- Pidgeon, R.T., Furfaro, D., Kennedy, A.K., Nemchin, A.A. and van Bronswijk, W., 1994, Calibration of zircon standards for the Curtin SHRIMP II, *In* Abstracts of the 8th International Conference on Geochronology, Cosmochronology and Isotope Geology, Berkeley, USA: U.S. Geological Survey Circular, **1107**, 251.
- Smith, J.B., Barley, M.E., Groves, D.I., Krapez, B., McNaughton, N.J., Bickle, M.J. and Chapman, H.J., 1998, The Sholl Shear Zone, West Pilbara: evidence for a domain boundary structure from integrated tectonostratigraphic analyses, SHRIMP U–Pb dating and isotopic and geochemical data of granitoids: *Precambrian Research*, **88**, 143–171.
- Stacey, J.S. and Kramers, J.D., 1975, Approximation of terrestrial lead isotope evolution by a two-stage model: *Earth and Planetary Science Letters*, **26**, 207-221.
- Wendt, I. and Carl, C., 1991, The statistical distribution of the mean squared weighted deviation: *Chemical Geology*, **86**, 275-285.
- Williams, I.S., 1998, U–Th–Pb geochronology by ion microprobe: *Reviews in Economic Geology*, **7**, 1-35.